N70-12050
NASA CR-106988

Second Quarterly Progress Report

THROTTLEABLE THRUSTOR SYSTEM

JPL Contract No. 952344
Report No. 69.4726.3-86

20 October 1969

CASE FILE
COPY

This work was performed for the Jet Propulsion Laboratory, California Institute of Technology, as sponsored by the National Aeronautics and Space Administration under Contract NAS7-100.

TRW SYSTEMS
One Space Park · Redondo Beach, California

Second Quarterly Progress Report

THROTTLEABLE THRUSTOR SYSTEM

JPL Contract No. 952344

Report No. 69.4726.3-86

20 October 1969

This work was performed for the Jet Propulsion Laboratory, California Institute of Technology, as sponsored by the National Aeronautics and Space Administration under Contract NAS7-100.

TRW SYSTEMS

One Space Park · Redondo Beach, California

ABSTRACT

This second quarterly report is a summary of the Phase I preliminary Design Study completed during the time period of 26 June through 26 September 1969. The nine candidate design concepts previously selected were further analyzed for engine performance, flow control requirements and total system weight. The relative advantages of each configuration were evaluated based on the ground rules established during the first quarter for a typical Mars lander mission. Engine thrust levels of 300, 600 and 1200 lbf were considered and the optimum chamber pressure and expansion ratio were determined for each system. System Eight, employing a light-weight catalytic chamber and conventional nozzle was recommended. This design incorporates an electro-mechanical throttle valve which is a high response version of a currently available valve. From the results of the system weight studies, the optimum design will employ a low chamber pressure ($\sim$200 psia) and low expansion ratio ($\sim$20:1). A more extensive examination of the operating parameters and design details will be completed during Phase II design effort which was commenced during this quarter.

This report contains information prepared by TRW Systems Group under JPL subcontract. Its content is not necessarily endorsed by the Jet Propulsion Laboratory, California Institute of Technology, or the National Aeronautics and Space Administration.

TABLE OF CONTENTS

		Page
ABSTRACT		ii
TABLE OF CONTENTS		iii
NOMENCLATURE		v
I	INTRODUCTION	I-1
II	TECHNICAL DISCUSSION	II.A-1
II.A	REQUIREMENTS	II.A-1
	II.A.1 Mission Characteristics	II.A-2
	II.A.2 Ground Rules and Assumptions	II.A-2
II.B	DESIGN CONCEPT SELECTION	II.B-1
	II.B.1 System Goals	II.B-1
	II.B.2 Potential Design Concepts	II.B-2
	II.B.3 Design Concept Comparison and Selection	II.B-22
II.C	PRELIMINARY SYSTEM DESIGN	II.C-1
	II.C.1 System Layouts	II.C-1
	II.C.2 Baseline Weight Analysis	II.C-5
II.D	SYSTEM EVALUATION	II.D-1
	II.D.1 Engine Performance	II.D-1
	II.D.2 Engine Weight	II.D-4
	II.D.3 Propellant Consumption	II.D-6
	II.D.4 Propellant Tank Weight	II.D-6
	II.D.5 Pressurant Weight	II.D-7
	II.D.6 System Weight Results	II.D-8
	II.D.7 Ideal Velocity Increment	II.D-9
	II.D.8 Conclusions	II.D-9

TABLE OF CONTENTS (Continued)

		Page
II.E	FLOW CONTROL SYSTEMS	II.E-1
	II.E.1 Throttling Concepts (Throttle Mechanizations)	II.E-1
	II.E.2 Throttle Valve Performance	II.E-9
	II.E.3 Electromechanical Throttle Actuator	II.E-17
	II.E.4 Control Systems	II.E-18
III	PHASE II RECOMMENDATION	III-1
IV	NEW TECHNOLOGY REPORTS	IV-1
	IV.1 Thermal Decomposition Engine	IV-1
	IV.2 Radial Flow Reactor	IV-2
	IV.3 High Efficiency Monopropellant Reactor	IV-6
	IV.4 Throttleable Monopropellant Rocket Engine	IV-9
APPENDIX A	SYSTEM PERFORMANCE PROGRAM	A-1
APPENDIX B	THRUST LEVEL OPTIMIZATION	B-1
APPENDIX C	THRUST LINEARITY	C-1

NOMENCLATURE

Symbol	Definition
A	= Area (in^2)
Av	= Catalyst bed specific surface area (in^2/in^3)
C*	= Characteristic exhaust velocity (ft/sec)
C_D	= Discharge coefficient (dimensionless)
C_F	= Thrust coefficient (dimensionless)
d	= Diameter (inch)
D	= Diameter (inch)
f	= Friction factor (dimensionless)
F	= Thrust (lbf)
F_{TU}	= Ultimate tensile strength (lbf/in^2)
F_v	= Catalyst bed porosity (dimensionless)
g	= 32.2 ft/sec^2 (Earth), 12.24 ft/sec^2 (Mars)
I_s	= Specific Impulse (lbf-sec/lbm)
J	= Moment of inertia ($oz\text{-}in\text{-}sec^2$)
k	= Specific heat ratio (dimensionless)
K	= Flow constant (lbm/lbf)
K_A	= Amplifier gain (volt/volt)
K_{FB}	= Feedback gain (volts/inch; volts/psi)
K_S	= Spring constant (lbf/inch)
K_T	= Motor torque constant (oz-inch/amp)
ℓ	= Length (inch)
ℓ	= Ball screw lead (inch/revolution)
L	= Length (inch)
L*	= Characteristic chamber length (inch)

NOMENCLATURE (Continued)

Symbol	Definition
Lc	= Chamber length (inch)
M	= Molecular weight
P_A	= Ambient pressure (lbf/in^2)
Pc	= Chamber pressure (lbf/in^2)
Pe	= Nozzle exit pressure (lbf/in^2)
P_T	= Tank pressure (lbf/in^2)
R	= Resistance (OHMS)
R	$= \left(C_2 - \frac{1}{C_1^2}\right)^{1/2}$
R	= Nitrogen gas constant (in-lbf/lbm°R)
S	= Laplace transform operator
T	= Temperature (°R)
V	= Valve pressure drop fraction (dimensionless)
V	= Volume ($inch^3$)
V	= Velocity (ft/sec)
V_c	= Control signal (volts)
$\dot{W}$	= Flowrate (lbm/sec)
W_c	= Component weight (lbm)
W_E	= Engine weight
WF	= Weld factor (dimensionless)
W_g	= Pressurant weight (lbm)
$\dot{W}_o$	= Design flowrate (lbm/sec)
W_P	= Propellant weight (lbm)
W_{PT}	= Propellant tank weight (lbm)

NOMENCLATURE (Continued)

Symbol	Definition
W_S	= System weight (lbm)
X	= Displacement (inch)
X	= Ammonia dissociation (percent)
X	= Flowrate fraction (percent)
Z	= Tank volume ratio (dimensionless)
γ	= Specific heat ratio (dimensionless)
ΔP_B	= Reactor bed pressure drop (lbf/in^2)
ΔP_{inj}	= Injector pressure drop (lbf/in^2)
ΔPs	= Feed system pressure drop (lbf/in^2)
ΔP_v	= Flow control valve pressure drop (lbf/in^2)
ϵ	= Expansion ratio (dimensionless)
ρ	= Specific weight (lbm/ft^3)
ρ_P	= Specific weight of liquid propellant (lbm/ft^3)
ρ_T	= Specific weight of propellant tank material (lbm/ft^3)
σ	= Working stress (lbf/in^2)
h	= Attitude (ft)
h	= Horizontal
v	= Vertical
$\dot{h}$	= Vertical velocity (ft/sec)
m	= Mass
$\dot{m}$	= Mass rate change (slugs/sec)
$\frac{\partial Meng}{\partial F}$	= Engine mass sensitivity, $.621 \times 10^{-3}$ $(\frac{slugs}{lbf})$
$\partial m_t/2m_p$	= Propellant tank mass sensitivity, .053 (slugs/slug)
t	= Time (seconds)
$\dot{y}_o$	= Ignition horizontal velocity, 250 (ft/sec)

I. INTRODUCTION

The simplicity and demonstrated reliability of monopropellant hydrazine propulsion systems has fostered their use on ever more ambitious missions. In addition, since the flow of a single propellant only must be regulated, throttling may be easily accomplished. These factors have led to the consideration of hydrazine systems for increasingly complex missions such as Voyager and Viking class planetary landers.

The objective of the Throttleable Thrustor System (TTS) contract is, therefore, to advance the state-of-the-art of hi-thrust throttleable monopropellant hydrazine thrustor systems. To this end, a three phase program is being accomplished by TRW Systems Group as follows:

- Phase I — Study and analysis, and comparison of different mechanizations capable of meeting stipulated performance requirements.
- Phase II — Detailed design of the candidate system selected as a result of the Phase I study.
- Phase III — Fabrication and test verification of the performance and response characteristics of the selected configuration.

This report is the second quarterly report for the subject contract covering the Phase I effort from contract initiation through the end of the third quarter of CY 1969. The initial section of the report shows how the TTS contractural goals are related to the mission requirements of the planetary lander mission which has been selected as a model for the study.

The first task undertaken was to select from the almost infinite number of potential designs for a TTS, a representative but manageable number to be studied in greater detail. The process and rationale used for this selection is presented in Section II.B.

Three types of detailed studies were then undertaken. Preliminary designs were completed for each selected system and these designs were analyzed to provide baseline weights. These studies are described in Section II.C. The performance of the various thrustor systems was then determined parametrically at thrust levels of 300, 600 and 1200 lbf for a

model Mars lander mission. These studies are described in Section II.D. Finally, design performance and response comparisons were completed for the flow control assembly as detailed in Section II.E.

Based on the results of these studies, a recommendation was made, Section III, of a candidate system to be used in the balance of the program. This recommendation was concurred in and Phase II, Detail Design, was initiated.

Because a large amount of graphic and tabular parametric information has been generated during the study, this information has been placed at the end of the various sections noted above. In this way it is hoped that the continuity of the text will be better preserved and that comparisons between the parametric data will be facilitated.

II.A. REQUIREMENTS

The performance requirements for any propulsion system are dictated by the specific application considered. The unmanned Mars soft-landing vehicle has been established as the mission model for the throttleable thrustor system. The intent of Phase I was to evaluate potential propulsion concept in the context of this model and recommend a system to be designed, fabricated and tested during Phases II and III. A brief summary of the mission model is therefore apropos.

II.A.1 Mission Characteristics

A representative Mars landing mission profile is illustrated in Figure II.A-1 where a three stage deceleration technique is employed. During the first stage, deceleration is initiated by a de-orbit burn and the vehicle orientation is adjusted to the correct angle for entry into the Mars atmosphere. This maneuver is followed by a parachute descent which settles the propellant and reduces the propulsion system impulse requirement. The terminal descent is accomplished entirely by the Mars lander propulsion system. Propulsion system ignition occurs at an altitude in the range of 1 to 5 kilometers. The atmospheric pressure versus altitude is shown in Figure II.A-2 along with a comparison to the contract specified value (0.3 psia). A typical system flow schematic and thrust profile are shown in Figure II.A-3.

Typical system characteristics for a mission with a lander initial mass of 3000 lbm are shown in Table II.A-1. It may be noted that a landing system impulse of 38,000 lbf-sec was required in this case which with the duty cycle of Figure II.A-3 yielded a thrust level of 1000 lbf for each of the three engines. The invariant percent thrust versus time of Figure II.A-3 results in a total impulse, and therefore vehicle size, which is a direct function of thrust level. This approach was selected over the possibility of considering a constant vehicle size with variable thrust engines on the basis of the analysis presented in Appendix A. As this analysis shows, an optimum lander thrust/weight ratio exists which is essentially independent of vehicle size. Therefore, studies which considered the vehicle weight fixed would indicate that a certain thrust level was optimal more or less independently of engine design. Since the purpose of the Phase I

study was to compare various engine designs, the variable vehicle size/total impulse approach was recommended and selected.

The contractual design goals are summarized in Table II.A-2 together with values which have resulted both from previous studies and from the currently on-going system definition of the 1973 Mars lander vehicle.

II.A.2 Ground Rules and Assumptions

For the purpose of this study the propulsion system configuration was identical for all the systems evaluated except for the design of the engine itself. The engine employs neat hydrazine fuel and spontaneous catalyst with a nitrogen blowdown pressurized system. A schematic of the basic system used in the performance studies has been presented in Figure II.A-3. Typical engine configurations are selected in Section II.B and described in detail in Section II.C. The weight and performance of each system was determined by the use of a digital computer program described in Appendix A. A summary of the basic ground rules and assumptions used in the performance study is contained in Table II.A-3. The primary measure of system performance was considered to be total system mass. Conceptually, at least, the system which had the best performance (least propulsion system mass) would be selected for the remainder of the program.

Table II.A-1. Typical Vehicle and Mission Characteristics

Initial Mass = 3000 lbm

Weight on Mars = 1170 lbf

Initial Thrust/Weight Ratio = F/W = 2.56

Mass of Aeroshell = 450 lbm

Mass of Parachute = 175 lbm

Mass of Vernier Rocket System - 330 lbm (3-1000 lbf engine systems)

Design $\frac{M}{C_D A}$ of Aeroshell - 0.20 slugs/ft^2

Design $\frac{M}{C_D A}$ of Parachute - 0.037 slugs/ft^2

Sequence	Altitude, ft	Time, sec
Deployment	24,000	0
A/S Separation	21,000	12
Minimum Ignition Complete	7,500	111
Landing (Terrain above zero altitude)	6,000	121

Vernier Impulse - 38,000 lb-sec
(3-1000 lbf engine system)

Table II.A-2. Throttleable Thrustor System
Design and Performance Requirements

PARAMETER	TTS REQUIREMENT	MARS LANDER REQUIREMENT
THRUST	600 LBF	600 LBF
THROTTLE RATIO (AT CONSTANT INLET PRESSURE)	6:1 MINIMUM 10:1 GOAL	6.7:1
NOZZLE SEPARATION CRITERIA	NO SEPARATION AT P_{AMB} = 0.3 PSIA	NO SEPARATION AT P_{AMB} = 0.29 PSIA
LIFE	500 SEC	300 SEC
SPECIFIC IMPULSE	$\geq$ 210 LBF-SEC/LBM (AMBIENT PRESSURE = VAC.)	227 LBF-SEC/LBM AT 600 LBF THRUST 200 LBF-SEC/LBM AT 90 LBF THRUST (AMBIENT PRESSURE = 0.29 PSIA)
HEAT STERILIZATION	6 CYCLES OF 64 HOURS/CYCLE AT 275°F	5 CYCLES OF 40 HOURS/CYCLE AT 275°F PLUS 3 CYCLES OF 60 HOURS/CYCLE AT 275°F
90%STEP RESPONSE	75 MSEC	80 MSEC
FREQUENCY RESPONSE (5 CPS)		
AMPLITUDE RATIO	0.70 @60 ± 10% THRUST	0.70@ 60± 25%THRUST
PHASE LAG	45°	45°
OVERSHOOT	25%	20%

Table II.A-3. Throttleable Thrustor System Performance Studies
Ground Rules and Assumptions

A. ENGINE SYSTEM - (THREE ENGINES PER SYSTEM)

1. F = 300, 600, 1200 LBF
2. Pc = 50 TO 500 PSIA
3. ϵ = 5 TO 80
4. C* EMPERICAL CURVE DEPENDENT ON % THRUST AND DECOMPOSITION BED
5. C_F THEORETICAL CURVE DEPENDENT ON % THRUST, ϵ AND NOZZLE TYPE
6. $\Delta P_{INJECTOR}$ = 75 FOR FLOW CONTROL INJECTOR, 110 FOR FIXED AREA INJECTOR
7. $\Delta P_{DECOMPOSITION\ BED}$ = 10 FOR THERMAL DECOMPOSITION, 50 FOR CATALYTIC BED
8. NOZZLE SEPARATION WHEN Pe < 0.12 PSIA
9. MATERIAL L-605 (MINIMUM GAGE = 0.015 IN.)

B. PROPELLANT SUPPLY SYSTEM - (ONE PRESSURANT AND PROPELLANT TANK COMBINED)

1. PROPELLANT MIL-P-26536B HYDRAZINE
2. PRESSURANT MIL-P-27401B NITROGEN
3. $\Delta P_V = V\ P_T$ WHERE V = 0.15 FOR A CAVITATING VALVE, 0.10 FOR A NON-CAVITATING AND 0 IF NO VALVE
4. ΔP_S = 10 PSI CONSTANT
5. SAFETY FACTOR = 2.2
6. BLOW DOWN PRESSURE RATIO = 50%
7. COMPONENT WEIGHTS = 4, 5, 6 LBM FOR 300, 600, 1200 LBF SYSTEMS RESPECTIVELY
8. TANK MATERIAL 6 AL 4V TITANIUM - F_{TU} = 150,000 PSI

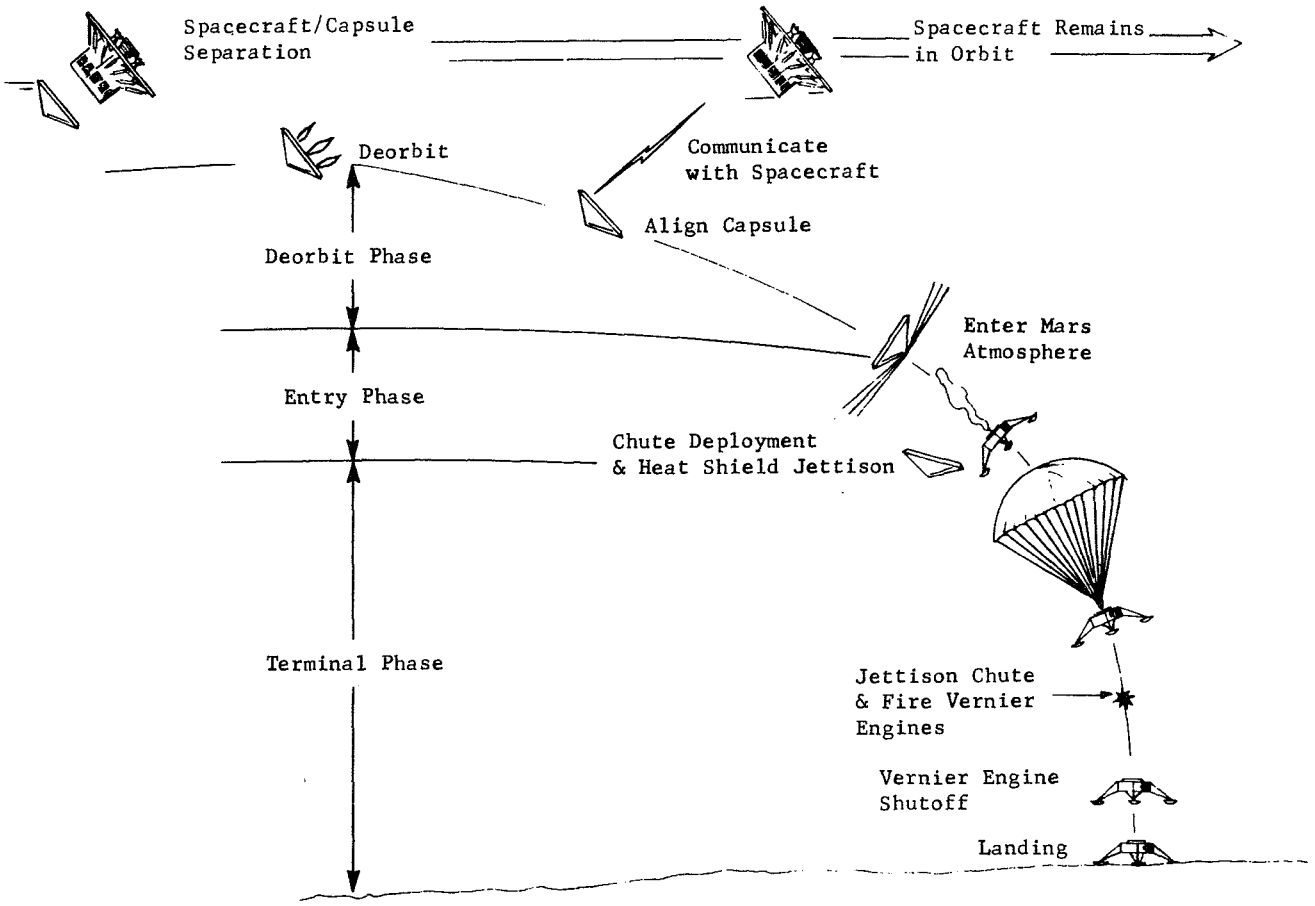

Figure II.A-1. Mission Profile for a Mars Soft Landing

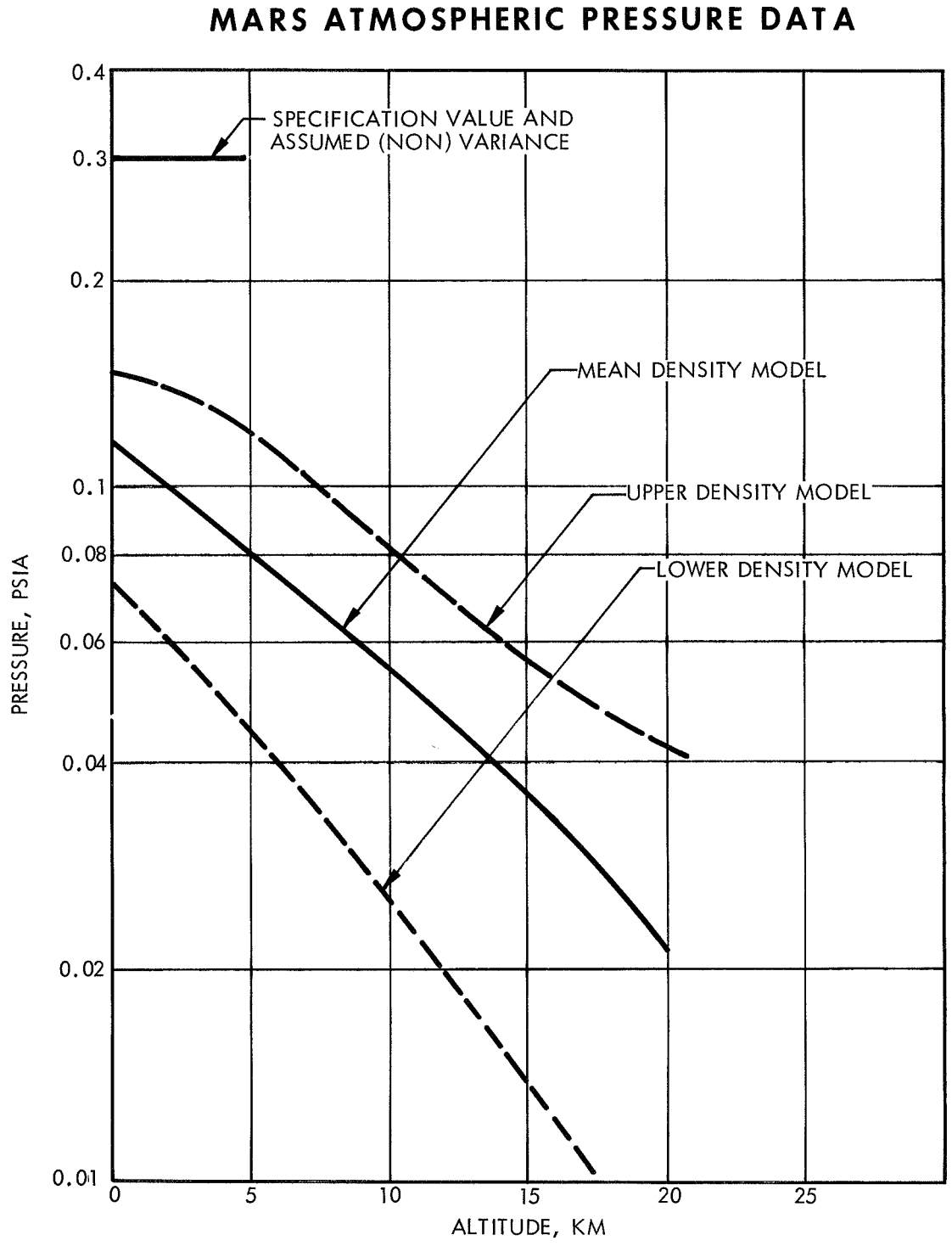

Figure II.A-2. Mars Atmospheric Pressure Data

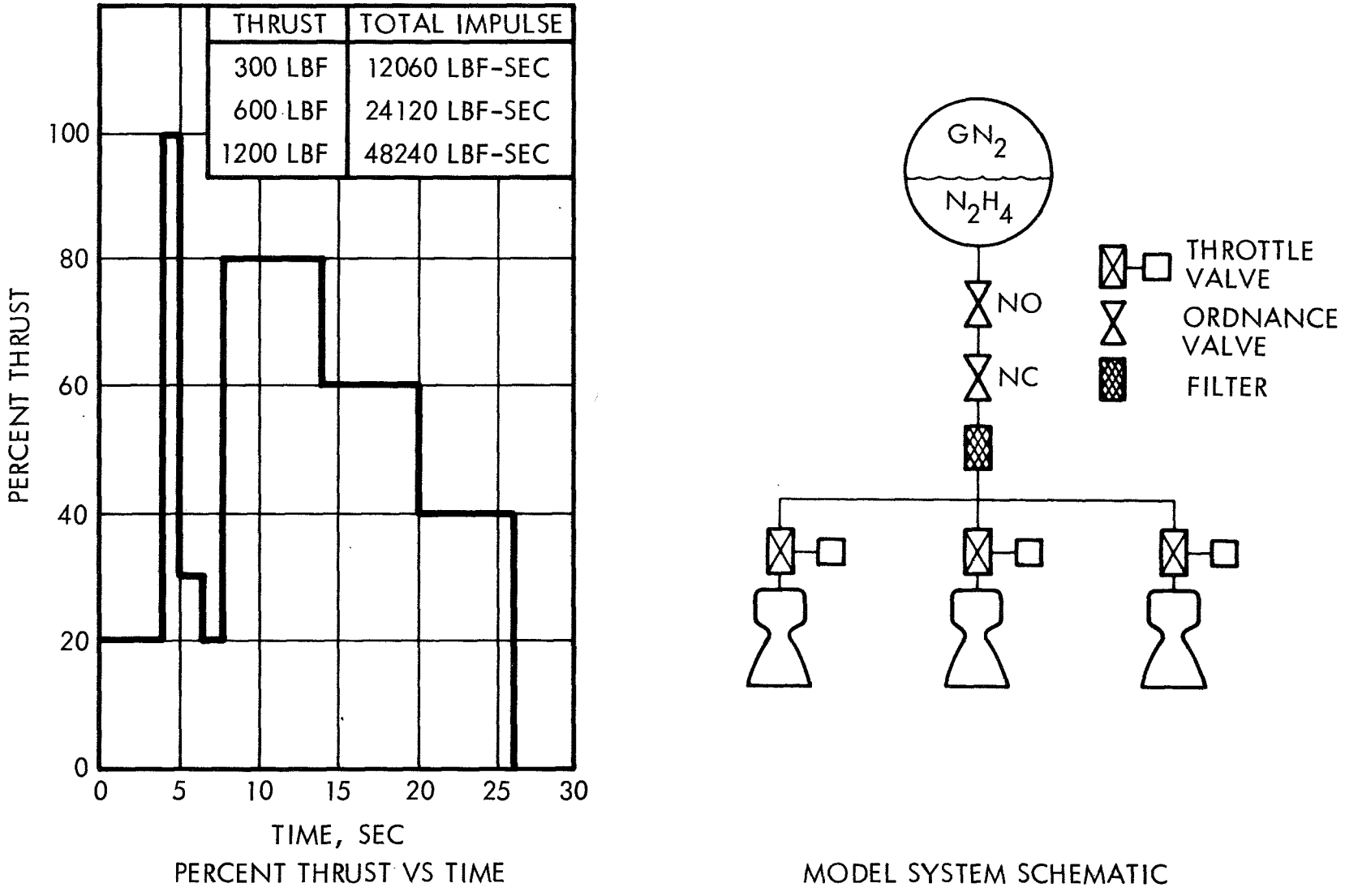

Figure II.A-3. Throttle Profile and Throttleable Thrustor System

II.B. DESIGN CONCEPT SELECTION

II.B.1 System Goals

A simplified rationale for selecting optimized TTS design features is outlined at the beginning of this section, followed by a description and evaluation of component designs. Finally the candidate engine configurations recommended for further study are presented. These recommended configurations are those judged to be most likely to meet the requirements outlined above.

Optimization of rocket engine design is a task which will be very complex and time consuming if the effects of all the pertinent variables are to be considered. Not only are there many alternate designs for each component part, but a multitude of interactions between parts must be considered. Within the present state-of-the-art many of these relationships are not fully understood let alone mathematically modelled. Therefore, in the interest of economy and schedule, the traditional compromise has been made of substituting engineering judgement for much of the time-consuming and tedious analysis (which is ofttimes of questionable validity).

The approach followed here consists of three steps: (1) identification of goals which act as criteria for gauging relative merit, (2) division of the engine design problem into discrete elements which can be individually analyzed in relation to one or more of the goals, and (3) assessment of the trade-offs which must be evaluated in selecting the optimal designs.

Based on the requirements of the contract, the selected goals are high specific impulse, low weight, durability, heat sterilizability, rapid transients and a 10:1 thrust range. For a monopropellant engine, the elements can be simply the different functional parts: the nozzle, throat, plenum, reactor bed, chamber, injector, manifold, shutoff valve,* throttle valve and actuator. Table II.B-1 shows how these primary goals are related

*The shutoff valve is included here because of its logical connection with engine operation. However, no further analysis is made because this component is not considered part of the TTS by contract definition.

to the basic elements of the engine (nozzle, reactor, etc.) by certain requirements which must be satisfied to attain the goals. The available methods for meeting these requirements are both general and specific to certain parts; the table lists available methods and available design approaches (i.e., the manner in which these could be implemented in each element of the engine).

In real systems, often it is not possible to use the exact configuration of each element which optimizes that particular element alone without regard to interfacial design problems and interactions, for these other considerations can be important enough to make the combination of features less than optimum. Geometric constraints and thermal problems are the most common limitations which force compromises in the overall optimization. These and some other interface subjects are mentioned in the discussions below. Operational characteristics are examined within the context of the four fundamental functions of the engine: propellant flow control, injection of the propellant into the reactor, generation of the gases within the reactor, and acceleration of the gases to produce thrust. This arrangement is preferrable to a strict adherence to the elemental breakdown because it permits a more logical narrative of the controlling phenomena and functional interactions.

II.B.2 Potential Design Concepts

This section contains a discussion of the design concepts which were considered for potential inclusion in the Throttleable Thrustor System. A listing of these concepts are presented in Table II.B-2.

II.B.2a Flow Control

Two general methods of throttling are considered: (1) those in which thrust of the engine is varied by changing the chamber pressure upstream of a constant area nozzle throat, and (2) those in which chamber pressure is maintained nearly constant by varying the nozzle throat area with concomitant changes in propellant flow rate. The first method is more conventional and requires only a mechanism for varying the propellant flow. The second method has never become operational because of its mechanical complexity even though it offers maximum performance (I_s) at reduced thrust levels.

Only those methods of varying liquid flow by mechanical adjustment are considered here. (Gas injection, density change, electrical effects,

and related methods are omitted because of the relatively massive auxiliary systems needed to implement them.) Propellant throttling mechanisms can be located at any point in the flow circuit above the injector face. Generally speaking, the closer they are to the injector face, the more directly the engine responds to their action but the more difficult they are to build. Mechanisms built into the injector elements obviously must increase in number as the number of elements increases; this form of complexity may decrease reliability, especially if each mechanism acts independently. Elemental mechanisms that are connected in parallel to a common actuator tend to be more reliable but the required actuator connections probably would influence the manifold design strongly or would require a multiplicity of dynamic seals. Throttle devices in the feedline are the most conventional. Usually these are easiest to build; one reason for this is that upstream throttling isolates the mechanism from the thermal environment which is most severe in the vicinity of the injector face.

Combination mechanisms are highly feasible and have been used with success. Generally these include active upstream flow control devices and feed pressure-operated mechanisms in the injector elements which improve the hydraulic characteristics of the elements (e.g., spring loaded poppets that prevent low injection velocities by narrowing the flow passage at low flow rates).

The precision with which valving elements control the flow rate is related to a number of factors such as the mechanical precision of the parts, the hydraulic characteristics of the valve, and the properties of the fluids over the range of interest. Mechanical precision in this context is mostly relative in the sense that errors or deviations should be a certain percentage of the parameter value. For example, accuracy of valve positioning is most easily attained when the total stroke is kept at intermediate values and there are no "floating" parts (i.e., all connected parts are firmly positioned relative to each other). Parts tolerances and sensing element resolution cannot be economically reduced below certain limits which means that they can add up to a noticeable percentage of very short strokes. For example, five machining tolerances of 0.001 inch plus a positioning resolution of 0.005 inch add up to four percent error for a quarter-inch stroke. At the other extreme, exceptionally long strokes are difficult to mechanize in compact, lightweight units.

Usually, valving mechanisms are designed so that stroking varies the cross-section of the minimum flow area within the valve; this variation may be linear or non-linear with stroke. Discharge coefficients may be constant over a considerable range of Reynolds Numbers but usually there will be at least some change, especially at the lower end of the range. Control schemes that depend on constant discharge coefficient (i.e., linearity between flow area and flow rate) are therefore limited to flows above the Reynolds Number where nonlinearity begins. Within systems that maintain a constant upstream pressure and develop a known downstream pressure relationship to flow rate, the throttling valve can be designed to deliver flow rates as a linear function of valve stroke by taking into account the concurrent effects of area change and discharge coefficients. Cavitating valves are unique in that they deliver a flow rate which is independent of downstream pressure (but they are sensitive to upstream pressure).

Repeatability of discharge rate versus valve position will be very dependent upon fluid density. Not only will this vary with temperature but also as gas desorbs or as vapor bubbles are formed due to the locally reduced static pressure in the valve mechanism. Fluid viscosity is a second order effect which is usually lumped into the C_D term when that coefficient is determined as a function of Reynolds Number.

For a constant feed pressure and chamber pressure directly proportional to flow rate, the valve pressure loss is approximately

$$\Delta P_V = P_T - P_C - \frac{K P_C^2}{\rho_P}$$

where

K = lumped flow coefficient for injector plus line losses

Figure II.B-1 shows this relation in the conventional manner.

The relationship between the flow rate and the valve discharge coefficient is illustrated in Figure II.B-2 for the case when the flow rate is to be linear with area (see curve marked $C_D/C_{D_{rated}}$).

Also illustrated in this figure is the relationship between the area and the flow rate if the discharge coefficient is constant (see curve marked A/A_{rated}). In practice, most pre-calibrated valves are designed so that the required area change is obtained (as a function of input or stroke) either by making the stroke linear with flow and tapering the throttling device as needed or by making the area change linear with stroke but programming the stroke to provide the area change needed as a function of flow rate by means of a cam or other non-linear element. Where either flow rate or chamber pressure is sensed, a closed-loop servo system can be used so that positioning according to calibration data is not required.

As flow rates are throttled, the velocities through fixed area flow passages will decrease proportionately. This is of little concern within manifolds but can lead to trouble in injectors. Generally there is some relation between injector stream velocity, stream flow stability, and reactor performance. Low velocities can result in flow instabilities which, in turn, can cause the reactor to operate roughly or unstably. Even when the streams remain adequately stable, the lowered stream momentums can lessen bed penetration, decrease atomization, or otherwise alter operating conditions in the reactor and may produce less efficiency. Generally the range of throttling is considered to be limited to 4:1 to 8:1 when fixed area injectors are employed.

Usually it is desirable from the standpoint of injector/reactor operation to maintain nearly constant flow velocities. This may be accomplished by varying the flow passage cross-sectional areas or by varying the number of flow passages in concert with the variation in flow rate. Injector flow passages (orifices, spray nozzles, slots, etc.) are the ideal location for flow throttling from a hydraulic viewpoint since this not only maintains the stream velocities but assures that the major flow resistance always separates the zone of energy release from the nearest capacitance in the system (the injector manifolding), which tends to maximize the system hydraulic stability. As mentioned before, this close coupling gives the greatest opportunity for fast hydraulic response. Variable area injectors have been found suitable for throttling over very wide ranges (30 to 1 or more). (Note, however, that engine performance may decrease substantially at very low thrust due to nozzle inefficiencies

unless compensating and/or variable throat area designs are used.) Difficulty in mechanization and the severity of the local thermal environment have tended to discourage exploitation of these potential advantages of variable area injectors.

Valve response depends on the power output of the actuator and the loads which the actuator must overcome. These loads are inertia of the parts, unbalanced pressure-area forces, spring forces and friction. In most cases the inertia will be low unless major segments of the injector face are moved or heavy linkages are required. Unbalanced pressure-area forces generally constitute nearly half of the load except where balanced areas can be arranged, then the seal forces (friction in dynamic seals or spring forces in bellows) become the largest contributors. Spring forces range up to half the average load; springs provide an unidirectional bias so the moving parts are held tight against the actuator to minimize backlash, provide bias to overcome excessive pressure-area unbalance, or provide return-stroke power where single-acting actuators are used. These loads, in at least one direction of stroking, must be substantially less than the stall load characteristic of the actuator if adequate response is to be achieved. Obviously, this requirement can exert a strong influence on the type of valving chosen since in some designs the seal loads or the amount of linkage cannot be easily reduced. A further complication is variation in response with position due to non-constancy of load or non-linearity of travel versus percent change in flow rate.

Regardless of the efficiency of liquid flow throttling, a performance loss will be experienced at low thrusts unless the nozzle is also throttled to keep it operating at a high pressure ratio.* When flow rates decrease, a high pressure ratio can be obtained only by decreasing the throat area. In the ideal case, the throat area is varied nearly linearly with flow rate so that chamber pressure remains nearly constant, and at the same time appropriate variation in flow areas are made to achieve constancy

*An ambient-pressure compensating expansion nozzle must be used where there is an atmosphere if maximum performance over the full range is to be achieved.

in terms of stability, tendency to cavitate or desorb gas, etc. This scheme theoretically enables the rocket to be varied over the widest range of thrust levels (in excess of 50 to 1).

Devices for varying the throat area of the nozzle fall into two geometric categories: plugs for circular throats and rings for annular throats. Plugs are usually controlled by a rod situated along the chamber axis and passing through the center of the injector. Centering of the plug to prevent thrust vectoring by slight lateral shifts requires great stiffness of the control rod unless spacer vanes are provided in the gas flow path; in either case the device is heavy and subject to large pressure-area loads and severe heating. A gas-tight seal at the injector end may not be so difficult since the region can be cooled by the propellant flow (at least until post-firing heat soak-back).

Rings for varying the annular throats probably require much greater actuator forces because of their size and proneness to cocking; balanced pressure-area seals and linkages that move the rings uniformly have not yet been reduced to practice. Heating loads are probably greater on these rings then on the plugs, but the ring actuator mechanism can be shielded from the gas flow whereas the central control rod for the plug is subject to heating. Cooling the ring seals with propellant flow appears to be almost impossible due to their large diameter and location in a region of high heat flux. Plug travel can be made reasonably large so that accuracy of throttling is attainable. Ring travel is limited since the throat gap at full thrust is very narrow. Table II.B-3 summarizes the throttling schemes outlined above.

II.B.2b Injectors

Propellant injectors considered here are limited to those which inject the propellant into the reactor as liquid jets, sheets, or sprays. Mechanical adjustments for performing throttling functions have been discussed in the previous section.

Injectors usually are classified by the type of elements used, the pattern of the element array, and the manifolding scheme. Generally the type of element determines the size and hydraulic character of the jets,

sheets, or sprays, as well as the local mass flux distribution pattern. The pattern of the array controls the gross mass flux distribution, and to some degree influences the local distribution if efflux from adjacent elements overlap. Manifolding affects the start and shutdown transients (rate and evenness of flow transients) as well as the hydraulic character of the jets, sheets, and sprays (cross-velocities and inlet pressures at the upstream end of the elements).

The most basic criterion for choosing an injector is whether or not the design supplies propellant in the manner required for highly efficient, smooth, reliable operation of the reactor. Practical considerations dictate careful examination of such other factors as freedom from detonation during heat soakback, system suitability, potential for becoming clogged, ease of fabrication, etc.

High efficiency operation of the reactor implies high performance and fast controlled transients. To achieve high performance the characteristic of the propellant injection pattern must be matched to the requirements of the reactor. Decisions must be made with regard to the degree of atomization prior to impingement on the bed, degree of penetration of the bed, local and overall distribution of the mass flux, and the hydraulic steadiness of the flow. Injector concepts which permit the designer to precisely control these factors should be emphasized, and those in which they are relatively uncontrollable should be downrated.

Fast, controlled transients require small manifold volumes which can be evenly filled and emptied, and which are otherwise passive in the control function (i.e., allow the active element, the valve, to control the flow rate vs. time profile).

Smooth operation of the reactor is linked to the injection conditions by the same characteristics which affect efficiency; however, injector/reactor combinations that yield high performance will not necessarily run smooth and vice versa.

Enhancing the reliability of reactor operation by the choice of injector concepts involves secondary effects that are not always self-evident. First of all, reliable operation implies repeatible injection characteristics; that is, hydraulic properties of the injector should be calibratible,

as linear as possible and not subject to wide variations as operating conditions shift slightly. The injection characteristics should be those which yield smooth operation so that agitation of the catalyst pellets is minimal in order to reduce powdering by abrasion; furthermore, oscillations of the thermal profile in the bed should be avoided to reduce thermal stress fatigue which might break up the pellets. Reliable starts depend upon controlled injection which doesn't flood the bed so severely that excessive delays occur. And finally, the injector and its manifolding must remain cool enough to avoid overheating the flowing hydrazine as this would produce uncontrolled flashing and detonation above the bed.

After shutdown, the injector and manifolding should not trap propellant which can be heated to the detonation point as heat soaks back from the bed and chamber wall. Generally this means the elements must be free-draining, and the manifolding must be: (1) insulated from the heat source, or (2) cooled by a conduction path to a cold sink, or (3) minimized to the extent that this effect is avoided altogether.

For this application, system suitability will be defined as the pressure loss required and the range of flows over which stable operation is obtained. Minimum pressure loss is especially desirable in this case so that the active throttling element (valve) is as effective as possible in shaping the flow rate vs. time profile. Minimum loss for a given element and manifold design will be fixed by either jet velocity or hydraulic stability requirements. Optimization of a given basic type of element and manifold design to achieve hydraulic efficiency and stability is necessary if the very lowest possible loss is to be realized; cross-velocities in the manifolding, entrance contours, friction losses, and exit geometry are the variables to be manipulated.

Clogging potential of injector elements is a function of flow passage lateral dimensions, tortuosity, and redundancy. Clusters of passages within an element (redundancy) tend to give some advantage against large-dimension particulate contamination but are more susceptible to clogging by small particles and gels or corrosion; the latter is true because the ratio of lateral dimension to coating thickness is less than

for larger passages. Since small particles, gels and corrosion are more likely to be present than large particles, injector elements with larger lateral dimensions and less tortuosity are judged to be the least prone to clogging. (Note: To some degree the clogging potential is also a function of the manifolding since manifold geometry may favor carrying contamination to certain elements of an array, as contrasted with a dissimilar tendency in different manifold layout.)

Ease of fabrication implies not only suitability for rapid, low cost construction, but also inherent ease of maintaining critical dimensions and surfaces so that part-to-part consistency is high. Usually these criteria are met by designs requiring no hard-to-machine or join materials, no close tolerances, and no extra smooth surfaces.

Table II.B-4 summarizes some engineering judgements made relative to these factors for several types of injector elements.

II.B.2c Reactors

The ultimate purpose of the reactor is to convert the injected propellant from liquid to high temperature gases which may be accelerated through the nozzle to produce thrust. Presumeably the ideal reactor would accomplish this purpose in a controlled manner with high efficiency and smoothness while introducing a minimum pressure loss in the system. The reactor design would be small, light in weight, and cheap to build. It would be durable and reliable.

Fundamentally, there are two alternate means used to cause hydrazine to decompose as a monopropellant: (1) catalytically, and (2) thermally. Since fast-starting thermal reactors require large energy inputs to achieve "ignition" they are often not competitive weightwise. Only one type of this class will be considered here, and it is actually a hybrid design in which a small catalytically-operated starter chamber supplies hot gas for heating the main chamber flow to ignition. Therefore, most of the discussion below applies primarily to the common reactor design containing a bed packed with catalyst.

From theoretical considerations it appears that, for a given pressure ratio, performance in any DeLaval nozzle will increase as the ratio T/M

increases and γ (ratio of the specific heats) decreases. In the case of hydrazine monopropellant, maximum performance is achieved when the hydrazine is completely decomposed and the ammonia dissociation (an endothermic process) is minimized. A well-designed reactor will decompose essentially all the hydrazine and allow no more than about 50% of the ammonia to dissociate before the gases reach the nozzle. The resulting gas composition at the entrance to the nozzle will be approximately 28% ammonia, 43% hydrogen, and 29% nitrogen and the temperature will be approximately 1850°F.

The design of catalytic reactors must be based on empirical data at this time, however, progress has been made in analytical modeling so that we know at least which tendencies must be encouraged and which ones discouraged in order to maximize performance. In this generalized description, only those phenomena which bear on the problem of reactor efficiency or control are given attention; other problems such as heat flow to the injector are too intimately bound up with design details to lend themselves to a brief generalization.

Starting with the simpler case of steady-state operation, the physical occurences may be viewed along the propellant path as follows, starting where the propellant impinges in the bed. Most of the liquid enters the catalyst interstitial spaces due to the momentum of the injected streams. The paths taken by the liquid in a bed are largely controlled by the particular surface configuration presented by the pellet orientations; this is usually random. Near the injector end the interstitial spaces between the pellets are nearly filled with liquid which is moving down the bed, primarily under the influence of its own momentum and surface tension forces since the pressure differential is low across this wetted region. Cross-wise and back flow circulation in this cooler region is largely a function of injector pattern, voids in the pattern acting as sinks receiving flow from adjacent areas of high mass flux. Thus, the flow tends to spread the liquid over a larger and larger fraction of the surface area. It is probable that only a few of the spaces within the spreading liquid zone contain vapor or gases except where very localized channelling dominates. Between the liquid zones the interstitial spaces are mostly filled with gases that have been carried upstream by recirculation. This condition must also be obtained in the headspace if such a design is to be successful.

The catalyst pellets within the liquid zone will tend to be wetted due to the surface forces. The heat of reaction will cause the liquid near the catalyst surface to boil and subsequently decompose into hot ammonia, hydrogen and nitrogen gases. Micro-scale counter-currents of bubbles stream from the catalyst pores while the liquid is drawn in. These streams of bubbles issuing from the pores of the catalyst pellets mark the transition to two-phase flow. The fraction of catalyst surface covered with liquid film vs. that which is ejecting froth decreases rapidly with distance down the bed. Close to the head end of the wetted zone, the propellant is relatively cold and a great excess of liquid is present per unit area. Further down the bed the hydrazine average temperature is higher and the catalyst warmer. Here the unreacted hydrazine liquid is closer to vaporization temperature, so a greater amount of it reaches the boiling point per unit surface area.

Gas (and vapor) experiences a greater propensity than liquid to be moved down the bed under the influence of the prevailing pressure differential. This creates a velocity difference between the gas and the liquid which, at this stage, is largely a surface film from which droplets are torn by the aerodynamic drag. This atomization radically increases the rate of heat transfer by convection so that much of the liquid is vaporized before it impacts a surface further down the bed. At this station in the bed the liquid flow is irregular patches of surface film and droplets entrained in the streaming gas. Entrained droplets undergo rapid vaporization on their surfaces and impinge catalyst surface with greater and greater frequency. Impact shatters the droplets into smaller globules which either ricochet back into the gas streams or spread to form an adhering film on the surface of the hot catalyst while furiously boiling and decomposing. Gas flow velocities are higher and higher with distance down the bed (for constant bed loading) due to the fact that a greater and greater proportion of the flow is in the gas phase. The average temperature of the gas is higher than that of the catalyst so the gas convectively heats the catalyst pellets and the entrained liquid droplets. Since the pellets are also hotter than the droplets, much of the heating is by conduction rather than catalytic.

Crosswise and back flow circulation is mostly eddy currents but uneven mass flux distribution, uneven reactivity of the bed, or uneven flow resistance in the bed may cause large scale patterns of non-axial flow to develop. The downstream propagation of mass flux patterns is dependent on a number of variables but generally the tendency is for inequalities to be reduced by crosswise currents.

Usually there is a fairly well defined demarcation between the region where the liquid flow is still apparant and where the liquid is atomized to a few residual droplets entrained in the gas. Temperatures in the bed are much higher on the side where the flow is dominantly gaseous. Stabilization of this "decomposition front" appears to be a key step in obtaining smooth operation of the reactor. Another important requirement is uniformly steady flow conditions so that propellant doesn't stagnate in isolated pockets where it can be heated to the point where explosively activated decomposition occurs; this process (in comparative isolation) of heating, decomposition, outflow and replenishment can be cyclical so that a self-sustaining pressure oscillation is generated.

The gases exit from the bed into a plenum at the entrance to the nozzle. In most cases the temperatures here are lower than those just downstream of the decomposition front because some ammonia dissociates in the space between these points. Beds that are too short, unevenly loaded, or channelled, may allow the wetted zone to extend to the exit. In this case, considerable raw hydrazine can enter the nozzle unless the plenum conditions are suitable for heating and decomposing this excess propellant. When the decomposition front is located well upstream of the exit, a considerable amount of ammonia in the gases may dissociate in the downstream part of the bed, thus lowering the temperature of the gases and decreasing the performance.

The starting transient response of a catalytic reactor depends upon several time-dependent actions. First, the propellant flow commences, the propellant impinges on and then infiltrates the bed. Liquid drops, ligaments, and films leave these first wetted surfaces and flow to adjacent surfaces or across interstitial spaces to the opposing surface. At this early stage the prime impetus for liquid motion is the liquid's own

residual momentum, the momentum it receives by exchange with later arriving liquid, and surface tension forces. Very little pressure differential to drive the liquid exists across the bed until the interstitial spaces are filled with either liquid or gas. The rate of gas evolution is relatively slow because it is largely limited to vaporization from internal heat so the advancing liquid front occupies a large fraction of the interstitial volume. During this initial wetting period the small amount of reaction that does occur is almost solely catalytic because the pellets are cold and the rate of gas evolution is insufficient to raise the bulk temperature of the liquid very much by regenerative heating.

This "flooding" of the catalyst reaches some maximum distance into the bed then starts to recede as the cummulative influence of regenerative heating and increased catalyst temperature begins to dominate at the edge of the flooded region. Recession of the wetted region marks the establishment of a fairly well defined transition zone beyond which very little liquid exists--this zone, where the liquid is very rapidly converted to gas, is sometimes called the "decomposition front".

Meanwhile, temperatures are also rising within the flooded region and these reach a critical level after a certain period of time; this time interval apparently is a function of mass flow rate per unit cross-sectional area. Ofttimes, a sudden pressure surge ("cook-off spike") marks the instant when the decomposition front flashes upstream to a new location much closer to the injector. This event is usually considered to be the end of the start transient since no variables change significantly after it occurs, except for temperatures which may continue to increase somewhat due to thermal lag considerations.

One of the most important relationships during the start transient is the one between the propellant flow rate and chamber pressure. Excessive flow rates may cause too much flooding of the bed which slows the rise in chamber pressure. Too much flooding means that the rate of added capacity for absorbing heat is too great compared to the rate at which heat is being generated. Heat generation is by a rate-limited process (catalysis) during the first part of the transient, so there is no optimum rate of liquid flow increase which will give the fastest

pressure rise. The optimum profile of flow rate versus time leads the pressure versus time relation because the amount of liquid injected up to a given point in time must be equal to the amount converted to gas (which generates the pressure), plus the amount existing as liquid in the bed. The quantity of liquid may be significant especially prior to the cook-off spike because an appreciable portion of the bed is flooded. Figure II.B-3 graphically illustrates the general relation of the flows as a function of time.

When the reactor is raised from a given operating level to a higher level, the pressure lags behind the flow rate increase. This is true because during the transition period the mass of liquid and gas in the reactor must be increased. An increase in the liquid present in the catalyst is due primarily to the recession of the decomposition front away from the injector as the flow rate increases (i.e., a greater length of bed is wetted). Some of the increased liquid mass is also due to the greater liquid concentration in the wetted region. Of course, the increased pressure means that the gas density also increases. Figure II.B-4 shows the general flow trends during an increase in thrust level. Operating trends are reversed when flow to the reactor is throttled back or shut down. Pressure lags behind flow rate because the load in the bed must be reduced as the decomposition front moves closer to the injector.

Steady-state operation of thermal decomposition chambers (containing no catalyst) is rate-controlled by the heat transfer process which vaporizes the propellant. Following vaporization, the hydrazine almost instantly decomposes at the prevailing conditions in the reactor. Initiating the decomposition reaction in a smoothly-controlled manner within a relatively small chamber is the design objective, and the complications of a multiplicity of gas phase reactions that are possible between the species are of little interest provided the ammonia dissociation is minimized. Therefore, the mechanics of heating and vaporizing the propellant are the factors to be optimized by the design.

Entering liquid propellant breaks up into ligaments and droplets due to residual motions, aerodynamic drag and surface tension. Ideally, the liquid is atomized to a fine mist in order to maximize the surface area

to mass ratio. Heat transferred to the liquid causes vapor to be expelled from the surface. To maximize the rate of vaporization there must be strong counter-current flows of heat to the droplets and vapor away from the surface. The vapor flow is probably a diffusion phenomenon at the surface but it appears to be dominated by convection only a very short distance away. Nothing can be done to enhance the diffusion process but the zone of its influence can be limited by inducing very strong convection in the surroundings.

Some heat is transferred to the cold propellant by radiation but the heat transfer depends mainly on convection (conduction is negligible). Convection heat transfer is most uniform where a high degree of mixing by small-scale eddies is achieved, but such a mixing mechanism draws on a very limited source of heat (the locally decomposed propellant) therefore, small-scale convection usually results in a slow, progressive increase in total heat content as the flow passes down the chamber. The conditions described are typical of those where turbulence is generated only by the viscous momentum exchanges with the incoming propellant and the irregularities in the pattern of volumetric expansion due to vaporization and heating (i.e., close to straight, parallel streaming flow). This kind of slow, progressive decomposition requires long stay times (large chambers) to reach completion.

Prompted by a desire to obtain high performance in small reactor chambers, it is usual practice to induce large-scale turbulence so that the hot gases are energetically mixed with the cooler volumes which contain atomized liquid. This may be done either with passive or active means. Here, "passive means" is defined as flow path configuration. "Active means" covers external power sources (injected gas, etc.) or secondary propellant injection; active devices will not be discussed.

Passive turbulence generators may be surfaces placed oblique or normal to the flow to cause sudden expansions or contractions in the flow passage or they may be baffles or flow channels which re-circulate all or a portion of the hot gas flow so it mixes with the upstream flow. Turbulence rings are the most commonly used, although grids, screens, baffles, flow reversing tubes also have been used successfully.

These devices usually become very hot and so also act as sources of radiant heat and surfaces on which impacting droplets may be vaporized by conduction.

Stability of reactor operation depends on: (1) maintaining steady flow into each volume, (2) constancy (with time) of the degree of atomization and the temperature of the propellant, and (3) a design which is dimensionally stable and acoustically non-resonant. The latter requirements are most easily met by de-tuning; none of the reactor dimensions are made close to the fundamental wave lengths of the relevant modes at the prevailing acoustic velocity. If de-tuning is not feasible, then the reactor must be either damped or decoupled. Damping can be accomplished by acoustic filters (such as perforated sleeves) which absorb the energy of the wave or by judicious distribution of the mass fluxes or atomization pattern across the lateral cross-section so that the acoustic velocity profile is discontinuous. Decoupling is accomplished by adjusting the acoustic impedances along the path traversed by the wave front.

Thermal decomposition chambers require an external source of energy to initiate decomposition during start-up. A compact and lightweight scheme for supplying this energy is to use a small starter chamber which exhausts hot gases into the main chamber. While this starter chamber could also be operated in a purely thermal mode, using a glow plug, for example, the fastest starts probably can be obtained using spontaneous catalyst. This hybrid design is very economical in terms of catalyst required and is essentially as reliable as the pure catalyst configuration. Catalyst life can be extended by shutting down the starter chamber once the main chamber is operating at steady-state.

Transients between levels of operation in thermal decomposition chambers behave in a manner similar to those in catalytic reactors. Although the total available heat is less at lower flow rates and the average turbulence level in the chamber is low, the mass flux which must be heated is less. Conversely, as the thrust level is raised, the heat and mass transfer rates increase and the amount of propellant in the chamber increases. Therefore, the response lag is greater than the transport time simply due to the accumulation process.

Although the thermal decomposition reactor is mechanically simpler than a catalytic reactor, the starting problem complicates it both in its design and operation; furthermore, the thermal decomposition chambers are usually physically larger due to restrictions in the rate of heat transfer to the incoming propellant. The design variations which can be made to optimize the operating characteristics discussed above are presented in Table II.B-5.

II.B.2d Nozzles

In this section the types of nozzle shapes from which optimized designs can be chosen, for the case of fixed throat areas, are briefly outlined. Variable throat area arrangements have been covered under throttling in Section II.B-2a. Novel designs, such as mechanically adjustable exit areas are not considered.

Nozzles may be optimized for performance or for minimum length and weight, but not for these opposing considerations simultaneously. Nozzle performance may be gauged by the traditional thrust coefficient (C_F). This is a lumped parameter method in which the losses arising from non-axial momentum components, viscous losses, etc., are subtracted from the idealized isentropic expansion based solely on area ratio and constant gas properties. The latest procedures for calculating nozzle flow are quite complicated and require computers so that changes in gas composition and properties, heat transfer, non-planar flow net surfaces, etc., can be simultaneously accounted for. However, simpler procedures are adequate for the present study since the essentially constant composition of decomposed hydrazine product allows composition effects to be neglected. Parameterized design calculations are available which describe nozzle contours and flow condition with sufficient accuracy to identify the pertinent trade-offs.

For a given pressure ratio and specific heat ratio the nozzle contours of a conventional conical nozzle can be selected for a maximum C_F based on the criteria of matching the nozzle exit pressure to the ambient. This results in a long nozzle with associated weight and size penalties, consequently a slight compromise is made to shorten its length and accept a

more divergent loss. Commonly the configuration chosen has a 15 degree half angle in the conical expansion section, while the radii blending the upstream and downstream contours to the throat are equal to the throat radius or less. This may be taken as the baseline conical nozzle.

Shorter expansion sections which compromise C_F still further by allowing a pressure mismatch with ambient can be used but the trend is to minimize this additional loss in short nozzles by adopting a so-called "bell" contour which allows shortening the nozzle while maintaining the area ratio. This shape expands the flow more rapidly just downstream of the thraot (introducing more flow turning), through an inflection section, then closer to the exit the surface curves towards the centerline (turning the flow in the opposite direction to make it more axial).

Several methods have been derived for calculating optimum or near optimum contours of this type; the most widely used is the method of Rao.* Dr. Rao derived a method of determing the optimum contour (maximum thrust coefficient) for nozzles in which the composition does not change during the expansion process (frozen flow, constant γ). In this method, the optimum contour and, consequently, the area ratio, are determined as a function of the nozzle length. Thus, for each nozzle length with a given given γ, a unique contour and area ratio exist which yield the highest thrust coefficient. This computation can be completed for a series of lengths yielding a set of optimum contours, each of which has a different area ratio. When the area ratio only is specified, as is the case here, the correct nozzle length is simply the length of the nozzle which has the specified area ratio. Such nozzles are generally 70 to 85 percent as long as a 15° conical nozzle of the same area ratio. While it is possible to provide a nozzle contour for the specified expansion ratio which has a higher thrust coefficient than the Rao optimum contour, that nozzle will, of necessity, be longer than the Rao nozzle.

The problem of choosing the correct nozzle length was, in a sense, compounded by Rao himself. Shortly after the publication of the exact

*G.V.R. Rao, "Exhaust Nozzle Contour for Optimum Thrust", Jet Propulsion, Vol. 28, No. 6, June 1958.

solution, he developed a simple method of geometrically approximating the contours of the optimum set of nozzles.* This method has come into wide use. However, since both the nozzle length and area ratio must be known, this method cannot be used to determine optimum nozzle lengths (or, indeed, the length of the optimum nozzle of a given expansion ratio, as we have just shown). Thus, fictitious lengths, such as 80 percent of the length of a 15 degree half-angle cone, have come into wide usage and such nozzles are occasionally referred to as "Rao optimum" nozzles. Of course, the difference in thrust coefficient produced by such errors are quite small with a maximum error of less than 1 percent. However, if the required performance is close to the maximum attainable, the use of optimum contours is essential. Or, to put it another way, small differences in the length of competing nozzles of the same area ratio should not be ignored.

The nozzles mentioned above which have circular throat cross-sections cannot be matched to more than one ambient pressure when flow and entrance pressure are fixed (unless, of course, mechanical adjustment is made). In other words, when these nozzles are operated over a range of parameter values, they will deliver less than optimum performance at all points other than the design point. Performance will be degraded by either over or under expansion.

At least two approaches to providing self-adjusting expansion to ambient pressures have been extensively worked. In these nozzles the ambient pressure controls, to a greater or lesser degree, the amount of expansion. Both feature annular throat cross-sections. The first is commonly called a "plug" or "Aerospike" nozzle, and the second, an "expansion deflection" (E-D) nozzle.

---

*G.V.R. Rao, "Approximation of Optimum Thrust Nozzle Contour," ARS Journal Vol. 30, No. 6, p. 561, June 1960.

Plug nozzles direct the exhausting gases inward so they expand along the outside surface of a tapered centerbody lying along the nozzle axis. This causes pressure loads to be generated on the centerbody which have an axial component. The surrounding gas plume expands until it is approximately in equilibrium with ambient pressure. As with DeLaval nozzles the maximum C_F is attained when the nozzle (centerbody) is fairly long. Compromised nozzles are fitted with shortened (truncated) plugs over which the axial pressure loads amount to less than those on the full-length plug, thus C_F is less. One method that has been tried for improving C_F is to raise the pressure on the surface by bleeding gases from the chamber into the region of low pressure. This shortened plug nozzle is termed the "Aerospike" nozzle. Its overall length is far shorter than any competing nozzle design.

If the plug nozzle is turned inside out so that the flow is directed more outward than inward, then a surface must be provided outside of the flow upon which the expanding gases can exert pressure. This outward flow direction makes the design different from a DeLaval nozzle in that a region of low to ambient pressure exists along the axis below the deflector plug. This low pressure region gives the flow sufficient space in which to adjust itself to ambient; in this respect the E-D nozzle is analogeous to a DeLaval nozzle but with centralized flow separation so that overexpansion cannot cause C_F losses. E-D nozzles tend to be about the same length as the very shortest contoured nozzles.

Nozzle weight is not directly a function of length because of the different shapes and different loading conditions. One shape parameter of the plug nozzle, the nozzle throat O.D., has a radical affect on weight of the chamber since the gases must be inward flowing towards a plug of sufficient area to achieve the desired C_F value. Fortunately, the reactors considered here are close to the correct diameter for an efficient plug or Aerospike nozzle. The weight of engines with E-D nozzles is increased due to the large circumference of the nozzle and the deflection plug and support. Bell nozzles are almost invariably lighter than baseline conical nozzles of the same expansion ratio.

Aside from the factors discussed above, the other considerations such as heat load, radiation pattern, etc., should be weighed in selecting a nozzle. These factors are too intimately related to details of design to permit generalizations here. Table II.B-6 summarizes the trade-offs for each of the basic types of nozzles mentioned above.

II.B.3 Design Concept Comparison and Selection

The design concepts discussed in the preceding section were combined into a number of potential system designs for throttleable thrustor systems. Designs were selected from the foregoing discussion for reactor concepts, nozzle concepts and flow control concepts, the latter of which included both the injector and flow control valve. It was not deemed necessary to include the throttle actuator in this comparison since this component is common to all system designs in function at least.

The criteria used in screening the design concepts for this comparison were drawn from the preceding discussion. Only the more attractive concepts were included and as a result it is felt that all of the potential systems selected for comparison are conceptually sound.

A comparative matrix was constructed for all the systems which survived this screening. This matrix is shown in Figure II.B-6. Each thrustor system concept consists of a reactor/flow control concept and a reactor/nozzle concept. The criteria used to rank the systems are defined in Table II.B-7. The results of this ranking are indicated in each matrix cell against the criteria of development required, concept feasibility and estimated performance. For the latter ranking, the currently proposed Mars lander engine was considered to offer median performance with the alternate systems being assigned above or below this median on the basis of estimates. While a ranking of this sort is admittedly imperfect, it does serve to identify the more interesting combinations. During the selection process of the final system concepts, the alternate approach criterion was applied by insuring that at least one member from each row and column was included.

The systems which were selected are indicated in Figure II.B-8. It is re-iterated that each selected system design consists of a reactor/nozzle combination and a reactor/flow control pairing so that two callouts

are required. The numbers assigned to the various systems have no special significance in terms of an order of preference but were simply assigned for convenience of identification in the remainder of the Phase I study. In this regard a descriptive listing of the systems by number is presented in Table II.B-9. It may be useful to mark this figure for easy reference when later sections of this report are being read.

Table II.B-1. System Goals and Potential Design Approaches

GOALS	REQUIREMENTS	AVAILABLE METHODS	DESIGN APPROACHES
HIGH SPECIFIC IMPULSE	LOW HEAT LOSSES	MINIMIZE CONDUCTION LOSSES	LOW CONDUCTIVITY MATERIALS THERMAL ISOLATORS AND INSULATION
		MINIMIZE RADIATION LOSSES	LOW EMMISSIVITY MATERIALS INSULATION
	OPTIMUM AMMONIA DISSOCIATION OPTIMUM $\overline{M}$ AND T_c	DECOMPOSE ALL N_2H_4	EVEN PROPELLANT DISTRIBUTION ADEQUATE BED DEPTH TURBULENT MIXING UPSTREAM OF NOZZLE
		DISSOCIATE $\leq$ 50% OF NH_3	MINIMIZE REACTOR VOLUME MINIMIZE CATALYTIC SURFACE CONTACT
	OPTIMUM THRUST COEFFICIENT	MINIMIZE CHANGE IN PRESSURE RATIO	VARIABLE AREA THROAT =>CONSTANT CHAMBER PRESSURE
		OPTIMIZE EXPANSION RATIO	VARIABLE AREA THROAT ALTITUDE COMPENSATING NOZZLE
		MINIMIZE LOSSES	OPTIMIZE NOZZLE CONTOUR
HIGH RESPONSE	FAST VALVING	MAXIMIZE FORCE TO LOAD RATIO	MINIMIZE LOAD MAXIMIZE FORCE USING MAXIMUM AVAILABLE POWER
		MINIMIZE TRAVEL	OPTIMIZE FLOW PATH USE LOW FRESSURE RECOVERY VALVING EASE ACCURACY REQUIREMENTS
	MINIMUM VOLUMES TO BE FILLED	MINIMIZE DRIBBLE VOLUME	MINIMIZE INJECTOR MANIFOLDING CLOSE COUPLE VALVE AND INJECTOR
		MINIMIZE CHAMBER VOLUME	OPTIMIZE REACTOR DESIGN
	MAXIMUM RATE OF GAS EVOLUTION	OPTIMIZE REACTOR DESIGN	EVEN PROPELLANT DISTRIBUTION MAXIMIZE CATALYTIC ACTIVITY =>FINE MESH CATALYST

Table II.B-1. System Goals and Potential Design Approaches (Continued)

GOALS	REQUIREMENTS	AVAILABLE METHODS	DESIGN APPROACHES
DURABLE	DURABLE REACTOR (CATALYST BED)	PREVENT POISONING	SEALED CONTAINER (OR NOZZLE CAP) DURING PRE-LAUNCH
		MINIMIZE CATALYST FINES GENERATION	EVEN PROPELLANT DISTRIBUTION LOW PROPELLANT INJECTION VELOCITY PRE-ANNEAL (PRE-SHRINK) CATALYST MATCH THERMAL EXPANSION COEFFICIENTS SPRING LOAD CATALYST BED
	DURABLE STRUCTURE	MINIMIZE HEAT DAMAGE	USE HEAT RESISTANT MATERIALS USE THERMAL ISOLATORS AND INSULATION PRE-ANNEAL CRITICAL STRUCTURES
		MINIMIZE ABRASION AND/OR WEAR	EROSION-RESISTANT MATERIALS AVOID RUBBING OR SLIDING PARTS AVOID HIGH IMPACT LOADS
HEAT STERILIZABLE	MINIMUM DISTORTION	MATERIAL SELECTION	USE MATERIALS WITH GOOD STRENGTH (LOW CREEP RATE) AT 300°F
		AVOID THERMAL STRESSES	DESIGN PARTS SYMMETRIC AVOID DIFFERENTIAL COEFFICIENTS OF EXPANSION STRESS RELIEVE COMPLEX PARTS PRIOR TO FINAL MACHINING
	MINIMUM THERMAL DEGRADATION	MATERIAL SELECTION	USE THERMALLY STABLE MATERIALS
10 TO 1 THRUST VARIATION	VARIABLE FLOW RATE	ADJUST POTENTIAL TO RESISTANCE RATIO	VARIABLE FLOW AREA IN PROPELLANT FEED SYSTEM VARIABLE AREA THROAT

Table II.B-2. Potential Design Concepts

CONTROL SYSTEMS

- POSITION FEEDBACK
- CHAMBER PRESSURE FEEDBACK $\dot{h}$, $\ddot{h}$
- GUIDANCE LOOP SENSING (h, $\dot{h}$, $\ddot{h}$)

ACTUATORS

- ELECTRO-MECHANICAL
- ELECTRO-HYDRAULIC
- ELECTRO-PNEUMATIC
- ELECTRO-FLUIDIC
- FLUIDIC-HYDRAULIC
- FLUIDIC-PNEUMATIC

THROTTLING METHODS

- UPSTREAM VALVING - INCREMENTAL OR CONTINUOUS
- INJECTOR VALVING - INCREMENTAL OR CONTINUOUS
- UPSTREAM PLUS INJECTOR VALVING - INCREMENTAL OR CONTINUOUS
- VARIABLE AREA THROAT PLUS INJECTOR VALVING - CONTINUOUS

THROTTLE VALVES

- LINEAR PLUG - CAVITATING, NON-CAVITATING OR COMBINATION
- BALL
- ROTARY PLUG
- BLADE
- SLIDE
- FLAPPER
- SPOOL

INJECTORS

- SPUD - SWIRL NOZZLES, IMPINGING SHEETS, IMPINGING JETS, MULTI JETS, WOVEN WIRE
- SHEET - CIRCULAR SLOTS, LAMINATIONS
- SHOWERHEAD - PARALLEL JETS, WOVEN WIRE

REACTOR TYPES

- CATALYTIC
- THERMAL WITH CATALYTIC PILOT

REACTOR GEOMETRIES

- CYLINDRICAL
- SPHERICAL
- ANNULAR

NOZZLES

- DELAVAL
- SPIKE OR AEROSPIKE
- EXPANSION DEFLECTION

Table II.B-3. Throttling Methods Design Concept Comparison

METHOD		REASONABLE RANGE	RESPONSE	FORCE OR POWER REQ'D	WEIGHT
UPSTREAM VALVING	INCRE-MENTAL	20 TO 1 OR GREATER	FAIR	MODERATE	FAIRLY LIGHT
	CONTIN-UOUS	10 TO 1 OR MARGINAL	GOOD	MODERATE	LIGHTEST
INJECTOR VALVING	INCRE-MENTAL	DEPENDS ONLY ON NO. OF ELEMENTS	EXCELLENT	FAIRLY HIGH	MODERATE
	CONTIN-UOUS	20 TO 1 OR GREATER	EXCELLENT	FAIRLY HIGH	MODERATE
UPSTREAM VALVING + VARIABLE INJECTOR [f(p)]	INCRE-MENTAL	20 TO 1	EXCELLENT	MODERATE	MODERATE
	CONTIN-UOUS	20 TO 1	EXCELLENT	MODERATE	MODERATE
VARIABLE AREA THROAT + THROTTLE VALVING		50 TO 1 OR GREATER WITH INJECTOR VALVING	FAIR	HIGH	HEAVY

CLASS	TYPE	CROSS-SECTION	PENETRATION ABILITY	ATOMIZATION WITHOUT AERODYNAMIC DRAG	MANIFOLDING TYPES	EVENNESS OF LOCAL	DISTRIBUTION GROSS	HYDRAULIC STEADINESS	POTENTIAL FOR THERMAL INTERFACE PROBLEMS	ΔP REQUIRI
SHOWER HEAD	PARALLEL JETS		EXCELLENT	POOR	ALL	POOR	EXCELLENT	POOR TO GOOD	MODERATE TO HIGH	MODER/
SHOWERHEAD	WOVEN WIRE		POOR TO FAIR	FAIR TO GOOD	PLENUM	EXCELLENT	EXCELLENT	POOR TO FAIR	HIGH	HIGH
SHEET	JET SPREADING	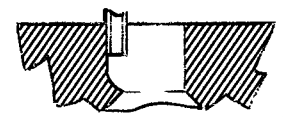	GOOD	POOR	ALL	POOR	FAIR TO GOOD	FAIR TO GOOD	LOW TO MODERATE	MODERA
SHEET	CIRCULAR SLOT		GOOD	POOR	ANNULAR OR PLENUM	POOR	POOR TO GOOD	FAIR TO GOOD	HIGH	MODERA
SHEET	SLOTS AND LAMINATED		GOOD	POOR TO FAIR	PLENUM	POOR	GOOD TO EXCELLENT	FAIR TO GOOD	HIGH	HIGH
SPUD	SWIRL NOZZLE	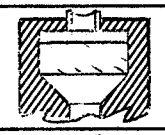	FAIR	GOOD	ALL	GOOD	POOR	POOR TO FAIR	LOW	LOW
SPUD	MULTI-JET		GOOD	POOR	ALL	POOR	POOR TO GOOD	POOR TO GOOD	MODERATE TO HIGH	MODER/
SPUD	IMPINGING JETS	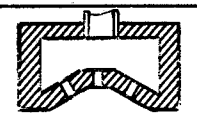	POOR TO FAIR	POOR TO GOOD	ALL	FAIR TO GOOD	POOR	POOR TO GOOD	MODERATE TO HIGH	MODER.
SPUD	IMPINGING SHEETS	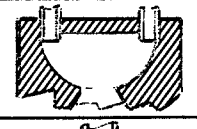	POOR	EXCELLENT	ALL	GOOD	POOR	FAIR TO GOOD	LOW TO MODERATE	MODER
SPUD	WOVEN WIRE	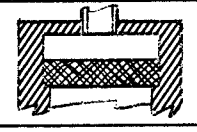	FAIR TO GOOD	FAIR TO EXCELLENT	ALL	EXCELLENT	POOR	POOR TO FAIR	HIGH	HIGH

Table II.B-4. Injector Design Concept Comparison

E	CROSS-SECTION	PENETRATION ABILITY	ATOMIZATION WITHOUT AERODYNAMIC DRAG	MANIFOLDING TYPES	EVENNESS OF LOCAL	DISTRIBUTION GROSS	HYDRAULIC STEADINESS	POTENTIAL FOR THERMAL INTERFACE PROBLEMS	ΔP REQUIREMENT	RANGE OF STABLE FLOW	POTENTIAL TO BECOME CLOGGED	EASE OF FABRICATION
LEL		EXCELLENT	POOR	ALL	POOR	EXCELLENT	POOR TO GOOD	MODERATE TO HIGH	MODERATE	MODERATE	MODERATE	FAIR
WIRE		POOR TO FAIR	FAIR TO GOOD	PLENUM	EXCELLENT	EXCELLENT	POOR TO FAIR	HIGH	HIGH	NARROW (?)	HIGH	GOOD
ING	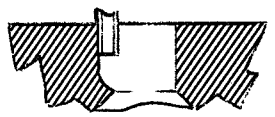	GOOD	POOR	ALL	POOR	FAIR TO GOOD	FAIR TO GOOD	LOW TO MODERATE	MODERATE		FAIRLY LOW	FAIR
LAR T		GOOD	POOR	ANNULAR OR PLENUM	POOR	POOR TO GOOD	FAIR TO GOOD	HIGH	MODERATE	MODERATE	MODERATE	POOR
AND ATED		GOOD	POOR TO FAIR	PLENUM	POOR	GOOD TO EXCELLENT	FAIR TO GOOD	HIGH	HIGH	MODERATE	FAIRLY HIGH	POOR
RL ZLE	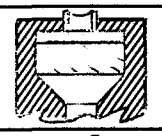	FAIR	GOOD	ALL	GOOD	POOR	POOR TO FAIR	LOW	LOW	WIDE	LOW	(COMMERCIAL)
-JET	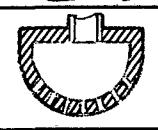	GOOD	POOR	ALL	POOR	POOR TO GOOD	POOR TO GOOD	MODERATE TO HIGH	MODERATE	MODERATE	MODERATE	FAIR
GING S	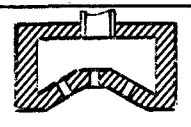	POOR TO FAIR	POOR TO GOOD	ALL	FAIR TO GOOD	POOR	POOR TO GOOD	MODERATE TO HIGH	MODERATE	NARROW	FAIRLY LOW	FAIR
GING TS	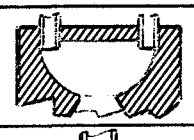	POOR	EXCELLENT	ALL	GOOD	POOR	FAIR TO GOOD	LOW TO MODERATE	MODERATE	MODERATE	FAIRLY LOW	FAIR
WIRE	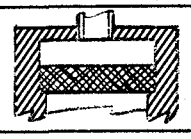	FAIR TO GOOD	FAIR TO EXCELLENT	ALL	EXCELLENT	POOR	POOR TO FAIR	HIGH	HIGH	NARROW (?)	HIGH	GOOD

Table II.B-5. Reactor Design Concept Comparison

MAJOR ADVANTAGE/ DISADVANTAGE			DESIGN VARIATIONS	COMMENTS
REACTOR TYPES	CATALYTIC	AMMONIA DISSOCIATION INCREASES WHEN THROTTLED	MESH CATALYST	HIGH ΔP/L SHORT BED
			PELLETS (1/8 X 1/8 CYLS)	LOW ΔP/L LONGER BED
			LAYERED BED	ADJUST ΔP/L - REQUIRES ADDITIONAL STRUCTURE
			ADVANCED (HONEYCOMB, PREFORMED, ?)	MAY IMPROVE LIFE BUT REQUIRES ADDITIONAL DEVELOPMENT
	THERMAL DECOMPOSITION	NEAR CONSTANT AMMONIA DISSOCIATION WHEN THROTTLED. REQUIRES HIGHER L*.	EMPTY CHAMBER	REQUIRES HIGHEST L*
			TURBULENCE DEVICES	ADD WEIGHT
			ATOMIZERS (SCREENS)	ADD WEIGHT
			HEAT TRANSFER DEVICES	ADD WEIGHT
			GAS RECIRCULATION DEVICES	ADD WEIGHT AND COMPLEXITY; MAY INCREASE AMMONIA DISSOCIATION
REACTOR SHAPES	CYLINDRICAL	CONVENTIONAL-STATE OF THE ART	AXIAL FLOW	CONVENTIONAL DESIGN
			FLOW RADIALLY IN	INCREASED MANIFOLDING AND HEAT SOAKBACK PROBLEMS
			FLOW RADIALLY OUT	INCREASED MANIFOLDING, HEAT SOAK BACK PROBLEMS, AND PLENUM VOLUME
	SPHERICAL	OPTIMUM PRESSURE VESSEL	AXIAL FLOW	INEFFICIENT VOLUME UTILIZATION
			FLOW RADIALLY IN	INCREASED MANIFOLDING AND HEAT SOAKBACK PROBLEMS
			FLOW RADIALLY OUT	COMPLEX CATALYST RETAINER
	ANNULAR OR TOROIDAL	INCREASED WEIGHT DUE TO INCREASED HOOP STRESSES AND 2 WALL CONSTRUCTION. MOST APPLICABLE TO HIGH ϵ ADVANCED NOZZLES	AXIAL FLOW	REQUIRES LEAST DEVELOPMENT
			FLOW RADIALLY IN	COMPLEX MANIFOLDING
			FLOW RADIALLY OUT	
	CONICAL		CONVERGING TO NOZZLE	INCREASING ΔP/L
			DIVERGING TO NOZZLE	NEARLY CONSTANT ΔP/L
			DIVERGING-CONVERGING (OR VICE-VERSA)	

Table II.B-6. Thruster System Comparison Chart

DEVELOPMENT REQUIRED: SA = STATE OF ART MD = MODERATE DEVELOPMENT ED = EXTENSIVE DEVELOPMENT
CONCEPT FEASIBILITY: QF = QUESTIONABLE FEASIBILITY RF = RELATIVELY FEASIBLE HF = HIGHLY FEASIBLE
ESTIMATED PERFORMANCE RANKING: 1-10 10 = HIGH PERFORMANCE 1 = LOW PERFORMANCE

REACTOR CONCEPT	FLOW CONTROL CONCEPT						NOZZLE CONCEPT		
	CAVITATING VENTURI		NON-CAVITATING VENTURI		FLOW CONTROL INJECTOR	FLOW CONTROL INJECTOR VARIABLE AREA NOZZLE	DE LAVAI	SPIKE	EXPANSION DEFLECTION
	FIXED AREA INJECTOR	VARIABLE LOSS INJECTOR	FIXED AREA INJECTOR	VARIABLE LOSS INJECTOR					
CATALYTIC									
CYLINDRICAL	SA	MD	SA	MD	MD	ED	SA 1	MD	ED
	HF	RF	RF	RF	RF	RF	HF	HF	RF
	5	5	5	5	7	8	5	6	8
ANNULAR	ED	ED	ED	ED	ED	ED	MD	MD	ED
	RF	QF	RF	QF	QF	QF	QF	HF	QF
	4	3	4	3	6	7	3	7	6
SPHERICAL	MD	MD	MD	MD	ED	ED	SA	MD	ED
	RF	QF	RF	RF	RF	QF	HF	QF	RF
	7	7	7	7	8	9	5	6	9
THERMAL DECOMPOSITION									
CYLINDRICAL	MD	MD	MD	MD	MD	ED	SA	SA	ED
	QF	HF	QF	RF	RF	RF	HF	HF	HF
	6	6	6	6	8	9	5	6	8
ANNULAR	MD	MD	MD	MD	ED	ED	SA	MD	ED
	QF	HF	QF	RF	RF	QF	QF	HF	QF
	5	5	5	5	7	8	3	7	6

Table II.B-7. Design Concept Selection Criteria

CONCEPT FEASIBILITY

WHAT IS THE INTRINSIC FEASIBILITY OF THE DESIGN CONCEPT? THIS JUDGEMENT TO BE INDEPENDENT OF THE CONCEPTS CURRENT DEVELOPMENT STATUS.

MISSION PERFORMANCE

WHAT IS ESTIMATED RANKING OF CONCEPTUAL SYSTEMS IN TERMS OF TOTAL PROPULSION SYSTEM WEIGHT FOR A TYPICAL MARS LANDER MISSION? HOW IS THE RANKING AFFECTED BY THRUST LEVEL?

DEVELOPMENT REQUIRED

HOW MUCH DEVELOPMENT IS NEEDED TO MAKE THE CONCEPT AN OPERATIONAL REALITY?

ALTERNATE APPROACH REPRESENTATION

AT LEAST ONE MEMBER FROM EACH ROW AND COLUMN OF THE TRADEOFF MATRIX WAS INCLUDED.

Table II.B-8. Selected Design Concepts

NUMBER	DESCRIPTION
1	CYLINDRICAL CATALYTIC BED, FIXED AREA INJECTOR, CAVITATING VENTURI FLOW CONTROL, DELAVAL NOZZLE
2	CYLINDRICAL CATALYTIC BED, FIXED AREA INJECTOR, NON-CAVITATING VENTURI FLOW CONTROL, DELAVAL NOZZLE
3	CYLINDRICAL CATALYTIC BED, FLOW CONTROL INJECTOR, VARIABLE AREA EXPANSION-DEFLECTION NOZZLE
4	ANNULAR CATALYTIC BED, FIXED AREA INJECTOR, CAVITATING VENTURI FLOW CONTROL, SPIKE NOZZLE
5	SPHERICAL CATALYTIC BED, FLOW CONTROL INJECTOR, EXPANSION DEFLECTION NOZZLE
6	CYLINDRICAL THERMAL DECOMPOSITION BED, VARIABLE LOSS INJECTOR, CAVITATING VENTURI FLOW CONTROL, DELAVAL NOZZLE
7	ANNULAR THERMAL DECOMPOSITION BED, VARIABLE LOSS INJECTOR, NON-CAVITATING VENTURI FLOW CONTROL, SPIKE NOZZLE
8	SPHERICAL CATALYTIC DECOMPOSITION BED, FIXED AREA INJECTOR, NON-CAVITATING VENTURI FLOW CONTROL, DELAVAL NOZZLE
9	CYLINDRICAL THERMAL DECOMPOSITION BED, FLOW CONTROL INJECTOR, VARIABLE AREA EXPANSION-DEFLECTION NOZZLE

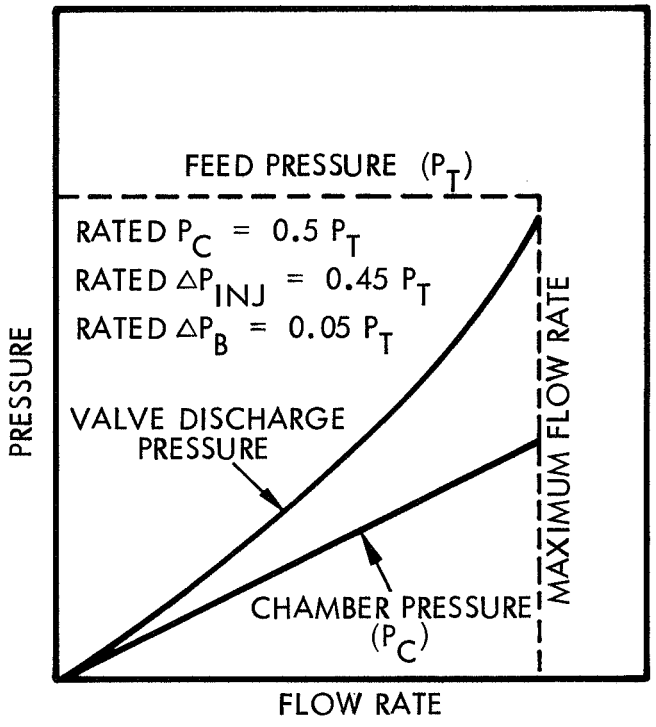

Figure II.B-1. Throttling Pressure Profile

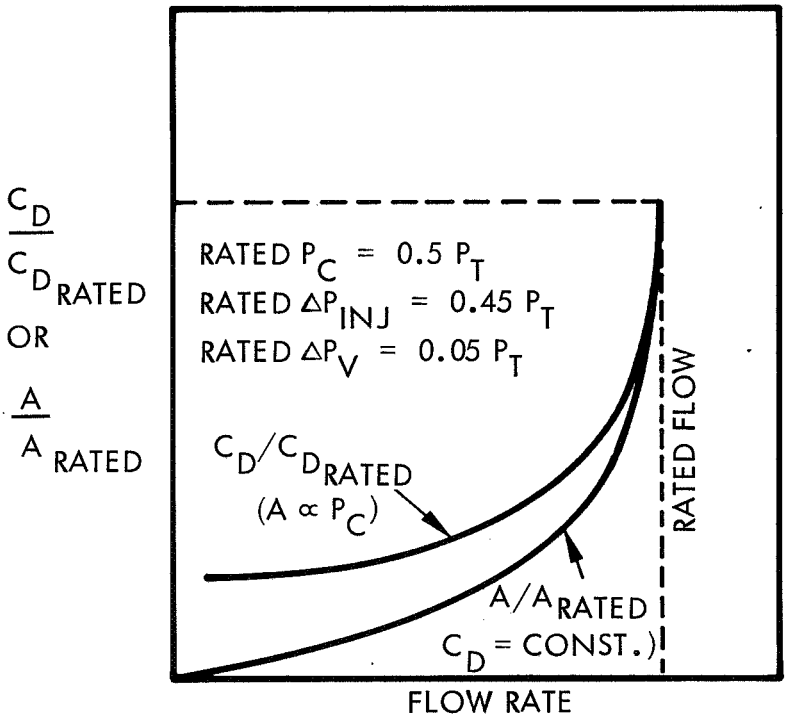

Figure II.B-2. Discharge Area or Discharge Coefficient Versus Flow Rate

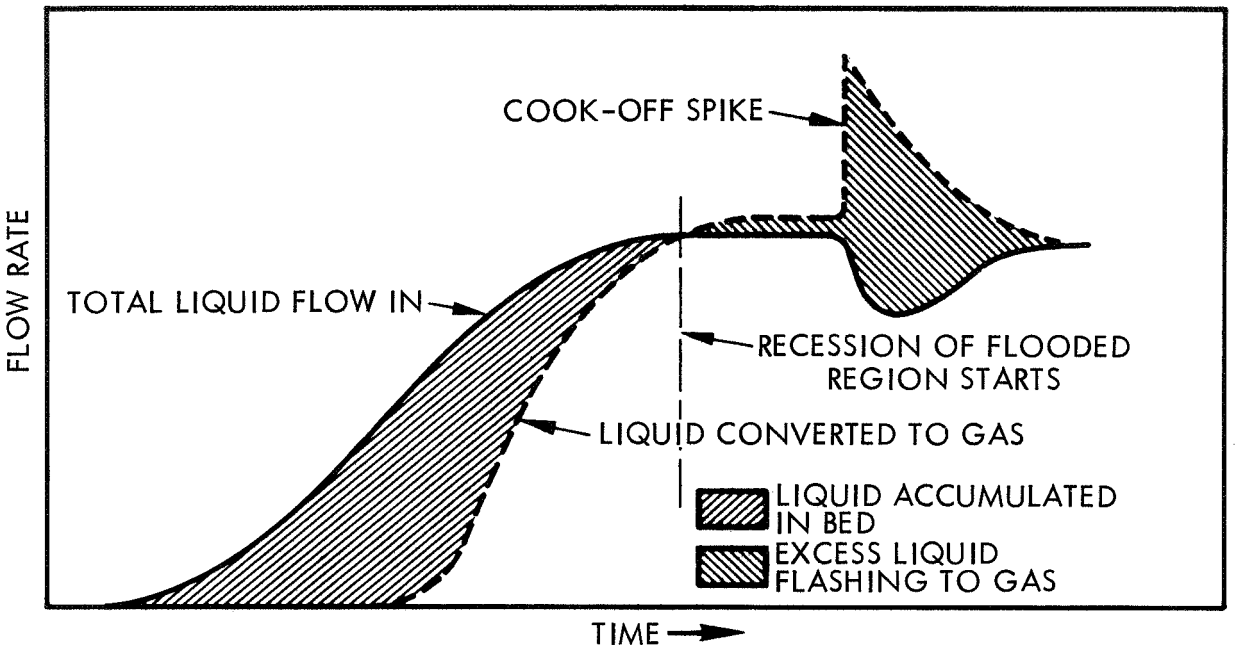

Figure II.B-3. Relationship Between Liquid and Gas Flow Rates During a Start Transient

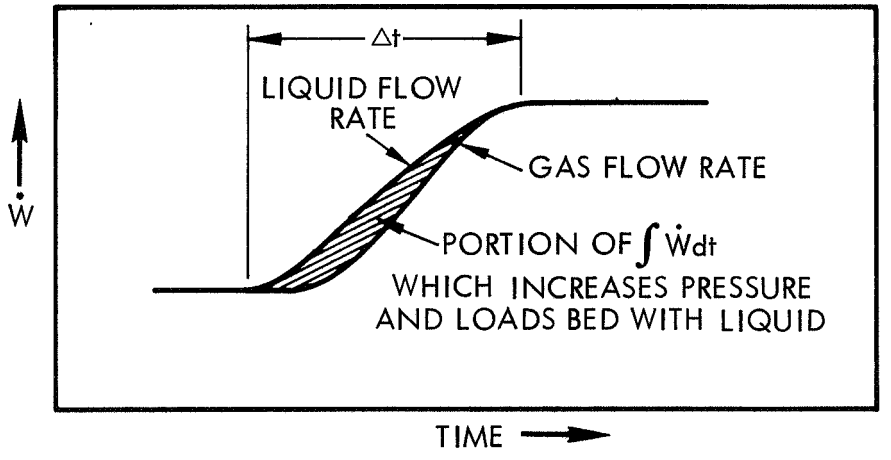

Figure II.B-4. Relationship Between Liquid and Gas Flow Rates During an Increase in Operating Level

Figure II.B-5. Nozzle Design Concept Comparison

F = 1000 LBF, P_c = 200 PSI

TYPE	THROAT GAP AT FULL THRUST, IN	THROAT GAP AT 1/10 THRUST, IN	RELATIVE LENGTH, NORMALIZED TO CONICAL	TOTAL RADIATION AREA, NORMALIZED TO CONICAL	CONFIGURATION
CONICAL	1.575	0.080	1.00	1.00	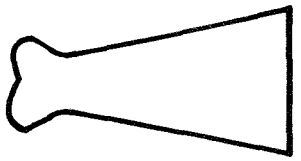
BELL (80%)	1.575	0.080	0.80	0.93	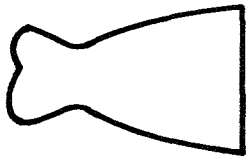
AEROSPIKE (20 TO 1)	0.093	0.009	0.63	0.43	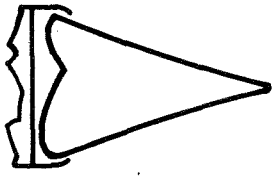
EXPANSION DEFLECTION (20 TO 1)	0.176	0.018	0.63	0.89	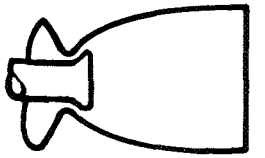

II.C. PRELIMINARY SYSTEM DESIGN

As a first step in analyzing the performance of the selected design concepts, a preliminary design study was completed for each system. The parameters selected for these studies were:

Thrust = 600 lbf
Chamber Pressure = 250 psia
Expansion Ratio = 20:1

The thrust was in the mid-range of the levels that were to be considered during Phase I and the other parameters were near optimal values based on the results of earlier, albeit less detailed, studies.

The resultant preliminary designs are discussed in paragraph 1 below. These layouts were used to determine 600 lbf baseline weights, paragraph 2, which could then be scaled to other operating conditions as shown in Section II.D.

II.C.1 System Layouts

The completed layouts are presented in Figures II.C-1 through II.C-7.

II.C.1a Systems 1 and 2 - Figure II.C-1

These concepts are identical except for the flow control valve design (non-cavitating for No. 1, cavitating for No. 2). Since this detail does not affect the engine layout as shown, only one drawing is required. On a system basis the performance will be different because the greater pressure drop of the cavitating valve leads to a higher tank pressure requirement (see Section II.D.5).

Several features shown in Figure II.C-1 are common to all of the designs. A thermal-isolating valve mounting structure is shown in all cases so that the designs are truly "thrustor systems". The injector concepts shown are versions of the "head-space" design which has been used on a wide variety of thrust levels by TRW with good success. A layered catalyst bed is also employed with fine mesh near the head-end (relatively standard practice). However, there are other injection concepts which have been demonstrated satisfactorily (see Section II.B-2b). While alternate

concepts could have been shown on some engines, the standardization on one type is felt to yield a better comparison. Subsonic struts are used to support the coarse-mesh catalyst retainer. Again this is a proven technique to which satisfactory alternative designs have been demonstrated.

In other respects, the design of system 1 and 2 is conventional. Indeed, these systems are probably most representative of a "baseline" from current practice. The performance figures quoted are derived in Section II.D-1.

II.C.1b System 3 - Figure II.C-2

In selecting the expansion-deflection nozzle for this system, it was noted that achievement of a variable area plug nozzle would be much more difficult since the larger annular throat gave a smaller throat gap with attendant difficulties in positioning the moveable element accurately. The flow control injector was incorporated as a natural companion to achieve full efficiency over the thrust range.

In this design the nozzle plug is positioned in the desired position by an electrohydraulic actuator. This type of device will probably be required since the loads are high. The injector is positioned by the chamber pressure acting on a spring-biased bellows. Chamber pressure is maintained reasonably constant over the throttling range by using a low-rate bias spring. (This concept requires some change in chamber pressure so that the error signal can position the injector at the proper flow rate.) The approach is attractive since only one actuator is required. System accuracy relies on accurate monitoring of thrustor acceleration as feedback to the nozzle plug actuator to compensate for thermal expansion effects on the plug actuation shaft.

II.C.1c System 4 - Figure II.C-3

The primary design intent here is to provide a compact, high expansion ratio engine. The design features a radial catalyst bed configuration with six single element injectors radiating from a common propellant manifold at the center. The six injectors insure uniform propellant distribution throughout the catalyst bed.

The combustion chamber is reinforced with ribs which are required to provide the necessary pressure chamber integrity and to maximize nozzle throat dimensional stability. The latter, is the most vulnerable feature of this design, considering the fabrication complexities and thermal expansion problems in operation.

A higher expansion ratio was selected for this engine on the basis that the pressure compensating feature would make such a choice more attractive and also on the basis that the 30:1 annular throat integrated much better with the dimensions of the annular bed. It may be seen that this engine is somewhat more compact, considering that the long dimension of the valve is included in the axial engine length.

II.C.1d System 5 - Figure II.C-4

The several unique features of this design include the spherical chamber, expansion-deflection nozzle and flow control injector. The spherical chamber is optimum pressure vessel shape for minimum (lightweight) wall thickness. The flow control injector is of the spray jet type with a notched pintle head for greater spray dispersion. The pintle is positioned by a torque motor/ball screw servo-actuator. The loads anticipated are within the force capability of this type of actuator. The expansion-deflection nozzle is heavier than a conventional DeLaval nozzle due to its greater dimensions. However, it is more efficient over a wider range of operating conditions. This design is notable for its light weight and low tank pressure requirement.

II.C.1e System 6 - Figure II.C-5

This is a straightforward thermal decomposition engine design with a cylindrical chamber sized for the relatively large L* necessary for complete propellant reaction. The pilot chamber is a single element injector, headspace type, catalytic-decomposition gas generator. Six spring loaded spray jets radially spaced about the pilot chamber distribute main propellant flow into the combustion chamber maintaining good atomization over the throttle range. A multiple layered, large mesh, screen pack is installed in the chamber, acting as a thermal reactor (heat sink). The notable features of this design are the minimum catalyst requirements

and the overall design simplicity. In this design it would be necessary to incorporate a shutoff feature in the flow control valve to allow system initiation on the pilot chamber only.

II.C.1f System 7 - Figure II.C-6

The key feature and design intent of this toroidal combustion chamber, spike nozzle, thermal decomposition engine is compactness. The weight penalty paid by this design is primarily due to the heavy structure necessary to reinforce the throat area. However, the chamber region is not penalized since low bending loads are transmitted. This allows a relatively low skin thickness for the toroid. Even so, this system was the heaviest concept studied. As in system No. 6, the pilot chamber is a small catalytic decomposition gas generator. Radial ports from the pilot chamber into the toroidal combustion chamber cause the hot gas to impinge on a multi-layered, screen pack, thermal reactor. Main propellant flow into the combustion chamber is through six spring loaded spray jets. Manifolding for the spray jets is incorporated in the valve/engine mount structure. The flow control shutoff feature would be necessary in this system also.

II.C.1g System 8 - Figure II.C-7

Three key parameters were the design objectives of this catalytic decomposition engine; optimum combustion chamber configuration (as a pressure vessel), even distribution of propellant over the surface area of the catalyst bed and maximum utilization of the catalyst. The spherical combustion chamber meets the requirements of the first parameter, yielding, maximum volume, thinnest walls, minimum weight and smallest size. Even distribution of propellant is accomplished by means of the "pin cushion" spherical injector and spherical configuration of the catalyst bed.

The spherical catalyst bed configuration provides a uniform bed depth, eliminating pockets and excess catalyst. The overal uniformity of the catalyst bed reduces the possibility of liquid propellant collecting at any specific point and the problem of channeling and avoids areas of high mass through-puts (i.e., high G). The most attractive feature of this design, however, is the low weight, achieved primarily through the efficient structure.

II.C.1h System 9

A layout of this concept was attempted but could not be completed with any chance of a competitive weight for the following reasons. Both the pilot chamber and the variable-area throat actuation rod are ideally located on the engine centerline. It appears that a distributed pilot chamber would be easier to mechanize than an external actuation linkage; however, the weight and complexity penalty would be large. Furthermore, it appears that separate actuators would be required for the plug and injector. The intrinsically variable pilot flow is too complex a factor to be able to utilize the "slave" injector positioning system used in Engine System 3. When preliminary estimates indicated that the engine overall length would approach 24 inches and that its weight would almost surely exceed 25 lbm, it was recommended and agreed that this system would be dropped from further consideration.

II.C.2 Baseline Weight Analysis

A weight breakdown for each of the systems under consideration has been presented together with each respective layout. These data are tabulated in more detailed form in Table II.C-1 where a breakdown by component parts is presented and compared. The criteria used to separate fixed and parametric weights and to scale the parametric weights to other operating conditions are discussed in Section II.D-2.

Table II.C-1. Preliminary Design Study Summary

THRUST = 600 LB_f CHAMBER PRESSURE = 250 PSIA EXPANSION RATIO = 20

COMPONENT \ SYSTEM	1	2	3	4	5	6	7	8
1. CHAMBER	4.52	4.52	4.52	9.22	2.20	4.78	9.77	2.24
2. NOZZLE	2.18	2.18	3.05	1.07	3.05	2.18	1.07	2.18
3. PLUG			0.72		0.55			
4. PLUG SUPPORT			0.13		0.84			
5. CATALYST	1.63	1.63	2.64	2.30	1.89	0.30	0.30	1.66
6. RETAINER HEADSCREENS	0.60	0.60	0.60	0.20	0.18			0.44
7. HEAT SINK						2.19	2.19	
8. CATALYST BED SUPPORT	1.36	1.36	1.74					
9. VALVE	2.80	2.80		2.80		2.80	2.80	2.80
10. INJECTOR	0.05	0.05	2.50	2.10	2.16		2.10	0.12
11. PILOT CHAMBER						1.12	1.12	
12. THERMAL BARRIER	0.32	0.32						0.87
13. MOUNT PLATE	1.15	1.15	0.91	0.80	0.91	1.47	2.23	
TOTAL WEIGHT	14.61	14.61	18.38	18.49	11.78	14.84	21.58	10.31

DESIGN PARAMETERS

MAXIMUM THRUST	600 LBF
CHAMBER PRESSURE	250 PSIA
EXPANSION RATIO	20:1
THROTTLE RATIO	10:1
LIFE	500 SECONDS
CHAMBER MATERIAL	L-605

PREDICTED PERFORMANCE

SPECIFIC IMPULSE

231 LBF-SEC/LBM

THRUST COEFFICIENT 1.70

CHARACTERISTIC VELOCITY 4360 FT/SEC

C_F EFFICIENCY = 99%

WEIGHT

CHAMBER AND NOZZLE	6.70
CATALYST AND SUPPORT	3.59
HEADEND STRUCTURE	1.52
THROTTLE VALVE	2.80
	14.61

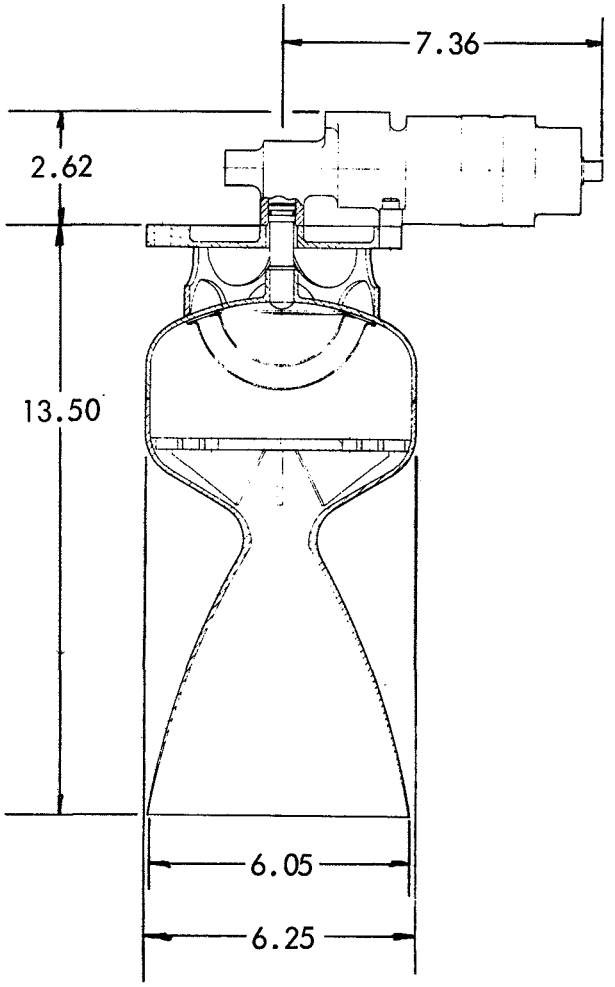

Figure II.C-1. System No. 1 and 2

DESIGN PARAMETERS

MAXIMUM THRUST 600 LBF

CHAMBER PRESSURE 250 PSIA

EXPANSION RATIO 20:1

THROTTLE RATIO 10:1

LIFE 500 SEC

CHAMBER MATERIAL L - 605

PREDICTED PERFORMANCE

SPECIFIC IMPULSE 225 LBF - SEC/LBM

THRUST COEFFICIENT 1.66

CHARACTERISTIC VELOCITY 4360 FT/SEC

C_F EFFICIENCY = 95%

WEIGHT

CHAMBER AND NOZZLE	7.57
CATALYST AND SUPPORT	4.98
HEADEND STRUCTURE	0.91
INJECTOR MECHANISM	4.07
PLUG AND SUPPORT	0.85
	18.38

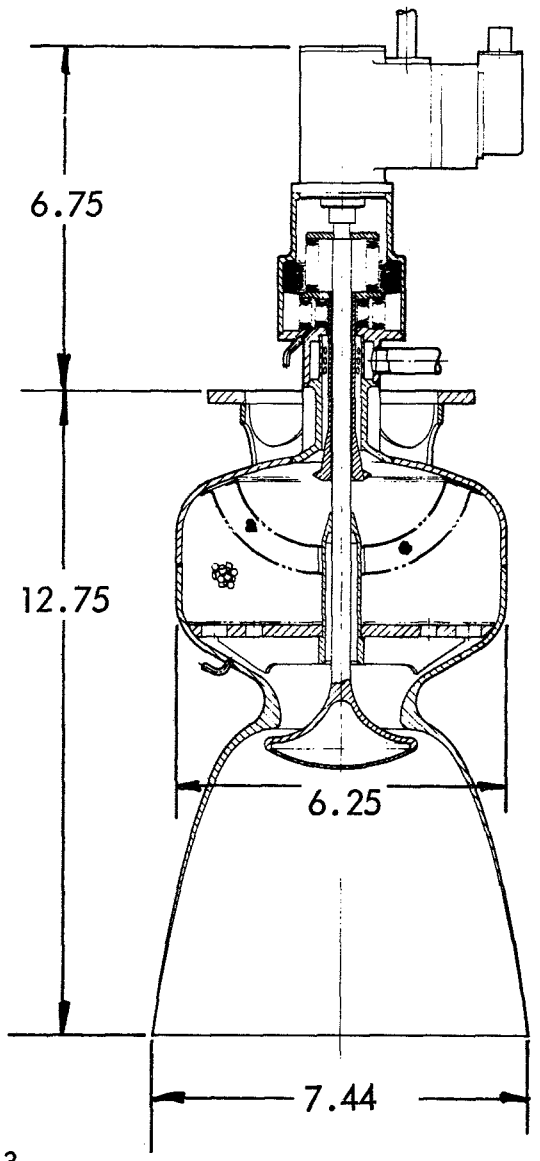

Figure II.C-2. System No. 3

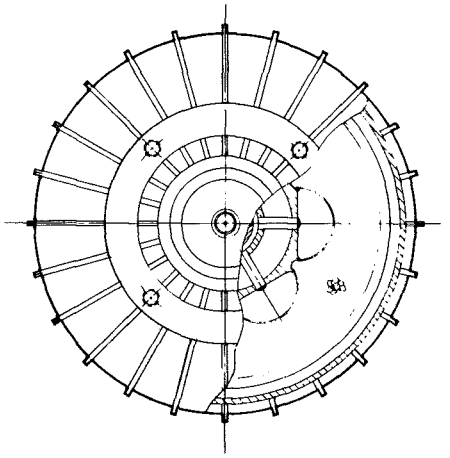

DESIGN PARAMETERS

- MAXIMUM THRUST 600 LBF
- CHAMBER PRESSURE 250 PSIA
- EXPANSION RATIO 30:1
- THROTTLE RATIO 10:1
- LIFE 500 SEC
- CHAMBER MATERIAL L - 605

PREDICTED PERFORMANCE

- SPECIFIC IMPULSE 228 LBF - SEC/LBM
- THRUST COEFFICIENT 1.68
- CHARACTERISTIC VELOCITY 4360 FT/SEC
- C_F EFFICIENCY = 96%

WEIGHT

CHAMBER AND NOZZLE	10.29
CATALYST AND SUPPORT	2.50
HEADEND STRUCTURE	2.90
THROTTLE VALVE	2.80
	18.49

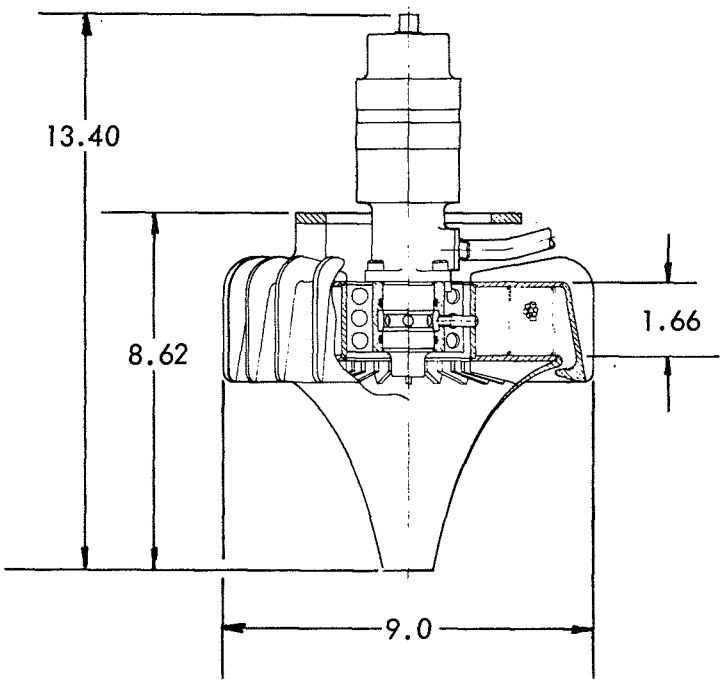

Figure II.C-3. System No. 4

DESIGN PARAMETERS

MAXIMUM THRUST 600 LBF

CHAMBER PRESSURE 250 PSIA

EXPANSION RATIO 20:1

THROTTLE RATIO 10:1

LIFE 500 SEC

CHAMBER MATERIAL L - 605

PREDICTED PERFORMANCE

SPECIFIC IMPULSE 225 LBF - SEC/LBM

THRUST COEFFICIENT 1.66

CHARACTERISTIC VELOCITY 4360 FT/SEC

C_F EFFICIENCY = 95%

WEIGHT

CHAMBER AND NOZZLE	5.25
CATALYST AND SUPPORT	2.07
HEADEND STRUCTURE	0.91
INJECTOR MECHANISM	2.16
PLUG AND SUPPORT	1.39
	11.78

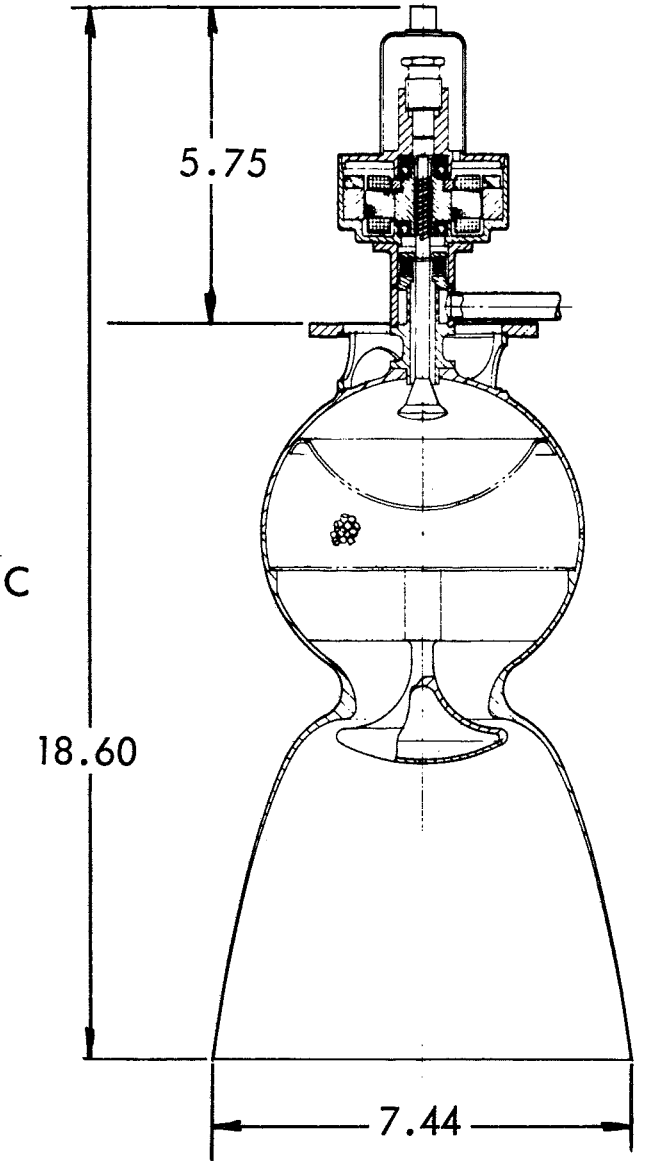

Figure II.C-4. System No. 5

DESIGN PARAMETERS

MAXIMUM THRUST	600 LBF
CHAMBER PRESSURE	250 PSIA
EXPANSION RATIO	20:1
THROTTLE RATIO	10:1
LIFE	500 SEC
CHAMBER MATERIAL	L - 605

PREDICTED PERFORMANCE

SPECIFIC IMPULSE	232 LBF - SEC/LBM
THRUST COEFFICIENT	1.70
CHARACTERISTIC VELOCITY	4400 FT/SEC
C_F EFFICIENCY = 99%	

WEIGHT

CHAMBER AND NOZZLE	6.96
PILOT CHAMBER	1.12
HEAT SINK	2.49
HEADEND STRUCTURE	1.47
THROTTLE VALVE	2.80
	14.84

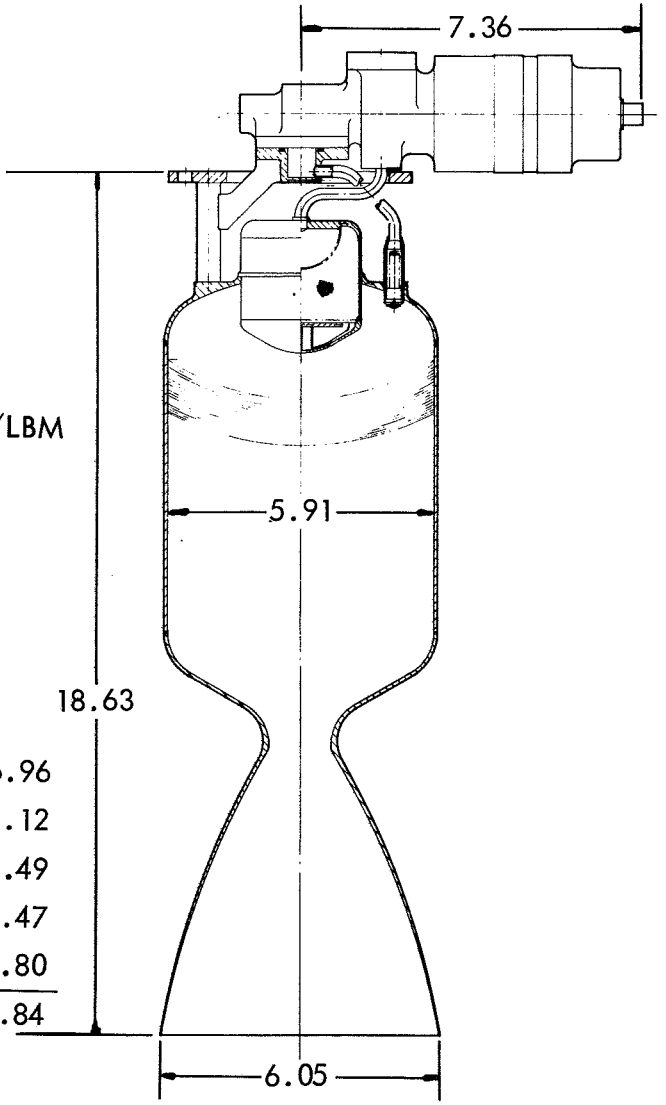

Figure II.C-5. System No. 6

DESIGN PARAMETERS

- MAXIMUM THRUST 600 LBF
- CHAMBER PRESSURE 250 PSIA
- EXPANSION RATIO 30:1
- THROTTLE RATIO 10:1
- LIFE 500 SEC
- CHAMBER MATERIAL L - 605

PREDICTED PERFORMANCE

- SPECIFIC IMPULSE 230 LBF - SEC/LBM
- THRUST COEFFICIENT 1.68
- CHARACTERISTIC VELOCITY 4400 FT/SEC
- C_F EFFICIENCY = 96%

WEIGHT

CHAMBER AND NOZZLE	12.94
PILOT CHAMBER	1.12
HEAT SINK	2.49
HEADEND STRUCTURE	2.23
THROTTLE VALVE	2.80
	21.58

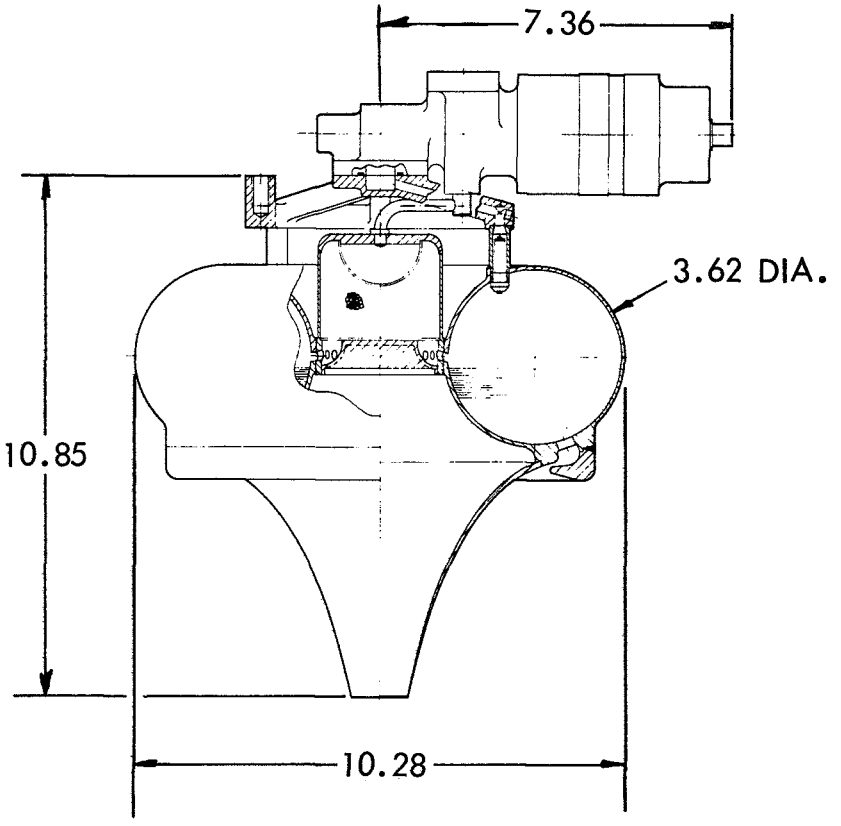

Figure II.C-6. System No. 6

DESIGN PARAMETERS

MAXIMUM THRUST 600 LBF

CHAMBER PRESSURE 250 PSIA

EXPANSION RATIO 20:1

THROTTLE RATIO 10:1

LIFE 500 SEC

CHAMBER MATERIAL L - 605

PREDICTED PERFORMANCE

SPECIFIC IMPULSE 231 LBF - SEC/LBM

THRUST COEFFICIENT 1.70

CHARACTERISTIC VELOCITY 4360 FT/SEC

C_F EFFICIENCY = 99%

WEIGHT

CHAMBER AND NOZZLE	4.42
CATALYST AND SUPPORT	2.10
HEADEND STRUCTURE	0.99
THROTTLE VALVE	2.80
	10.31

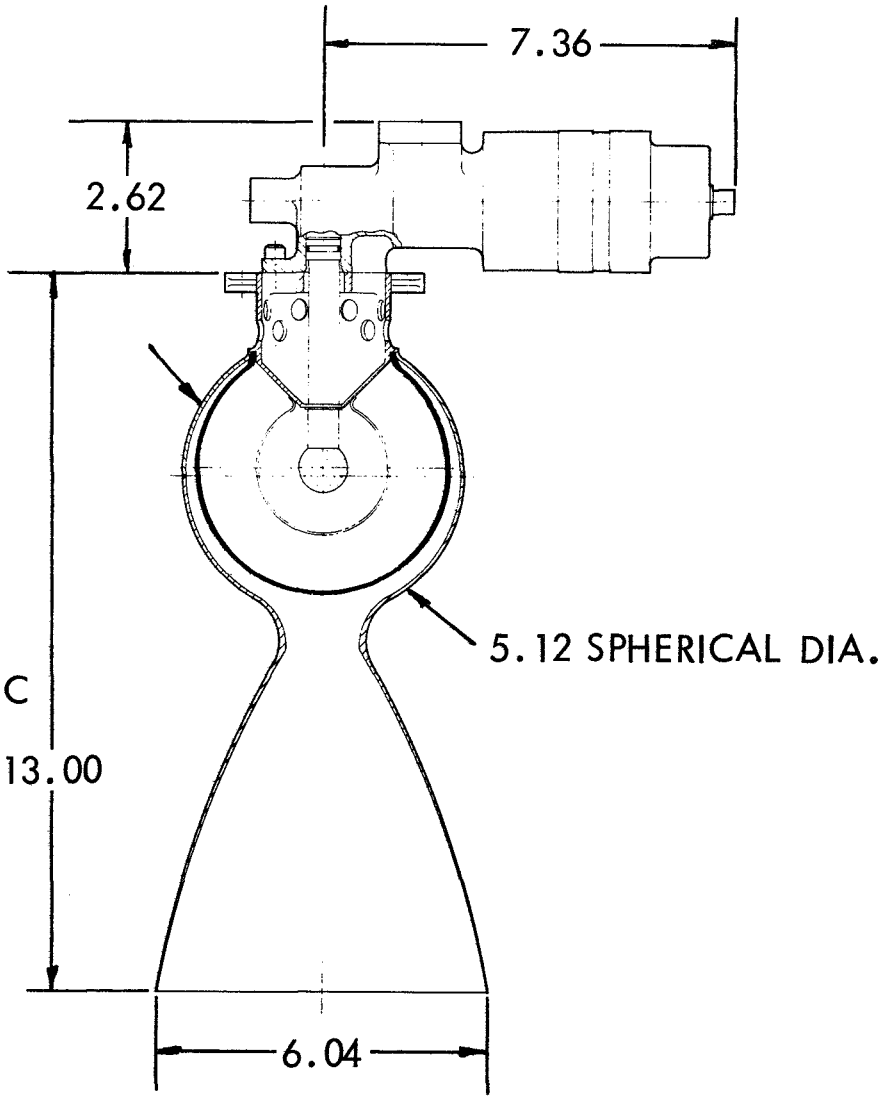

Figure II.C-7. System No. 8

II.D. SYSTEM EVALUATION

Based on the established requirements and ground rules described in Section II-A, the eight candidate systems were evaluated for performance and weight by a consistent analytical technique. A valid comparison of the various systems was achieved by developing practical engine configurations using identical propellant feed systems in all concepts. The method of analysis involved two basic computations; first to determine the performance of each engine over the range of operating variables considered, and second to compute the system weight and ideal velocity increment for each case. The digital computer programs used in this study are discussed in Appendix A.

II.D.1 Engine Performance

The engine performance was determined for each of the candidate engine configurations based on a combination of emperical and theoretical considerations. Two reactor designs were evaluated (catalytic and thermal decomposition) and four nozzle types (DeLaval, fixed and variable throat expansion deflection and plug). The characteristic exhaust velocity (C*) was established for each chamber design based on test experience for the range in thrust surveyed. Figure II.D-1 shows a comparison of C* for each design as a function of percent thrust with the fraction of ammonia dissociation (X) indicated. The data presented were measured on engines which had a chamber pressure of approximately 300 psia at a thrust level of 400 to 600 lbf. Note that a slight performance increase can be realized with the thermal decomposition reactor and this advantage increases as the engine is throttled to lower thrust levels. The primary reason for this increase in performance with the thermal decomposition chamber is due to the decrease in ammonia dissociation achieved with the lower surface area heat sink material as compared to catalyst. The decrease in performance occurs under throttling conditions due to the lower mass velocity through the reactor. However, the change in residence time is much less for the thermal reactor which results in its superior throttling characteristic. The decomposition of hydrazine is expressed chemically as:

$$2\ N_2H_4 + \text{Catalyst} \rightarrow 2\ NH_3 + N_2 + H_2 + 83{,}000\ \text{BTU}$$

As dissociation of the ammonia increases, the molecular weight and adiabatic flame temperature decrease while the effective specific heat ratio (γ) increases. The net effect is a decrease in performance with an increase in dissociation. The C* performance was considered to be independent of chamber pressure based on theoretical and experimental results. Theoretical values are indicated in Figure II.D-1; it is felt from the comparison of this figure that the the C* efficiency is on the order of 98 percent.

The thrust coefficient (C_F) is influenced primarily by the particular nozzle type and expansion ratio. Values for the nozzle efficiency and effective specific heat ratio were selected on the basis of experiemental evidence. A summary of the design parameters and C_F efficiencies used in this study is shown in Table II.D-1. The thrust coefficient was assumed independent of chamber decomposition method. The basic expression for thrust coefficient assuming one dimensional flow and isentropic expansion is:

$$C_{F_{vac}} = \sqrt{\left(\frac{2\gamma^2}{\gamma-1}\right)\left(\frac{2}{\gamma+1}\right)^{(\gamma+1)/(\gamma-1)}\left[1-\left(\frac{P_e}{P_c}\right)^{(\gamma-1)/\gamma}\right]} + \frac{P_e\,\varepsilon}{P_c}$$

The Rao nozzle C_F was used in the DeLaval nozzle engine configurations and the one dimensional C_F was used in defining nozzle performance of the advanced nozzle concepts. The thrust coefficient was corrected for back pressure as follows:

$$C_F = C_{F_{vac}}\left(\eta C_F\right) - \frac{P_a\,\varepsilon}{P_c}$$

For the altitude compensating nozzles, the term $\frac{P_a\,\varepsilon}{P_c}$ was replaced by $\frac{P_e\,\varepsilon}{P_c}$ if the exit pressure was equal or less than ambient pressure. With the variable area throat design, it was necessary to adjust the C_F for the change in area ratio during the throttling. The vacuum C_F was based on an effective specific heat ratio which is a function of the expected dissociation at the various thrust levels during throttling. Figure II.D-2 indicates the assumed conditions at various locations in the engine and the

effective specific heat ratio used in this study. It is noted that the change in γ during flow is due solely to the variation of the specific heats with temperature since the gas composition is a function only of X and remains constant throughout the nozzle. Therefore in specifying a γ as an input to the Rao nozzle optimization, an "average" value must be selected such as the line marked "design" in Figure II.D-2. Incorrect nozzle contours will result if the chamber value is used, although the resulting errors in contour and C_F will be small (on the order of 1 percent). Figure II.D-3 shows the isentropic nozzle pressure ratio as a function of expansion ratio for the expected range in specific heat ratio. The resultant vacuum thrust coefficient under various throttling conditions is shown as a function of area ratio in Figure II.D-4 for the DeLaval and advanced nozzle concepts.

Engine performance with the conventional nozzle was computed over the entire range in chamber pressure and expansion ratio without consideration of possible separation at the nozzle exit because of the possible variations in ambient pressure, expansion characteristics and separation criteria. Figure II.D-5 shows the range in separation conditions based on the Summerfield criteria, i.e., separation in the nozzle occurs when the exit pressure is equal or less than 40 percent of ambient pressure. Applying this criteria to the optimum designs which employs a DeLaval nozzle and a relatively low chamber pressure and expansion ratio indicates that separation will not occur with a 10:1 throttle ratio and 0.3 psia ambient pressure based on the two dimensional results. The performance of the two dimensional nozzle is different from the one dimensional result due to the difference in static pressure at the nozzle wall. For optimum contour nozzles designed by the method of Rao, the pressure varies across the nozzle exit and the wall pressure is appreciably higher than the one dimensional result thus allowing higher expansion ratios.

The specific impulse was computed for each system over the expected throttling range based on the relationship:

$$I_s = \frac{C^* C_F}{g}$$

The performance of the various configurations at a chamber pressure of 200 psia and expansion ratio of 20:1 is shown in Figure II.D-6 with a

comparison showing the performance loss due to the specified ambient atmospheric pressure (0.3 psia) displayed in Figure II.D-7. The advantage of the advanced nozzle concepts is shown clearly by the higher performance achieved during throttling operation.

Figure II.D-8 shows the conventional catalytic engine performance as a function of area ratio for 5:1 throttle ratio with the one dimension separation points indicated. As indicated from this data, the optimum area ratio is a function of the amount of part throttle operation performed. For the mission conditions used in this study, approximately 30 percent of the propellant is consumed at thrust levels less than 50 percent, hence the optimum expansion ratio lies between the high expansion ratio required for optimum performance at full thrust and the low expansion ratio required for optimum performance at low thrust operation of the engine.

The effects of chamber pressure on engine performance is shown in Figure II.D-9. For hydrazine engines, the specific impulse is less sensitive to chamber pressure than for bipropellant engines due to the small effect on the generated gas properties and reaction temperature. As can be seen from the data presented, a significant performance decrease occurs with a chamber pressure less than 200 psia. When comparing the engine performance at an ambient pressure of 0.3 psia to vacuum performance, it is apparent that if the Mars atmospheric pressure is lower than expected, the optimum chamber pressure would be lowered.

II.D.2 Engine Weight

The throttleable thrustor system employs three throttleable fixed-vector radiation cooled hydrazine engines. The engine weight was determined utilizing the detailed weight breakdown given for each of the preliminary designs in Section II.C as a baseline and developing scaling criteria as detailed below. The effects of the following variables were studied:

Thrust	300, 600, 1200 lbf
Chamber Pressure	50 to 500 psia
Expansion Ratio	5:1 to 80:1

Since the preliminary designs had considered only a thrust level of 600 lbf, the first step was to establish corresponding baseline engine weights for the 300 and 1200 lbf thrust engines. The chamber dimensions

were established based on maintaining the catalyst bed loading specified ($G = 0.06$ lb/sec-in^2). A minimum wall thickness of .015 inch was maintained for manufacturing reasons. The baseline nozzle thickness contour was based on structural buckling criteria for an expansion ratio of 80:1 and this contour was simply truncated for lower expansion ratios. This technique yielded nozzle weights that were somewhat conservative, but the relative effect on the various engine configuration is identical so that comparisons are valid. Included in the engine weight is a fixed weight which includes the following components: throttle valve, catalyst, screen, retainer and plate, thermal standoff and injector. The plug nozzle engines were sized for a range in expansion ratio between 20:1 and 40:1. A larger range was not considered practical because the reactor bed imposes size limitations on the annular throat radius. For the expansion deflection engine, a full range in area ratio was investigated since there are no practical limitations on this concept.

The engine weight for conditions other than those of the baseline design were found by identifying the influence parameters. Chamber diameter was computed as follows:

$$D_c = \sqrt{\frac{4\,\dot{M}}{\pi\,G}}$$

where $\dot{M}$ = N_2H_4 flow rate, lb/sec

Chamber weight was found to be proportional to chamber pressure and to thrust to the 3/2 power. Nozzle weights were determined from the Rao nozzle computer data which prints out nozzle surface area as a function of expansion ratio and throat radius squared. With the established thickness contour, the baseline nozzle weight was computed as a function of area ratio. Nozzle weight was found to be influenced inversely as the square root of the chamber pressure and directly as the square root of the thrust level. Catalyst weight is roughly proportional to thrust, however, slight adjustments had to be made to maintain the minimum bed depth of one inch. The mounting plate weight and head and lower catalyst screens weight were assumed proportional to thrust or chamber diameter squared while the thermal standoff weight was a function of chamber diameter.

The results of the engine weight computations are shown in Figures II.D-10 through II.D-30 for systems No. 1 through No. 8 at thrust levels of 300, 600, and 1200 lbf, respectively. (It is noted that there are only 21 curves instead of the 24 that might be expected since the engine weights for systems No. 1 and No. 2 are identical. The system weights for these cases will be different, since the two cases have different types of throttle valves which yield different tank pressure requirements and concomitantly different system weights.)

II.D.3 Propellant Consumption

The quantity of hydrazine used for the representative Mars landing mission was based on the thrust profile presented previously in Figure II.A-3. This mission profile was evaluated for a range in thrust level (or total impulse) to identify the approximate payload capability. The thrust-time curve was integrated to obtain a total impulse which corresponds to the approximate landed payload weight shown in Table II.D-2. Since the specific impulse of the engine is a function of the throttle ratio, it was necessary to integrate the propellant consumption for each thrust increment by dividing the corresponding total impulse by the specific impulse as follows:

$$W_p = 3F\left(\frac{1}{I_{s\ 1.0F}} + \frac{4.8}{I_{s\ 0.8F}} + \frac{3.6}{I_{s\ 0.6F}} + \frac{2.4}{I_{s\ 0.4F}} + \frac{0.6}{I_{s\ 0.3F}} + \frac{1}{I_{s\ 0.2F}}\right)$$

II.D.4 Propellant Tank Weight

The propellant tank was sized to allow sufficient ullage for employing a nitrogen blowdown pressurization system at a ratio of 2 to 1. A single spherical 6 Al-4V titanium tank was employed in this study with a safety factor of 2.2. Assuming an isentropic blowdown with a 50 percent pressure decay, the resultant tank volume is approximately 2.7 times the volume of propellant. Figure II.D-31 shows the effects of specific heat ratio on required tank volume for a range in pressure ratio. The pressurization factor (Z) is the ratio of tank volume to propellant volume which may be expressed as follows for an isentropic expansion of the pressurant gas:

$$Z = (P_1/P_2)^{1/\gamma} \Big/ (P_1/P_2)^{1/\gamma} - 1$$

where P_1/P_2 is the blowdown pressure ratio and γ is the specific heat ratio of the pressurant

As can be seen, a significant decrease in tank volume can be achieved with a higher blowdown pressure ratio. If helium rather than nitrogen were used as the pressurant, a larger tank would be required for the same blowdown pressurization ratio.

The tank weight calculation was derived from elementary stress relationships and an emperical weld factor (WF) which allows for welds, bosses and local stiffening. Figure II.D-32 shows the weld factor as a function of tank diameter. By combining the above factors, the tank weight can be expressed as:

$$W_T = \frac{1.5\ Z\ W_p\ P_T\ \rho_T\ WF}{\rho_p\ \sigma}$$

Figure II.D-33 shows a comparison of the theoretical tank weight with some actual data as a function of pressure and diameter. Reasonable agreement over the range of tank diameters of interest may be observed; however, if the actual data of this figure had been available earlier, it would have been utilized.

II.D.5 Pressurant Weight

Propellant tank pressure was determined by summing the chamber pressure and system pressure losses at full thrust for each system per the following equation: $P_T = P_c + \Delta P_b + \Delta P_i + \Delta P_v + \Delta P_s$. The particular pressure loss of the throttle valve, injector and catalyst bed is shown in Table II.D-1 for the various system investigated. In this study, the pressure loss for the various components was assumed based on practical experience and is believed valid for the expected range in operating conditions. Figure II.D-34 shows a comparison of the resultant tank pressures for the eight system configurations with an engine chamber pressure of 200 psia. As noted in Table II.A-3, the pressure loss of the cavitating valve was assumed to be 15 percent of tank pressure and the non-cavitating valve was 10 percent of P_T. Where a throttling injector is used, the valve loss does not exist and a lower tank pressure results. On this basis as well as others which will be presented in Section II.E, the use of a flow control injector appears to be very desirable.

It is noted with the initial tank pressure established, the pressurant weight was computed from the perfect gas law as follows:

$$W_g = \frac{(Z-1)\ P_T\ W_P}{\rho_P\ RT}$$

By combining the tank weight and pressurant weight equations and solving in terms of tank pressure, we can see that hardware weight is directly proportional to tank pressure:

$$W_{Hardware} = P_T\ (K_{Tank}\ K_{Gas})$$

where K_{Tank} and K_{Gas} are constants defined by the propellant quantity and blowdown pressurization ratio. For this application, the hardware weight represents approximately 40 percent of the total system dry weight with more conventional engine systems. Consequently, a dry weight saving of 2 percent can be achieved with a non-cavitating throttle valve or 5 percent with a throttling injector (assuming the injector weight is equal to the throttle valve weight) due to the lower tank pressures required.

II.D.6 System Weight Results

The system weight was based on the simplified propulsion system concept shown in Figure II.A-3 and does not include payload, support structure or avionics. The expression for system weight can then be stated as:

$$W_s = 3W_E + W_P + W_{PT} + W_g + W_c$$

The component weight includes two squib actuated valves, a filter and associated service connections and plumbing. The component weight estimates are shown below as a function of engine thrust:

THRUST	COMPONENT WEIGHT
300 lb_f	4 lb_m
600 lb_f	5 lb_m
1200 lb_f	6 lb_m

The engine, propellant, tank and pressurant weight calculations were previously described. The propulsion system dry weight is defined as the system weight minus the propellant weight. Each of the eight configurations were evaluated for the effects of thrust level, operating pressure and expansion ratio and the results are shown in Figures II.D-35 through II.D-58 for systems No. 1 through No. 8 at F = 300, 600, and 1200 lbf, respectively. The results have also been summarized in Figures II.D-59 through II.D-63 for near optimum conditions with a chamber pressure of 200 psi and expansion ratio of 20:1.

II.D.7 Ideal Velocity Increment

The ideal velocity increment generally represents the most significant parameter for propulsion system evaluation and is expressed as:

$$\Delta V = I_{SA}\, g\, \ln (\text{initial system weight} + \text{payload}/\text{dry weight} + \text{payload})$$

where the effective specific impulse I_{SA} = total impulse/weight propellant

An example of the results of this computation for system No. 6 with 600 lb thrust engines and 1500 payload are shown in Figure II.D-64 for an expansion ratio of 20:1. Due to the relatively small variation in I_{SA} with chamber pressure for N_2H_4 engines, the performance optimization is not as apparent as the weight optimization. Since both optimization methods produced the same conclusions, the more meaningful weight data was presented in greater detail.

II.D.8 Conclusions

From the results presented, it is apparant that there is not an extreme range in the system weight for any of the engine systems considered. For example, the maximum difference between the highest and lowest performing systems was on the order of 15% for the range of variables investigated. On the other hand, the differences in terms of landed payload is not so insignificant (15 to 50 lbm).

On the dual considerations that the best performing system should be selected and that there should be a high probability that the selected engine will work with the minimal development which is allowed in the test

plan, a modified version of system No. 8 was recommended for Phase II and III. The modification consists in changing the radial outflow injector to an axial flow version as shown in Figure II.D-65. It is felt that this choice has a high success probability and it is only slightly heavier than the version shown in Figure II.C-7.

The results clarly indicated that low chamber pressure and low expansion ratio were optimal. An examination of the governing bed pressure drop equations shows that the assumed constant catalyst bed ΔP of 50 psia is optimistic for chamber pressures below 200 psia. Also the effect of using a constant thickness contour for the nozzles and truncating this contour for shorter nozzles leads to unrealistically low values of optimum ε. Thus, while a chamber pressure of 200 psia and an expansion ratio of 10:1 to 20:1 have been tentatively established, it is clear that these recommendations should be reviewed in detail during Phase II.

It is apparent also that the thermal decomposition thrustor did not offer any performance improvement. For example, compare system No. 6 (employing a thermal decomposition chamber) with system No. 8 (employing a catalytic chamber). Although the performance of system No. 6 was higher than system No. 8, the lower engine weight of system No. 8 produced a significant weight advantage for the range in total impulse investigated. Therefore, the catalytic reactor was recommended for this application. This advantage, however, would diminish for longer duration missions.

The effects of total impulse on subsystem weight are shown in Figure II.D-62 for system No. 8. Figure II.D-63 is a weight comparison of the eight systems as a function of total impulse or thrust level. The expected advantage of the higher performing systems at high total impulse is not readily apparent since the burn time in this study was constant and of relatively short duration. As can be seen from Figure II.D-63, system weight is roughly proportional to total impulse with a constant burn duration. The results indicate that there is no significant system weight advantage with the advanced nozzle configurations to warrant the increased risk associated with the development of these configurations for this particular application.

An examination of the various segments of propulsion system weight shows that the engine and hardware weight make up a significant part of the total system weight due to the relatively small quantity of propellant required for the short duration mission. For this reason, the small gain in the specific impulse of the various advanced nozzle configurations was offset by the increased engine weight and use of an advanced nozzle was not recommended.

A significant decrease in tank pressure can be achieved by the flow control injector and the development of this throttling technique should be encouraged. Based on hardware availability, however, a non-cavitating flow control valve was recommended for Phases II and III. This component produces a larger weight penalty than the flow control injector but has a weight advantage over the cavitating design.

Table II.D-1. Performance Study Input Parameters

SYSTEM	C*	C_F	V	$\triangle P_I$	$\triangle P_B$
1	CD	1	0.15	110	50
2	CD	1	0.10	110	50
3	CD	4*	0.0	75	50
4	CD	3*	0.15	110	50
5	CD	2*	0.0	75	50
6	TD	1	0.15	75	10
7	TD	3*	0.10	75	10
8	CD	1	0.10	110	50

CD CATALYTIC DECOMPOSITION
TD THERMAL DECOMPOSITION

1 99% C_F VAC — RAO NOZZLE C_F (See Figure II.D-4)

2 95% C_F VAC
3 96% C_F VAC
4 95% C_F VAC (VARIABLE ϵ)
— ONE DIMENSIONAL C_F (See Figure II.D-4)

* ALTITUDE COMPENSATING

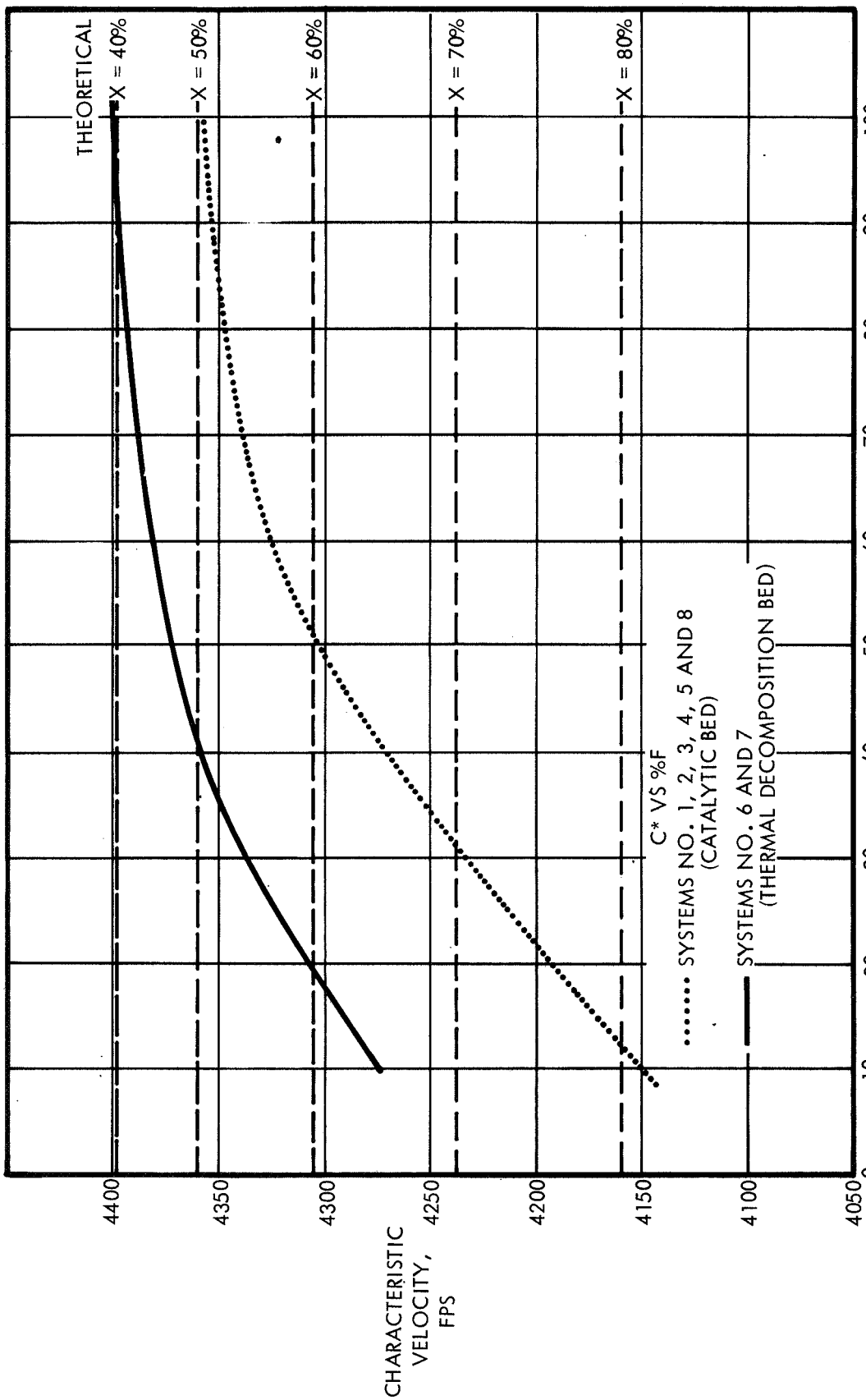

Figure II.D-1. Characteristics Velocity Throttling Performance

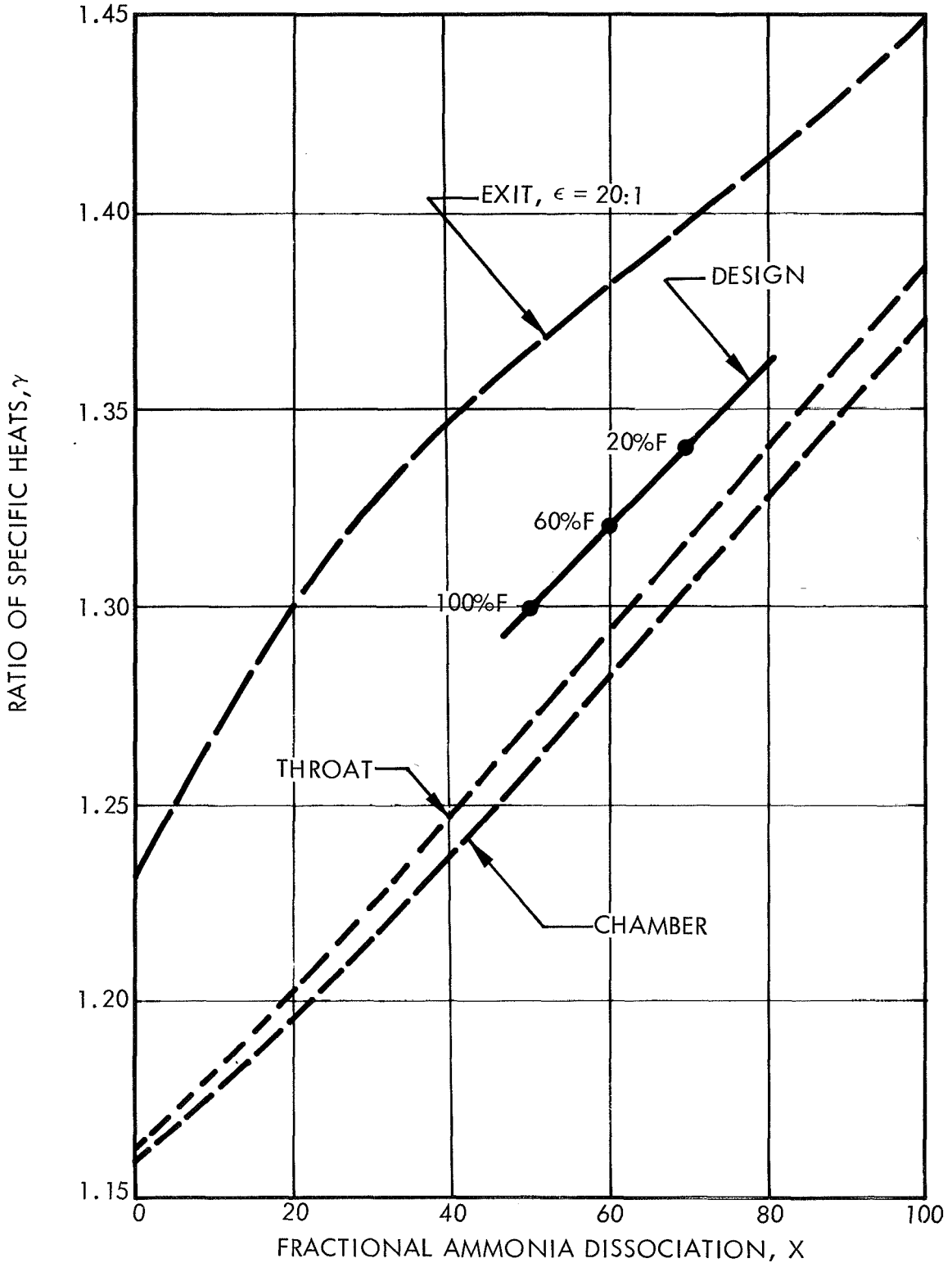

Figure II.D-2. Effective Specific Heat Ratio

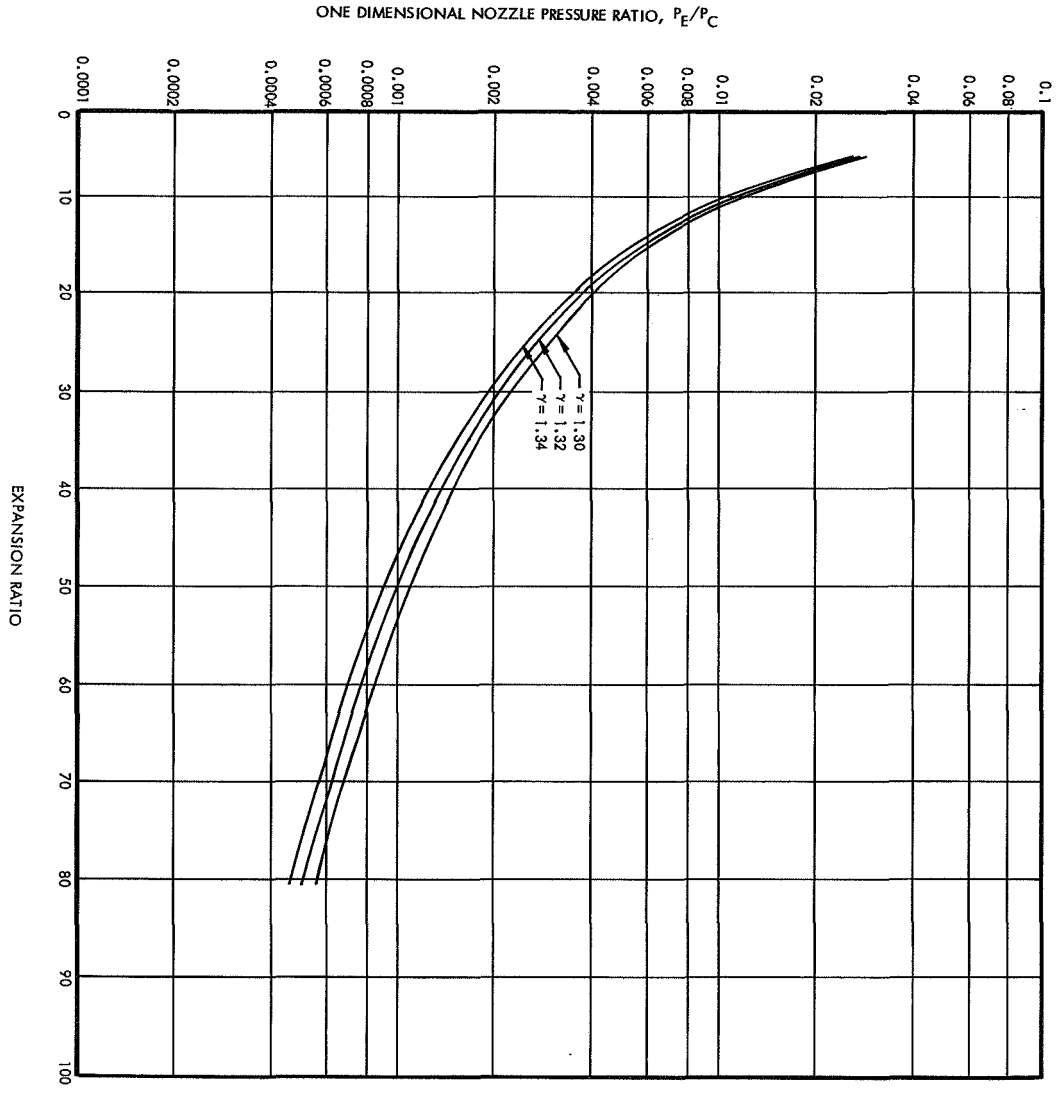

Figure II.D-3. Nozzle Pressure Ratio as a Function of Expansion Ratio and Gamma

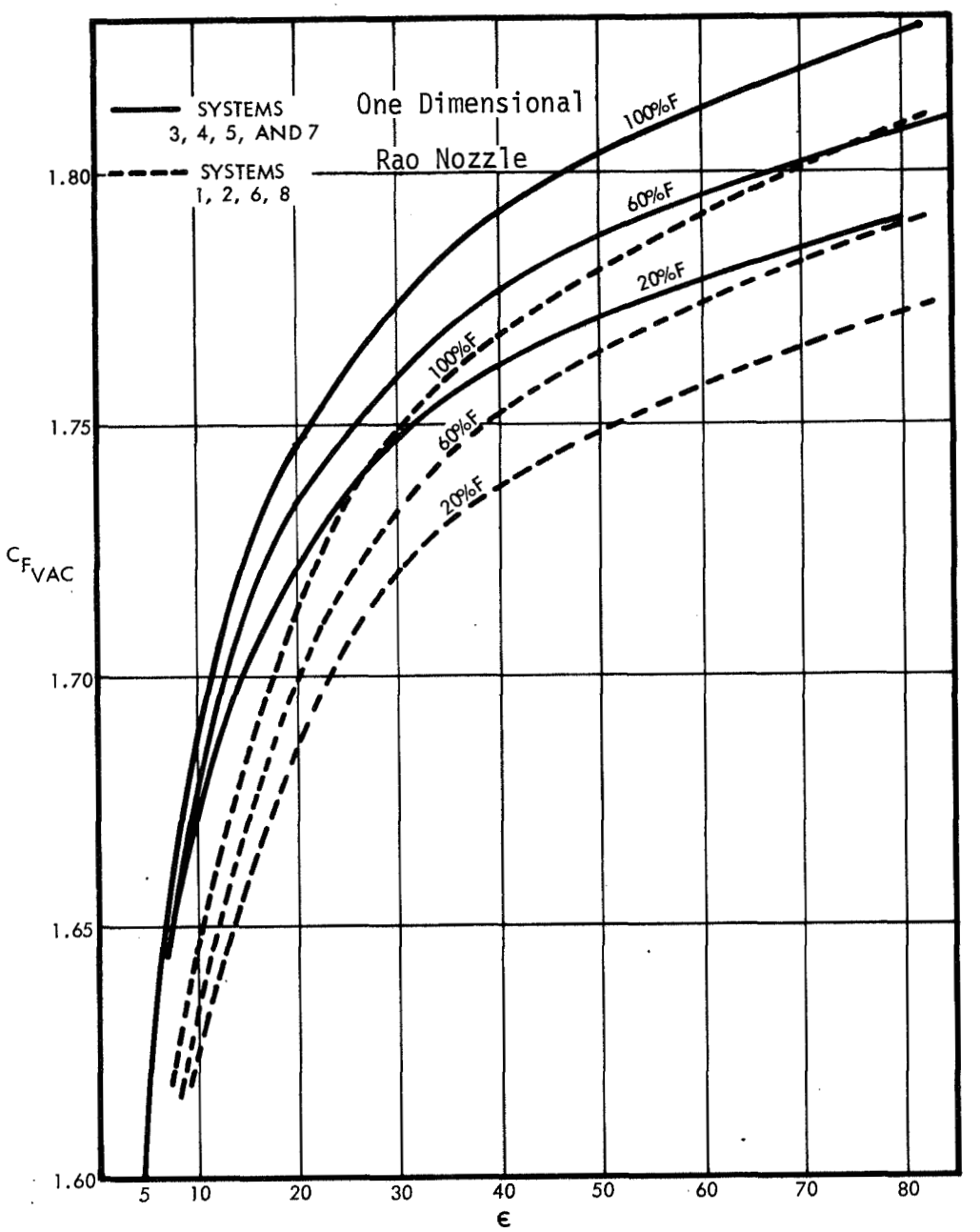

Figure II.D-4. Theoretical Thrust Coefficient

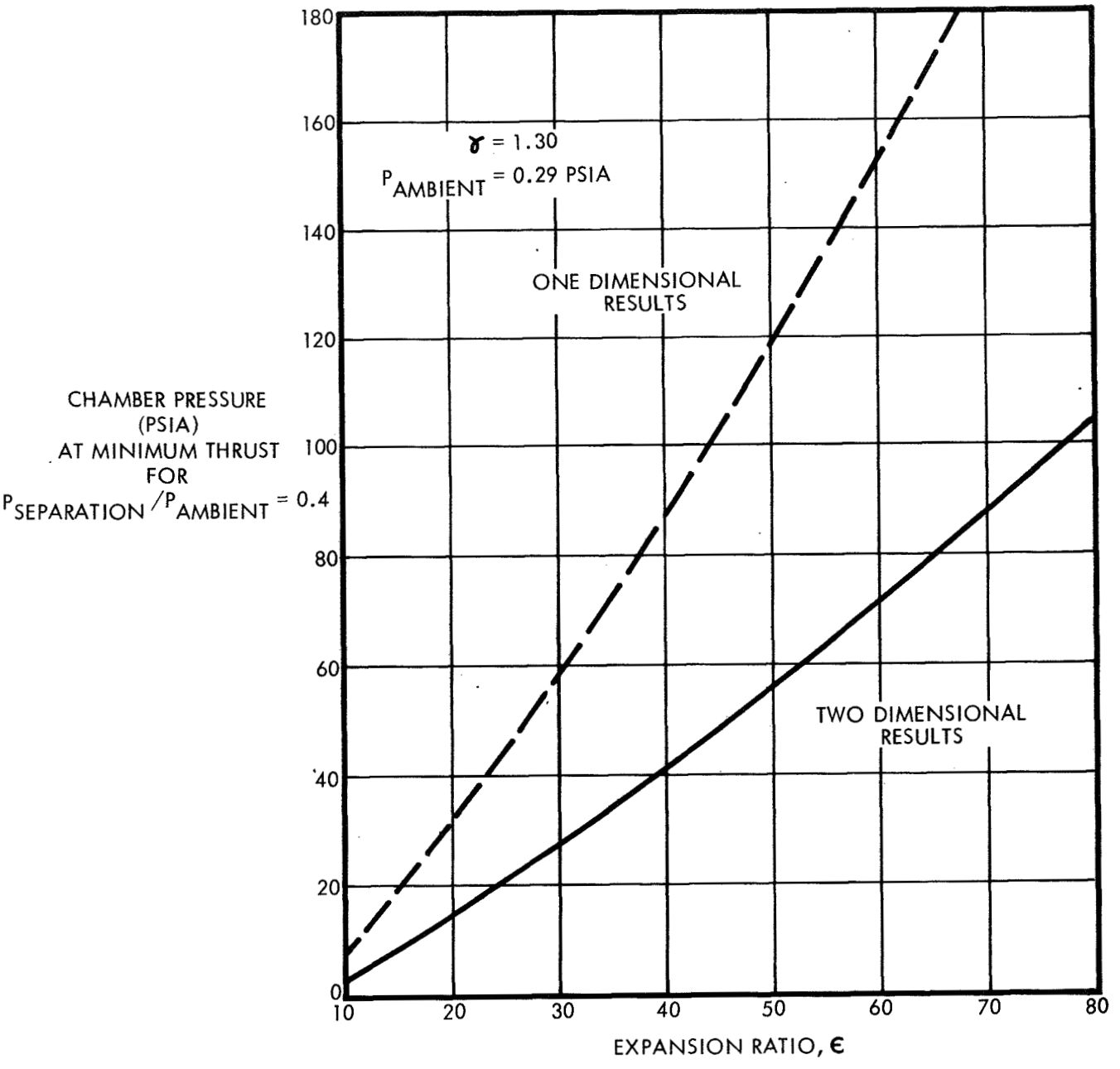

Figure II.D-5. Nozzle Separation Criteria

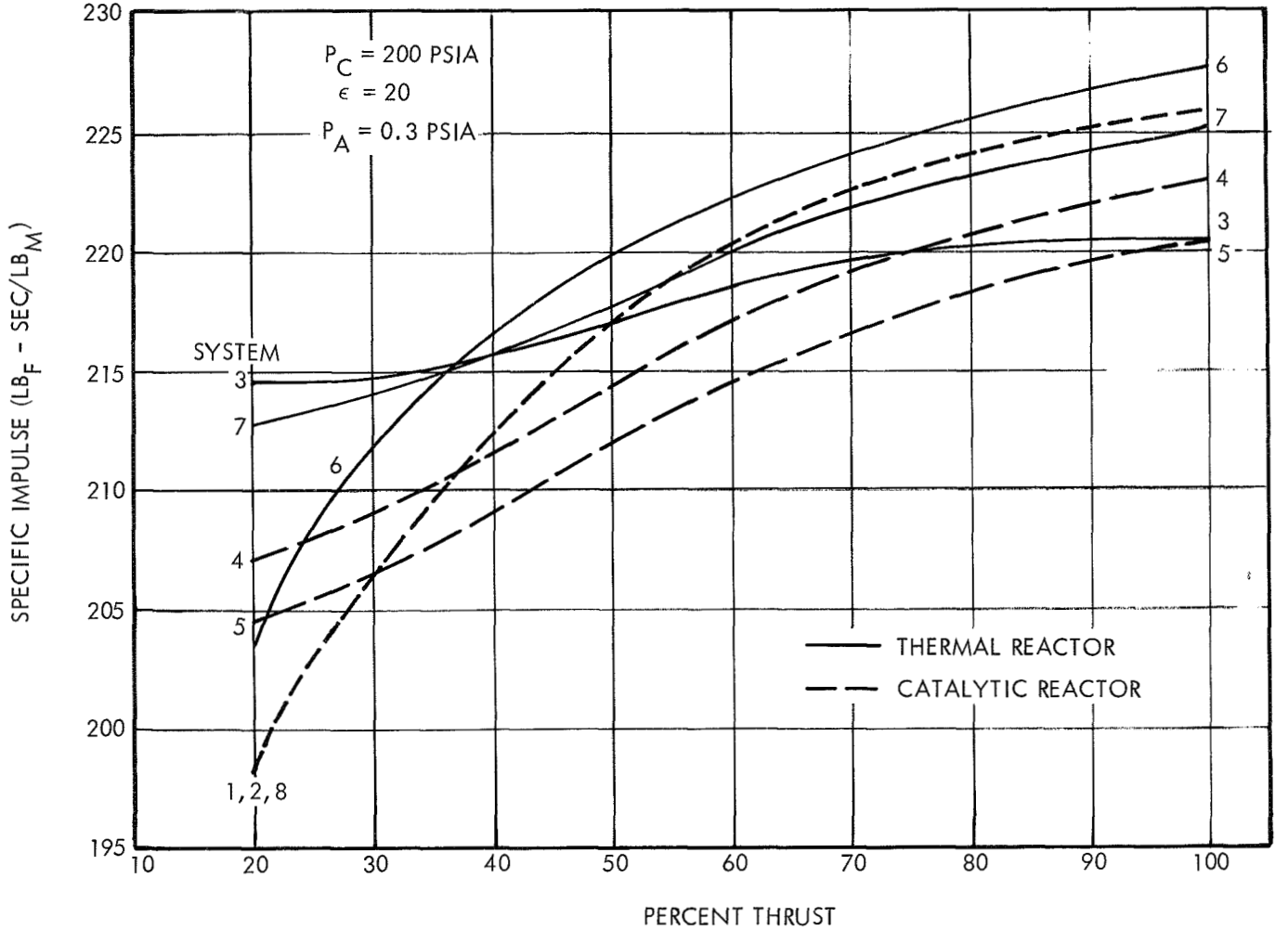

Figure II.D-6. Throttling Performance of Various TTS Mechanizations

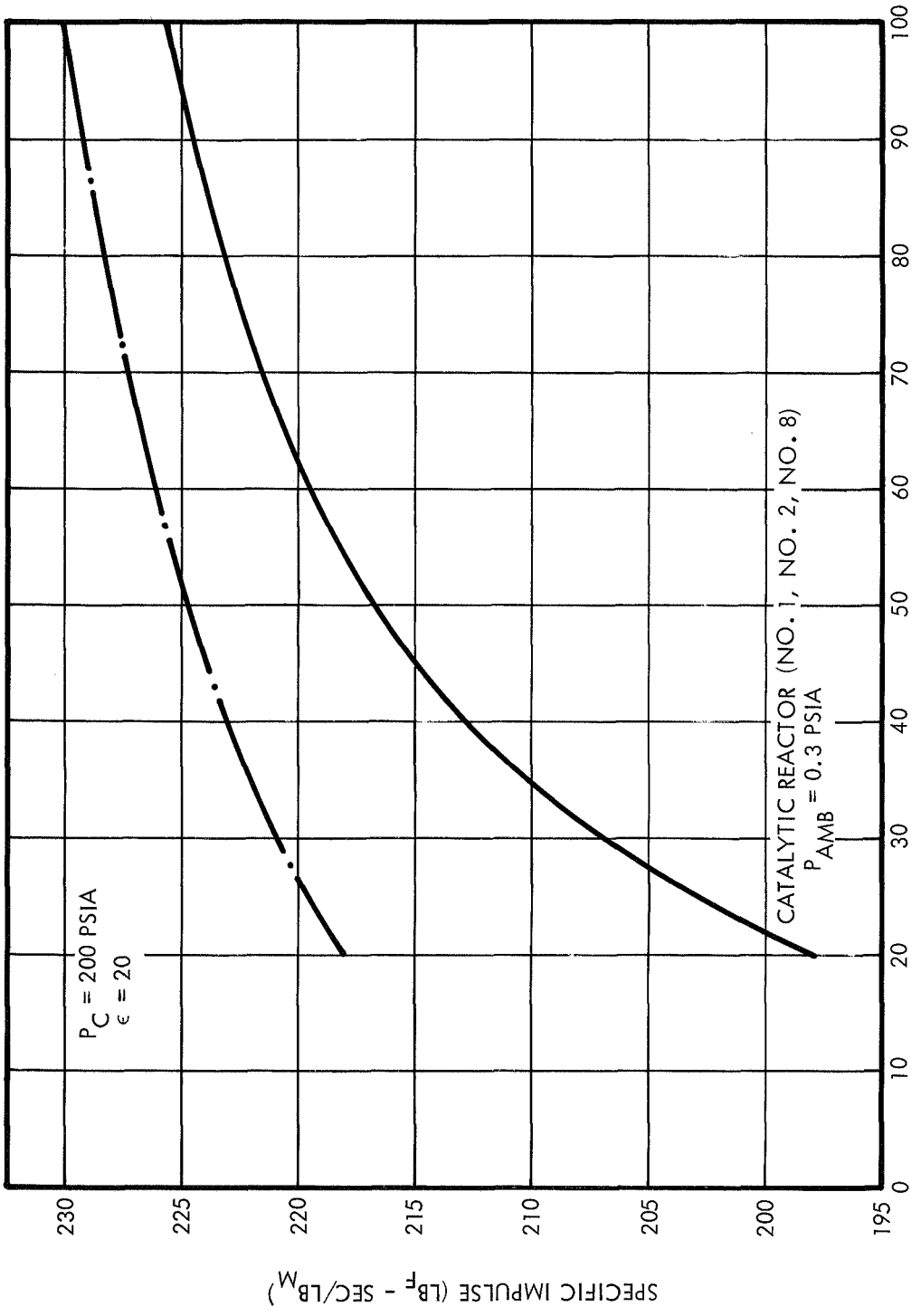

Figure II.D-7. Effect of Ambient Pressure on Throttling Performance

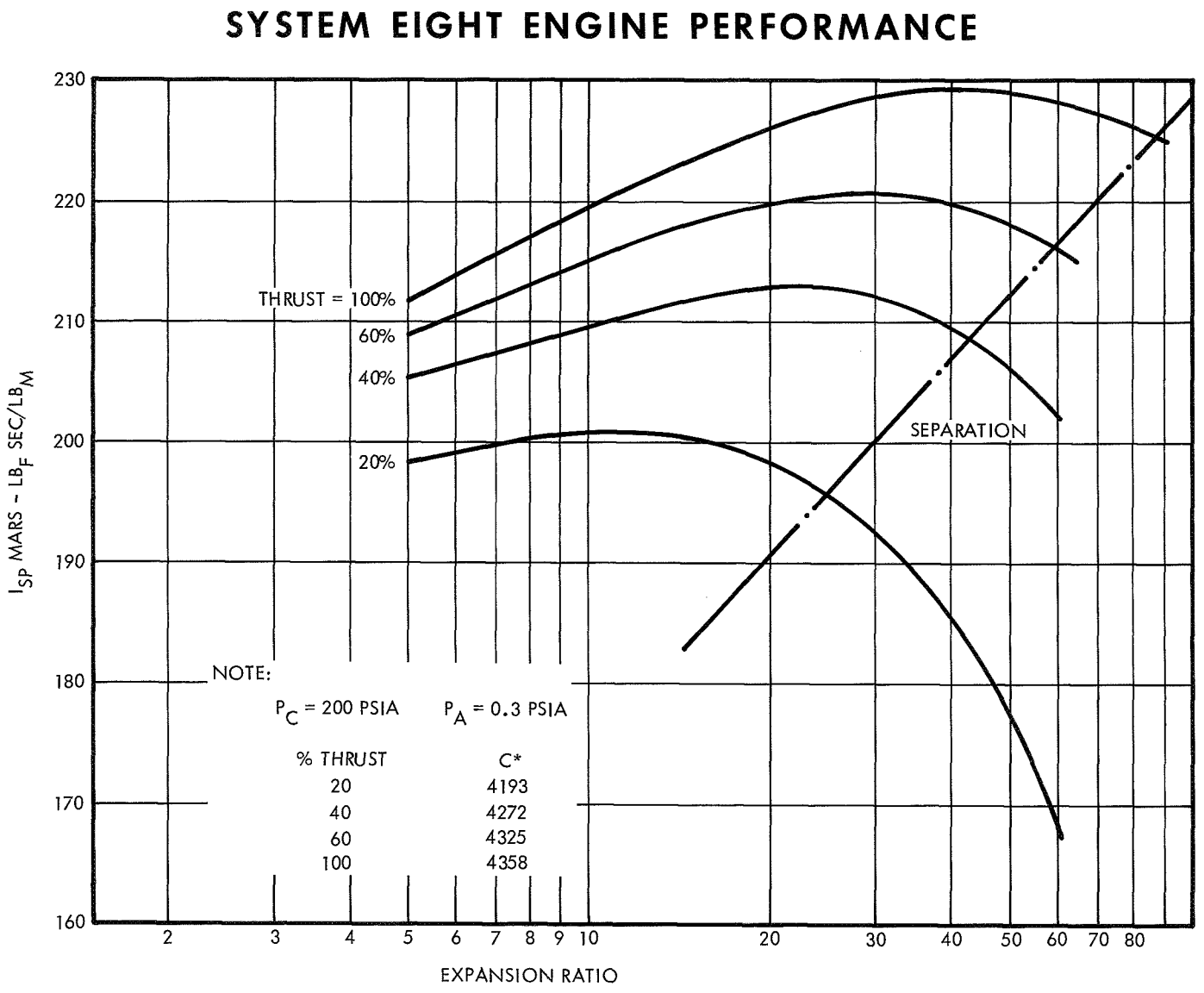

Figure II.D-8. Throttling Performance of Systems Number 1, 2 and 3

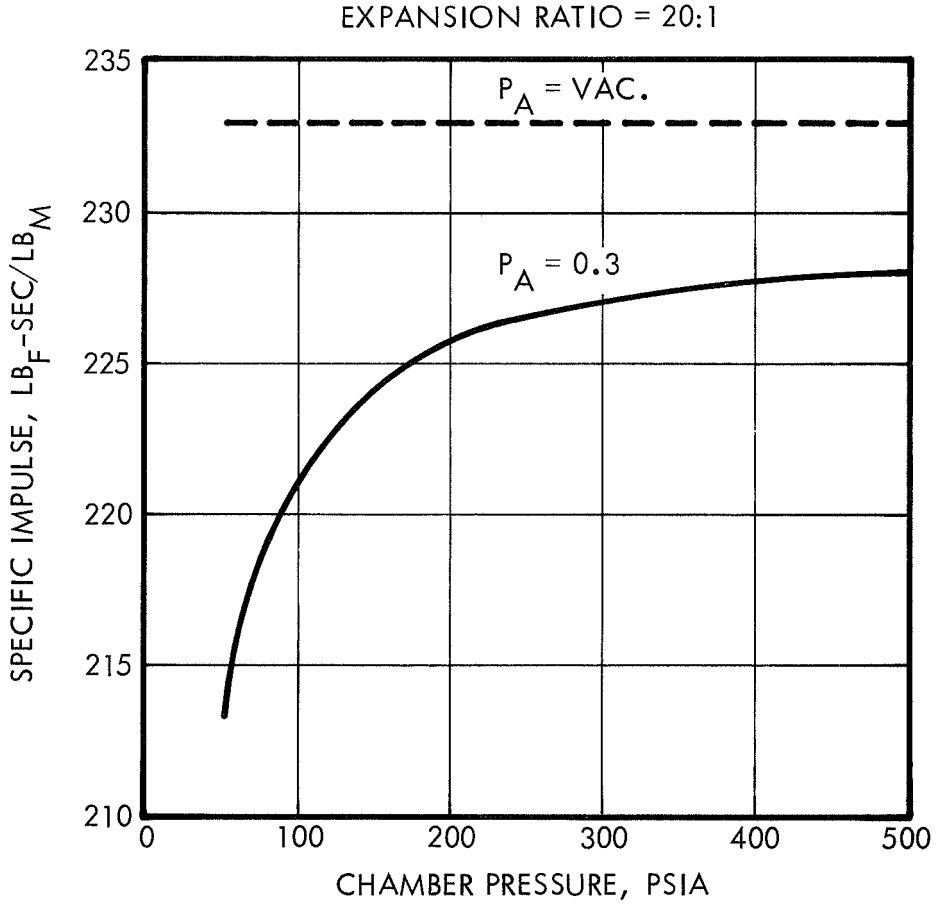

Figure II.D-9. Chamber Pressure Effects on Engine Performance at Full Thrust for Systems 1, 2 and 3

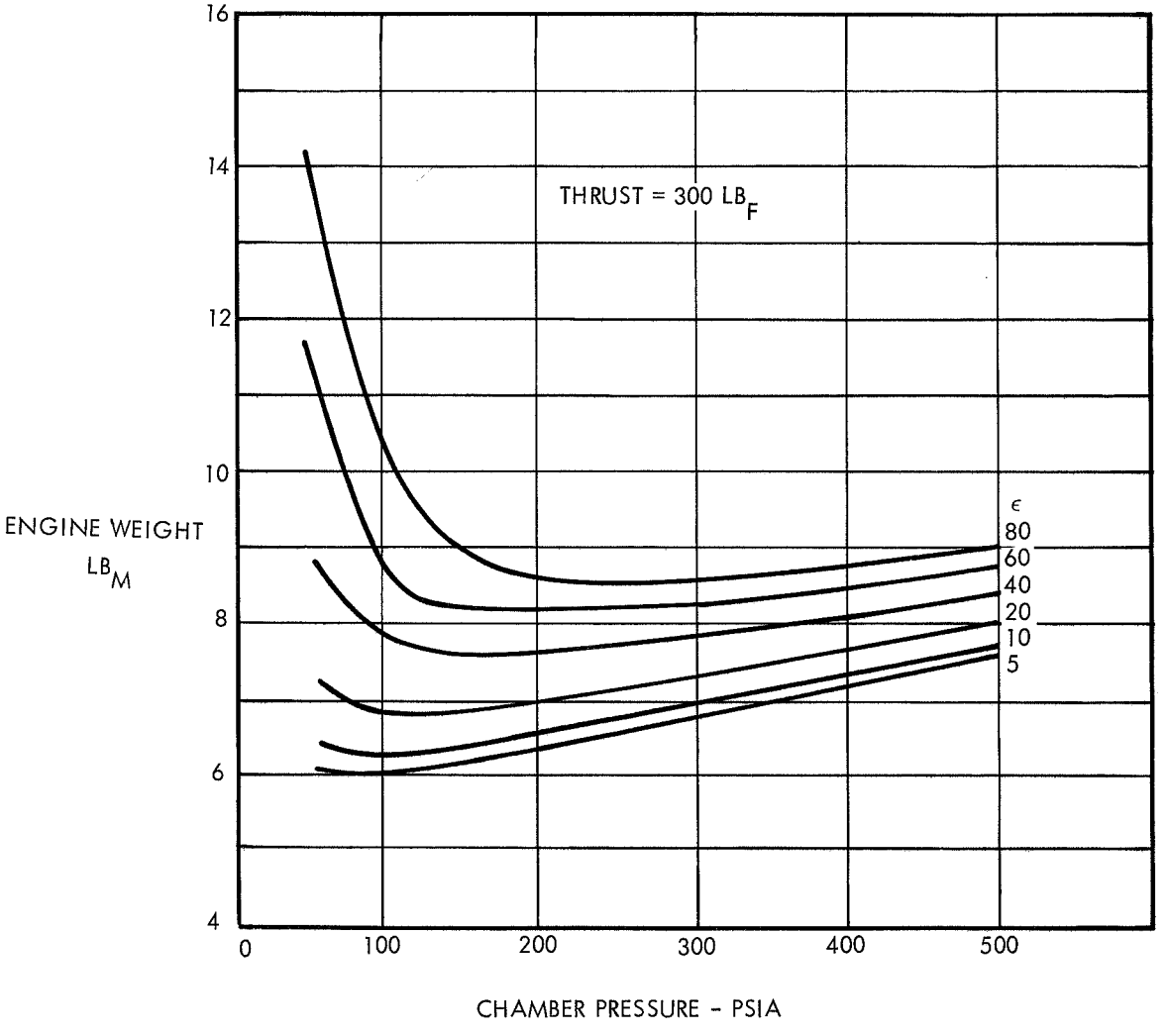

Figure II.D-10. Engine Weight as a Function of Chamber Pressure and Expansion Ratio for Systems Number 1 and 2

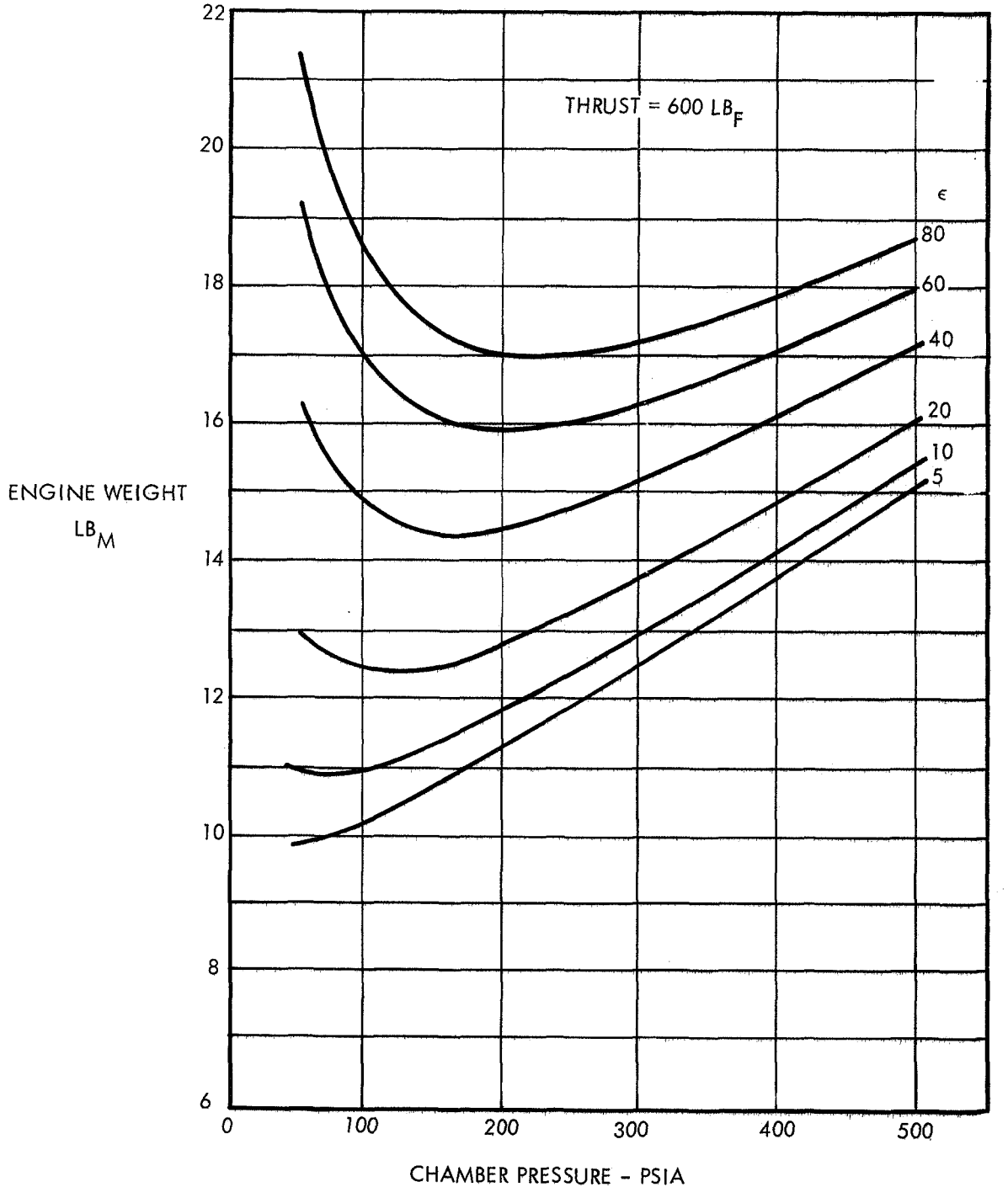

Figure II.D-11. Engine Weight as a Function of Chamber Pressure and Expansion Ratio for Systems Number 1 and 2

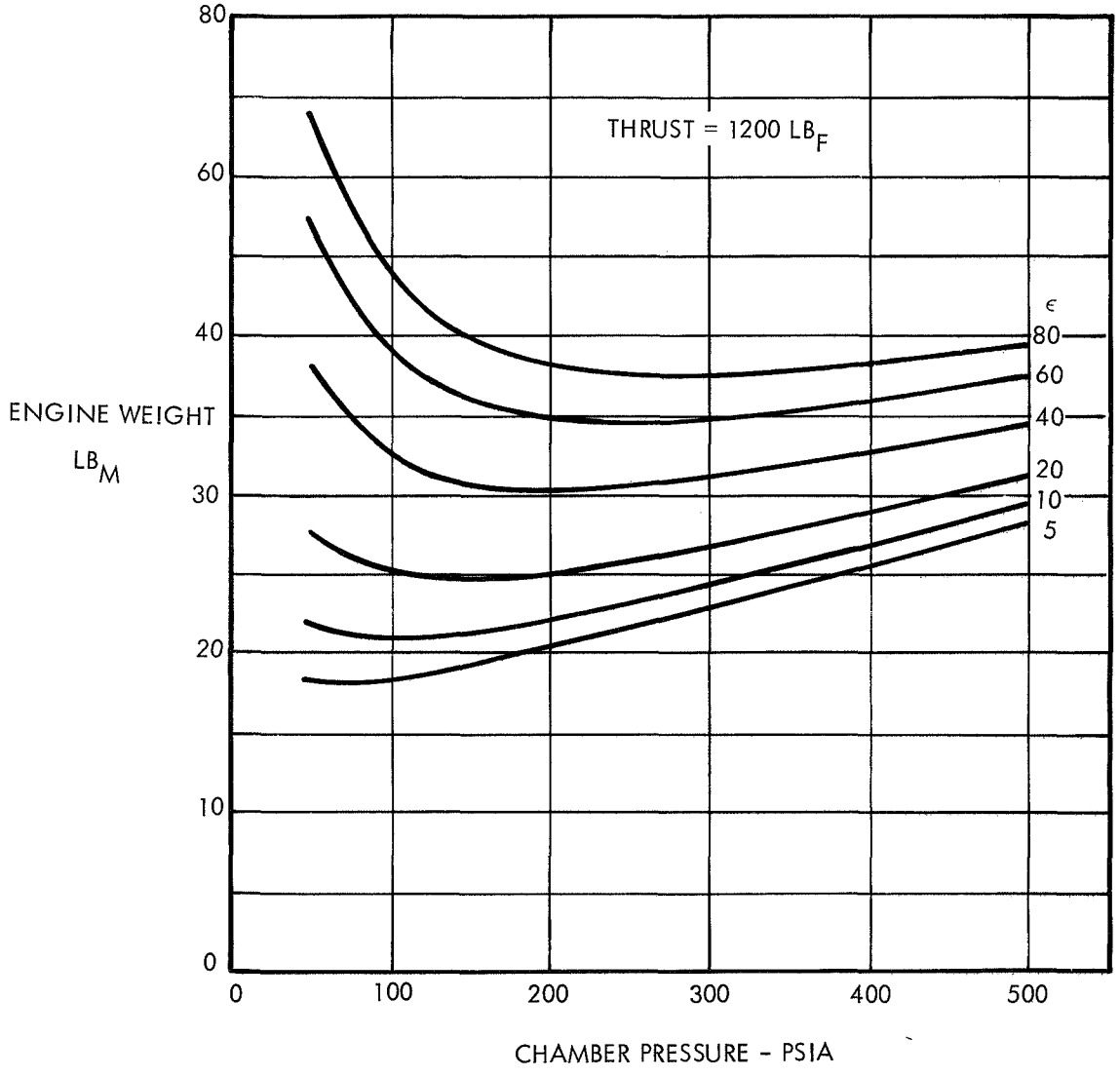

Figure II.D-12. Engine Weight as a Function of Chamber Pressure and Expansion Ratio for Systems Number 1 and 2

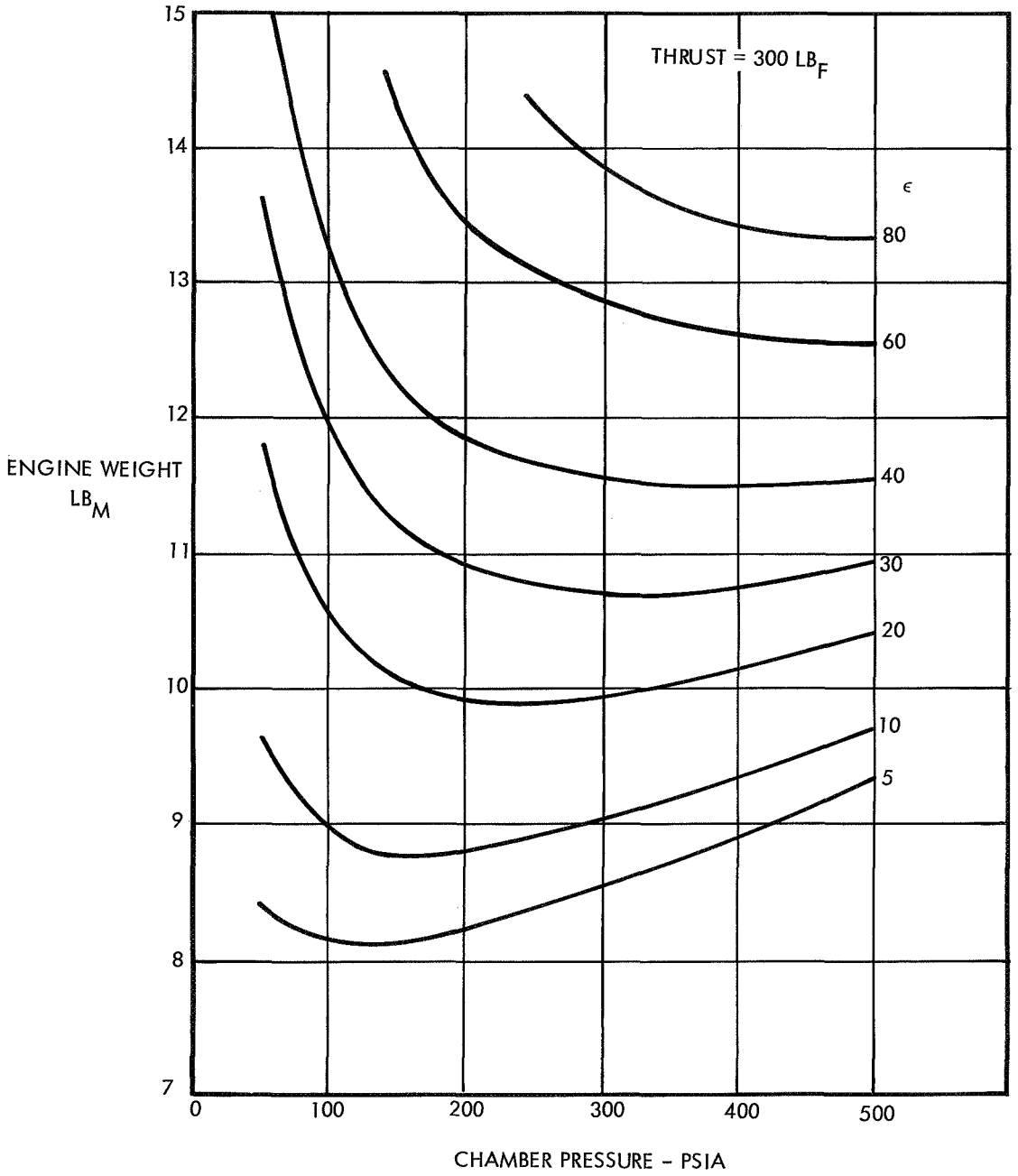

Figure II.D-13. Engine Weight as a Function of Chamber Pressure and Expansion Ratio for System Number 3

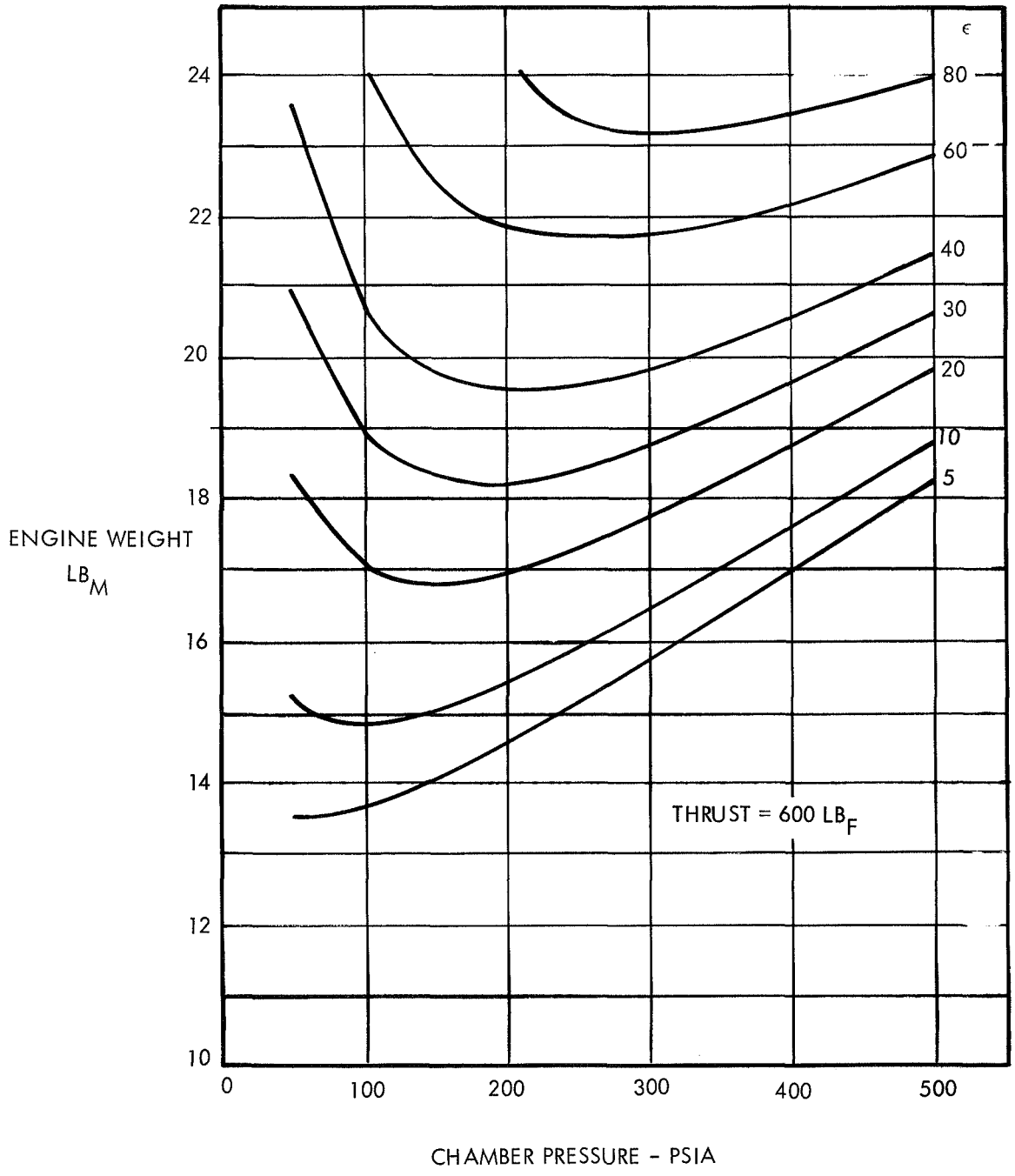

Figure II.D-14. Engine Weight as a Function of Chamber Pressure and Expansion Ratio for System Number 3

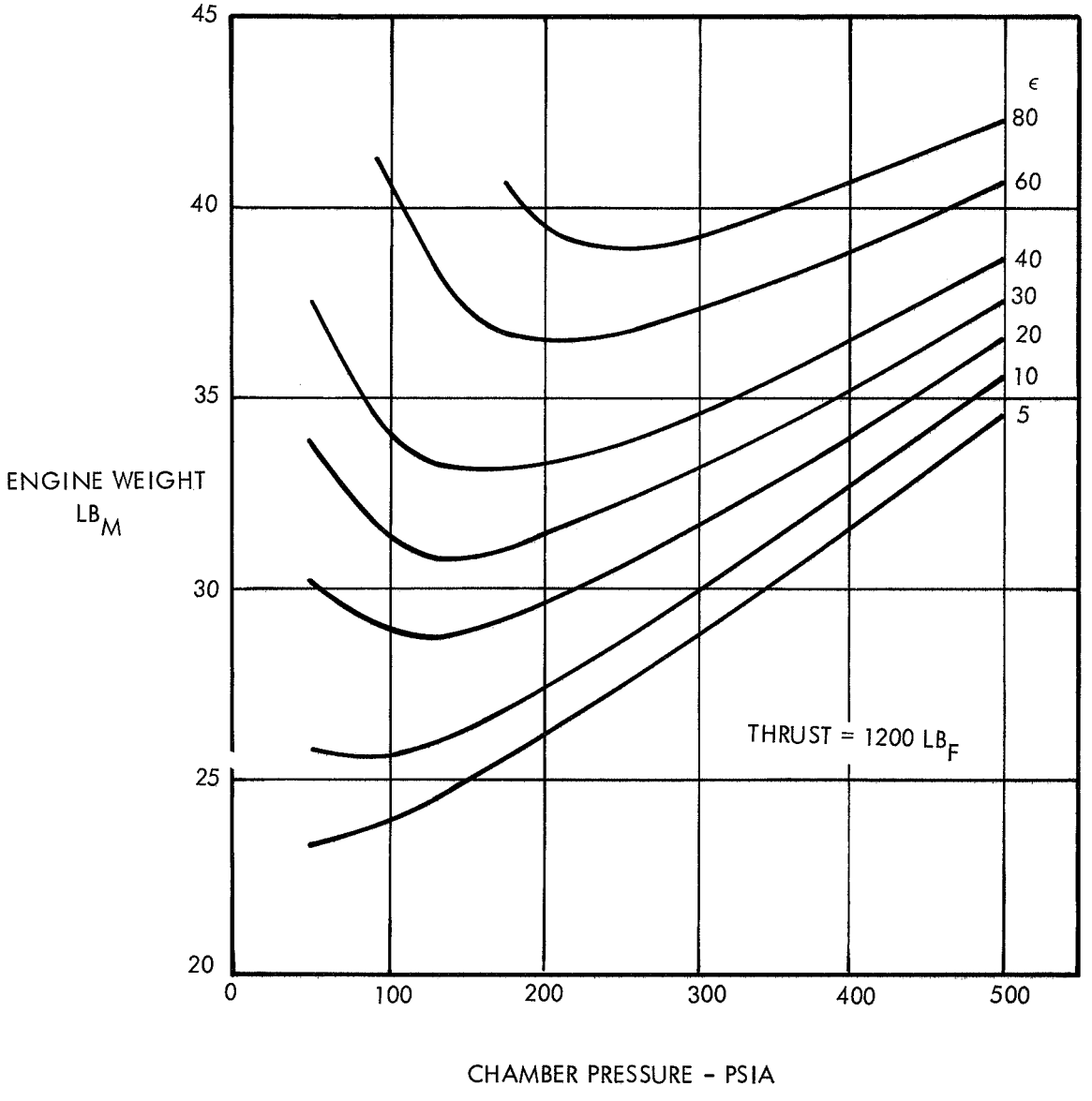

Figure II.D-15. Engine Weight as a Function of Chamber Pressure and Expansion Ratio for System Number 3

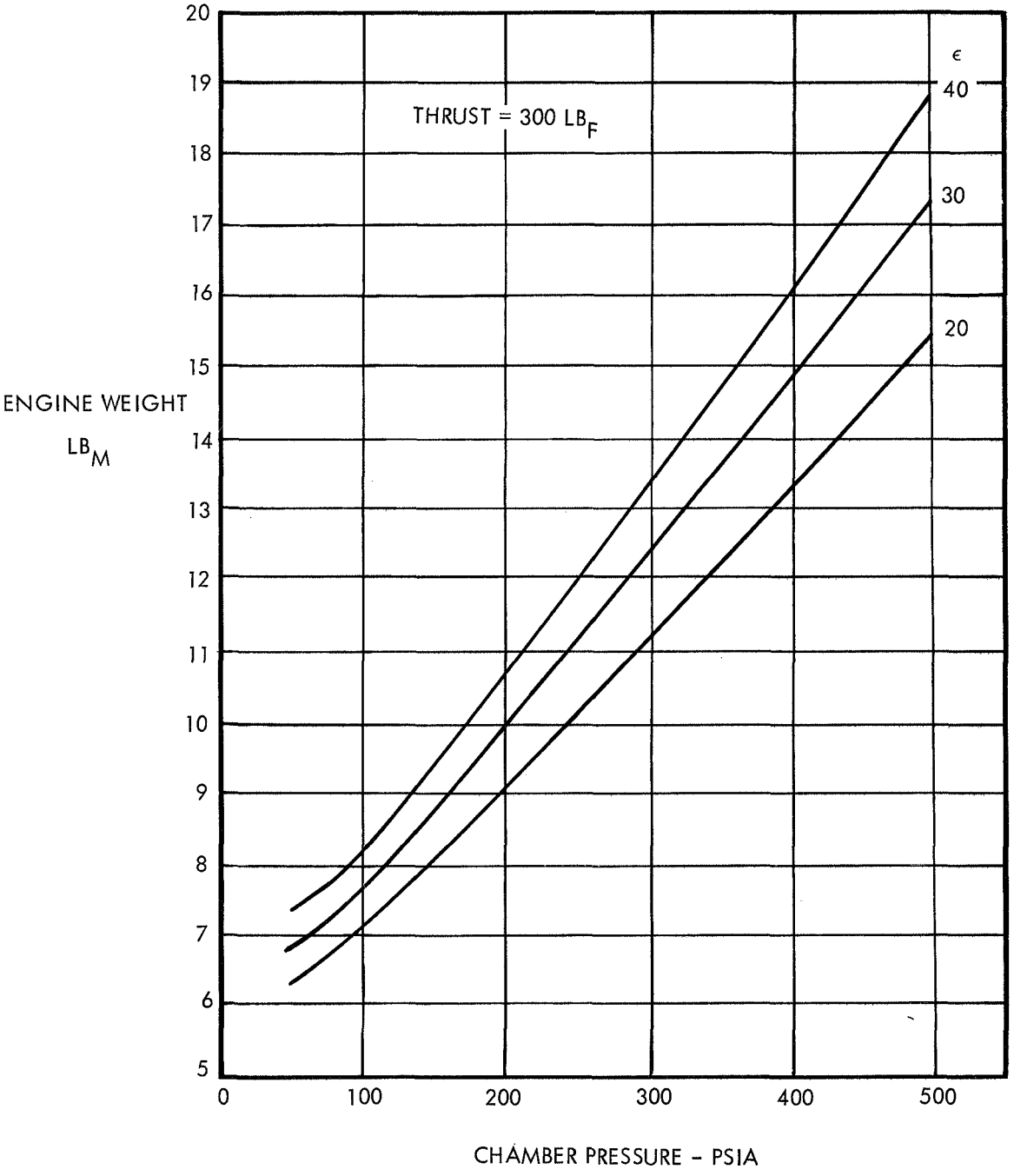

Figure II.D-16. Engine Weight as a Function of Chamber Pressure and Expansion Ratio for System Number 4

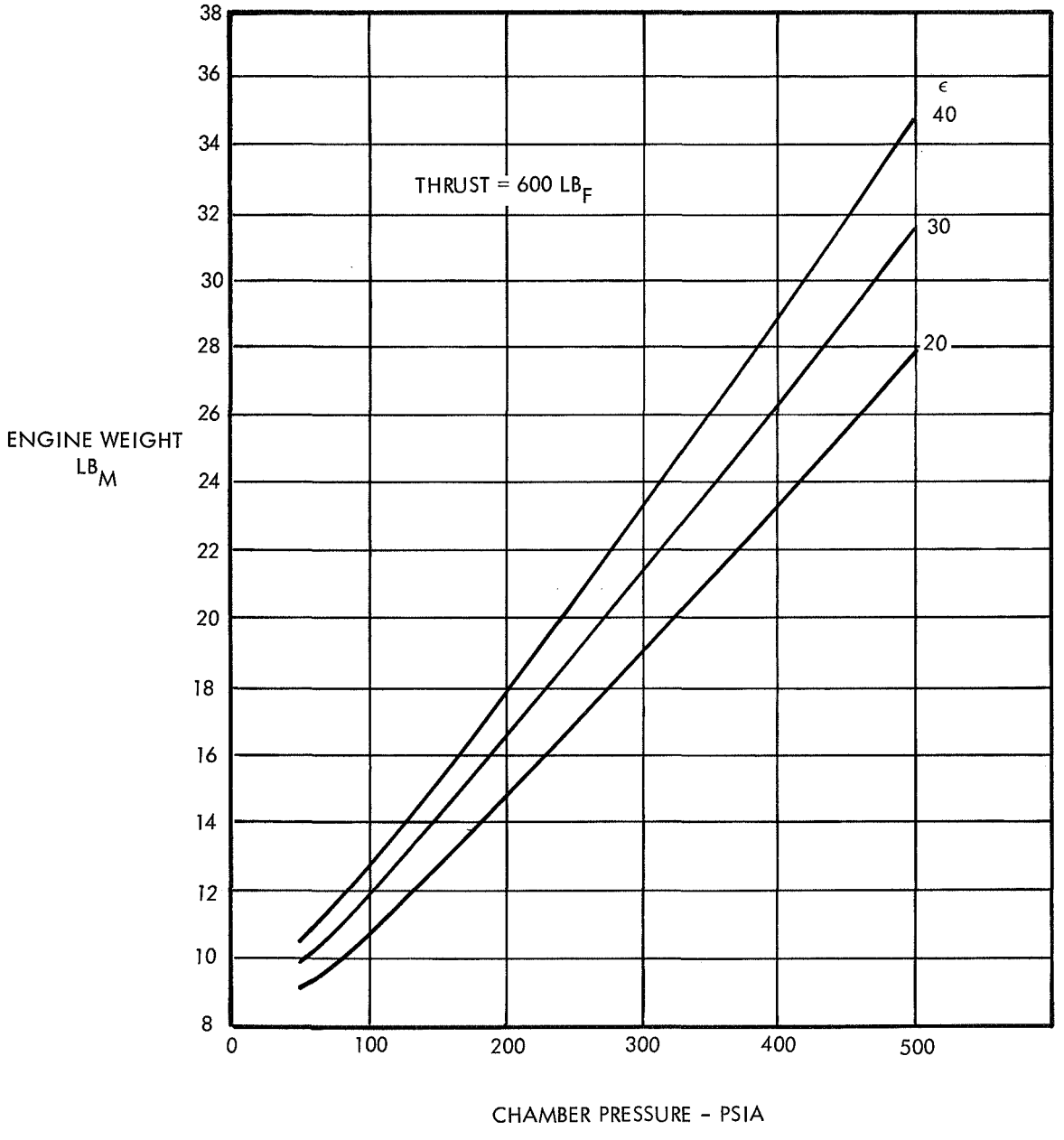

Figure II.D-17. Engine Weight as a Function of Chamber Pressure and Expansion Ratio for System Number 4

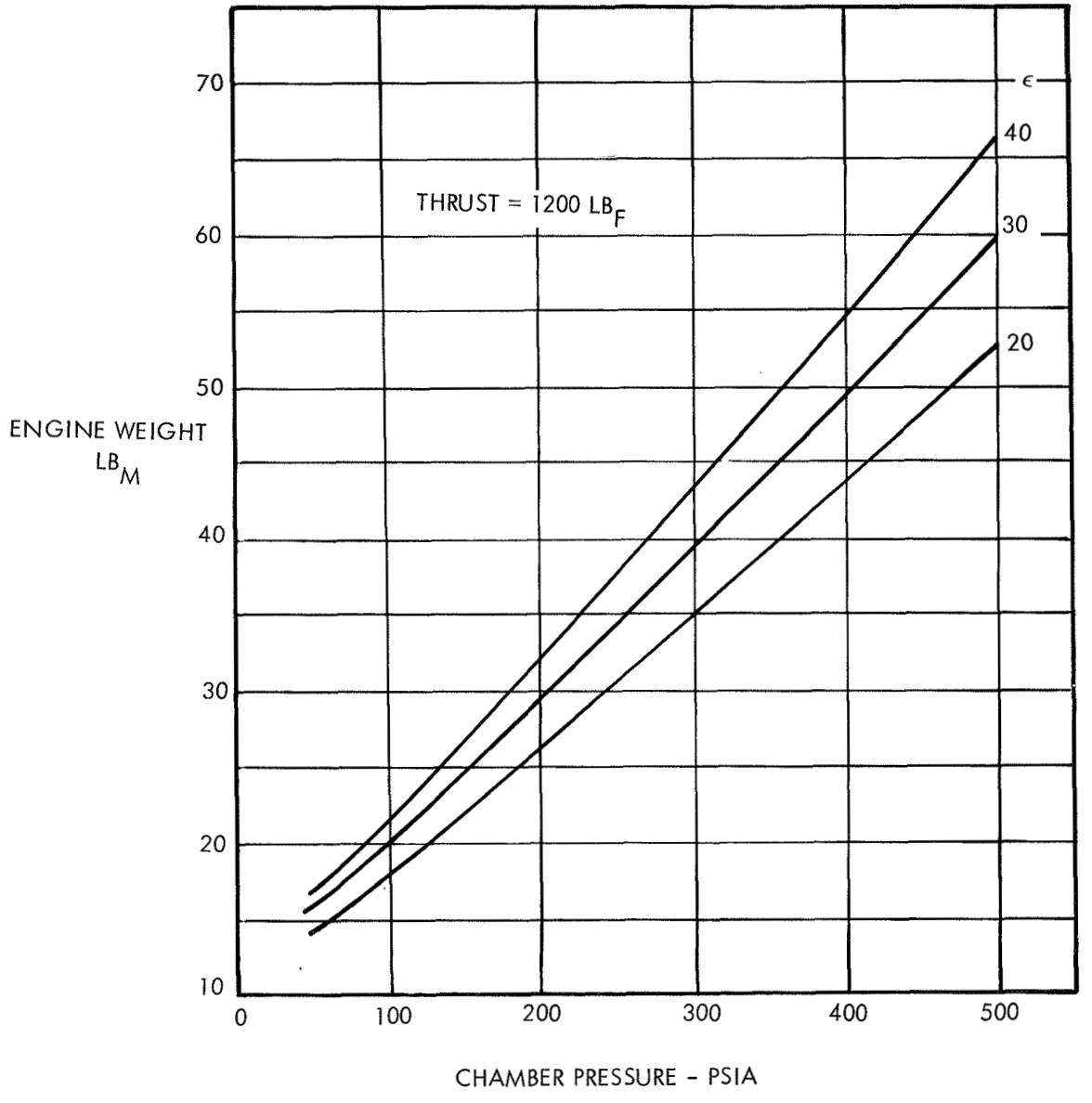

Figure II.D-18. Engine Weight as a Function of Chamber Pressure and Expansion Ratio for System Number 4

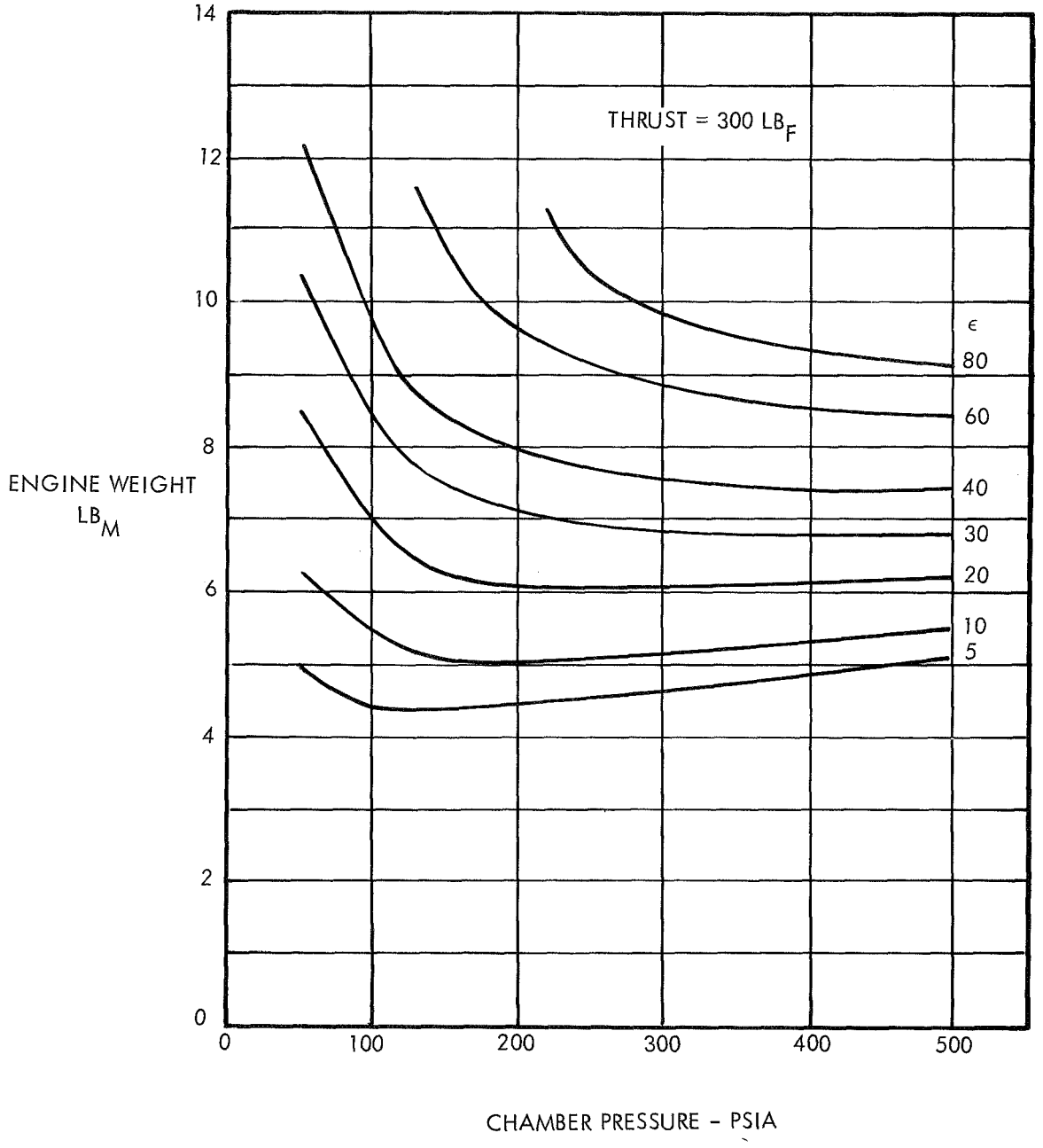

Figure II.D-19. Engine Weight as a Function of Chamber Pressure and Expansion Ratio for System Number 5

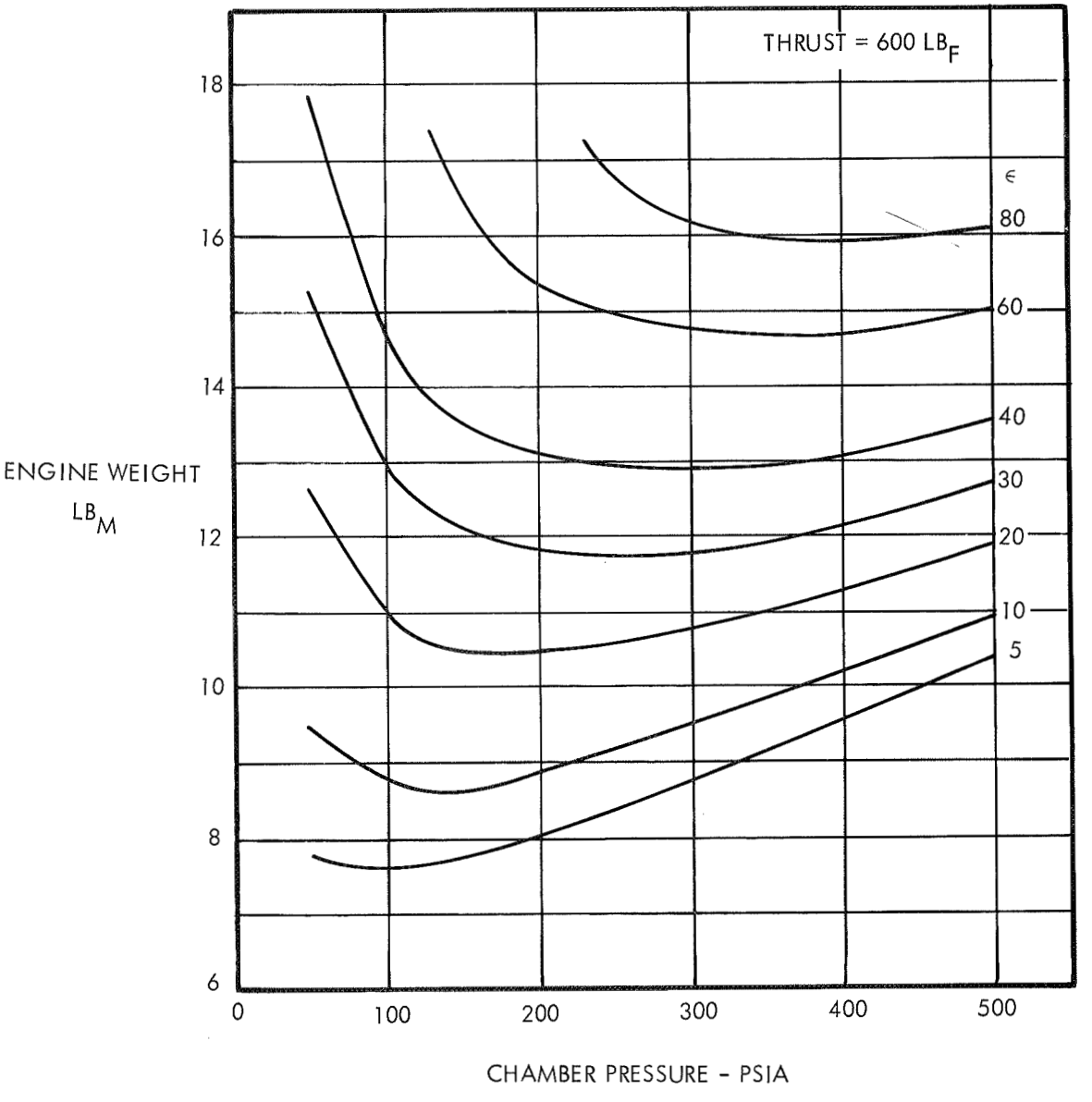

Figure II.D-20. Engine Weight as a Function of Chamber Pressure and Expansion Ratio for System Number 5

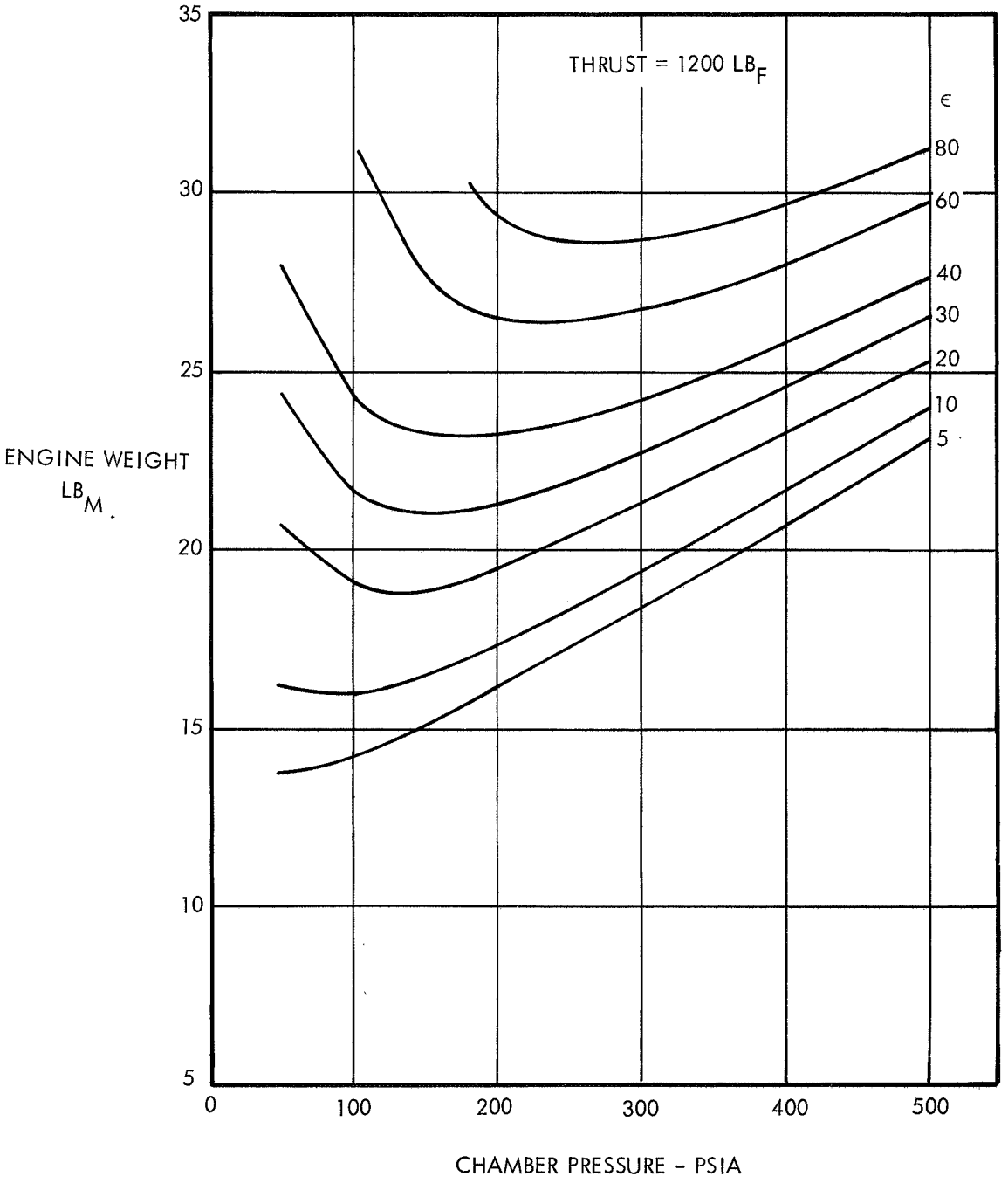

Figure II.D-21. Engine Weight as a Function of Chamber Pressure and Expansion Ratio for System Number 5

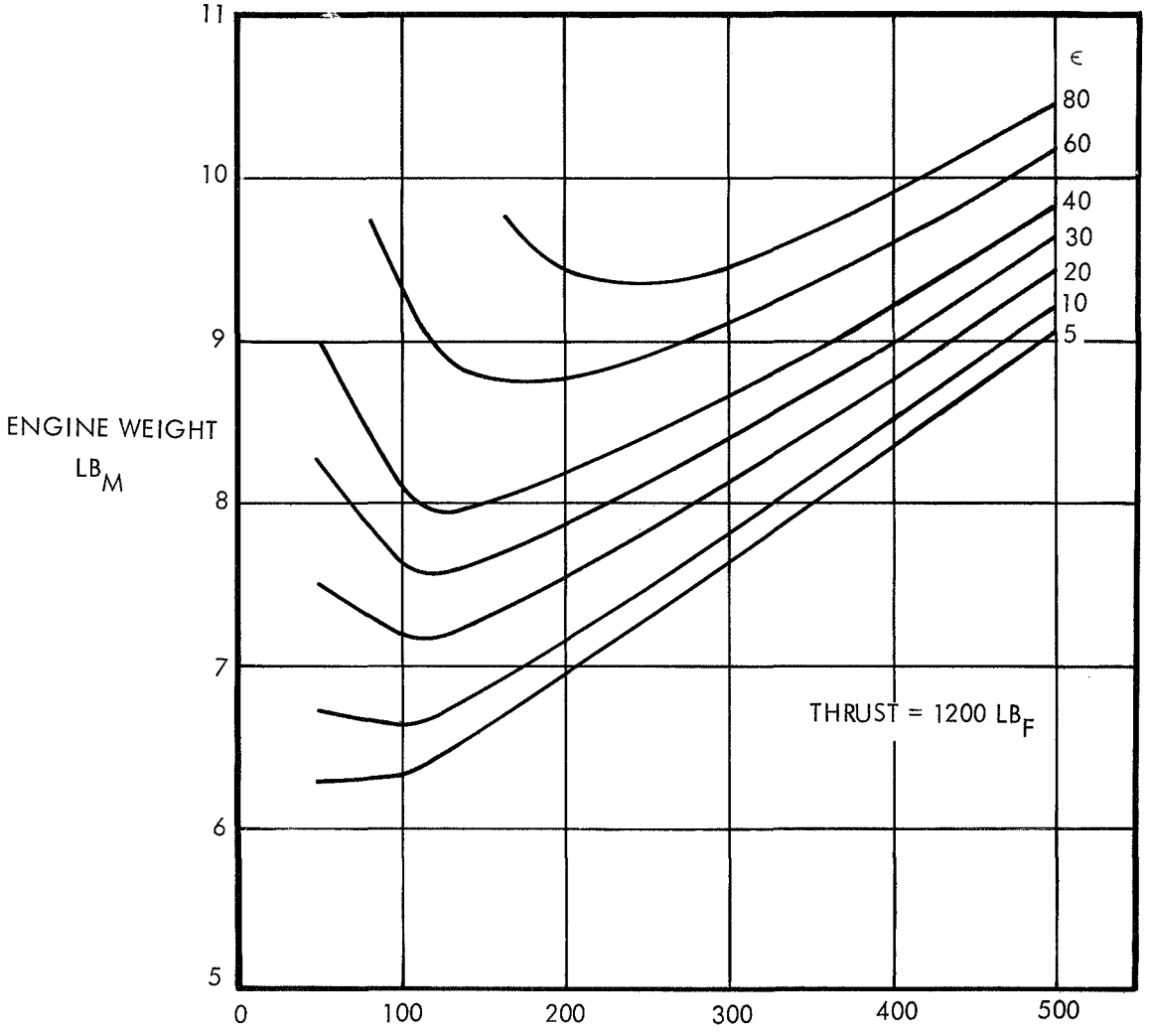

Figure II.D-22. Engine Weight as a Function of Chamber Pressure and Expansion Ratio for System Number 6

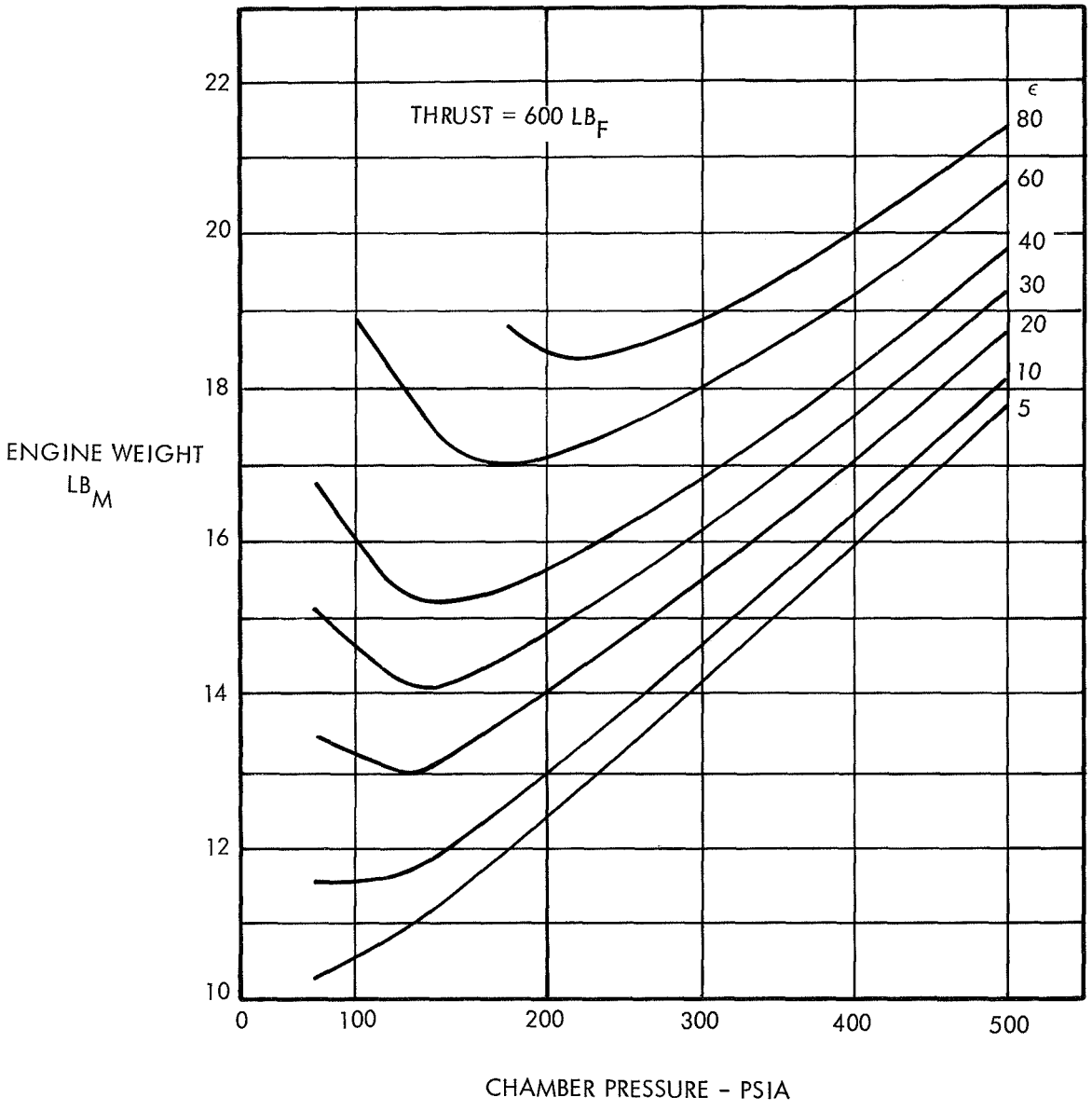

Figure II.D-23. Engine Weight as a Function of Chamber Pressure and Expansion Ratio for System Number 6

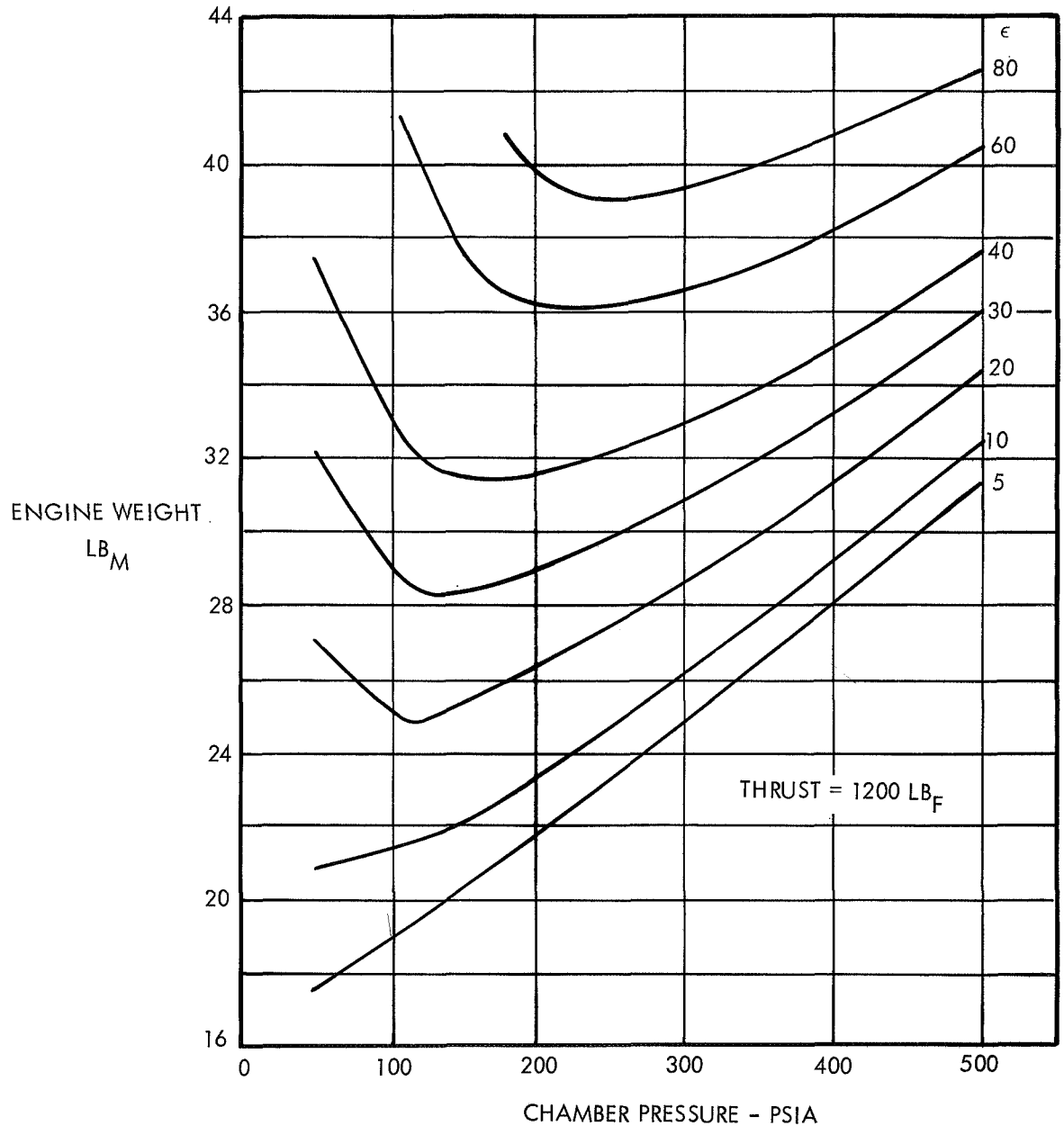

Figure II.D-24. Engine Weight as a Function of Chamber Pressure and Expansion Ratio for System Number 6

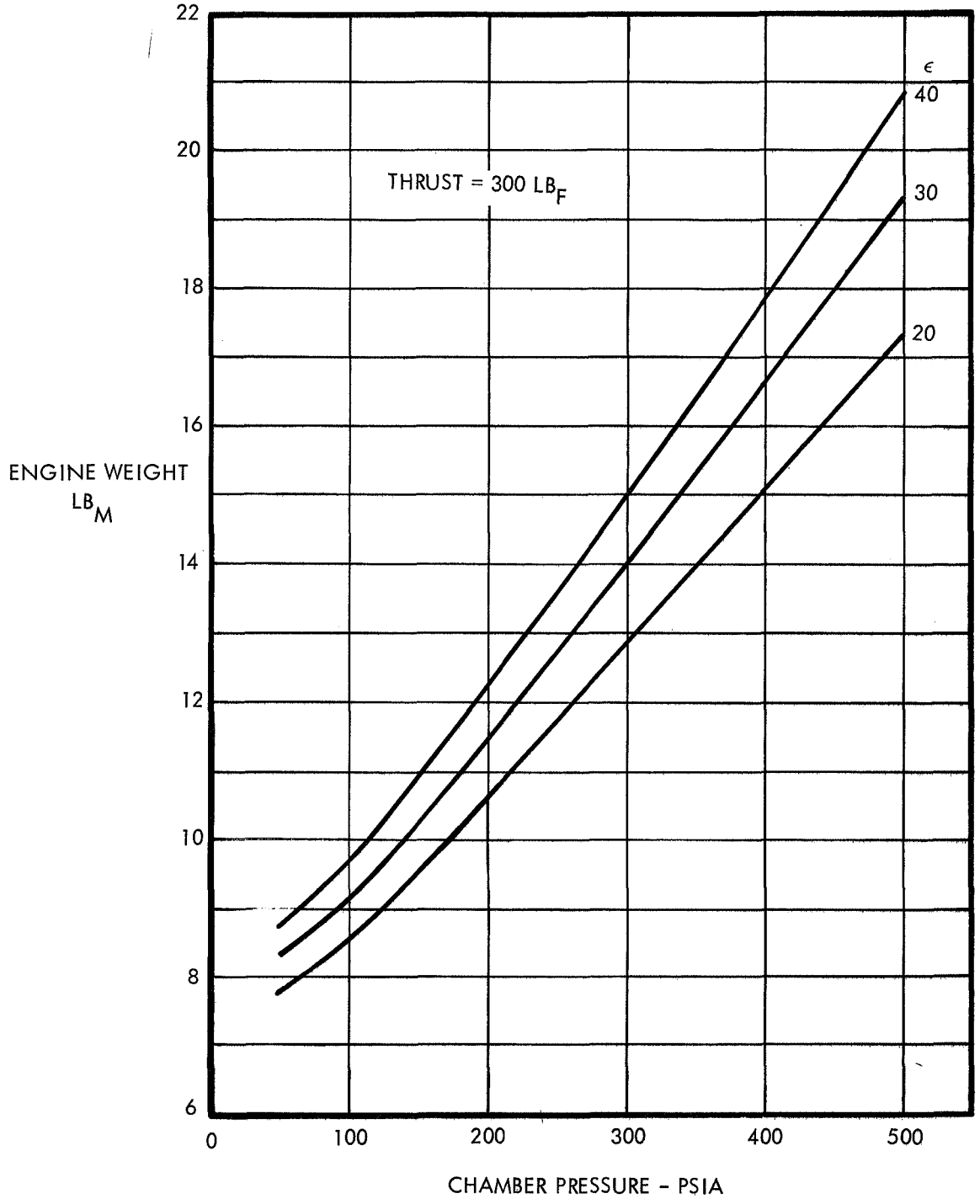

Figure II.D-25. Engine Weight as a Function of Chamber Pressure and Expansion Ratio for System Number 7

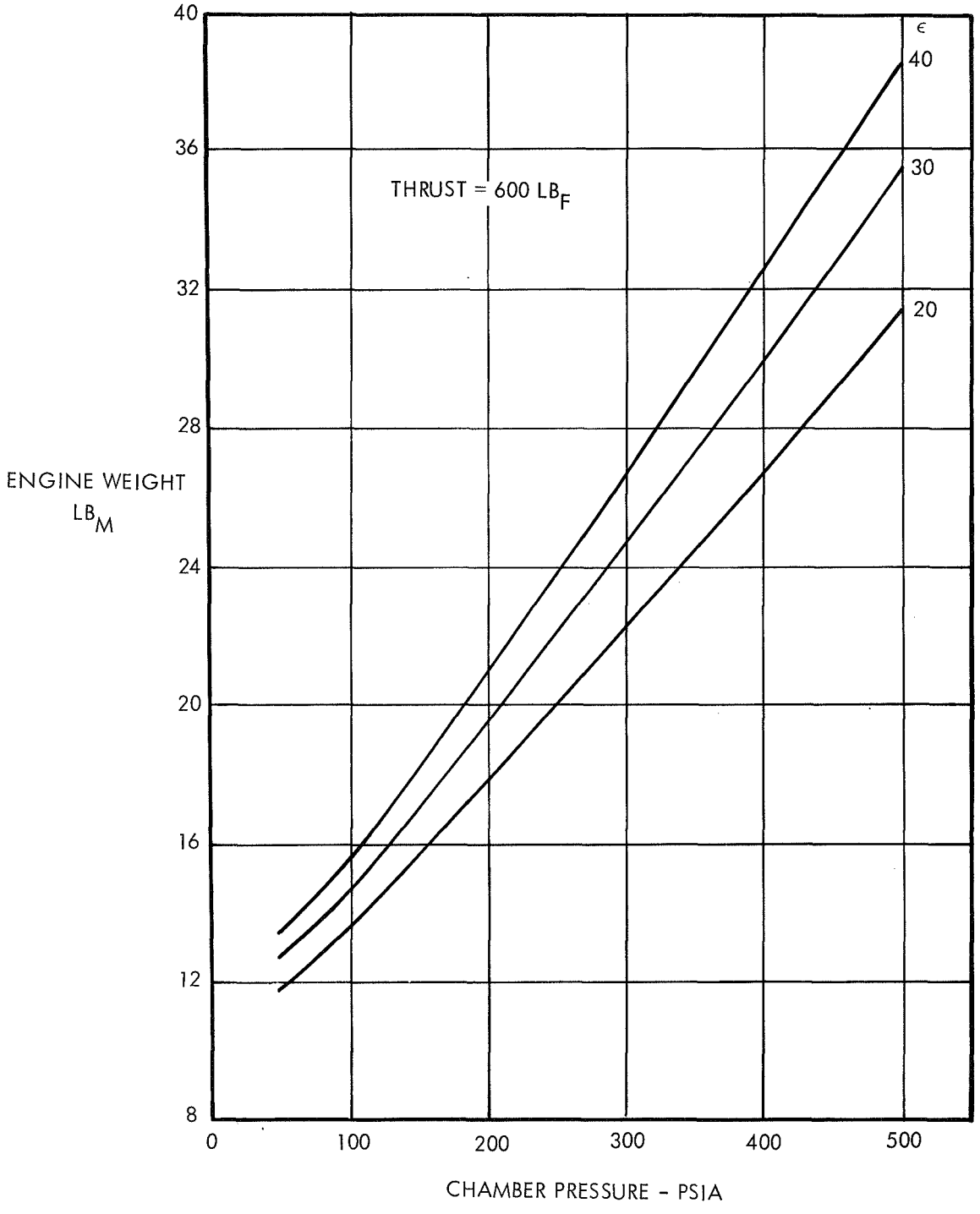

Figure II.D-26. Engine Weight as a Function of Chamber Pressure and Expansion Ratio for System Number 7

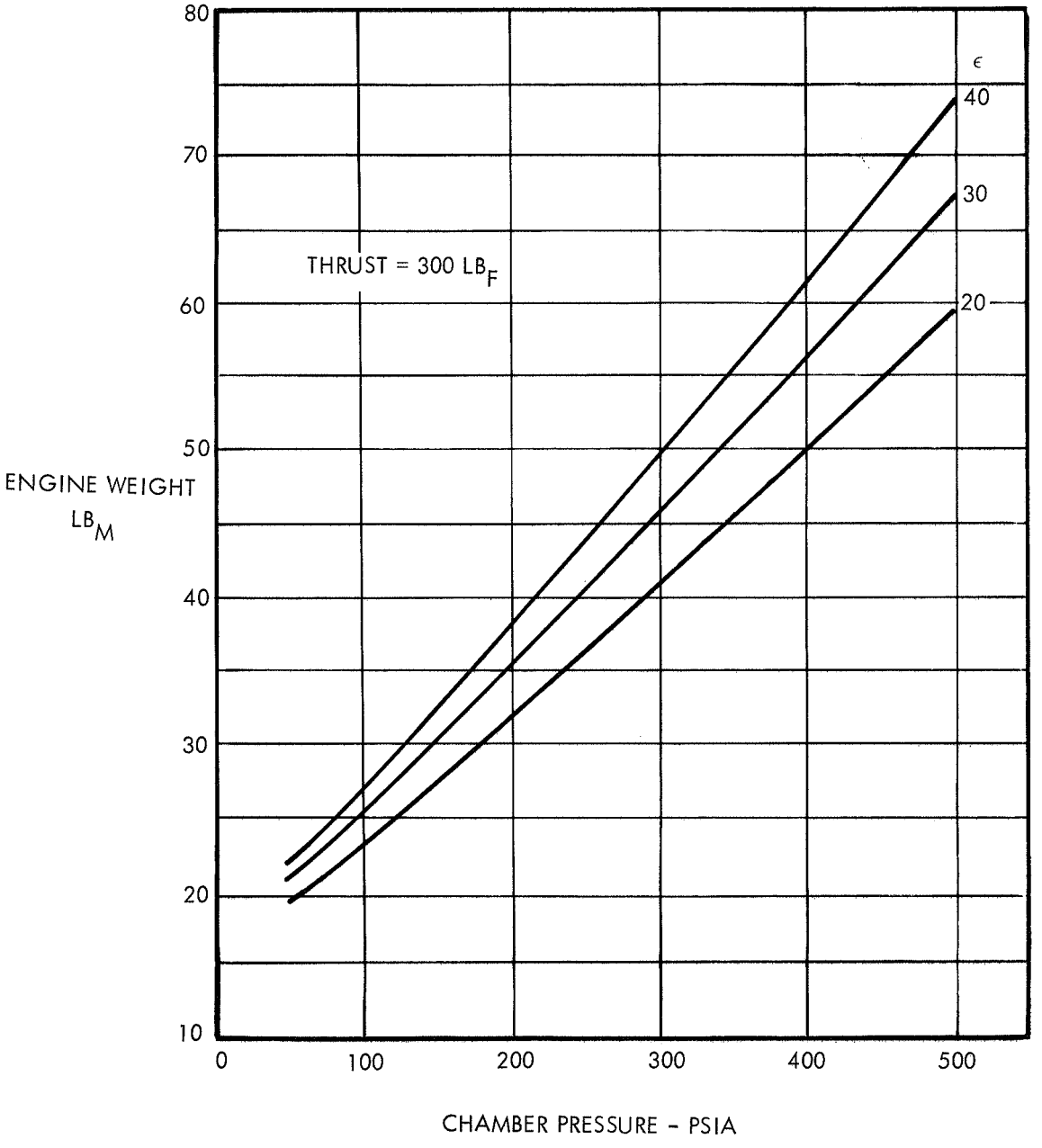

Figure II.D-27. Engine Weight as a Function of Chamber Pressure and Expansion Ratio for System Number 7

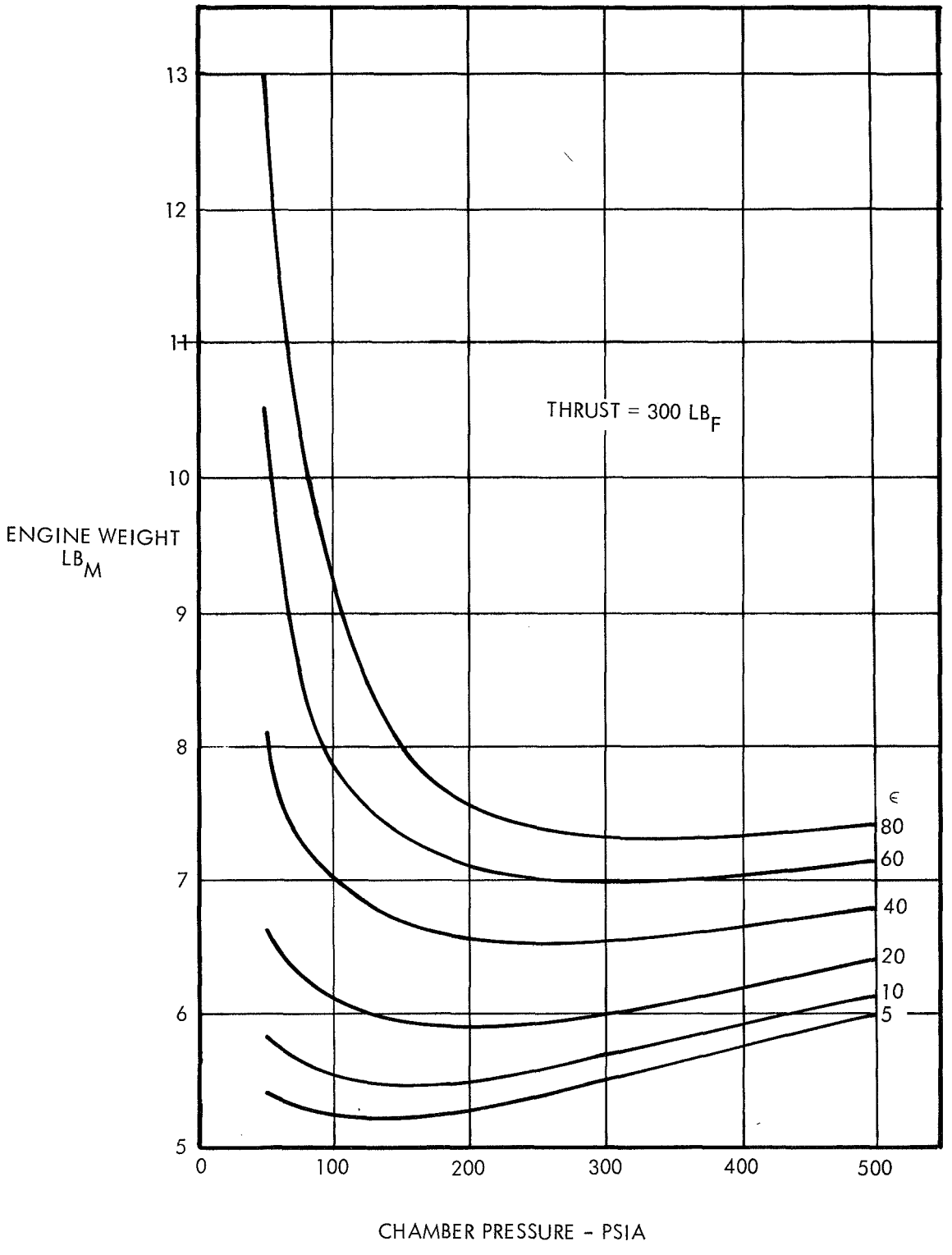

Figure II.D-28. Engine Weight as a Function of Chamber Pressure and Expansion Ratio for System Number 8

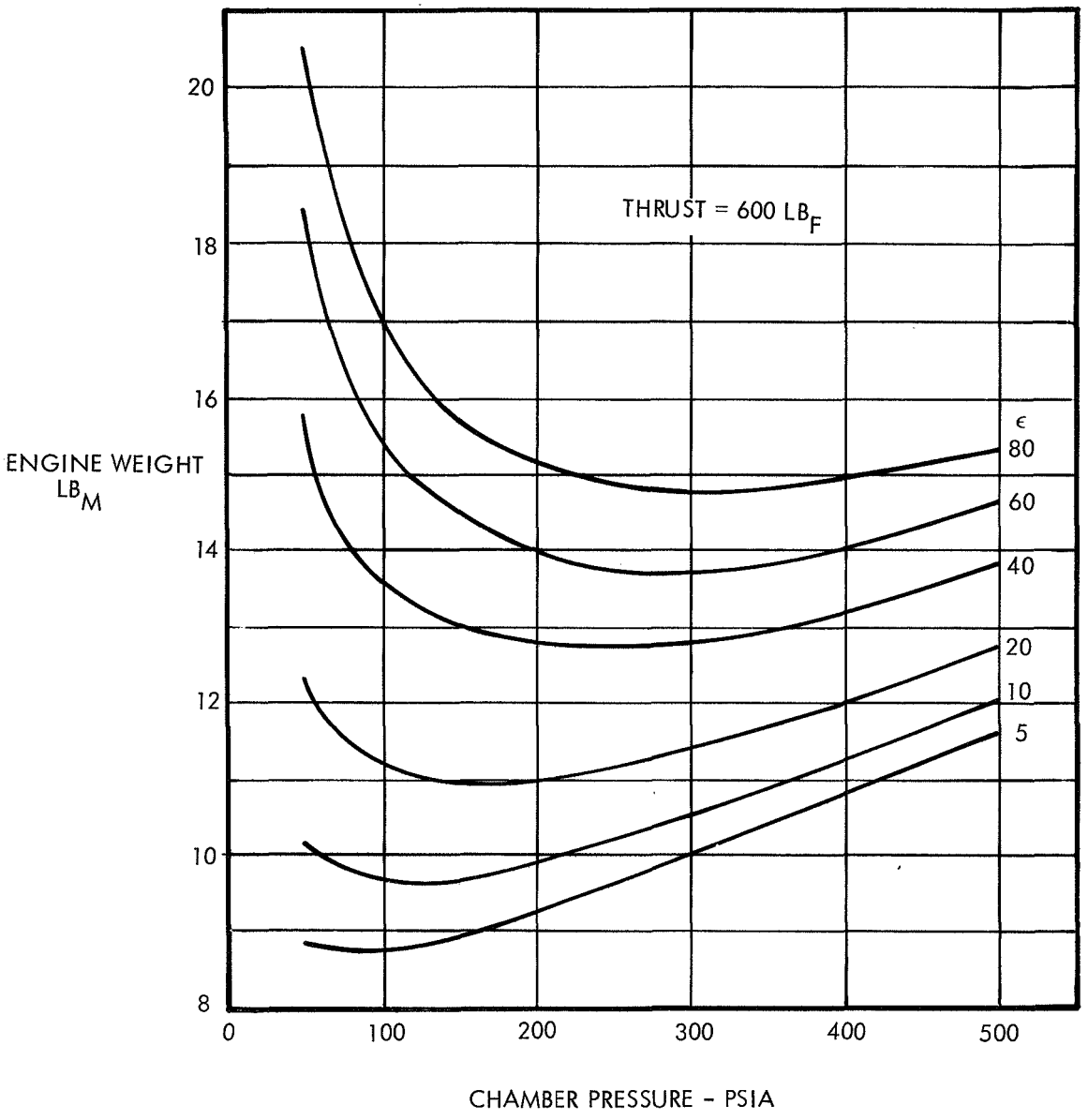

Figure II.D-29. Engine Weight as a Function of Chamber Pressure and Expansion Ratio for System Number 8

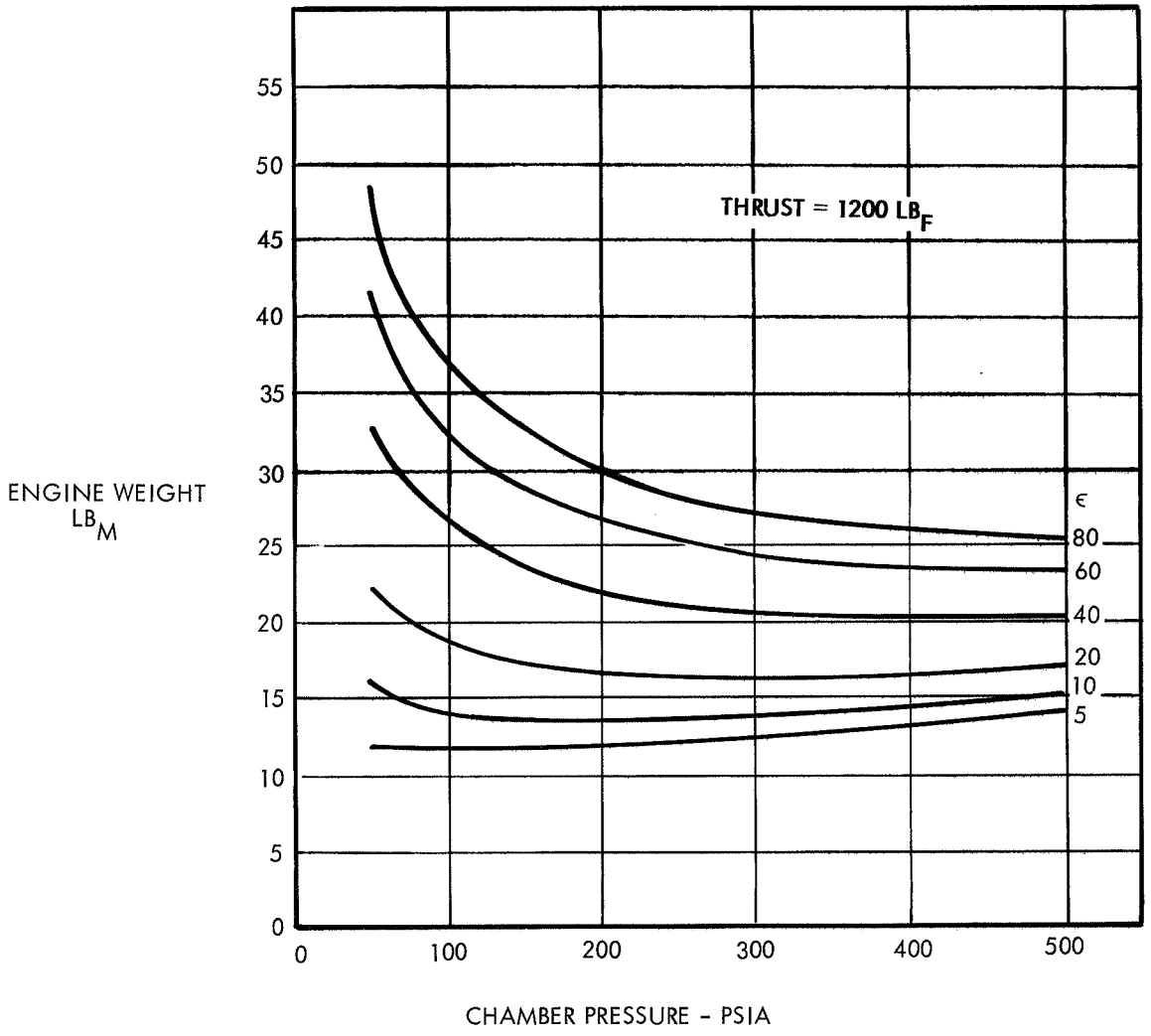

Figure II.D-30. Engine Weight as a Function of Chamber Pressure and Expansion Ratio for System Number 8

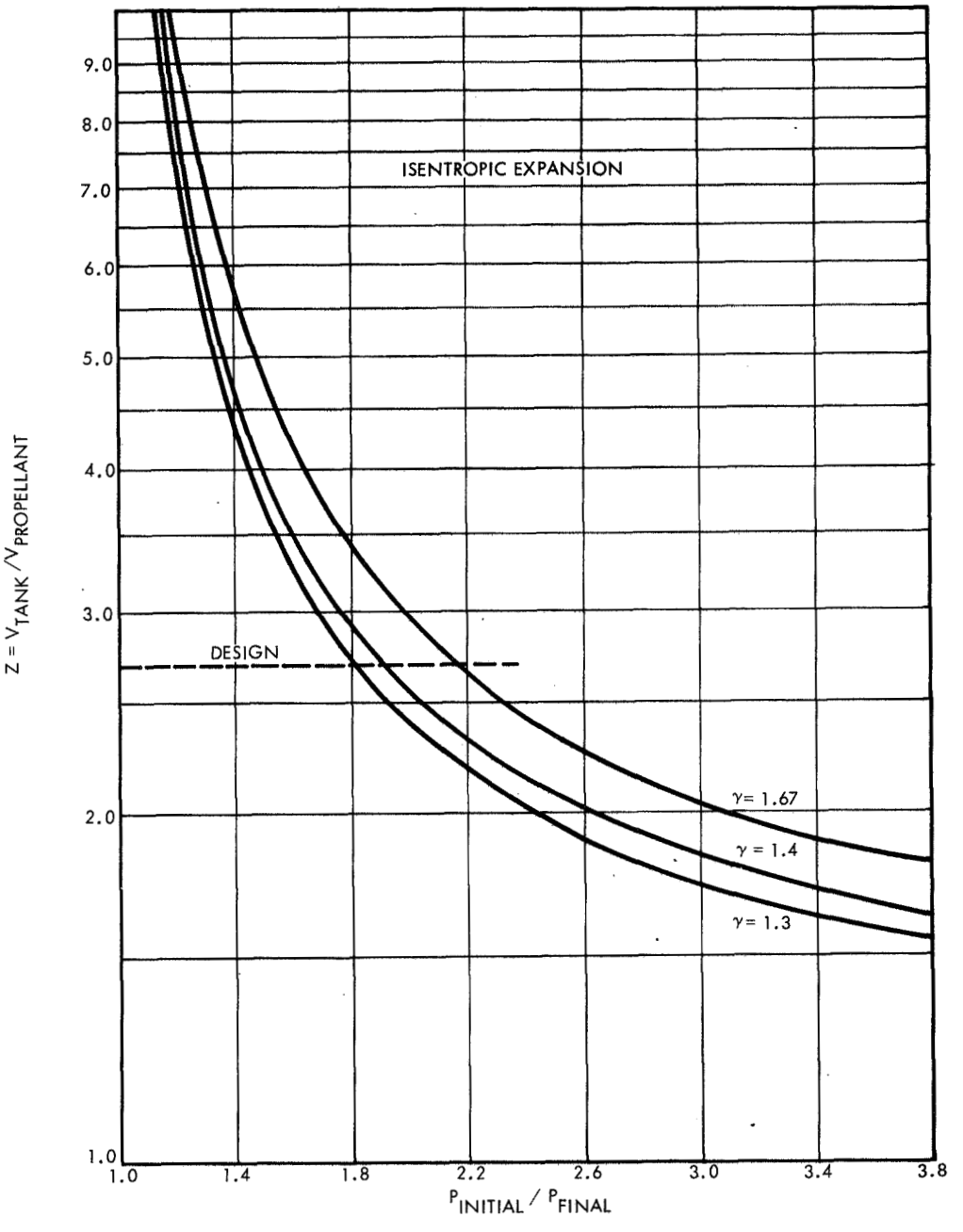

Figure II.D-31. Propellant Tank Volume Ratio

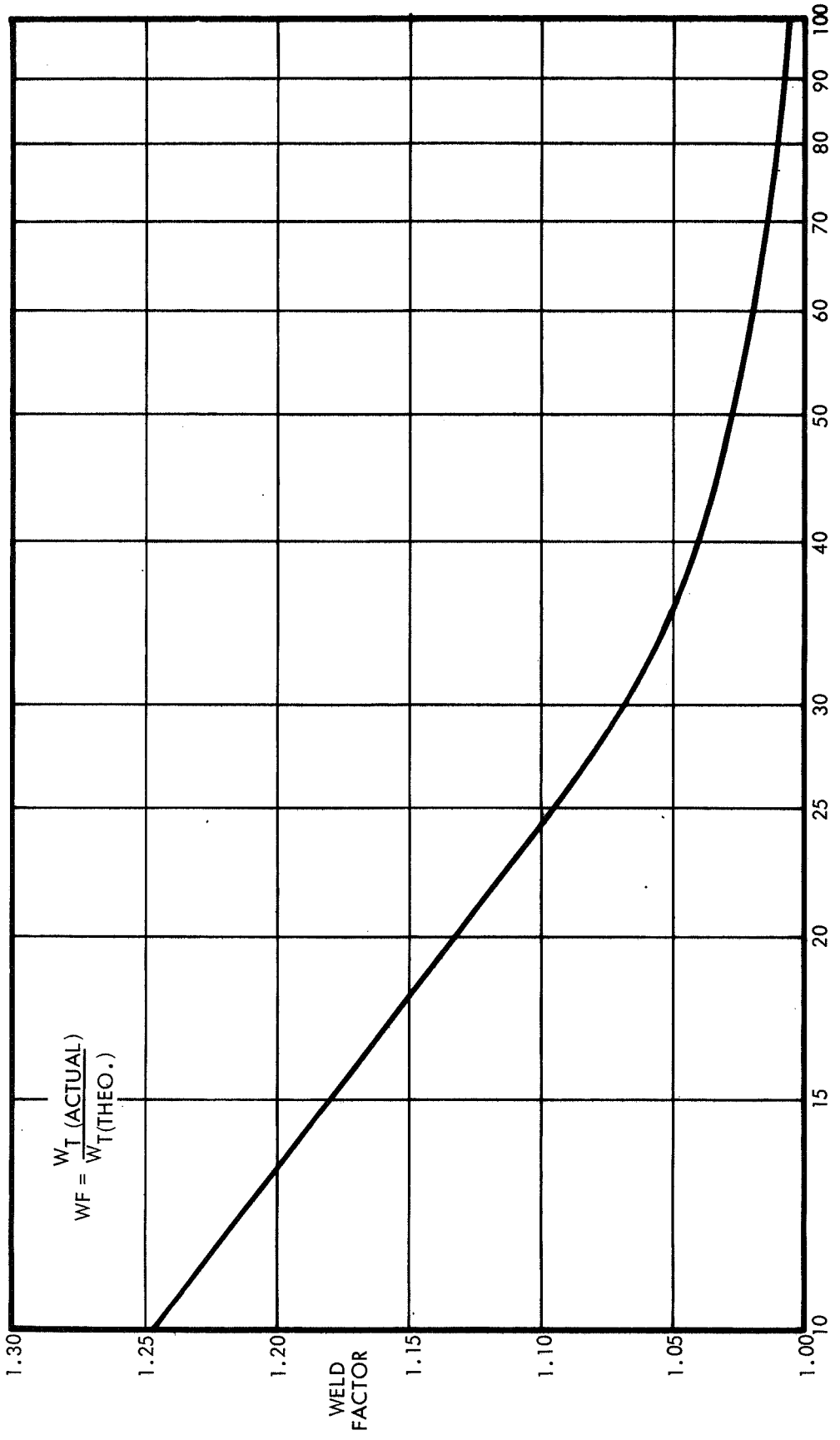

Figure II.D-32. Weld Factor Vs Tank Diameter

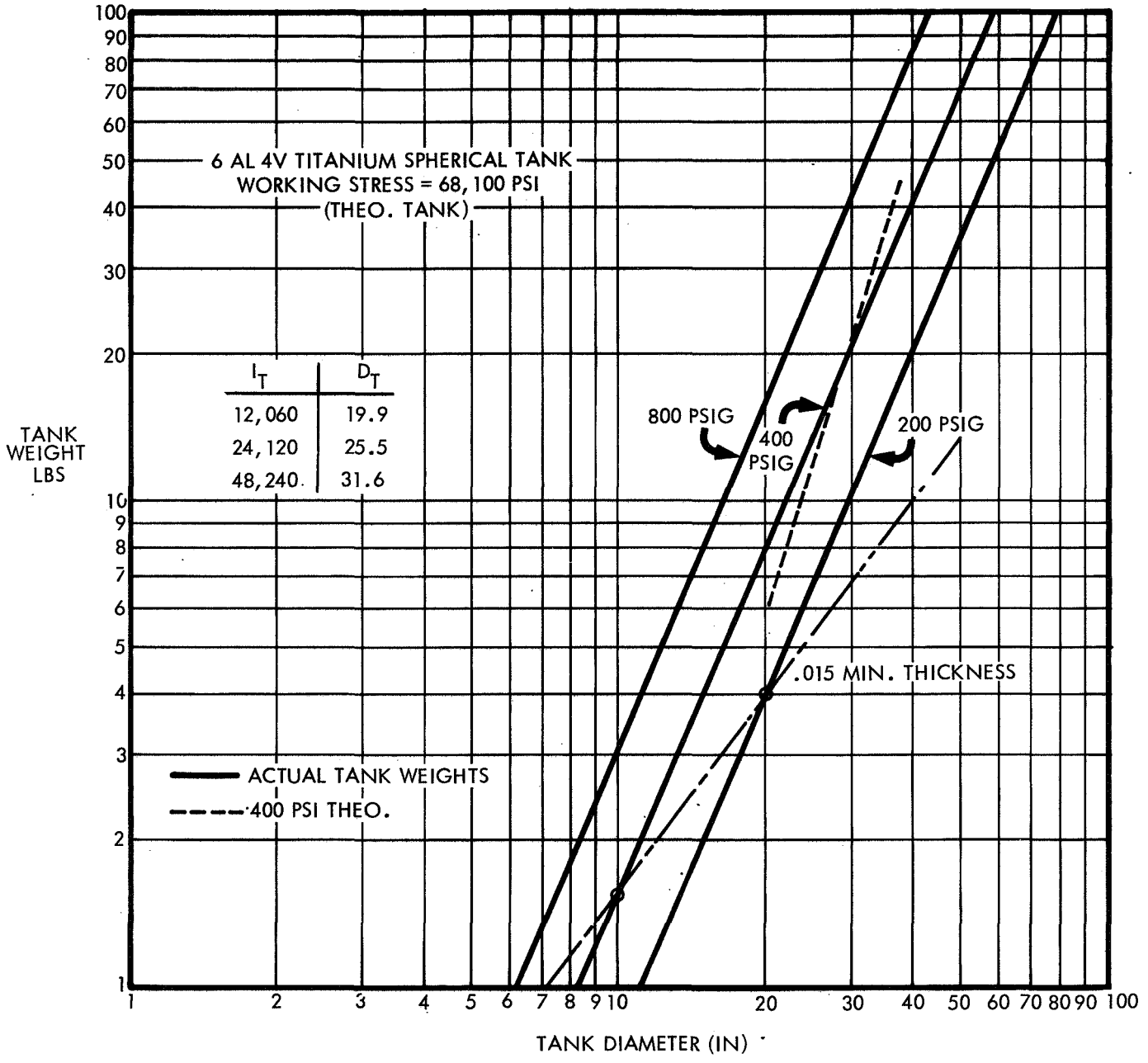

Figure II.D-33. Spherical Propellant Tank Weight Comparison

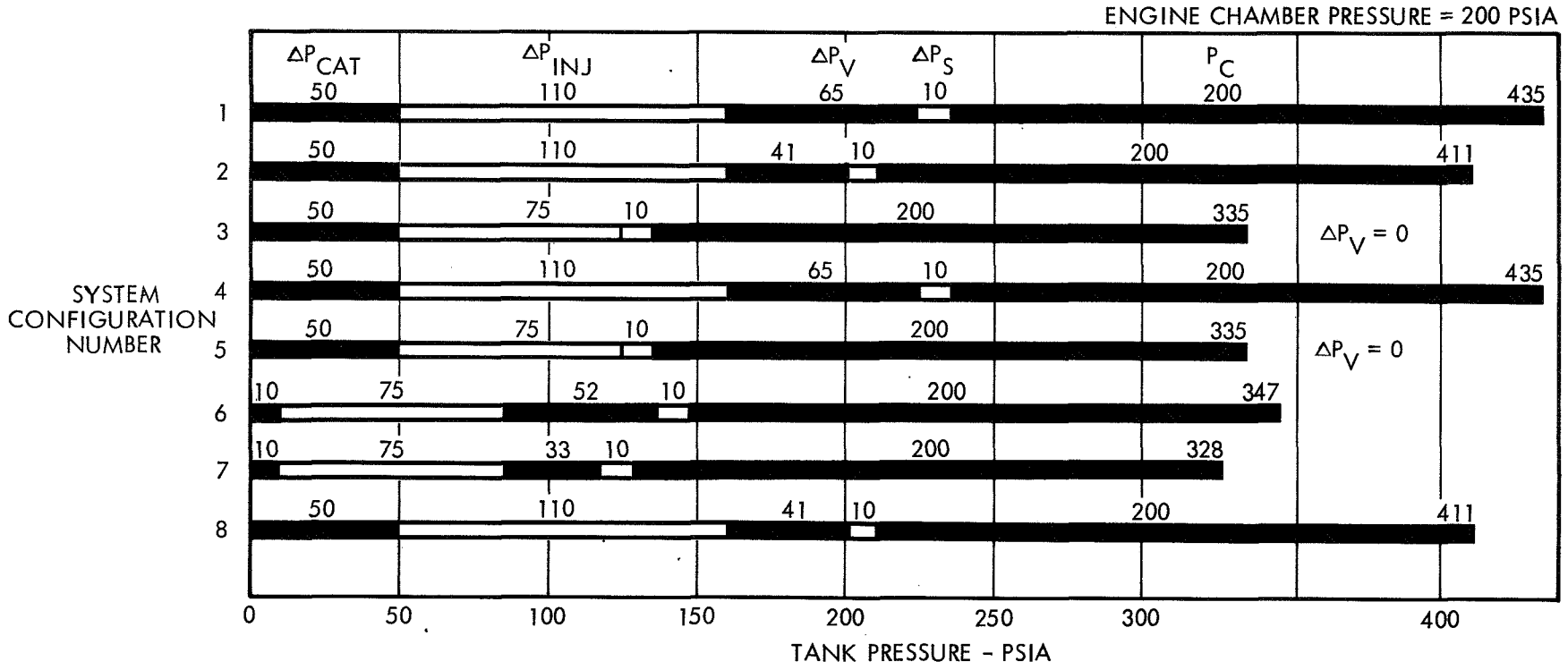

Figure II.D-34. System Pressure Comparison

FIGURE II.D-35
SYSTEM WEIGHT AS A FUNCTION OF CHAMBER PRESSURE AND EXPANSION RATIO FOR SYSTEM NUMBER 1

THRUST = 300 LB_F

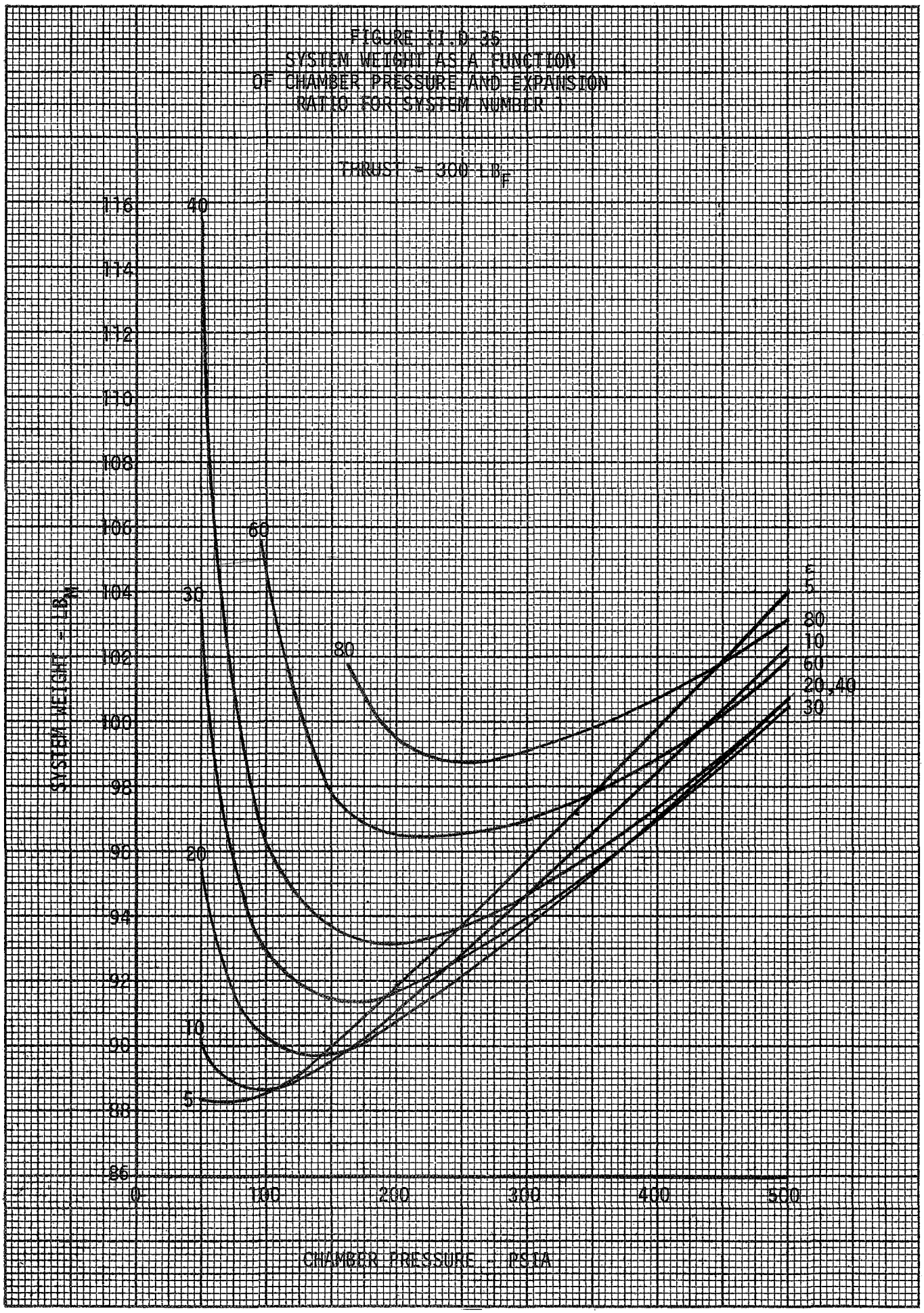

FIGURE II.D-36
SYSTEM WEIGHT AS A FUNCTION
OF CHAMBER PRESSURE AND EXPANSION

THRUST = 600 LB_F

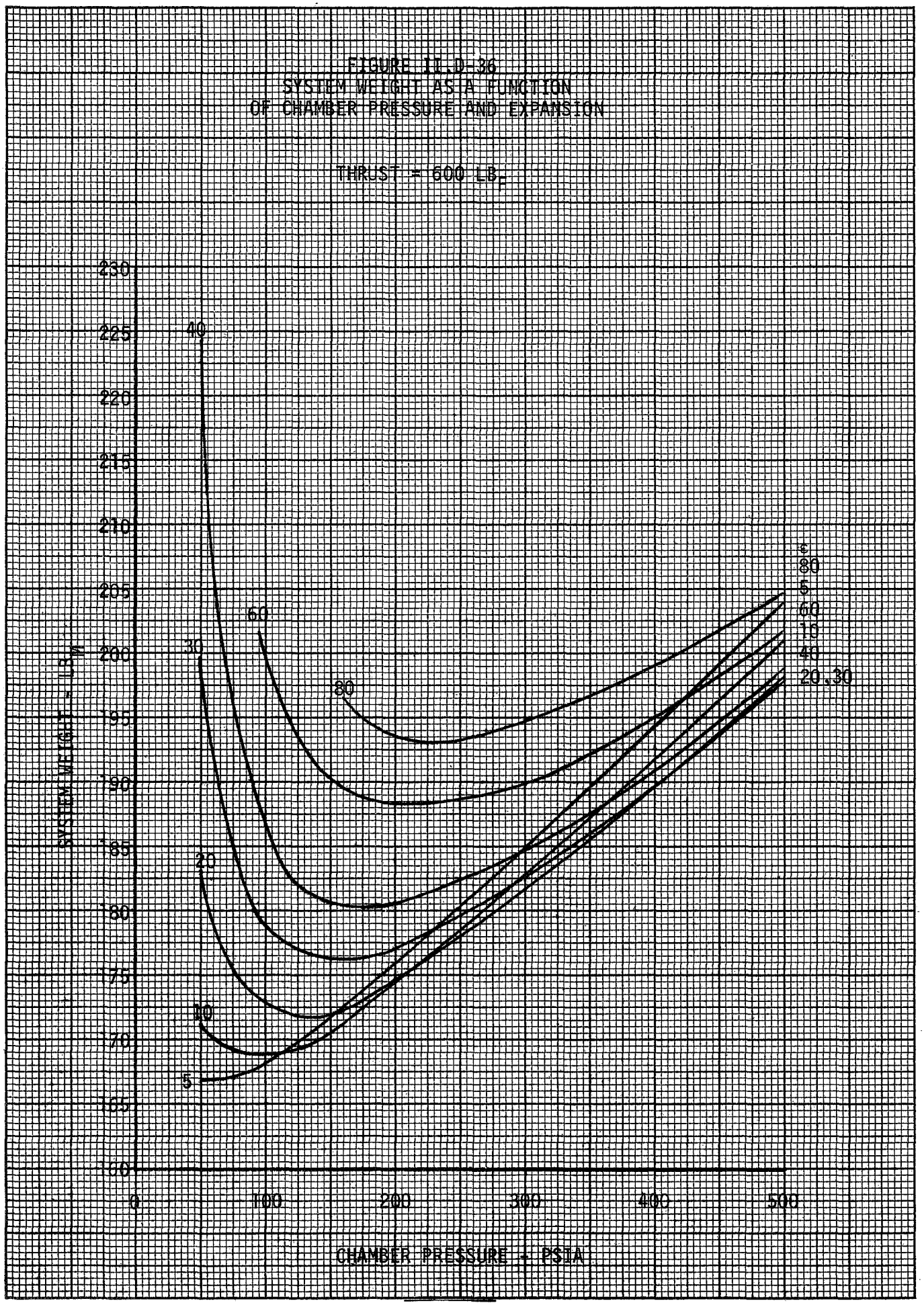

FIGURE II.D-37
SYSTEM WEIGHT AS A FUNCTION OF CHAMBER PRESSURE AND EXPANSION RATIO FOR SYSTEM NUMBER 1

THRUST = 1200 LB_F

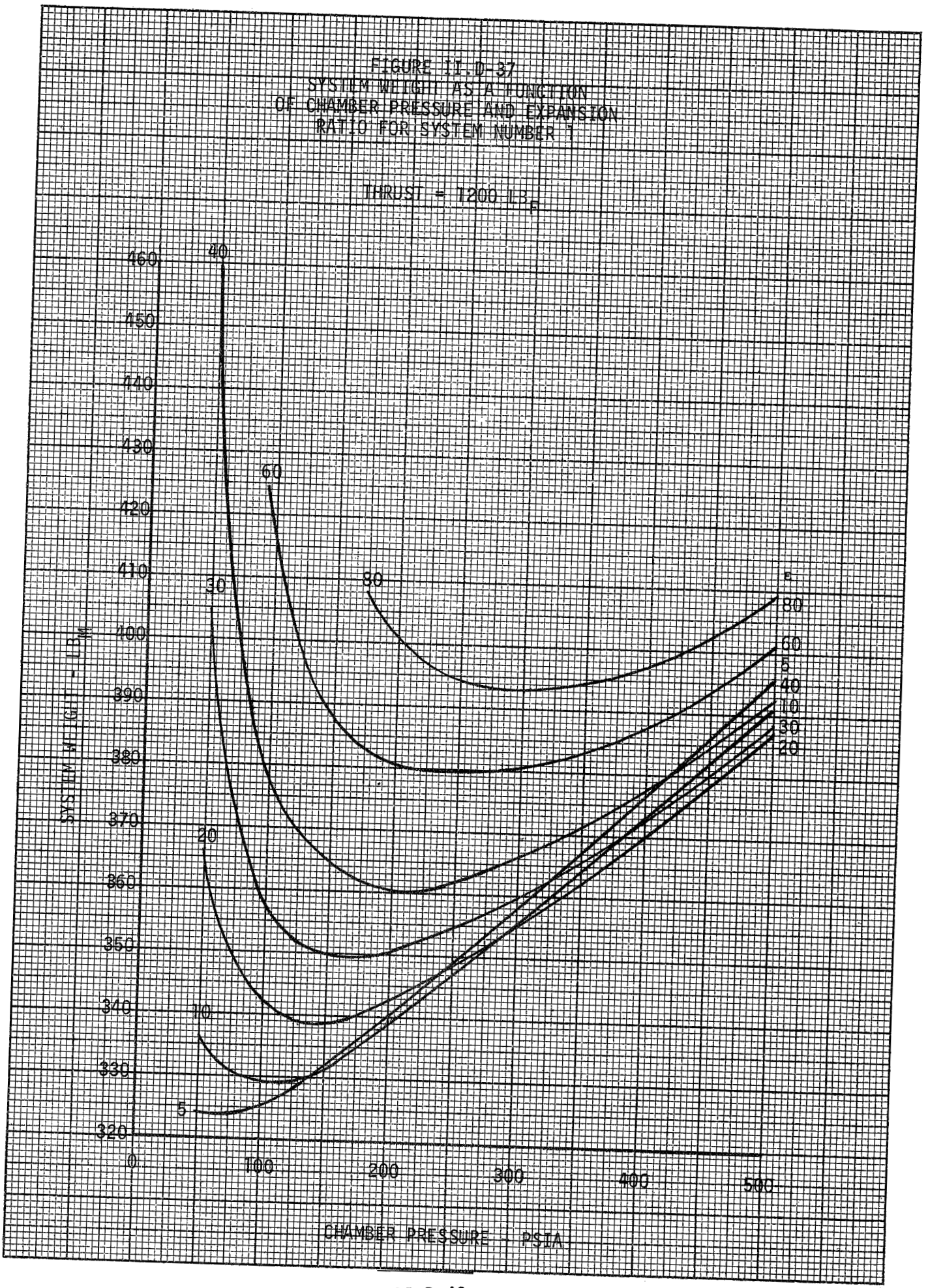

FIGURE II.D-38
SYSTEM WEIGHT AS A FUNCTION
OF CHAMBER PRESSURE AND EXPANSION
RATIO FOR SYSTEM NUMBER 2

THRUST = 300 LB_F

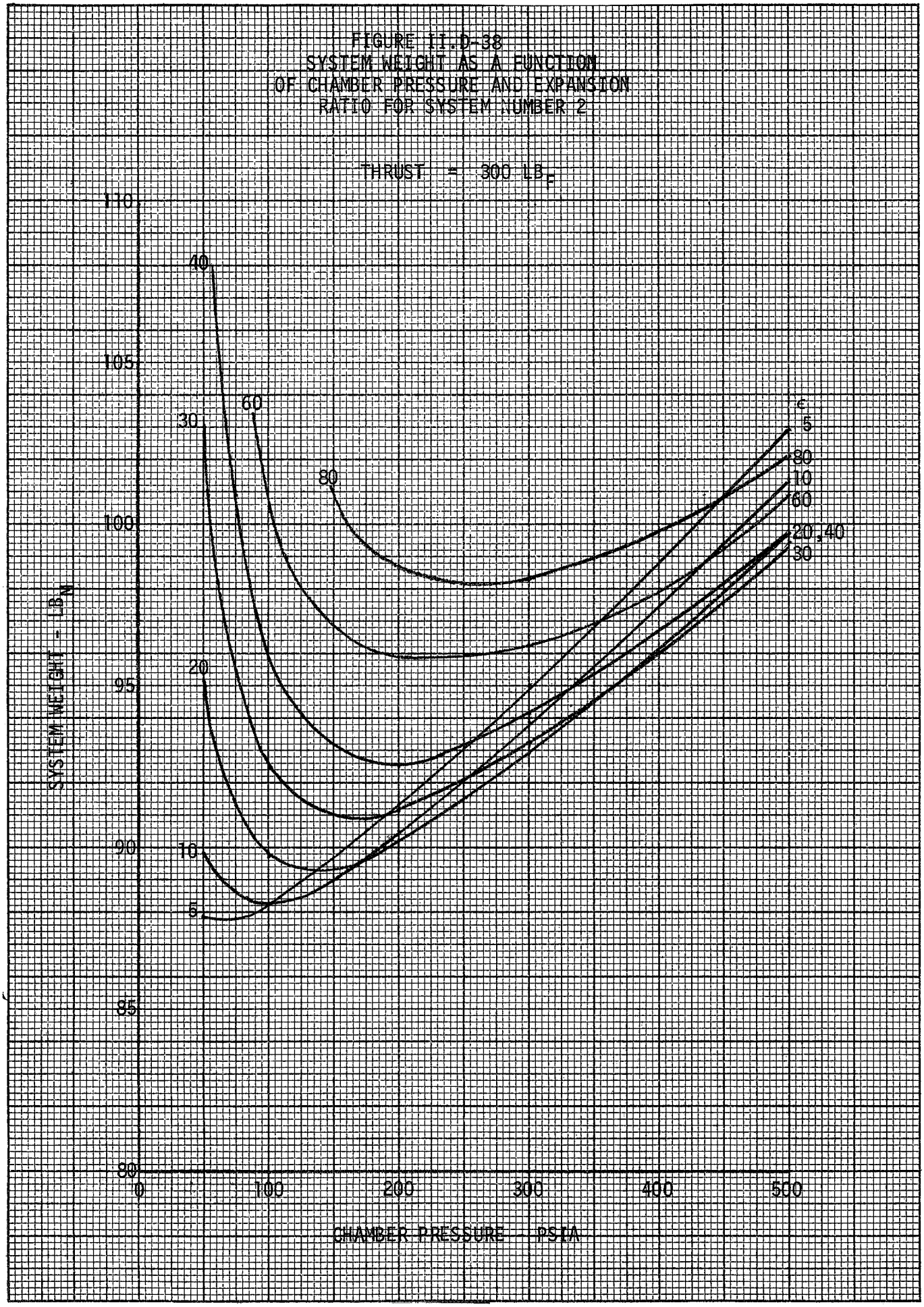

FIGURE II. D-39
SYSTEM WEIGHT AS A FUNCTION
OF CHAMBER PRESSURE AND EXPANSION
RATIO FOR SYSTEM NUMBER 2

THRUST = 600 LB_f

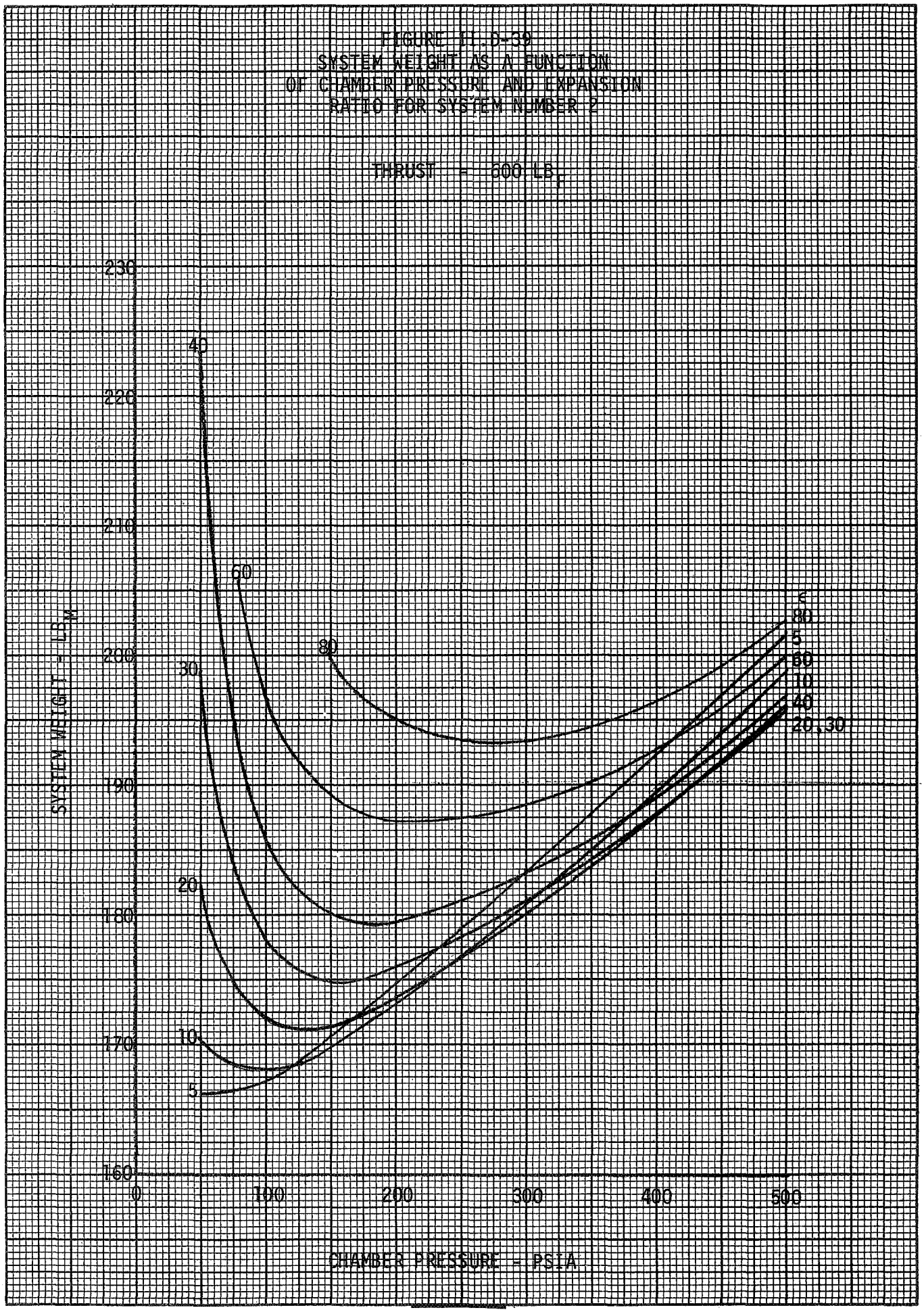

FIGURE II.D-40
SYSTEM WEIGHT AS A FUNCTION
OF CHAMBER PRESSURE AND EXPANSION
RATIO FOR SYSTEM NUMBER 2

THRUST = 1200 LB_F

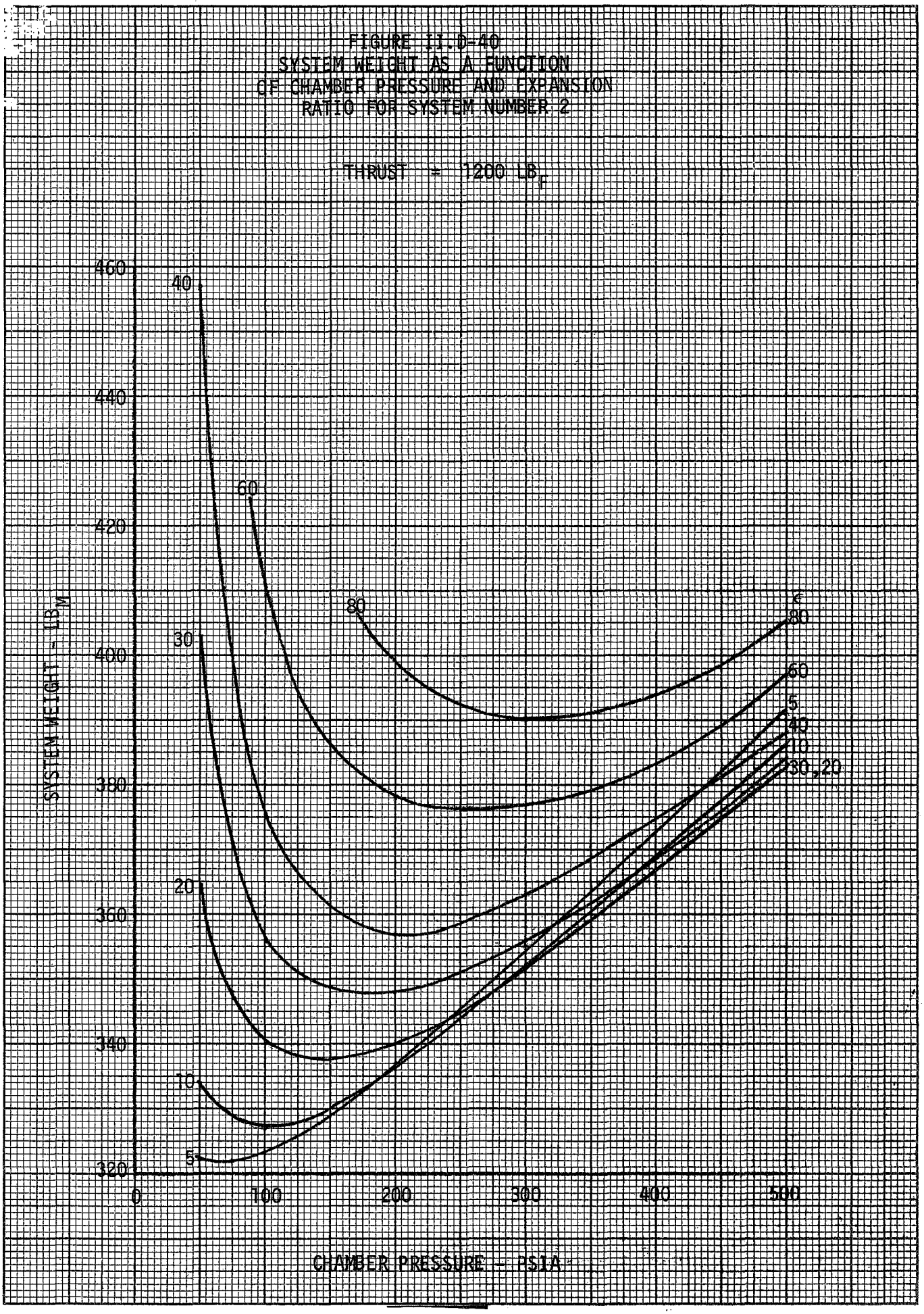

FIGURE II.D-41
SYSTEM WEIGHT AS A FUNCTION
OF CHAMBER PRESSURE AND EXPANSION
RATIO FOR SYSTEM NUMBER 3

THRUST = 300 LB_f

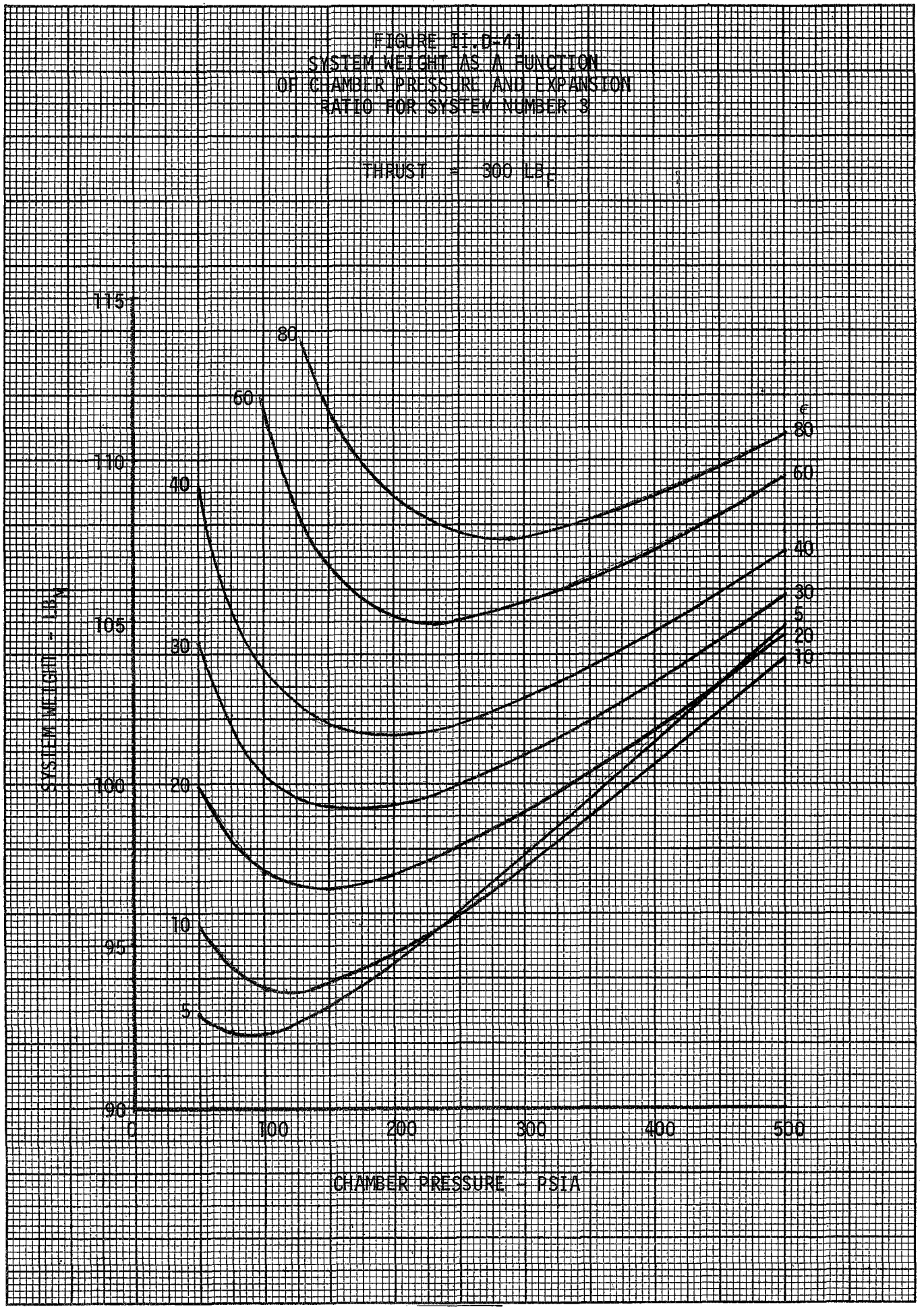

FIGURE II.D-42
SYSTEM WEIGHT AS A FUNCTION
OF CHAMBER PRESSURE AND EXPANSION
RATIO FOR SYSTEM NUMBER 3

THRUST = 600 LB_F

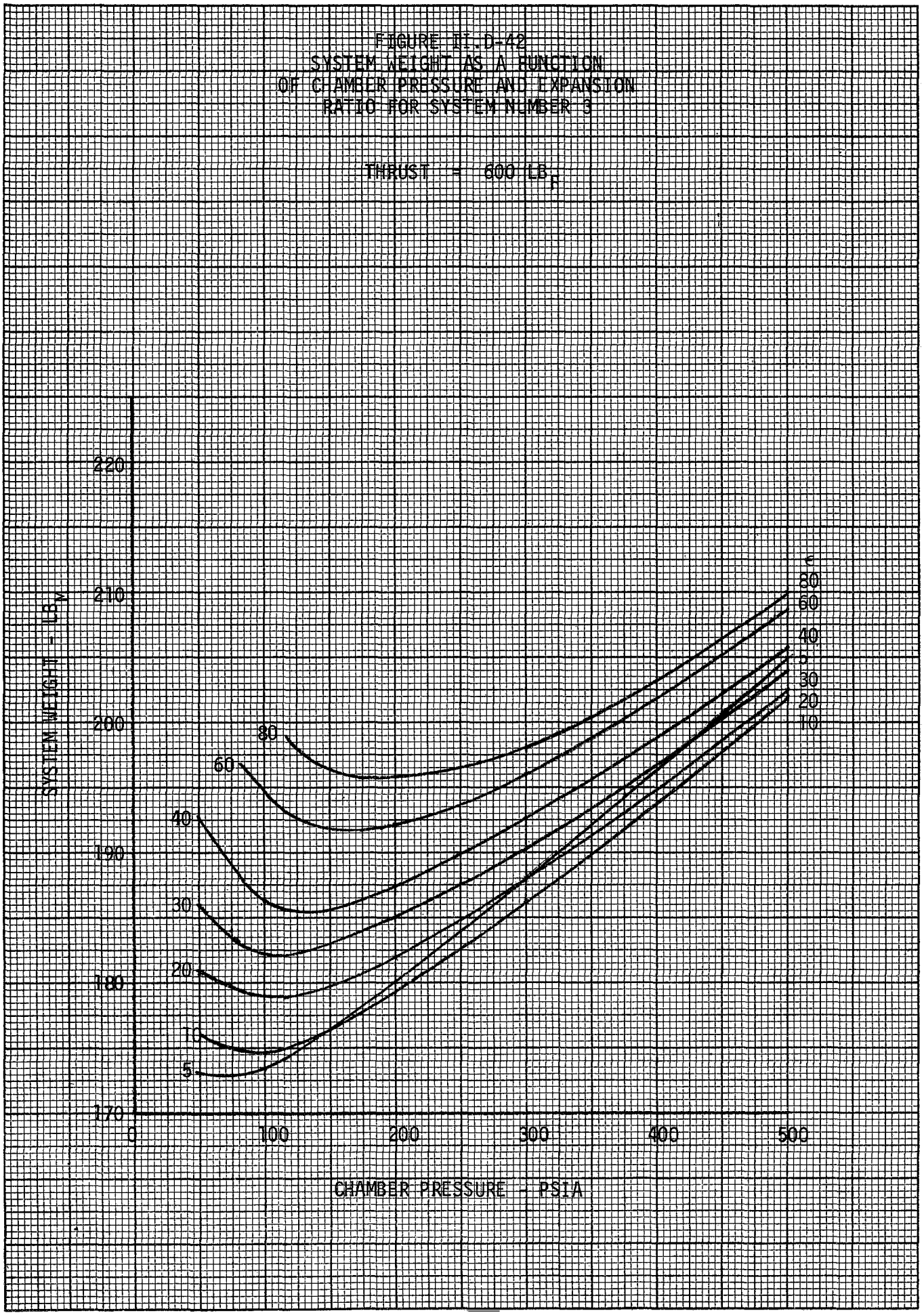

FIGURE II.D-48
SYSTEM WEIGHT AS A FUNCTION
OF CHAMBER PRESSURE AND EXPANSION
RATIO FOR SYSTEM NUMBER 3

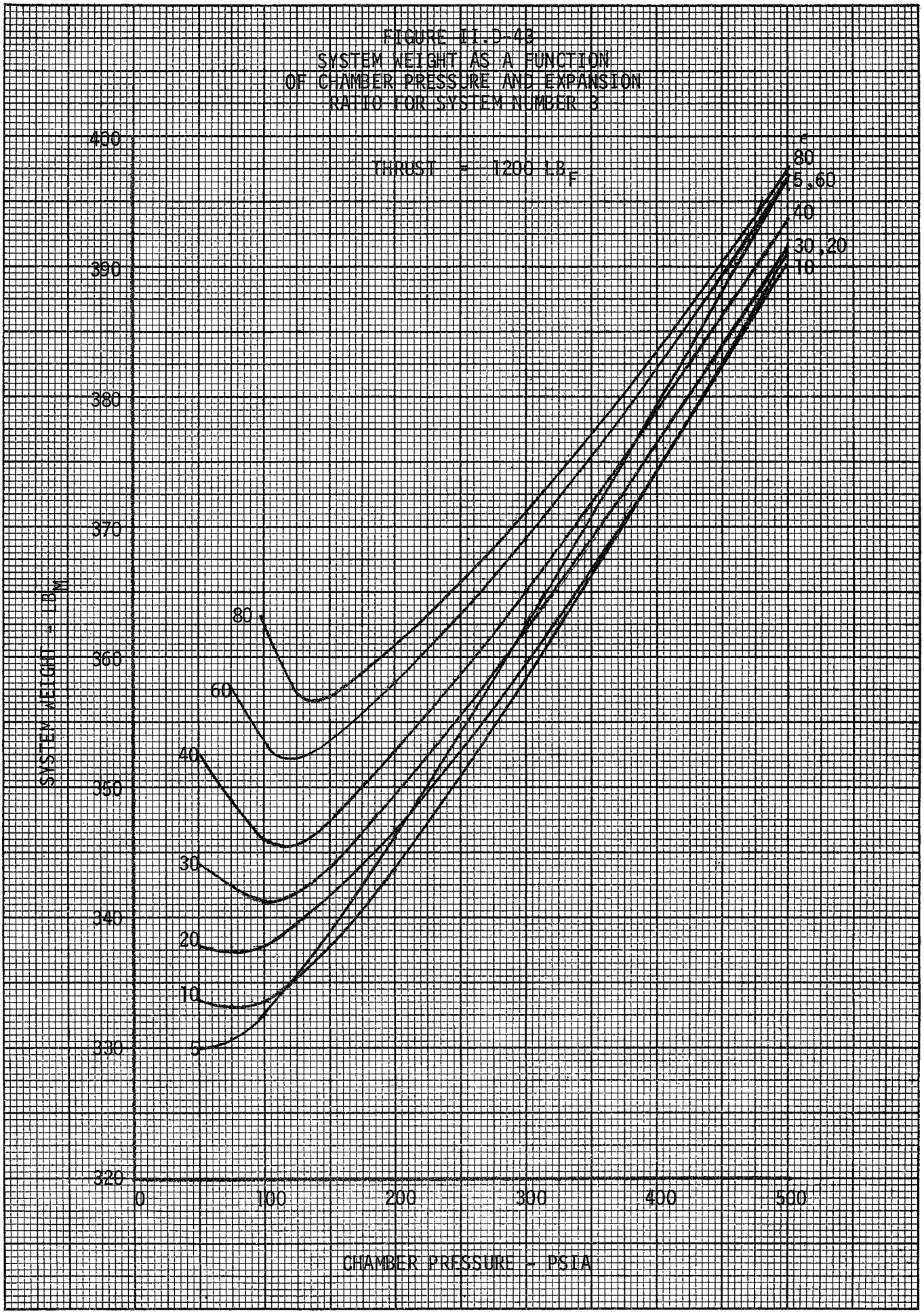

FIGURE II.D-44
SYSTEM WEIGHT AS A FUNCTION
OF CHAMBER PRESSURE AND EXPANSION
RATIO FOR SYSTEM NUMBER 4

THRUST = 300 LB_F

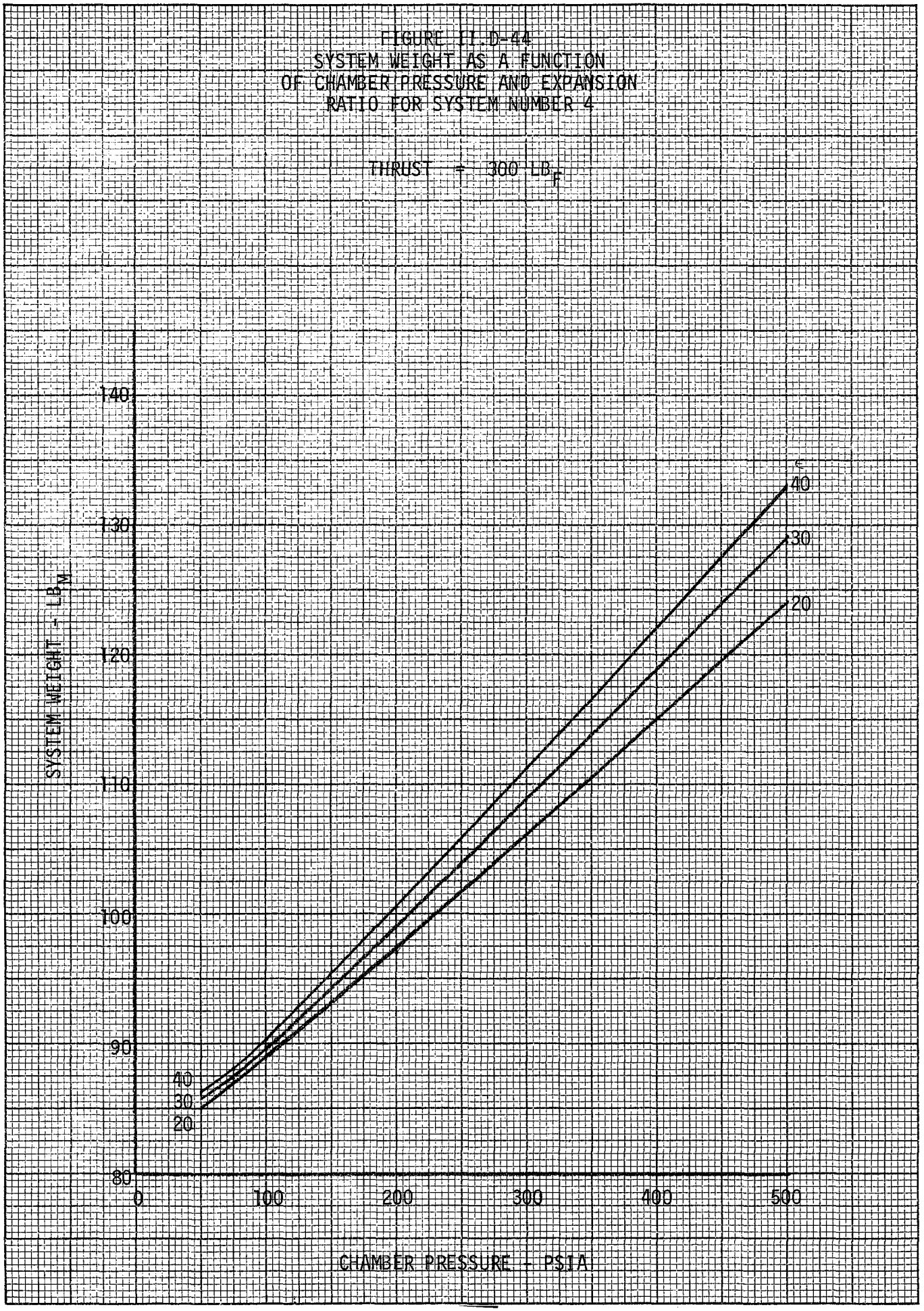

FIGURE II.D-45
SYSTEM WEIGHT AS A FUNCTION OF CHAMBER PRESSURE AND EXPANSION RATIO FOR SYSTEM NUMBER 4

THRUST = 600 LB_F

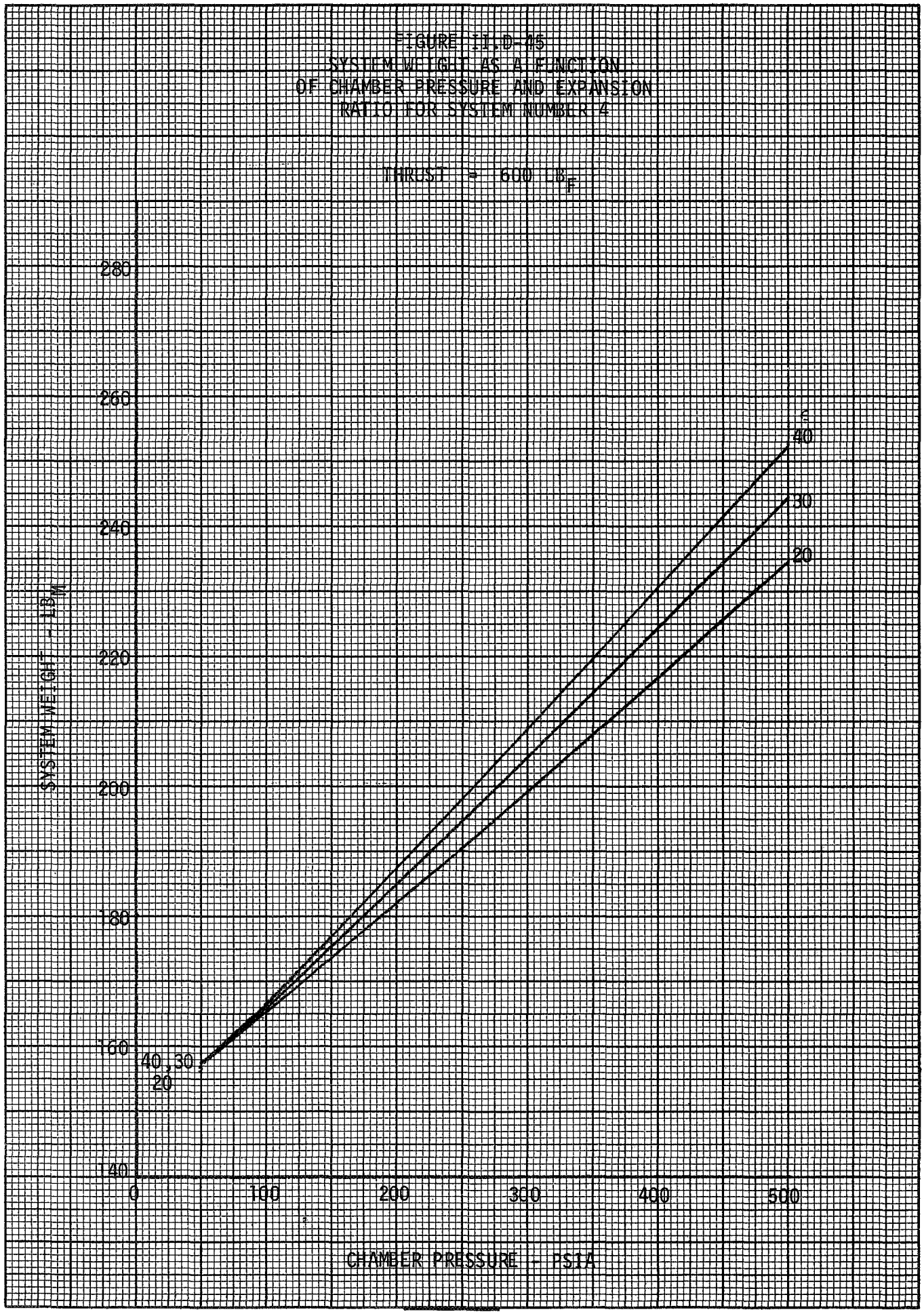

FIGURE II.D-46
SYSTEM WEIGHT AS A FUNCTION
OF CHAMBER PRESSURE AND EXPANSION
RATIO FOR SYSTEM NUMBER 4

THRUST = 1200 LB_F

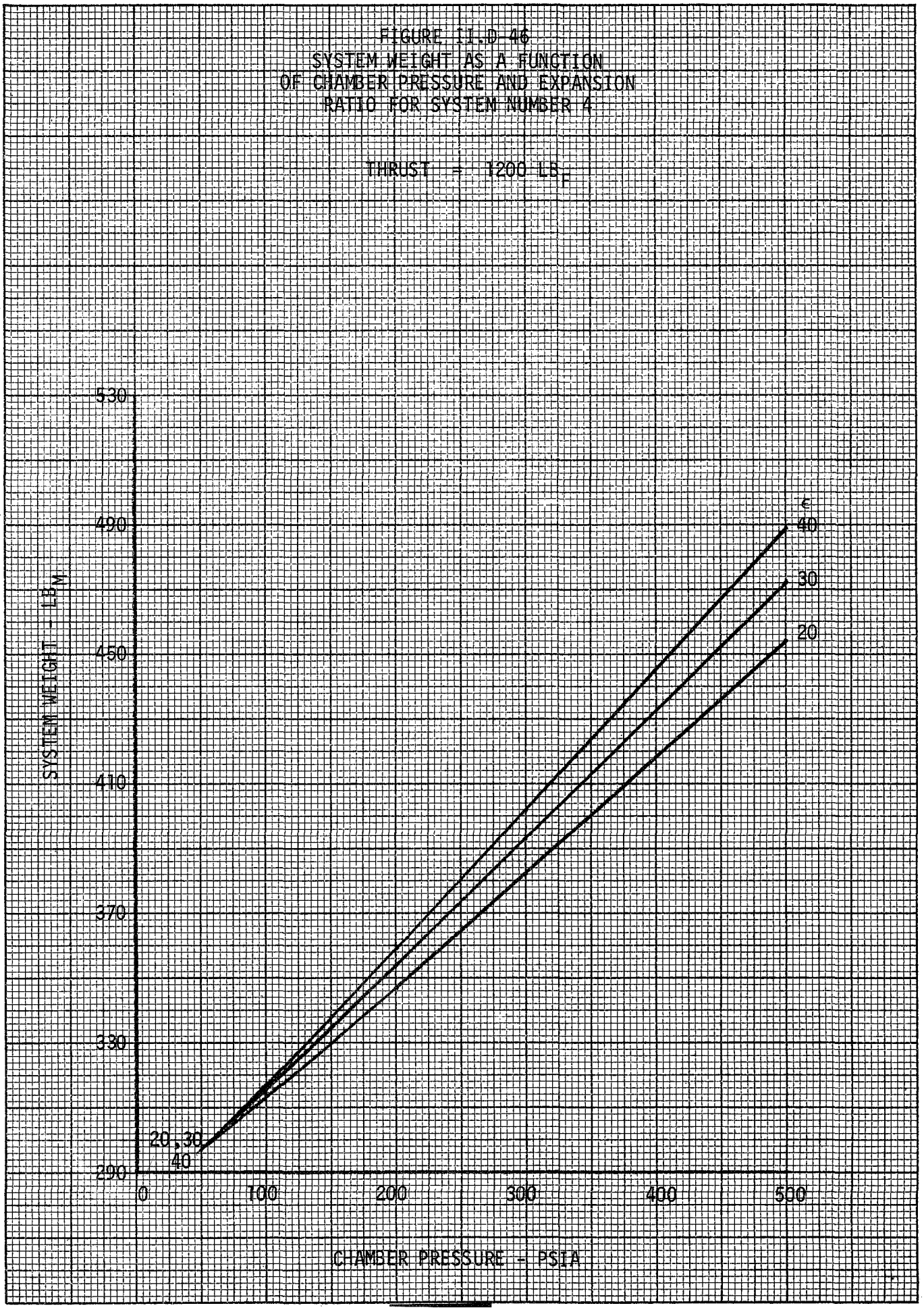

FIGURE II.D-47
SYSTEM WEIGHT AS A FUNCTION
OF CHAMBER PRESSURE AND EXPANSION
RATIO FOR SYSTEM NUMBER 5

THRUST = 300 LB_F

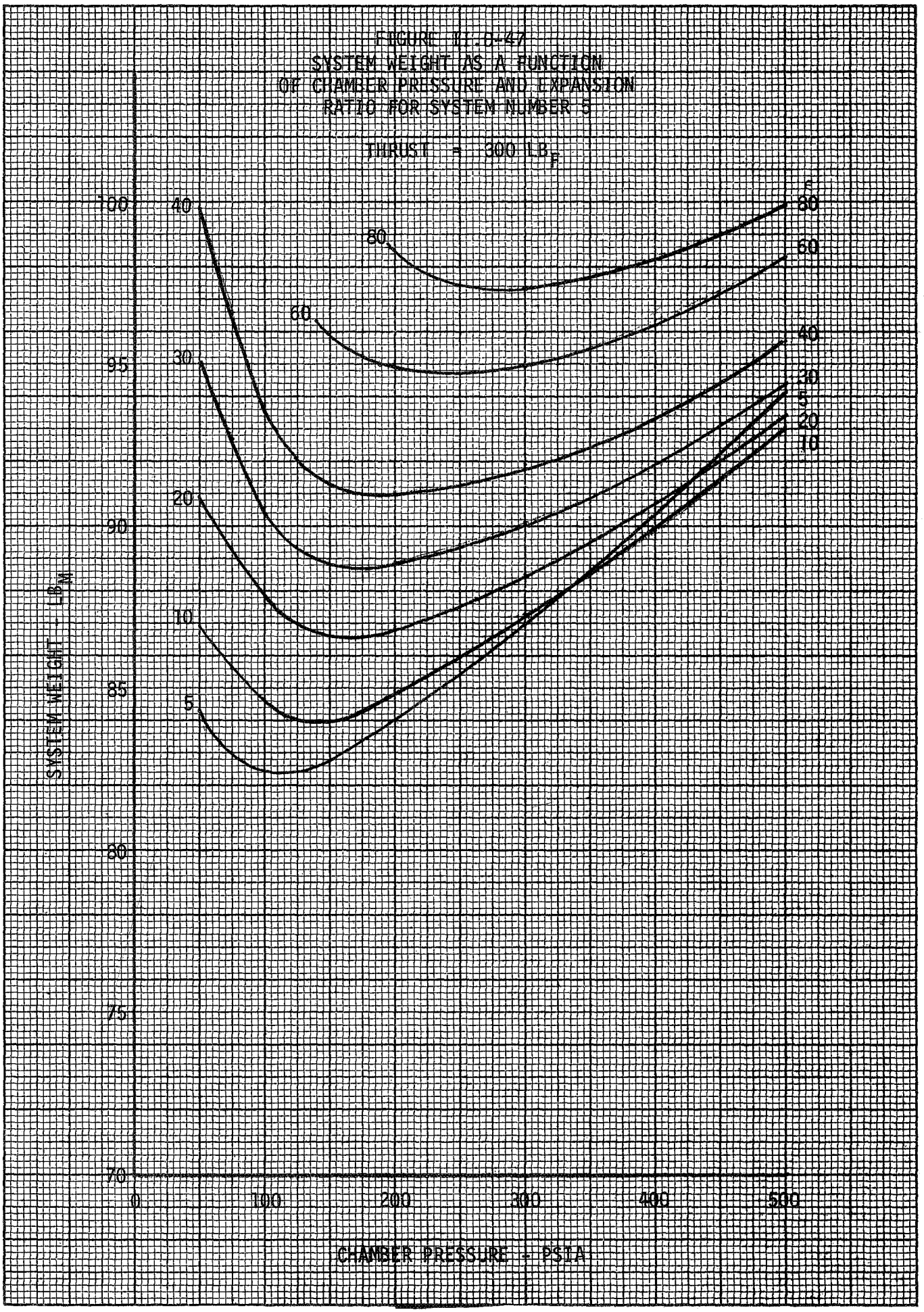

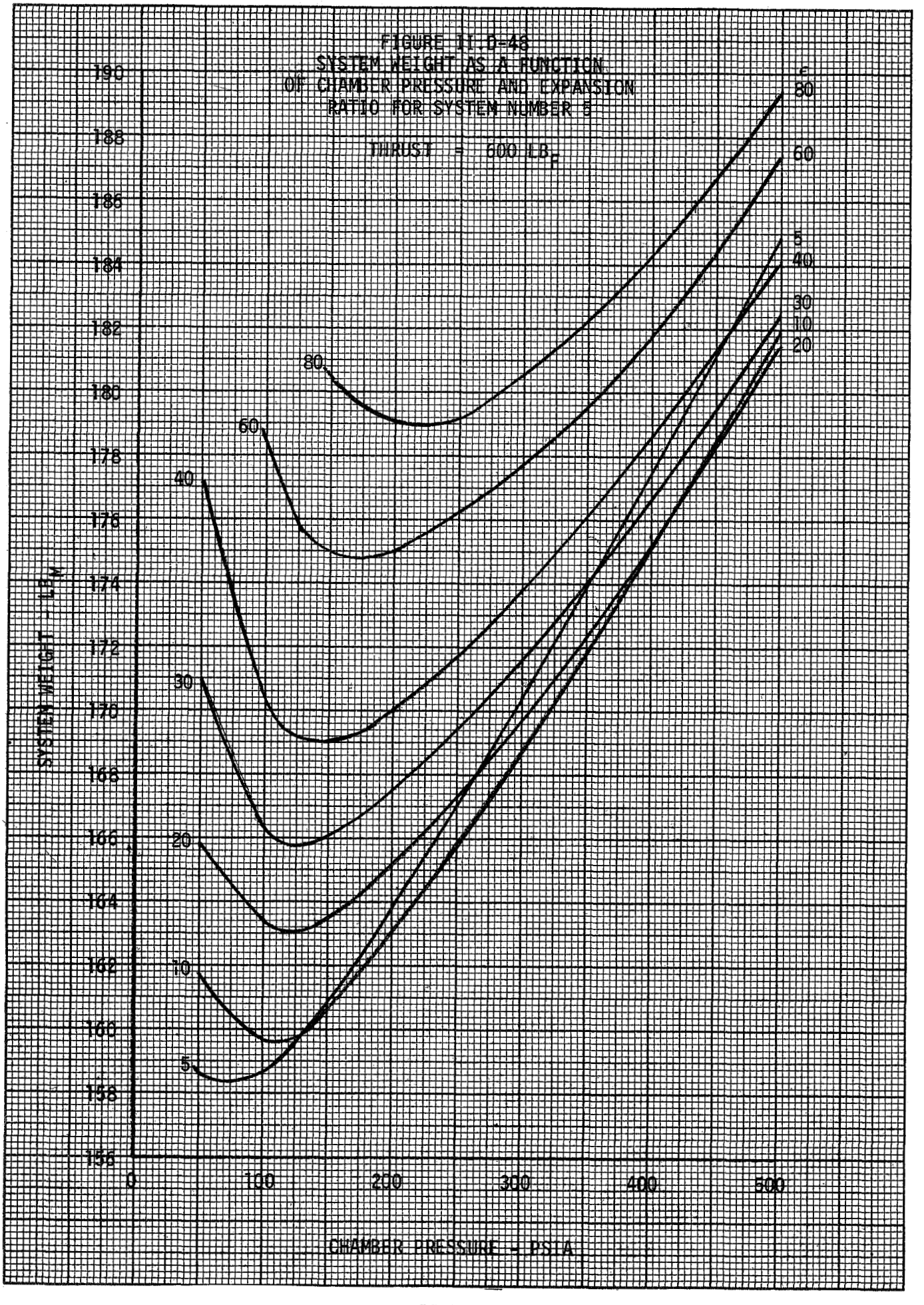
FIGURE II.D-48
SYSTEM WEIGHT AS A FUNCTION
OF CHAMBER PRESSURE AND EXPANSION
RATIO FOR SYSTEM NUMBER 8
THRUST = 600 LB$_F$
SYSTEM WEIGHT - LBM
190
188
186
184
182
180
178
176
174
172
170
168
166
164
162
160
158
156
0
100
200
300
400
500
CHAMBER PRESSURE - PSIA
ε
80
60
40
30
20
10
5

FIGURE II. D-49
SYSTEM WEIGHT AS A FUNCTION
OF CHAMBER PRESSURE AND EXPANSION
RATIO FOR SYSTEM NUMBER 5

THRUST = 1200 LB_F

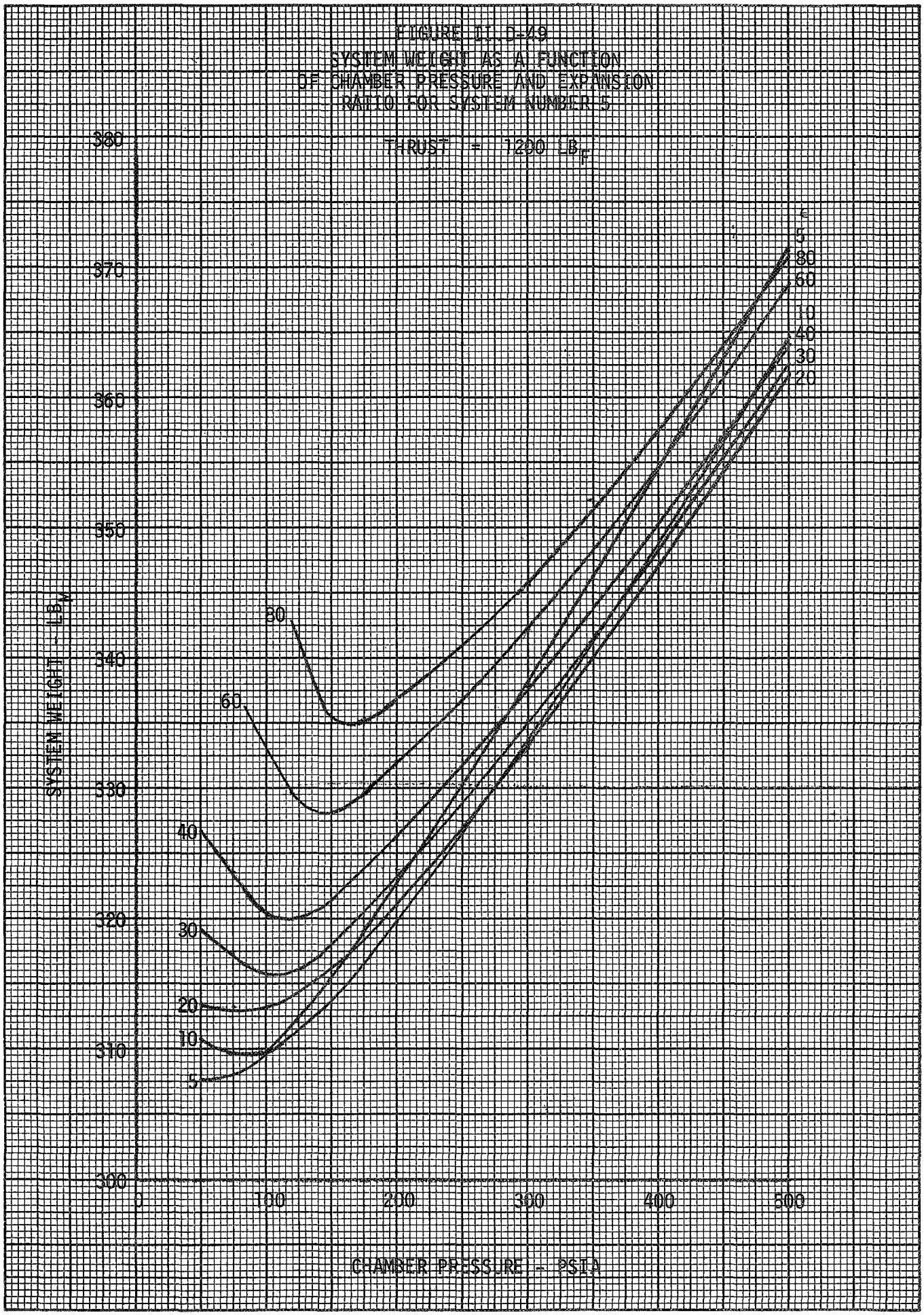

FIGURE II.D-50
SYSTEM WEIGHT AS A FUNCTION
OF CHAMBER PRESSURE AND EXPANSION
RATIO FOR SYSTEM NUMBER 6

THRUST = 300 LB_F

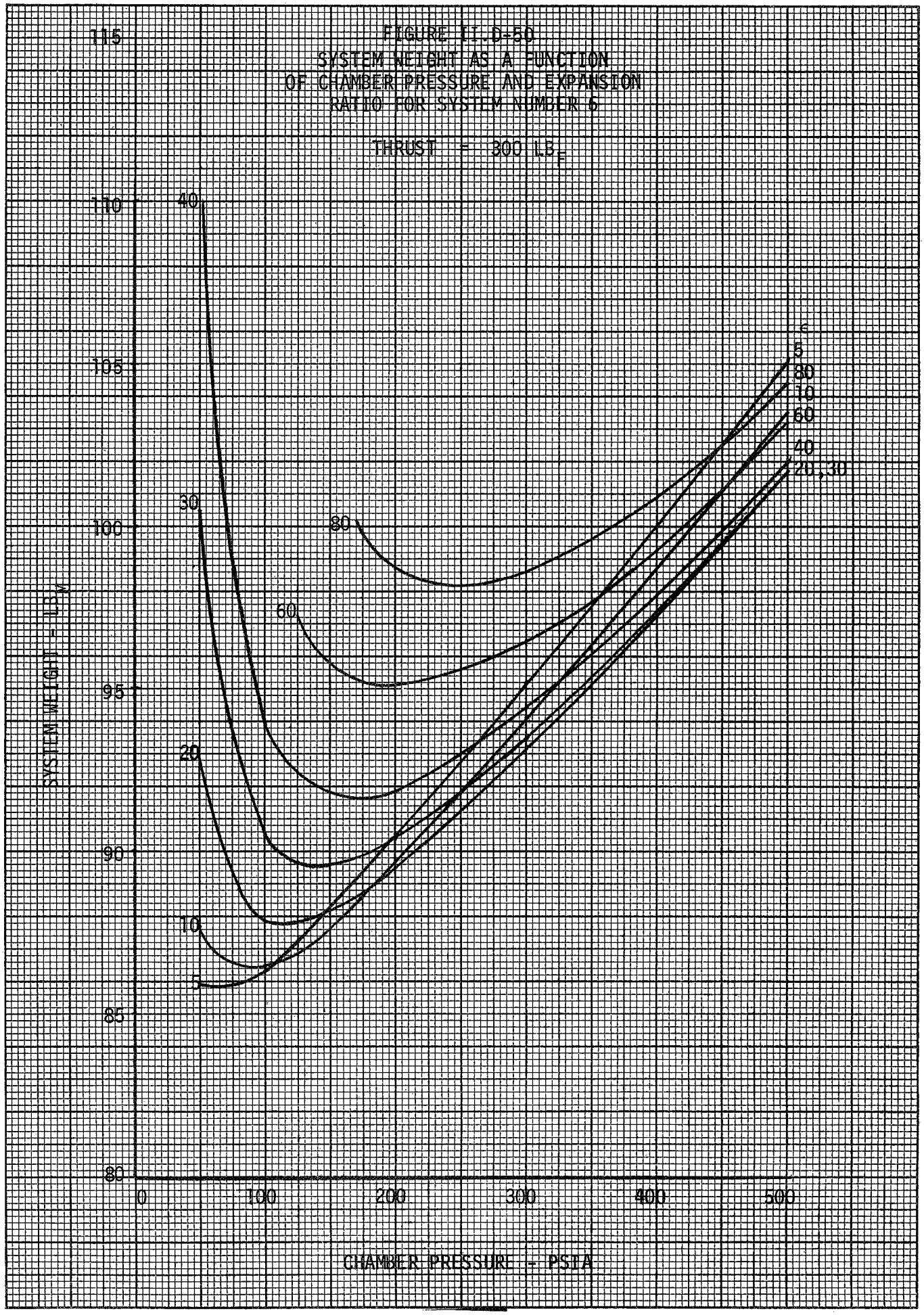

FIGURE II.D-50
SYSTEM WEIGHT AS A FUNCTION
OF CHAMBER PRESSURE AND EXPANSION
RATIO FOR SYSTEM NUMBER 6

THRUST = 600 LB$_F$

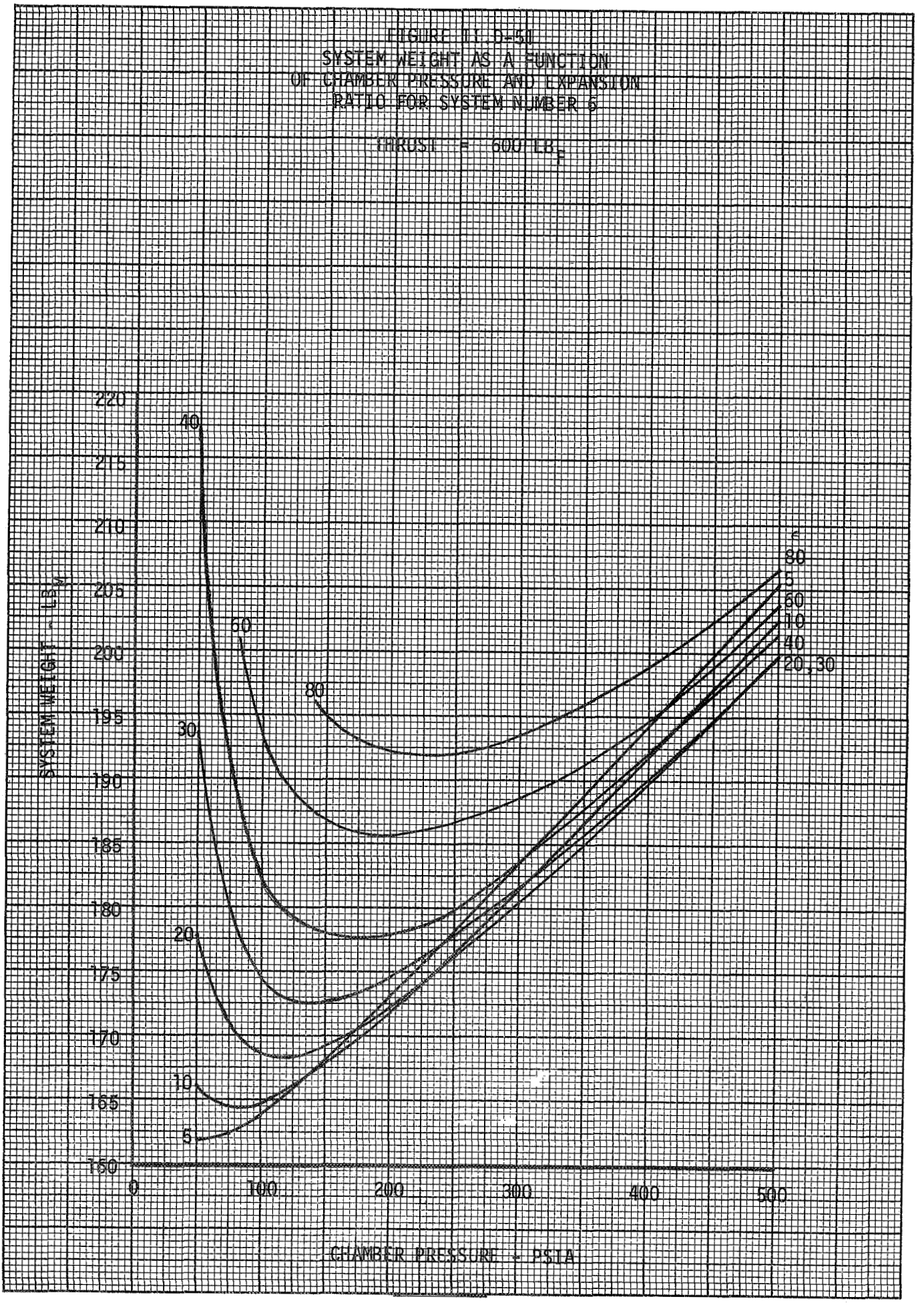

FIGURE II.D-52
SYSTEM WEIGHT AS A FUNCTION
OF CHAMBER PRESSURE AND EXPANSION
RATIO FOR SYSTEM NUMBER 6

THRUST = 1200 LB_F

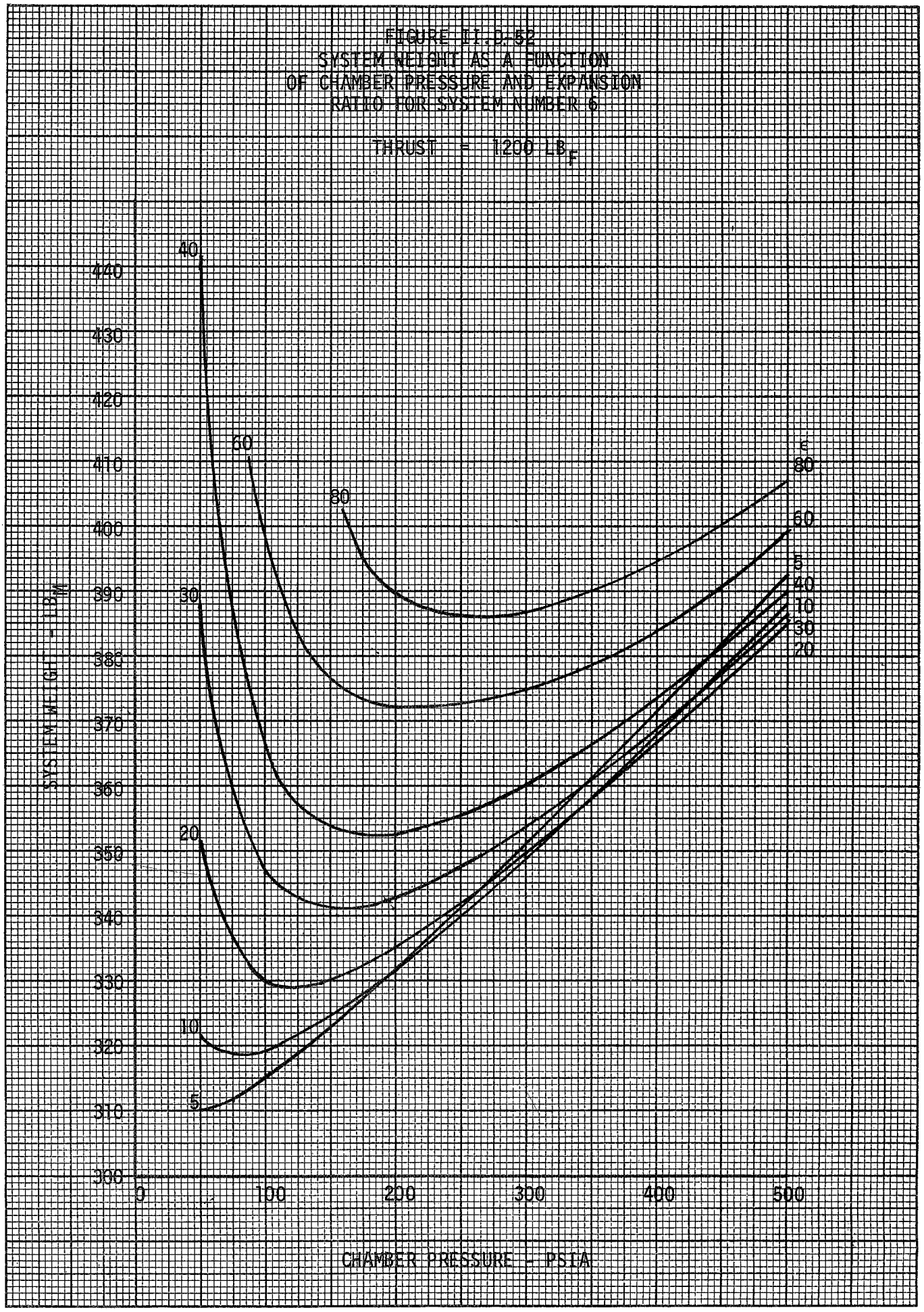

FIGURE II.D-53
SYSTEM WEIGHT AS A FUNCTION
OF CHAMBER PRESSURE AND EXPANSION
RATIO FOR SYSTEM NUMBER 7

THRUST = 300 LB_F

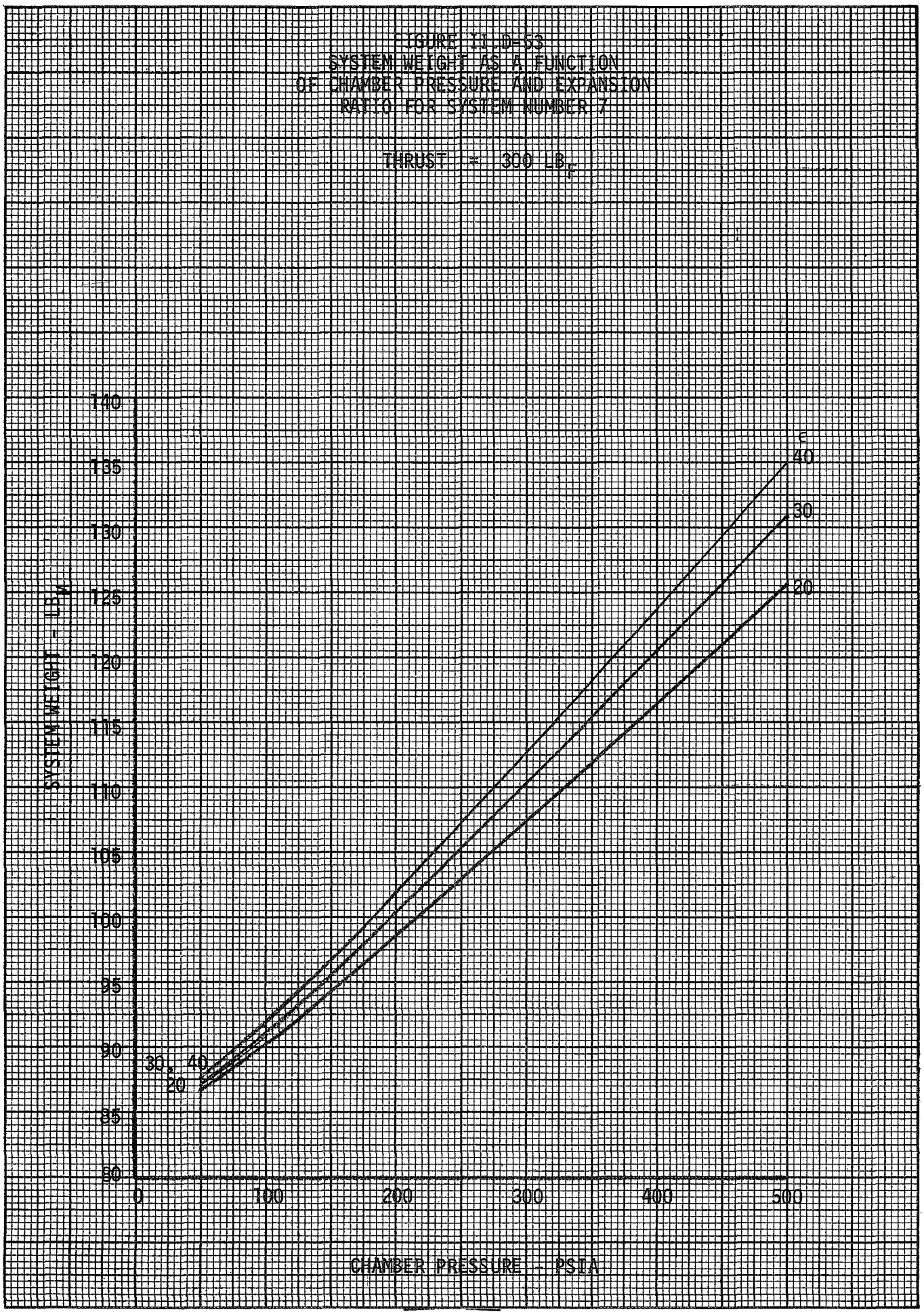

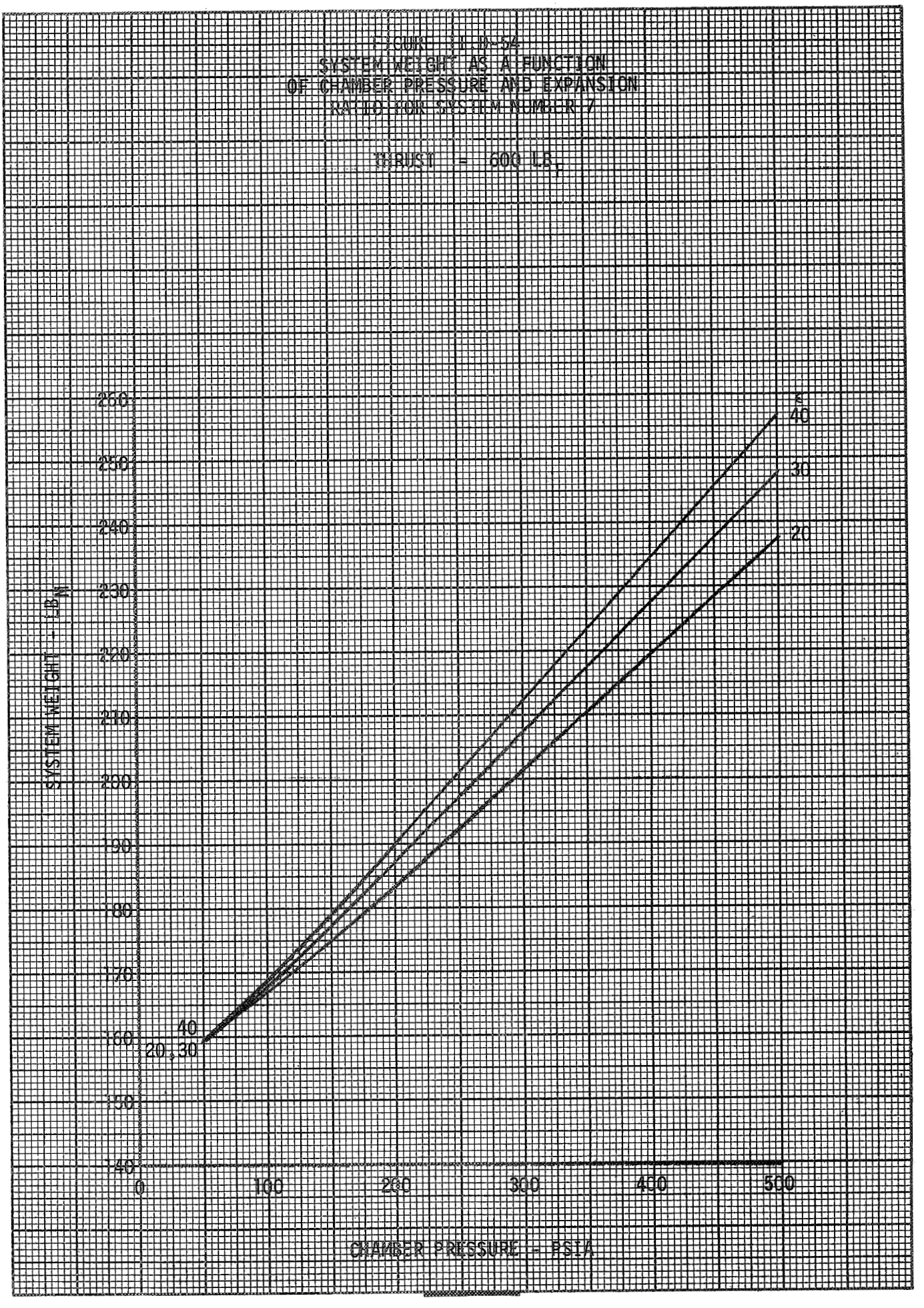
FIGURE II.D-54
SYSTEM WEIGHT AS A FUNCTION
OF CHAMBER PRESSURE AND EXPANSION
RATIO FOR SYSTEM NUMBER 7
THRUST = 600 LB$_f$
SYSTEM WEIGHT - LB$_m$
260
250
240
230
220
210
200
190
180
170
160
150
140
0
100
200
300
400
500
CHAMBER PRESSURE - PSIA
40
30
20
40
20, 30

FIGURE II.D-55
SYSTEM WEIGHT AS A FUNCTION
OF CHAMBER PRESSURE AND EXPANSION
RATIO FOR SYSTEM NUMBER 7

THRUST = 1200 LB_F

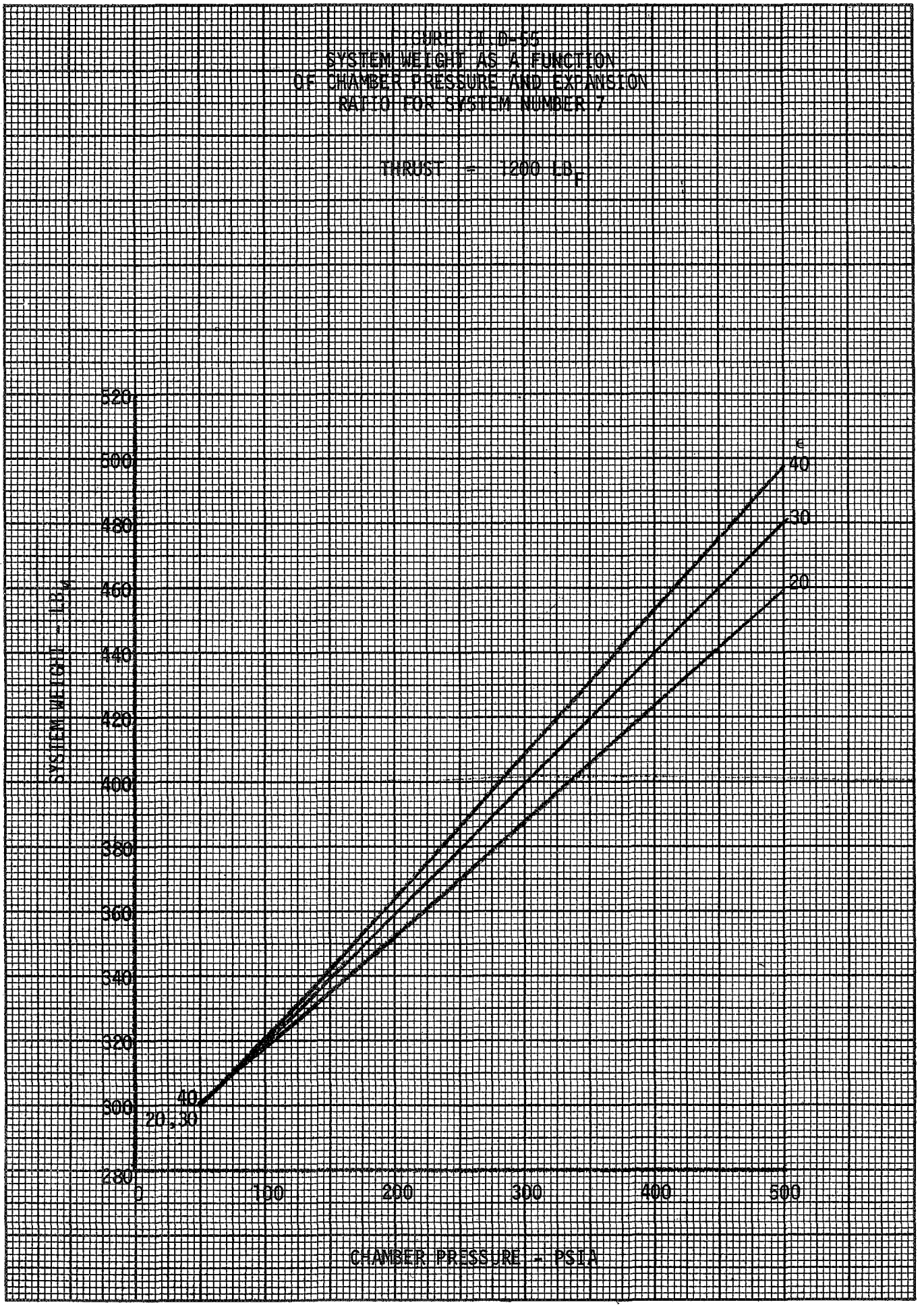

FIGURE II.D-56
SYSTEM WEIGHT AS A FUNCTION
OF CHAMBER PRESSURE AND EXPANSION
RATIO FOR SYSTEM NUMBER 8

THRUST = 300 LB_f

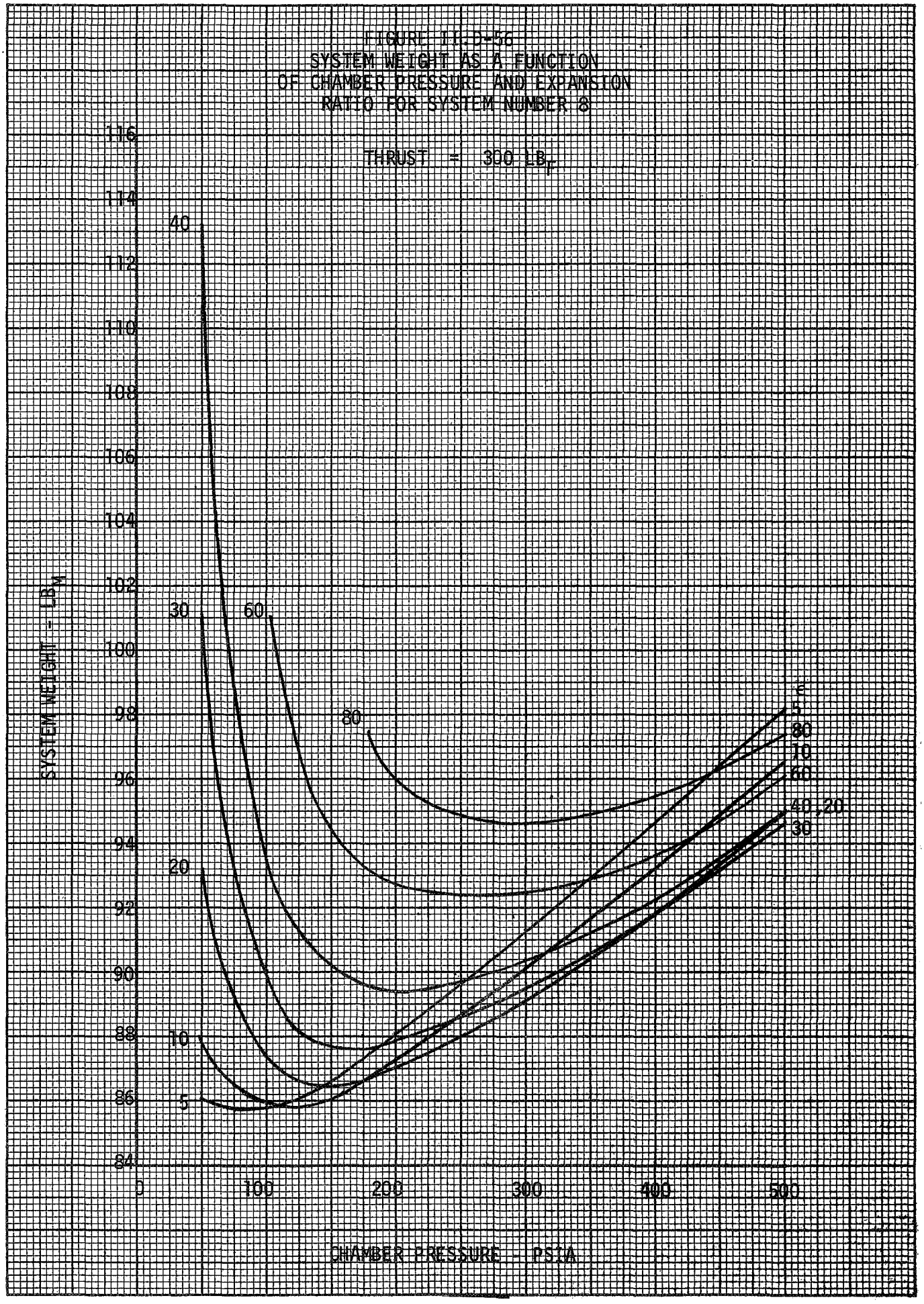

FIGURE II.D-57
SYSTEM WEIGHT AS A FUNCTION
OF CHAMBER PRESSURE AND EXPANSION
RATIO FOR SYSTEM NUMBER 8

THRUST = 600 LB_F

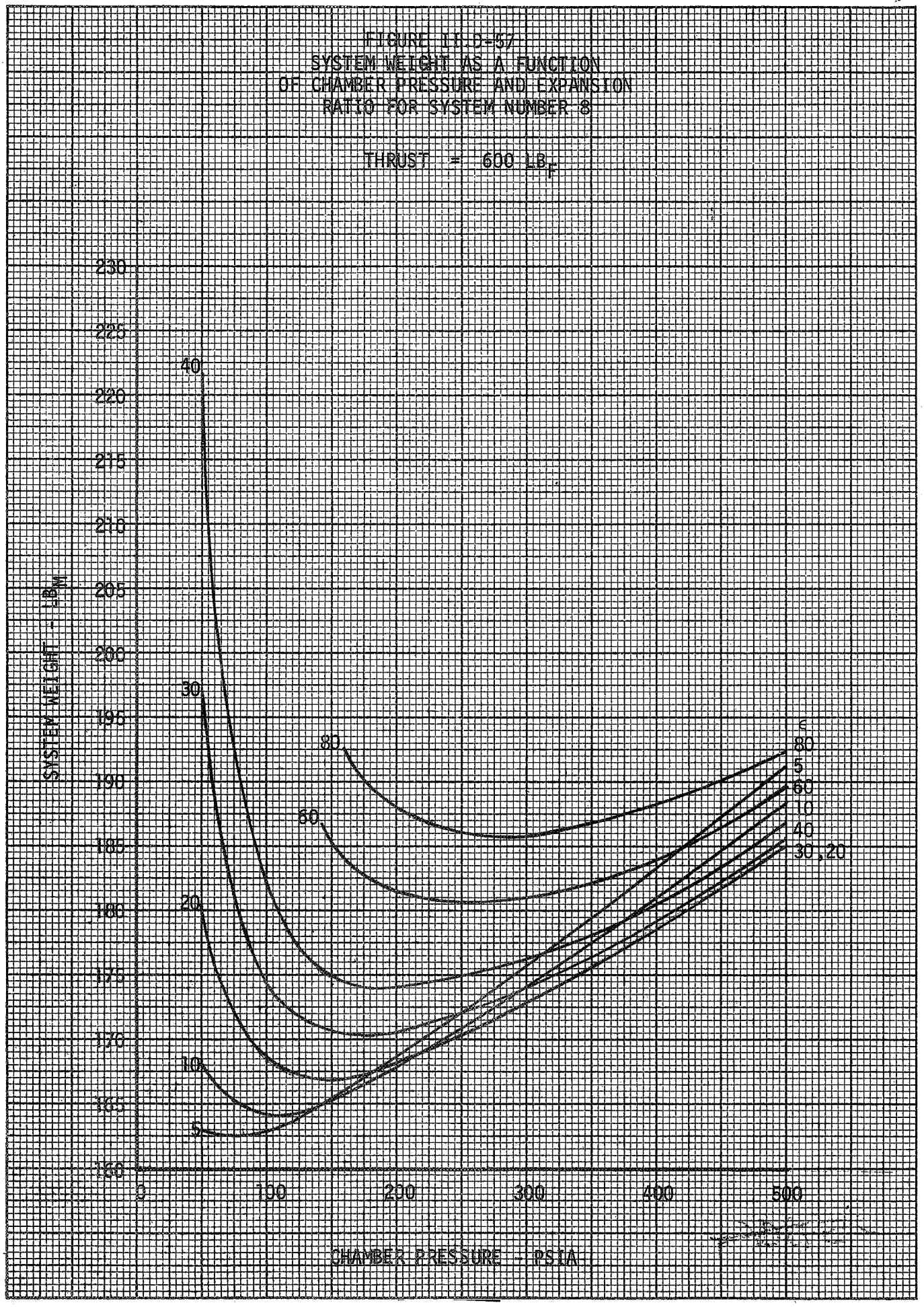

FIGURE II.D-58
SYSTEM WEIGHT AS A FUNCTION
OF CHAMBER PRESSURE AND EXPANSION
RATIO FOR SYSTEM NUMBER 8

THRUST = 1200 LB_F

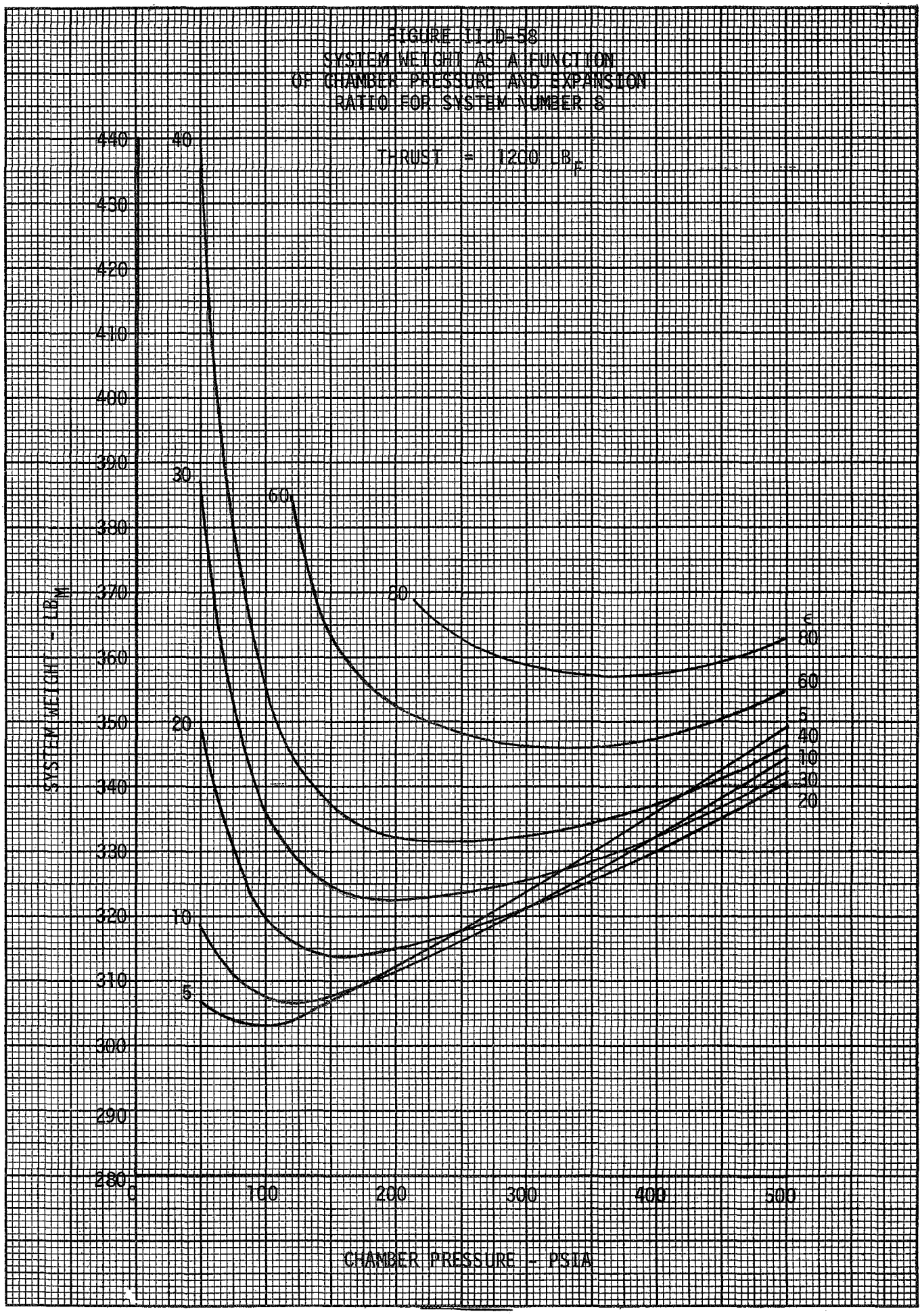

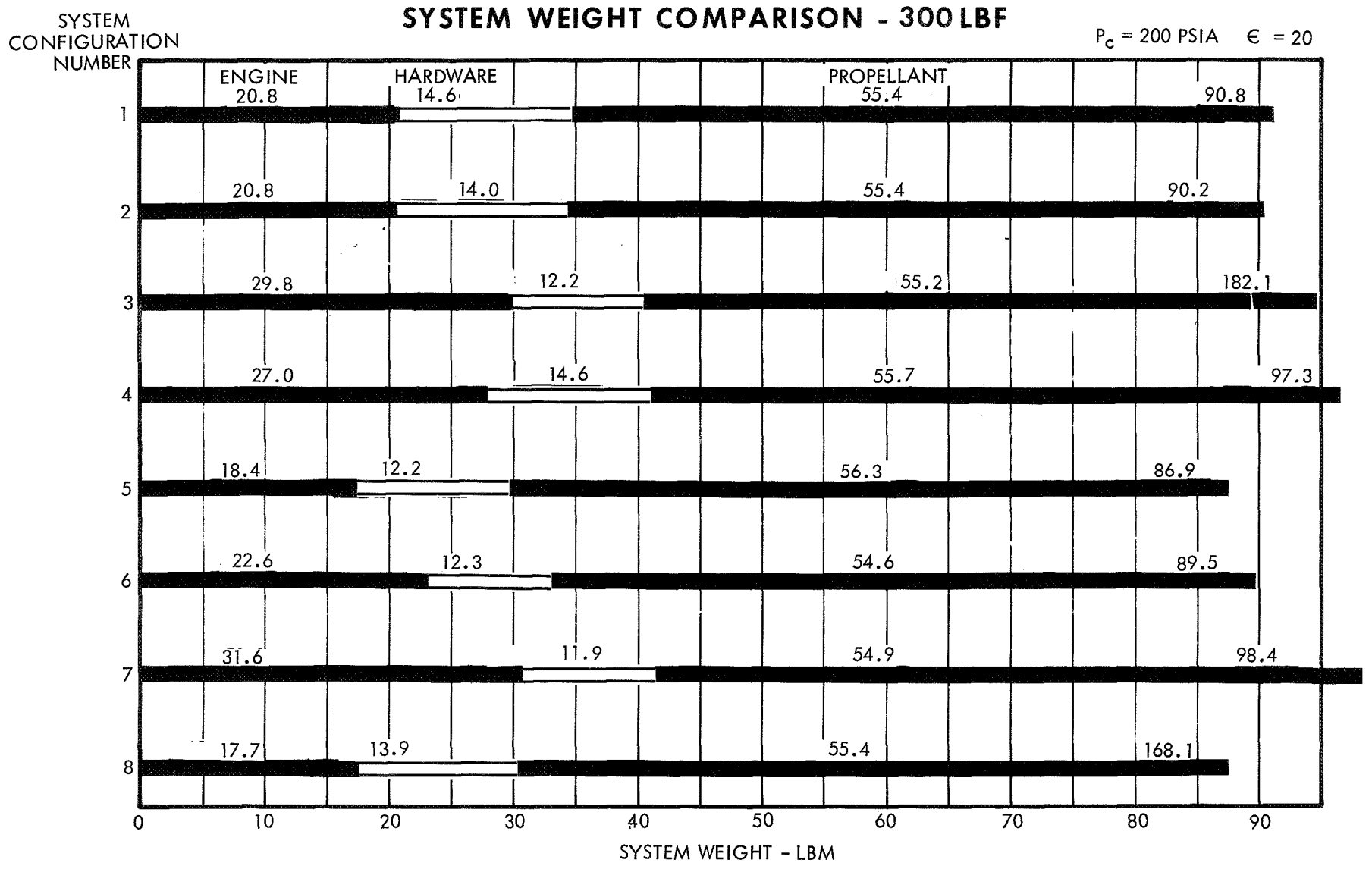

Figure II.D-59. System Weight Comparison - 300 LBF

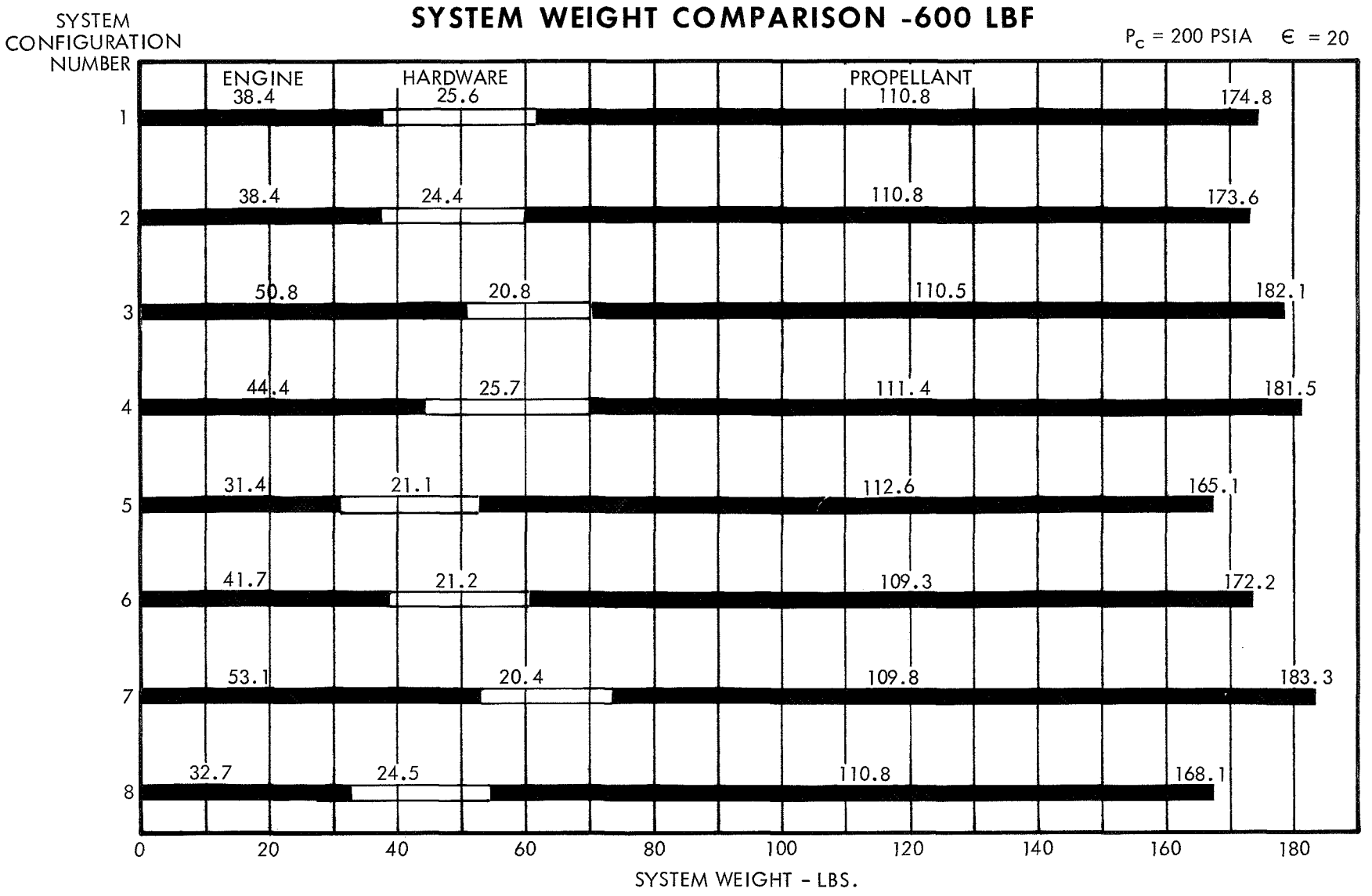

Figure II.D-60. System Weight Comparison - 600 LBF

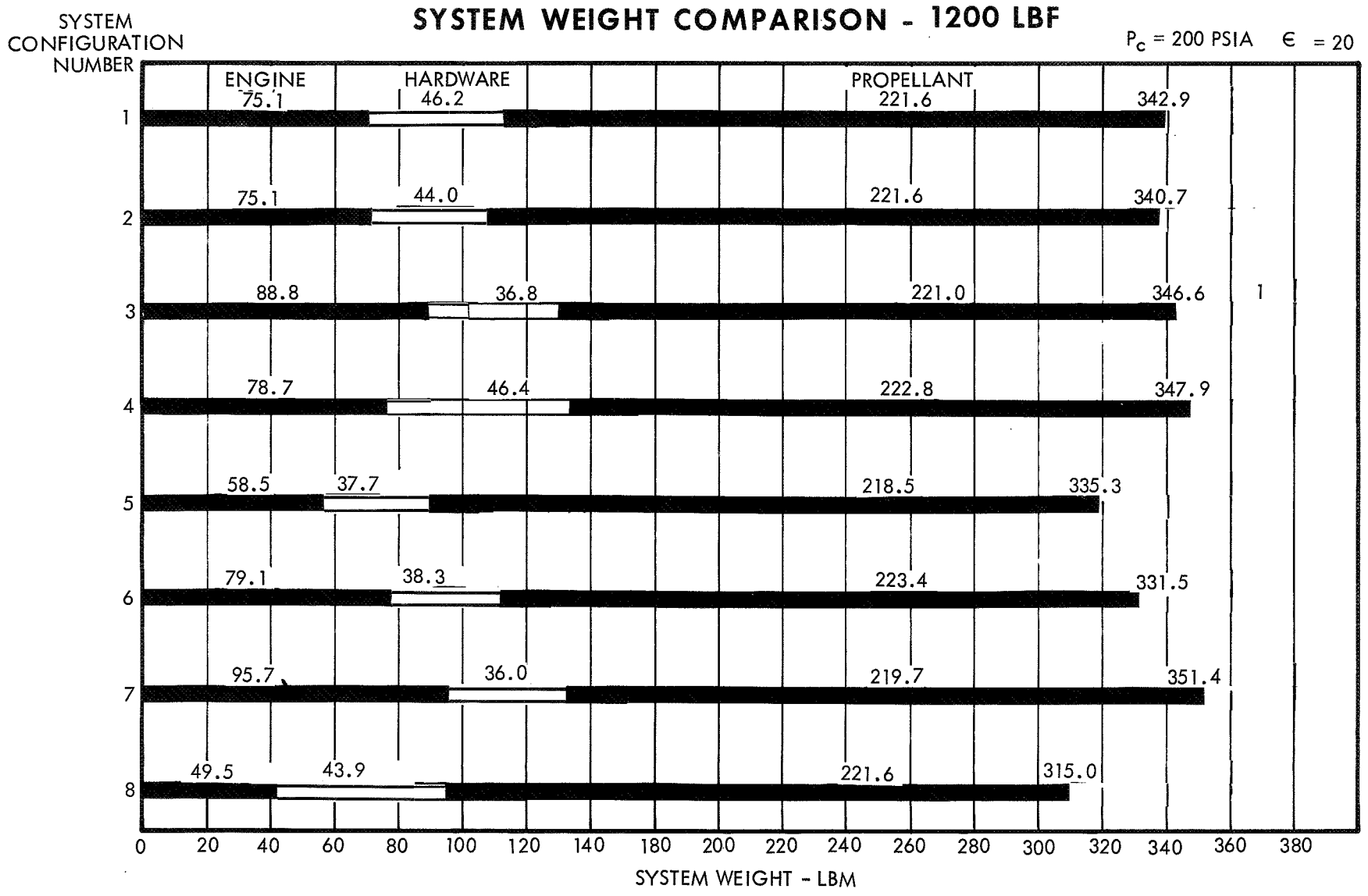

Figure II.D-61. System Weight Comparison - 1200 LBF

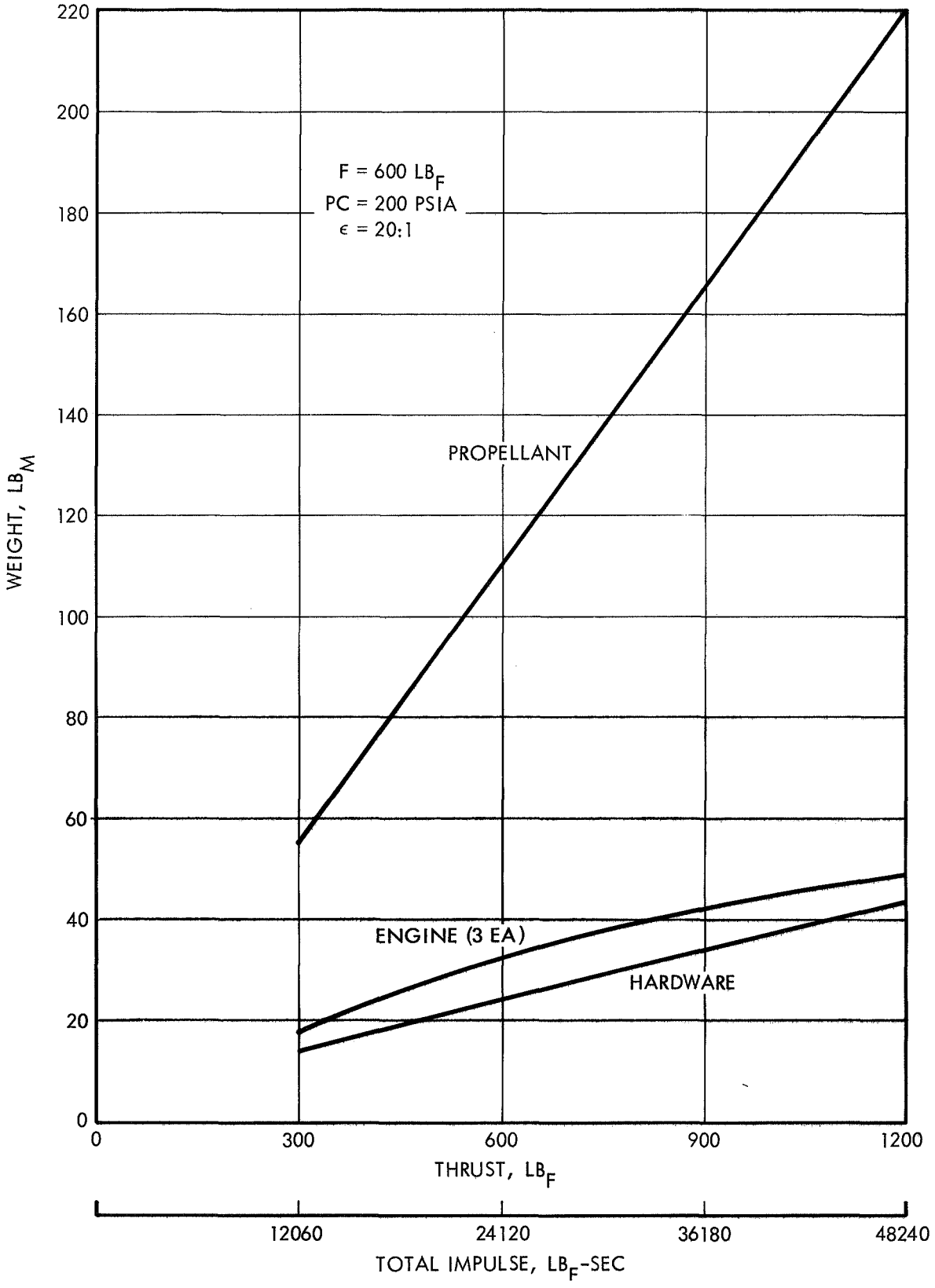

Figure II.D-62. Mission Effects on System Weight for Configuration Number 8

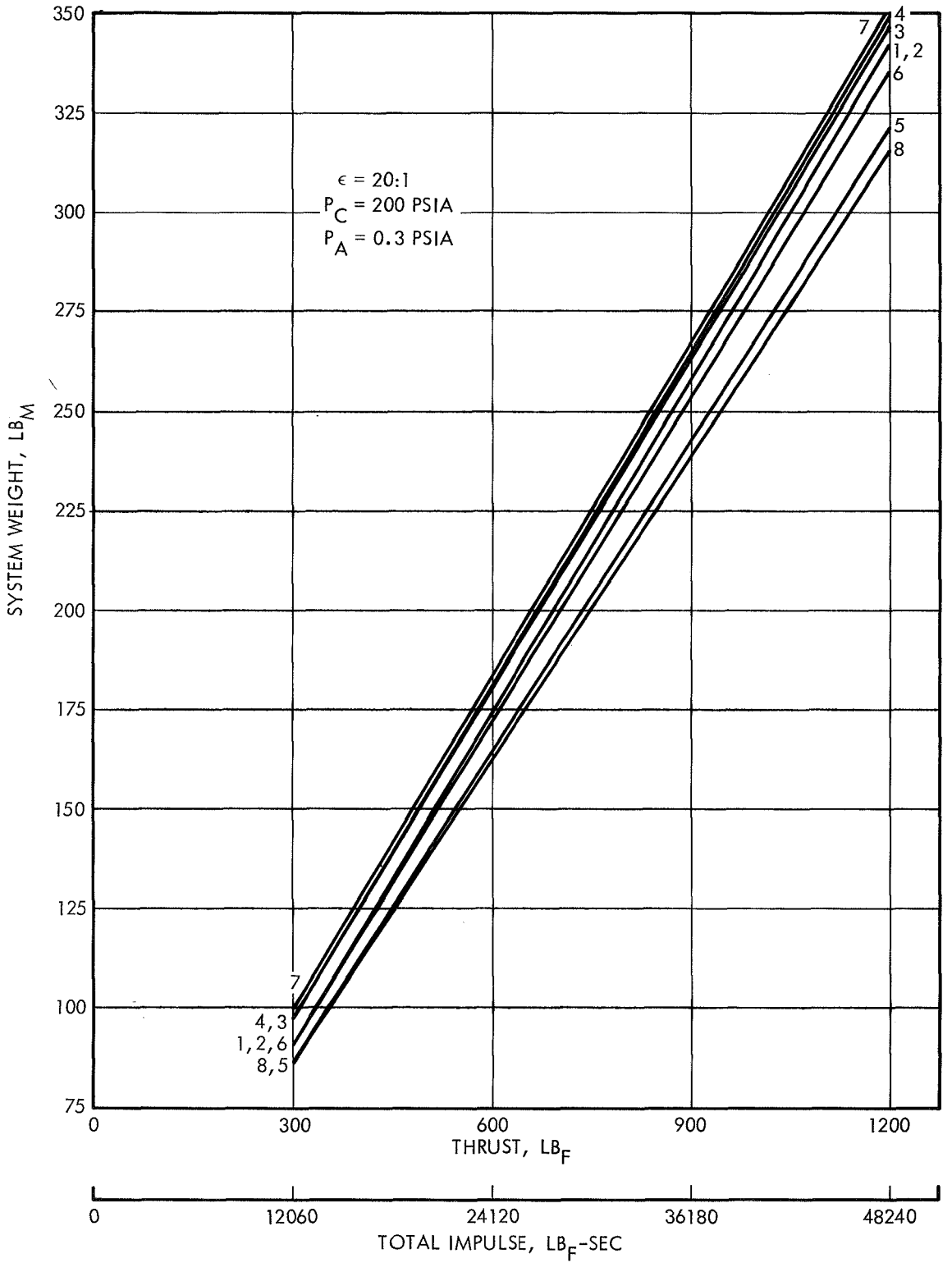

Figure II.D-63. System Weight Comparison Versus Thrust

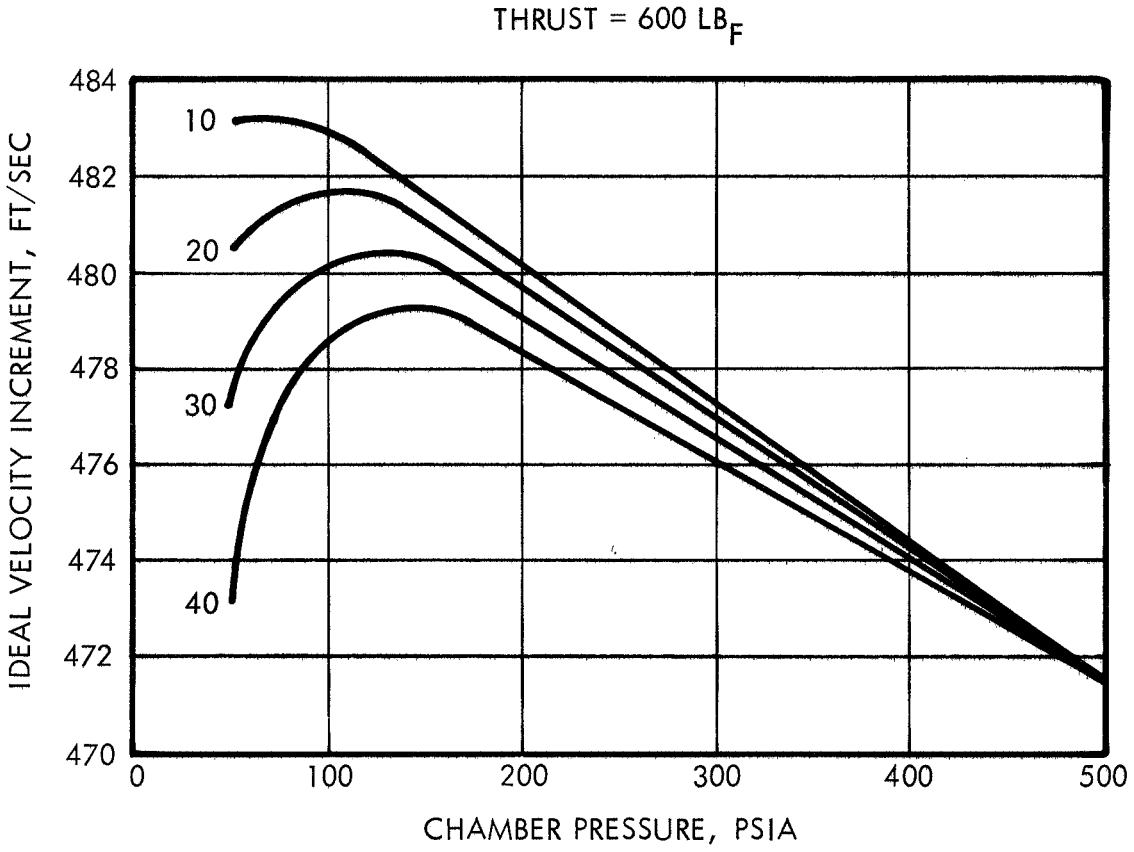

Figure II.D-64. Ideal Velocity Increment as a Function of Chamber Pressure and Expansion Ratio For System Number 6

DESIGN PARAMETERS

- MAXIMUM THRUST 600 LBF
- CHAMBER PRESSURE 200 PSIA
- EXPANSION RATIO 10 TO 20:1
- THROTTLE RATIO 10:1
- LIFE 500 SEC
- CHAMBER MATERIAL L - 605

PREDICTED PERFORMANCE

- VACUUM SPECIFIC IMPULSE 220 LBF - SEC/LBM
- VACUUM THRUST COEFFICIENT 1.64
- CHARACTERISTIC VELOCITY 4360 FT/SEC

WEIGHT	LBM
● CHAMBER AND NOZZLE	3.70
● CATALYST AND SUPPORT	2.81
● HEADEND STRUCTURE	2.06
● THROTTLE VALVE	2.80
	11.37

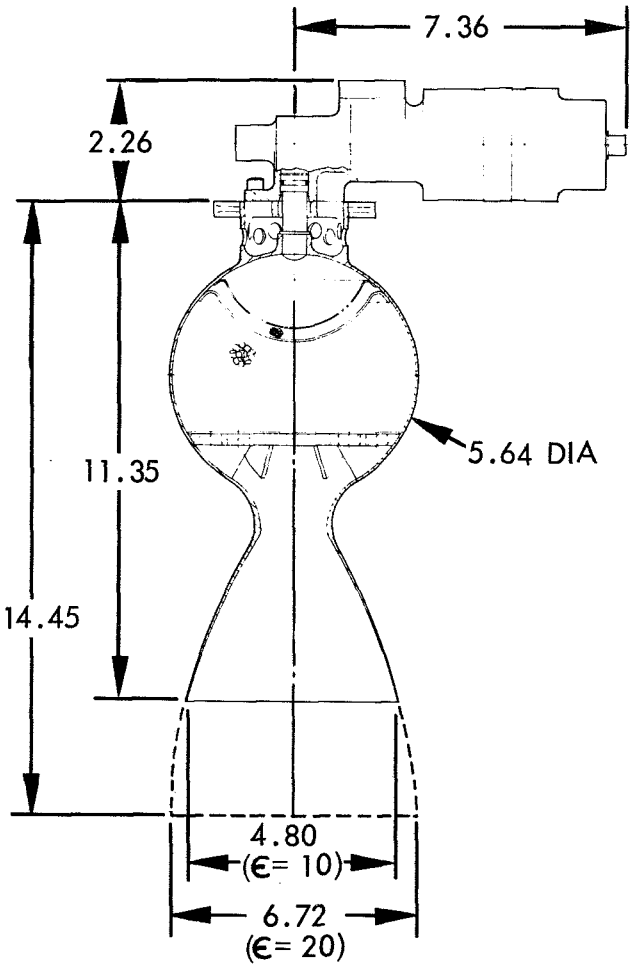

Figure II.D-65. Recommended System

II.E. FLOW CONTROL SYSTEMS

II.E.1 Throttling Concepts (Throttle Mechanizations)

Selection and mechanization of a monopropellant engine throttling concept is basically governed by the type of reactor used and the desired throttle range. Additional factors which influence these decisions are (1) available tank pressure, (2) injector design requirements, (3) chamber pressure characteristics, (4) engine response requirements, (5) thrust linearity criteria, and (6) integrated throttling/shutoff capabilities. This section includes a comparison of the relative advantages of potential throttling concepts and a summary of the basic operating characteristics of each.

II.E.1a Basic Approaches

Control of propellant flow rate or thrust level for a monopropellant engine is simplified in comparison to the bipropellant case in that the mixing requirements of the injector do not exist. However, there are constraints on the injector configuration and pressure drop as dictated by hydrazine vaporization, catalyst bed utilization and heat transfer considerations. These factors were discussed in Section II.B.2b; the following discussion is primarily concerned with the pressure budgets and related effects associated with various flow control concepts.

Thrust control can essentially be implemented at three points in the propulsion system:

- Upstream of the injector
- At the injector
- At the thrustor nozzle throat

Implementation of any of these for the catalytic decomposition engine is relatively straightforward while the thermal decomposition engine generally requires control of parallel flow paths (1) the pilot stage, and (2) the main reactor. In addition, it is possible to combine actively or passively two of these control modes if there is some advantage to be gained. The possible approaches which were considered are as follows.

Upstream Control

The application of flow control valves to throttling is a commonly used approach in which the throttling mechanism can be developed separate from the

engine at the component level. The basic flow relationship of equation (1) indicates that the flow rate can be controlled by varying either the minimum (throat) flow area or the differential pressure across the valve. The former is generally

$$\dot{w} = C_D A_t \sqrt{2 \rho g (P_1 - P_2)} \qquad (1)$$

a more acceptable approach since the pressure losses can be minimized. The latter, which is characterized by two-stage throttling, was successfully used in the Surveyor vernier control system. However, relatively high tank pressures on the order of 700 to 800 psia were required for a maximum chamber pressure on the order of 100 psia. The advantage of the variable area valve is that at maximum flow rate the valve pressure loss can be reduced to a few psi. However, other factors such as flow linearity for tank pressure blow-down systems, engine dynamic coupling (hydraulic) and general flow control-lability including metering plug design limit the minimum acceptable pressure drop.

An extension to this type of valve is one in which the pressure at the throat reaches the vapor pressure of the fluid. Through this phenomena the flow rate can be made proportional to the effective flow area ($C_D A_t$) of the throat and independent of any downstream resistances (injector, catalyst bed, nozzle, filters, etc.). On the other hand, a valve diffuser section must be included to maximize pressure recovery which generally does not exced 85 percent of the valve inlet pressure. This can be compared to a 90 percent recovery (10 percent loss) design guideline for non-cavitating valves. The use of a cavitating/non-cavitating valve design such as in the Lunar Module Descent Engine combines the best features of each type. However, the achievement of good flow linearity and repeatability in the incipient cavitation or transition region is at best very difficult. The relative advantages and disadvantages of these valves are discussed in more detail in Section II.E.2 below.

Mechanization of this type of throttle control is easily implemented by packaging the valve and actuator separately and then mounting the sub-assembly to the engine. In the case of monopropellant engines, an integral throttle valve/actuator assembly is easily implemented and hermetically

where required. In the case of thermal decomposition engines, an additional problem arises in that the pilot chamber flow rate characteristics limit the engine throttle range unless the pilot can be shut down after ignition. If continuous flow is required then a maximum throttle range on the order of 5:1 is achievable. This is based on the need for a 10 percent (of maximum) pilot flow rate and a main valve throttling capability of 10:1. These values would have to be improved to about 5 percent and 20:1 respectively to obtain a 10:1 thrust range. Neither of these is considered obtainable at this time based on performance and accuracy criteria. In addition, a cavitating valve would be required in the pilot line to maintain a fixed flow rate as the pilot flow rate would tend to increase with decreasing main chamber pressure, thus further limiting the throttle range. There are two further alternates: (1) design the pilot chamber such that the gas flow into the main chamber chokes at some point in the throttle range, thus limiting the pilot flow rate or (2) locate the inlet to the pilot downstream instead of upstream of the main flow control valve thus providing a decreasing pilot inlet pressure characteristic with decreasing thrust. The former eliminates the need for a cavitating pilot valve but is not as effective while the latter presents problems during start-up because of the need for 3-5 seconds of pilot operation prior to main injector flow. If the main shutoff valve can be located between the throttle valve and engine, this approach is very feasible. The effect of injector selection on the pilot operation is discussed further in the following paragraphs.

Injector Control

A second fundamental approach to throttle control is to use the injector element directly. This type of throttling has been demonstrated with bipropellant engines through the use of a concentric injector in which a sleeve is used to meter both fuel and oxidizer flow rates. In this throttling mode, the injector area must be reduced sufficiently to offset the increase in injector pressure drop as chamber pressure decreases. The main advantage to this approach is the total elimination of a separate throttling mechanism and associated pressure loss as well as the integral packaging of throttle actuator and injector. Conversely, the large increase in injector pressure drop and thus injection velocity will tend to erode or channel the catalyst bed unless appropriate splash plates or series resistances are provided.

For use with thermal decomposition thrustors, the fixed cavitating venturi pilot valve would be required since no fuel pressure reduction occurs prior to the main injector element.

Nozzle Control

The relatively low combustion temperature of hydrazine engines makes the use of nozzle throat area control very feasible. In its simplest form the throat area could be reduced to control throttling while using a fixed area injector and no flow control valve. During throttling the chamber pressure would actually increase instead of decreasing as with the other concepts. The main advantages to this approach include (1) the lower tank pressure due to throttle valve elimination, (2) integral packaging of the actuator and chamber, and (3) higher I_{sp} performance at the low thrust levels due to the higher chamber pressure. The main disadvantages include potential thrust inaccuracies due to thermal deformation and the possibility of strong feed system/engine dynamic coupling at the low thrust levels due to the absence of any resistance between the chamber and tank. The latter would almost certainly necessitate the use of a chamber pressure or guidance control loop instead of the position feedback appraoch most commonly used with throttle valves. As an example, it is shown in Section II.E.1b that a 500 psia chamber pressure (catalytic decomposition) requires a 700 psia tank pressure excluding a throttle valve. (See Figure II.E-17). This requires a nozzle throat diameter of about 1.0" for a 600 lb_f engine; throttling to 10:1 would increase the chamber pressure to about 700 psia and would require an annular gap of 0.010" at the throat, which represents a throat area reduction of 14:1. This approach would be equally feasible for the catalytic and thermal decomposition engines.

Constant Pressure Drop Injector

One of the disadvantages to upstream throttling (throttle valve) is that the injector pressure drop at the low thrust levels is very small. For example, at the 10:1 throttle point the pressure drop is $1/100^{th}$ of the value at maximum throttle or on the order of 1 psi. This can lead to potential performance and stability problems under certain conditions. One method of avoiding this is to use a pressure balanced injector which maintains a relatively constant pressure differential across the injector. This is most easily implemented by spring loaded poppets which are closed

off as the fuel pressure downstream of the flow control valve decreases during throttling. Among the disadvantages of such an approach is the possibility of dynamic instability resulting from the combustion, hydraulic and mechanical frequency characteristics. However, efficient injector atomization over the entire throttle range is possible.

Fixed Chamber Pressure

Another alternate approach to thrust control is to maintain a constant engine chamber pressure while throttling the propellant flow at the injector (variable area). This requires the reduction of nozzle throat area as the engine is throttled. This approach has the advantage of maintaining nearly constant performance over the entire throttle range while providing separate flow control. This is somewhat similar in concept to the Lunar Module descent engine in which flow control is done at the throttle valves (cavitating) and optimum propellant injection is achieved by varying the injector setting (rather than the throat area); a single actuator simultaneously positions both the valves and the injector. In the constant chamber pressure approach it would be necessary, however, to include a position feedback control loop for the injector and a chamber pressure feedback for pressure control.

The use of a fixed pressure drop injector in this system would be best since the same pressure schedule would be maintained over the entire throttle range thus allowing complete optimization of performance. In this case, it would also be possible to use a passive fixed pressure drop injector control thus requiring only the single active (chamber pressure feedback) control loop.

II.E.1b Pressure Budget Evaluation

Selection of an "optimum" chamber pressure, catalyst bed ΔP, injector ΔP or feed system ΔP is essentially dependent on overall system performance requirements and/or other design constraints such as weight, envelope, etc. In order to evaluate the effects of ΔP allocation the flow control system, a set of ΔP values at maximum thrust were selected to be used as a baseline. The values selected are shown in Table II.E-1. Allocations of the pressure losses as a function of

percent flow rate for the various flow control concepts are shown in Figure II.E-1 through II.E-15. The graphs are based on the above ΔP schedule at 100% flow rate.

Non-Cavitating Throttle Valve

Figures II.E-1 through II.E-3 show the pressure budget for the fixed area injector engine with a non-cavitating throttle valve. The throttle valve ΔP schedule is shown to range between .10 P_{tank} at maximum thrust to approximately 100% P_{tank} at the 10:1 throttle point. The high ΔP across the valve at 10% throttle for engines designed for high chamber pressures indicates that cavitation with its attendant problems may occur in the valve. Among these are flow limiting and material pitting unless properly accounted for in the valve design.

The throttle valve flow area change computed by assuming a constant discharge coefficient is equal to $(w_{X\%}/w_{100\%})\ \sqrt{\Delta P_{100\%}/\Delta P_{X\%}}$. For a 10:1 throttling range the area reduction is approximately 97% or 30:1. The large area reduction required for a 10:1 throttling capability may present physical design problems depending upon the valve stroke, seat diameter and pressure balancing requirements. It should be noted that the injector ΔP at the 10% flow condition is only 1% (1.5 psi) of the original value of 150 psi indicating that the propellant injection pattern will be significantly altered. The effect of this low injector ΔP on engine performance and stability has been further discussed in Section II.B-2b. The primary advantage of the non-cavitating valve is that the ΔP requirement at the 100% flow condition can be reduced to a very low value if valve weight or size is not a limiting factor. The reduction in required tank pressure associated with a 5% pressure loss is also shown in Figure II.E-1 through II.E-3. However, a low valve ΔP may introduce undesirable engine/feed system dynamic coupling problems as well as a degradation in flow accuracies.

Cavitating Throttle Valve

Cavitating venturi throttle valves are often used to improve flow accuracies over wide throttle ranges and tank pressure blowdown ranges as well as to avoid hydraulic dynamic coupling. Since the cavitating

valve operates at a pressure differential equal to P_{tank}-$P_{vapor\ pressure}$, the variable valve ΔP schedule as a function of percent flow rate has no effect on valve design. The valve design is established only by the allowable ΔP at the maximum flow condition and the required throttling range. The flow area requirement is directly proportional to the flow rate requirement; i.e., for a 10:1 throttle range a 10:1 area change is required assuming a constant discharge coefficient as compared to a 30:1 area reduction required for a non-cavitating throttle valve. It should also be noted that since the valve flow rate is independent of downstream pressure, all engine generated pressure perturbations are effectively isolated from the propellant feed system, thus eliminating all engine-feed system dynamic coupling problems. The slightly lower pressure recover (85%) attained with the cavitating valve necessitates a slightly higher system operating pressure. The pressure schedules for a fixed area injector engine with a cavitating flow control valve are shown in Figure II.E-4 through II.E-6 as a function of maximum chamber pressure.

Variable Area Injector

The pressure budgets for the variable area injector flow control system (Figures II.E-7 through II.E-9) show that the operating ΔP requirement is essentially similar to the engine with the fixed area injector less the throttle valve pressure loss. Unlike the preceding configurations, the ΔP across the injector increases from 150 psi to approximately the supply pressure as the propellant flow is throttled from 100% down to 10% flow rate. This results from the fact that the variable injector area is used to throttle the flow. The injector area ratio for a 10:1 throttle range is approximately equal to $(w_{10\%}/w_{100\%})\sqrt{150/P_{tank}}$ or .072 (14:1) for an engine with a chamber pressure of 100 psia and approximately .039 (26:1) for an engine with a maximum steady-state chamber pressure of 900 psia. This represents an improvement compared to the non-cavitating throttle valve area ratio although the absolute areas are smaller by a factor of between 1/2 and 4/5 for maximum chamber pressures between 100 and 900 psia. The propellant velocity leaving the injector will increase by 39% when the engine

designed for a chamber pressure of 100 psia is throttled from 100% to 10% thrust and approximately 258% for an engine designed for a chamber pressure of 900 psia. The higher propellant injection velocity can result in an accelerated break-up of the catalyst granules unless appropriate splash plates or similar devices are provided.

Constant Pressure Drop Injector

The constant ΔP injector flow control system pressure budgets shown in Figures II.E-10 through II.E-15 indicate that the valve operating ΔP range for a 10:1 throttling range is greatly reduced for the low chamber pressure (100 psia) design condition. The valve ΔP ratio (i.e., $\Delta P_{10\%}/\Delta P_{100\%}$) is on the order of approximately 5.1:1 as opposed to 9.5:1 for the fixed injector engine with the non-cavitating valve. This effectively reduces the flow area ratio requirement for the flow control valve. At the higher design chamber pressure case (900 psia), the effect of the constant ΔP injector on reducing the valve ΔP range is considerably less (8.0:1 for the constant ΔP injector and 9.3:1 for the fixed area injector and non-cavitating valve configuration). The primary advantage afforded by the fixed ΔP injector system is that the propellant injection velocity and pattern remain essentially invariant with flow rate changes and thus can be set for highest engine performance.

Variable Area Nozzle

Figures II.E-16 through II.E-18 show the operating characteristics of the variable area nozzle control concept. As can be noted, the chamber pressure increases as thrust is reduced thus maintaining high theoretical performance. The maximum thrust nozzle expansion ratio and chamber pressure must be properly controlled, however, to obtain maximum performance. In addition, the low injector ΔP at low thrust makes this approach very susceptible to feed system perturbations and may introduce multiple engine stability problems.

Tank Pressure Requirements

The propellant tank pressures required for the catalytic and thermal decomposition engine are summarized in Figures II.E-19 and II.E-20 as a function of maximum chamber pressure and throttle valve pressure loss.

II.E.1c Throttling Concept Selection

The somewhat conventional upstream flow control system has been selected for further investigation due to the separate flow control component (valve) capability and the near-term schedule limitation. Future missions, however, might be more effectively fulfilled by using the variable-area-injector control approach which will reduce both the number of components and the required tank pressure. This approach would, therefore, be recommended for future applied research investigations.

II.E.2 Throttle Valve Performance

II.E.2a Steady-State Performance

Flow Relationships

Figures II.E-21 and II.E-22 show the derivation of equations relating propellant flow rate to supply pressure and system design parameters. Steady-state flow equations are derived for both the catalytic and thermal decomposition engines with a non-cavitating flow control valve, cavitating flow control valve and variable area injector.

The resulting general form of the flow equations for the catalytic decomposition engine (with a non-cavitating valve or a variable area injector) is a quadratic (Equation 2) in terms of flow rate.

$$\left(C_8 + \frac{1}{C_5} + C_4 + \frac{1}{C_3}\right) \dot{w}^2 + \left(C_2 + \frac{1}{C_1^2}\right)^{1/2} \dot{w} - P_1 = 0$$

$$\frac{1}{C_5} = \frac{P_1 - \left(C_2 + \frac{1}{C_1^2}\right)^{1/2} \dot{w}_o - \left(C_8 - C_4 + \frac{1}{C_3}\right) \dot{w}_o^2}{\dot{w}_o^2} \qquad (2)$$

and

$$\dot{w} = \frac{\left(C_2 + \frac{1}{C_1^2}\right)^{1/2} + \left[C_2 + \frac{1}{C_1^2} + 4P_1 \left(C_8 + \frac{1}{C_5} + C_4 + \frac{1}{C_3}\right)\right]^{1/2}}{2\left(C_8 + \frac{1}{C_5} + C_4 + \frac{1}{C_3}\right)}$$

By substituting the valve resistance $\left(\frac{1}{C_5}\right)$ into Equation (1) it can be shown* that the flow rate at any given throttle setting as a function of supply pressure is independent of distribution of total resistance between injector, feed system and throttle valve (Equation 3). Therefore, in order to minimize flow nonlinearities at other than design tank pressure, it is necessary only to minimize the catalyst and nozzle resistances; i.e., low design chamber pressure and catalyst bed ΔP; another alternative is to reduce the tank pressure blowdown range.

$$\dot{w} = \frac{\left\{\left(C_2 + \frac{1}{C_1^2}\right) + \frac{4P_{tank}}{\dot{w}_o^2 X^2}\left[P_{To} - \left(C_2 + \frac{1}{C_1^2}\right)^{\frac{1}{2}} \dot{w}_o X\right]\right\}^{\frac{1}{2}} - \left(C_2 + \frac{1}{C_1^2}\right)^{\frac{1}{2}}}{2\left[\frac{P_{To} - \left(C_2 + \frac{1}{C_1^2}\right)^{\frac{1}{2}} \dot{w}_o X}{\dot{w}_o^2 X^2}\right]}$$

where:

$\frac{1}{C_1}$ = nozzle resistance

C_2 = catalyst bed resistance

$\dot{w}_o$ = maximum design flow rate

$\dot{w}$ = flow rate

P_{To} = design tank pressure at which the valve flow is linearized

P_{tank} = tank pressure

X = fraction of maximum flow rate

*See the subsequent paragraphs on Tank Pressure Effect on Flow Linearity

The steady-state propellant flow equation for the catalytic engine with the cavitating flow control valve is shown to be essentially independent of downstream pressure, i.e., $w \propto \sqrt{P_{inlet} - P_{vapor}}$. As noted in Section II.E-1b, 15% of tank pressure is lost in the cavitating valve; if the maximum tank pressure is based on this requirement, the valve will come out of cavitation at some throttle setting less than 100% as tank pressure is reduced. Under these conditions Equation (3) must be used to determine the system flow rate.

The steady-state flow equation for the thermal decomposition engine is shown in Figure II.E-22 to be more complex than for the catalytic decomposition engine due to the parallel propellant flow paths. The equations were derived for a configuration using a fixed area non-cavitating type valve in the pilot propellant flow path and with the pilot propellant supply obtained upstream of the main throttle valve. The equation for the thermal decomposition engine with a non-cavitating flow control valve shows that the minimum propellant flow rate that can be obtained with the main throttle is limited by the pilot flow. The flow rate to the engine with the throttle closed is shown by Equation (4).

$$\left[C_{12} + \frac{1}{C_{11}} + \frac{\left(C_{10} + \frac{1}{C_9}\right)}{P_5 + P_8} + C_8\right] \dot{w}^2 + \left(\frac{1}{C_1^2} + \frac{1}{C_2}\right) \dot{w} - P_1 = 0 \qquad (4)$$

The pilot flow in effect limits the overall throttle range of the engine irrespective of the main throttle capability. The variation in the pilot flow can be eliminated simply by using a cavitating valve in the pilot flow circuit or by obtaining the pilot flow downstream of the main throttle valve. However, the latter method appears to be design limited at the low throttle range for a fixed area injector due to the low ΔP across the injector (1.5 psi at 10%).

Tank Pressure Effect on Flow Linearity

Evaluation of the engine control system indicates that a linear relationship of flow rate versus percent command voltage over the operating range of the engine will greatly simplify the design of the engine control system and the vehicle guidance and control system. Linearity is defined in this section as the slope of the flow rate versus percent command voltage curve at any given throttle setting. Analysis of the steady-state flow equations presented in the preceding section indicates that the non-cavitating flow control valve resistances can be scheduled to provide linear flow characteristics only at the one inlet pressure. If the propellant inlet pressure is changed from the selected design point, a non-linear effect will result. The slope of the flow rate percent command voltage will be greater than the design value if the inlet pressure is greater than the design value or the slope will be less if the inlet pressure is reduced below the design value.

This section presents the characteristic flow rate versus percent command voltage curves for representative flow control systems (Figures II.E-23 through II.E-33). The flow control systems shown plotted are:

(a) Fixed area injector engine with a non-cavitating valve

(b) Fixed area injector engine with a cavitating valve

(c) Variable area injector engine

(d) Constant ΔP injector engine with a non-cavitating valve

The figures shown are for the case where the systems have been linearized at the maximum design pressure.

Figures II.E-23 through II.E-25 show the non-cavitating flow control valve flow characteristics for a 2 to 1 tank blowdown range. The non-linearity (slope change) noted at the lower tank pressure is due to the effect of the catalyst bed and nozzle resistance. The figures also show that the non-linearity increases as the design chamber pressure is increased from 100 to 900 psia. As indicated in the preceding section, the overall flow non-linearity can be reduced by using the midpoint of the propellant tank blowdown range as the design pressure.

The flow characteristic of the control system using a cavitating throttle valve (Figure II.E-26) is shown to be linear for any tank pressure; i.e., no slope change, since the valve flow rate is independent

of downstream pressure. The ratio of the slopes at design tank pressure and .5 design tank pressure is equal to the square root of the ΔP ratio or .707. As discussed earlier, this relationship does not hold at the higher throttle settings due to the fact that the cavitating valve goes out of cavitation at some point. It should be noted, however, that higher throttle settings are not commanded late in the models duty cycle when tank pressure has decayed.

The flow rate versus percent command voltage characteristics of the variable area injector system (Figures II.E-27 through II.E-29) is similar to the flow control system with the non-cavitating valve with the exception that the non-linearity is slightly greater.

The constant ΔP injector engine flow characteristic is shown in Figures II.E-30 through II.#-32. The large slope changed noted for this system is due primarily to the fixed injector pressure drop (150 psi) which is equivalent to increasing the supply pressure blowdown range (Equation 5).

$$P_1 - \Delta P_{inj} = \left(C_8 + \frac{1}{C_5} + \frac{1}{C_3}\right) \dot{w}^2 + \left(C_2 + \frac{1}{C_1^2}\right)^{1/2} \dot{w} \qquad (5)$$

The flow maps show that the cavitating valve flow control system provides the best flow control "linearity" over the 2 to 1 tank blowdown. This analysis also indicates that the non-linearity of the non-cavitating valve flow control system can be minimized by reducing the design chamber pressure. The constant ΔP injector flow control system is shown by the figures to exhibit the worst performance characteristic of those systems considered. A significant improvement, however, can be obtained by operating the system at the higher propellant supply pressure.

II.E.2b Flow Gain Ratio

Flow gain ratio is defined in this section as the ratio of the flow slope (linearity) at a given throttle setting and tank pressure to the slope at the same throttle setting and any other tank pressure (Equation 6).

$$\text{Flow Gain Ratio} = \frac{\text{actual slope}}{\text{design slope}} \qquad (6)$$

The flow gain that will occur with a change in the propellant supply pressure has been evaluated (Equation 7) to illustrate the relative performance characteristics of the various flow control systems.

$$\text{slope} = \frac{\partial w}{\partial V_c} = \frac{2P_{tank}\, w_o^2\, X - 2R\, w_o^2\, X + R\, w_o\, w^2}{[P_{To} - R\, w_o\, X]\, 2w + R\, w_o^2\, X^2} \qquad (7)$$

where:

$$R = \left(\frac{1}{C_1^2} + C_2\right)^{1/2}$$

Figure II.E-34 shows the gain ratio that will occur with a 2 to 1 tank pressure blowdown with the flow control valve in the full-open position (100% command voltage). The slope at the 100% command voltage point is shown since the largest gain change occurs at the 100% throttle position. The results show essentially that the cavitating valve provides the least change (30% reduction) in flow gain and the gain is independent of chamber pressure. Although not shown in the figure, the gain is also independent of throttle position.

The non-cavitating valve and the variable area injector flow control systems show a larger variation in flow gain with a 2:1 tank pressure blowdown than the system using a cavitating flow control valve. The normalized flow gain characteristic decreases from about 55% to 33% as the design chamber pressure is increased from 100 to 900 psia. The normalized gain for the cavitating valve system remains constant at 70.7%.

The normalized flow gain for the constant ΔP injector system ranges between 2% and 3% for design chamber pressures ranging between 100 psia and 900 psia, respectively. The gain is almost zero for the low design chamber pressure case because of the high injector ΔP.

The flow gain change over the total tank pressure blowdown range can be minimized for the control systems which do not use a cavitating venturi flow control valve by linearizing the flow schedule at the mid tank pressure. This is a necessity in current vehicle design since the guidance and control

system can only tolerate gain changes up to some limit; a flow gain change of 2.4:1 is currently acceptable. In order to demonstrate the effect of system pressure distribution on the flow gain change, the flow control system using the non-cavitating flow control valve and fixed area injector was evaluated quantitatively. The detailed analysis is presented in Appendix C. Figure II.E-35 shows the variation in the flow gain ratio as a function of chamber pressure and catalyst bed pressure drop for a tank pressure of 500 psia and a maximum thrust level of 600 lb_f. Examination of Figure II.E-35 and equations (C-10)*, (C-11) and (C-12) shows that once the catalyst bed pressure drop and chamber pressure are established, the distribution of the remaining pressure between lines, valve and injector has no effect on the gain ratio (assuming a square law pressure loss for these elements). Therefore, this distribution can be made on the basis of injector and valve design criteria without affecting the flow gain ratio.

Valve Weight

A cursory valve weight study was conducted to estimate the valve weight as a function of design thrust. The results indicate that the weight increase due to increasing the design throat level from 300 to 1200 lb_f will be negligible. This study is based on a valve design using an electromechanical actuator and a pressure balanced pintle. Essentially no weight increase is anticipated for the following reasons:

(a) No increase in the inlet and exit port dimension from the baseline design is required (i.e., the valve body dimension will be the same).

(b) The small increase in the valve pintle weight (0.5 oz) will not affect the E/M actuator torque requirement. The pintle weight increase of 0.5 oz will only increase the effective actuator rotor inertia by 0.5×10^{-6} oz-in-sec^2.

(c) The pintle-seal friction, return spring preload, spring rate, etc., will not increase with an increasing flow requirement.

The estimated flight valve weight for the above range of thrust is 2.75 lbm.

---

*See Appendix C

II.E.2c Dynamic Considerations

During engine head end priming, the throttle valve and/or engine injector will be subjected to high surge pressures caused by the throttling of the high transient flow rates at the valve and the injector. In order to determine the magnitude of these peak surge pressures, the feed system was mathematically modeled and the system (including a non-cavitating throttle valve) analyzed with the aid of an on-line computer program. A schematic of the feed system used in the analysis is shown in Figure II.E-36. The results of the analyses are discussed in this section and shown in Figures II.E-37 through II.E-39 as a function of maximum chamber pressure for a 400 lbf engine. A summary of the data is presented in Figure II.E-40. It was assumed for the purpose of this analysis that the engine priming sequence will be initiated with either a squib or fast response solenoid valve and with the system pressurized to the design tank pressure up to the squib valve. A line volume between the squib valve and the throttle valve of 1.84 cubic inch was used in this analysis as an approximation of the priming volume.

The analysis indicated that peak surge pressure at the inlet of the non-cavitating throttle valve will be of the order of 1650 psia (ΔP = 872 above tank pressure) with the throttle in the full-open position and approximately 3900 psia (ΔP = 3122 above tank pressure) when the valve is at the 60% open position. The resulting high surge pressure is due to the combined effect of a high initial transient flow rate of 9.8 lb/sec (compared to 1.04 lb/sec during steady-state operation) during priming coupled with the high resistance of the throttle valve. The calculated peak flow rate during the priming sequence of 9.8 lb/sec is equivalent to a flow velocity of 75 ft/sec. The effect of the throttle valve resistance on peak surge pressure can be seen by the difference in the magnitude of the over-pressure with the valve partially closed.

The analysis also indicates that the time duration of the surge pressure generated during the priming sequence is relatively short (approximately 5 milliseconds) and damped out in a short time, therefore, the over-pressure may not be critical. However, the throttle valve structural design must be consistant with these stress levels.

The results indicated that in general a priming sequence initiated with a downstream void volume of 1.84 cubic inch will generate surge pressures in excess of 1650 psia (ΔP = 872). Higher peak surge pressures are generated as the valve resistance is increased. In order to minimize the pressure transient, the void volume should be less than 1.84 in^3 and the valve resistances less than $25\left(\frac{psi\text{-}sec^2}{LBm^2}\right)$. Specific design analyses need to be conducted for each system; in general, the priming volume should be small enough that priming occurs before the line flow velocity can reach its peak or maximum allowable value. The time for this to occur is a function of the feed system inertia and resistance levels.

II.E.2d Valve Selection

Table II.E-2 shows the relative merits of the various valve configurations evaluated with the highest value indicating the best selection. The linear plug valve is recommended for further investigation due to the relative accuracy capabilities and the absence of an integral shutoff requirement. The non-cavitating operating mode has been selected primarily because of the lower tank pressure requirement. Figure II.E-41 shows a cutaway view of a typical non-cavitating linear plug valve with an electromechanical actuator.

If faster response is required, a rotary plug type valve should be considered; this would eliminate the short linear stroke requirements which limits the capability of meeting desired pressure and flow rate schedules.

II.E.3 Electromechanical Throttle Actuator

II.E.3a Actuator Response

A typical electromechanical throttle valve step response characteristic was evaluated parametrically using a mathematical model and typical motor constants (Figure II.E-42). The step response times (0 to 90% of commanded step) were computed using the CSMP on-line computer program. For this analysis, the power supply voltage to the torque motor was varied between 18 and 36 volts to cover nominal expected range of operating voltages. In addition, the valve spring force, as a function of position, was varied between 320 and 1280 oz/inch. The lower limit represents the spring constant used in the present LTV Minuteman III LITVC throttle valve design and the upper limit represents the estimated rate for a valve designed to operate with a 1200 psia inlet pressure.

The effect of the 1.0 to 7.36 inch-oz bias torque on the step response time was also considered in the analysis. The lower value of 1.0 inch-oz represents the nominal minimum design limit (i.e., motor coulomb friction only) and the upper limit represents the estimated extremes of seal friction, spring bias load and pressure load reflected to the motor as a bias torque. (A motor torque of 1.0 inch-oz is required to hold a pintle load of 3.15 lbs). Both the spring force and pintle friction forces act to increase the valve response time since the torque motor must operate against the effects of the combined load.

During valve closure, the spring force will aid the actuator and therefore decrease slightly the closing response time. The results indicate that a valve response time of 60 ms (for an engine response time of 75 ms) can be met at 28 vdc only if the friction torque is very low. However, since no failed-close requirement exists, the spring can be removed which will shift the curves down approximately 10 ms. If further design margin is required, the valve stroke must be reduced.

II.E.3b Actuator Selection

Actuator selection was based on the rating criteria shown in Table II.E-3. By applying a numerical rating technique to the seven feasible concepts, a relative appraisal of the inherent features was possible. Table II.E-4 presents the results of the actuator rating study with a high value indicating the most desirable approach. While both the electromechanical (E/M) and electrohydraulic (E/H) actuator concepts are capable of fulfilling the mission requirements, the need for pre-launch checkout places such an excessive burden on the electrohydraulic system that the electromechanical actuator becomes the only feasible approach. In the event that response times become more critical and confidence is generated that pilot valve (servovalve or solenoid valve) displacement is a suitable operational indication, the electrohydraulic actuator should be re-examined.

II.E.4 Control Systems

II.E.4a Accuracy

A propellant control system using a throttle valve with an electromechanical actuator was analyzed to determine the parameters affecting resolution, hysteresis, linearity and static error. For the purpose of

this evaluation, the control accuracy definitions are as follows:

(a) Resolution - defined as the change in control signal required to obtain a change in the controlled output.

(b) Hysteresis - defined as the change in control signal required to reverse the direction of the controlled output.

(c) Static Error - defined as the total deviation of the controlled output variable from the theoretical or commanded input.

(d) Linearity - defined as the slope of the controlled variable versus input command signal curve or alternatively as the ratio of the slope at any given command point or over a given range to the design slope.

In this study, three control concepts were evaluated and are described in general form in Figure II.E-43. The block diagrams of the three candidate control systems are shown in Figure II.E-44 through II.E-46 and the equations relating the control system parameters to the above accuracy criteria are given in Figure II.E-47. A comparative evaluation of the three control systems indicate that resolution and hysteresis are controlled by the forward loop gain, valve control electronics and the actuator static friction. Feedback loop gain has no effect on either resolution or hysteresis. The latter is due to the fact that the criteria is based on essentially open-loop characteristics. In general, the equation indicates that resolution and hysteresis can be reduced by increasing the forward loop gain, motor torque constant, or by reducing internal friction. The static error of the controlled output variable, however, is controlled by the forward loop gian, the feedback loop gain and the internal errors associated with the actuator and the actuator control electronics. Therefore, the static error can be reduced by increasing the feedback loop gain and also by including all the control system components in the loop.

The linearity of the controlled output variable for chamber pressure feedback and guidance system feedback control system is controlled only by the feedback loop. All forward loop gain variations such as the valve flow gain variation due to tank pressure variation is compensated by the feedback loop. The position feedback control system, however, does not compensate for valve flow rate gain changes.

II.E.4b Response and Stability Characteristics

Figures II.E-48 and II.E-49 show the open loop root locus of the position feedback and chamber pressure feedback control systems, respectively. The root locus for the position feedback system (Figure II.E-48) shows that the position feedback control system (Figure II.E-44) is stable except at very high gain. Instability at the high gain is indicated since there are asymptotes located at 60° and 300° indicating that the root locus will cross over the jw axis if the gain is increased to a very high value. The response characteristics of the position feedback control system can be improved by the addition of compensation in either the forward loop or the feedback loop. This is also illustrated in Figure II.E-48 with a simple lead-lag compensation in the feedback loop. The compensation allows the system to be operated with higher gain thus improving the system response characteristics. If the gain and time constants are properly selected, the effective damping will be the same, therefore, the overshoot characteristics will remain essentially unchanged.

The root locus for a control system using chamber pressure feedback is shown in Figure II.E-49. The engine dynamics in the root locus plot are represented as a simple second order system and the throttle valve is modeled as a third order system (See Figure II.E-45). It should be noted that if the engine is characterized by a lightly damped oscillation, it will always exist in the position feedback. With the chamber pressure feedback, there is an opportunity to attenuate these oscillations although the possibility of creating a further instability also exists. The root locus plot indicates that the control system stability limit is reached when the controller gain is increased to 5.9×10^{12}. If, however, a lead compensation with a transfer function of (.015 +1/.00335 +1) is integrated into the feedback loop the gain can be increased to 16.3×10^{12} before the system stability limit is reached. It should be noted here that the compensation techniques can be used to either stabilize a control loop or to improve its performance characteristics. Optimum selection of the compensation time constants not only improves the response characteristics but also improves overshoot as well as system settling time.

II.E.4c Control System Selection

The control system evaluation was performed by a numerical rating technique and the results are shown in Table II.E-5. For near term missions, the conventional valve position feedback loop has been selected due to inherent transducer reliability and inner loop stability enhancement. Improvements in chamber pressure transducers would, however, provide the capability for greater thrust accuracy, thrust response, and possible roughness attenuation through the use of the chamber pressure feedback loop. It is also recommended that joint guidance and control propulsion studies be made to evaluate the possibility of eliminating the engine control loop completely and working strictly with the prime vehicle control loops.

Table II.E-1. Pressure Budget Assumptions

ITEM	CATALYTIC THRUSTOR	THERMAL DECOMPOSITION THRUSTOR
ΔP DECOMPOSITION BED	40 PSI	10 PSI
ΔP INJECTOR	150 PSI	100 PSI
PILOT FLOW	NONE	10% OF MAX. THROTTLE
CHAMBER PRESSURE	100 - 900 PSIA	100 - 900 PSIA
BLOWDOWN RANGE (TANK PRESSURE)	2:1	2:1
ΔP FEED SYSTEM	10 PSI	10 PSI
ΔP THROTTLE VALVE	*	*

*Cavitating, .15 P_{tank}; Non-Cavitating, .10 P_{tank}; Non-Cavitating, .05 P_{tank}.

Table II.E-2. Valve Comparison Chart

(A) BASIC RATING
(B) WEIGHTED RATING
(C) COULD SHAPE STROKE
(D) UNBALANCED OVERFLOW RANGE
(E) THE WEIGHTED VALUE EQUALS PRODUCT OF BOTH RATINGS.

CHARACTERISTIC	VALVE TYPE												
	LINEAR PLUG												
	WEIGHTING FACTOR	CAVITATING	NON CAVITATING	CAVITATING/ NON-CAVITATING	BALL	BUTTERFLY	ROTARY PLUG	GATE	SLIDE	FLAPPER	SPOOL	POPPET	PINCH
(C) EASE OF CHARACTERISTIC SHAPING FOR TRAVEL VS FLOW LINEARITY (LINEAR OR ROTATION TRAVEL	3	5(A)	4	2	3	1	3	4	4	2	4	3	1
		15(B)	12	6	9	3	9	12	12	6	12	9	3
FULL OPEN PRESSURE LOSS	4	3	5	5	5	4	5	5	3	3	3	4	4
		12	20	20	20	16	20		12	12	12	16	16
(D) (E) TORQUE OR FORCE REQUIREMENTS (PRESSURE LOADS)		4	3	3	4	5	4	2	2	1	4	1	2
(E) EASE OF PRESSURE BALANCING		4	4	4	3	3	3	1	3	1	5	1	2
		16	12	12	12	15	12	2	6	1	20	1	4
STARTUP AND SHUTDOWN TIME OF ENGINE	4	2	4	3	5	5	5	5	5	5	5	4	5
		8	16	12	20	20	20	20	20	20	20	16	20
ACCURACY CHARACTERISTICS	5	5	4	3	3	1	3	4	4	2	3	2	1
		25	20	15	15	5	15	20	20	10	15	10	5
PRESSURANT GAS SATURATION EFFECTS	1	1	5	3	2	2	2	3	3	2	3	4	4
		1	5	3	2	2	2	3	3	2	3	4	4
RELATIVE WEIGHT	4	4	4	4	3	5	3	4	3	5	3	4	2
		16	16	16	12	20	12	16	12	20	12	16	8
SHUTOFF CHARACTERISTICS	1	3	3	3	5	4	5	5	5	3	5	5	2
		3	3	3	5	4	5	5	5	3	5	5	2
EASE OF FABRICATION	3	5	4	3	3	1	3	3	2	1	2	1	1
		15	12	9	9	3	9	9	6	3	6	3	3
		111	116	96	104	91	104	107	96	77	102	80	65

Table II.E-3. Actuator Rating Criteria

PARAMETER	WEIGHTING FACTOR
RESPOND	3
POWER	4
LOAD SENSITIVITY	2
WEIGHT	5
PACKAGING (VALVE INTEGRATION)	1
ACCURACY	
RESOLUTION	1
REPEATABILITY	1
LINEARITY	1
HYSTERESIS	1
NOISE SENSITIVITY	1

PARAMETER	WEIGHTING FACTOR
TRANSMISSION REQUIREMENTS	1
RELATIVE COST	1
RELATIVE RELIABILITY	5
CHECKOUT CAPABILITY	5
ENVIRONMENTAL SENSITIVITY	
VACUUM STORAGE	1
VIBRATION	1
STERILIZATION	1
EMI	1
N_2H_4 COMPATIBILITY	1

Table II.E-4. Actuator Rating

TYPE	RATING
ELECTROMECHANICAL (PWM)	148.5
ELECTROHYDRAULIC	
• SOLENOID PILOT VALVE	149.5
• SERVOVALVE	146.0
ELECTROPNEUMATIC	
• SOLENOID PILOT VALVE	116.5
• SERVOVALVE	104.5
FLUIDIC/HYDRAULIC	
• DIGITAL	129.5
• PROPORTIONAL	130.0

Table II.E-5. Control System Evaluation

CHARACTERISTIC	WEIGHTING FACTOR	POSITION	CHAMBER PRESSURE	VEHICLE ($\ddot{H}$, $\dot{H}$, H)
STABILITY (BASIC) NOISE SENSITIVITY	5	5	3	4
		25	15	20
THRUST RESPONSE	4	3	5	5
		12	20	20
COMPENSATION REQUIREMENTS	1	5	4	3
		5	4	3
COMPATIBILITY WITH G AND C SYSTEM	2	4	4	5
		8	8	10
EFFECT OF TIME DEPENDENT SYSTEM PARAMETERS	2	3	4	5
		6	8	10
STARTUP/SHUTDOWN TIMES	3	3	5	5
		9	15	15
TRANSDUCER REQUIREMENTS	1	4	3	5
		4	3	5
RELATIVE COST	1	4	3	5
		4	3	5
RELATIVE RELIABILITY	5	4.5	4	5
		22.5	20	25
RELATIVE DEVELOPMENT TIME	1	5	4	4
		5	4	4
CALIBRATION	2	4	5	3
		8	10	6
LINEARITY	4	2	4.5	5
		8	18	20
ACCURACY	5	4	4.5	5
		20	22.5	25
CHECKOUT	5	5	2	2
		25	10	10
		161.5	160.5	178

Figure II. E-1

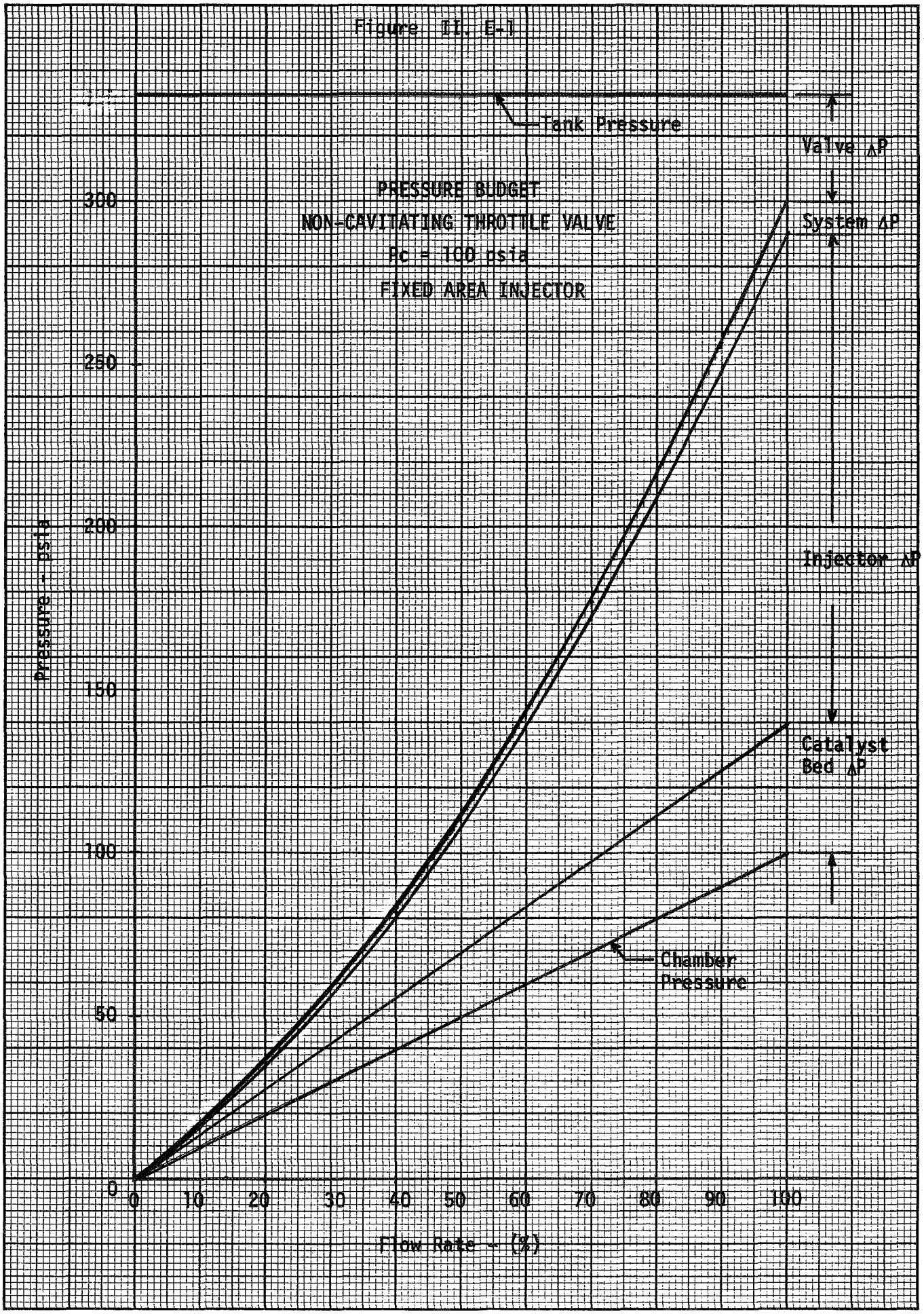
PRESSURE BUDGET
NON-CAVITATING THROTTLE VALVE
Pc = 100 psia
FIXED AREA INJECTOR
Tank Pressure
Valve ΔP
System ΔP
Injector ΔP
Catalyst Bed ΔP
Chamber Pressure
Pressure - psia
300
250
200
150
100
50
0
0
10
20
30
40
50
60
70
80
90
100
Flow Rate - (%)

Figure II. E-2

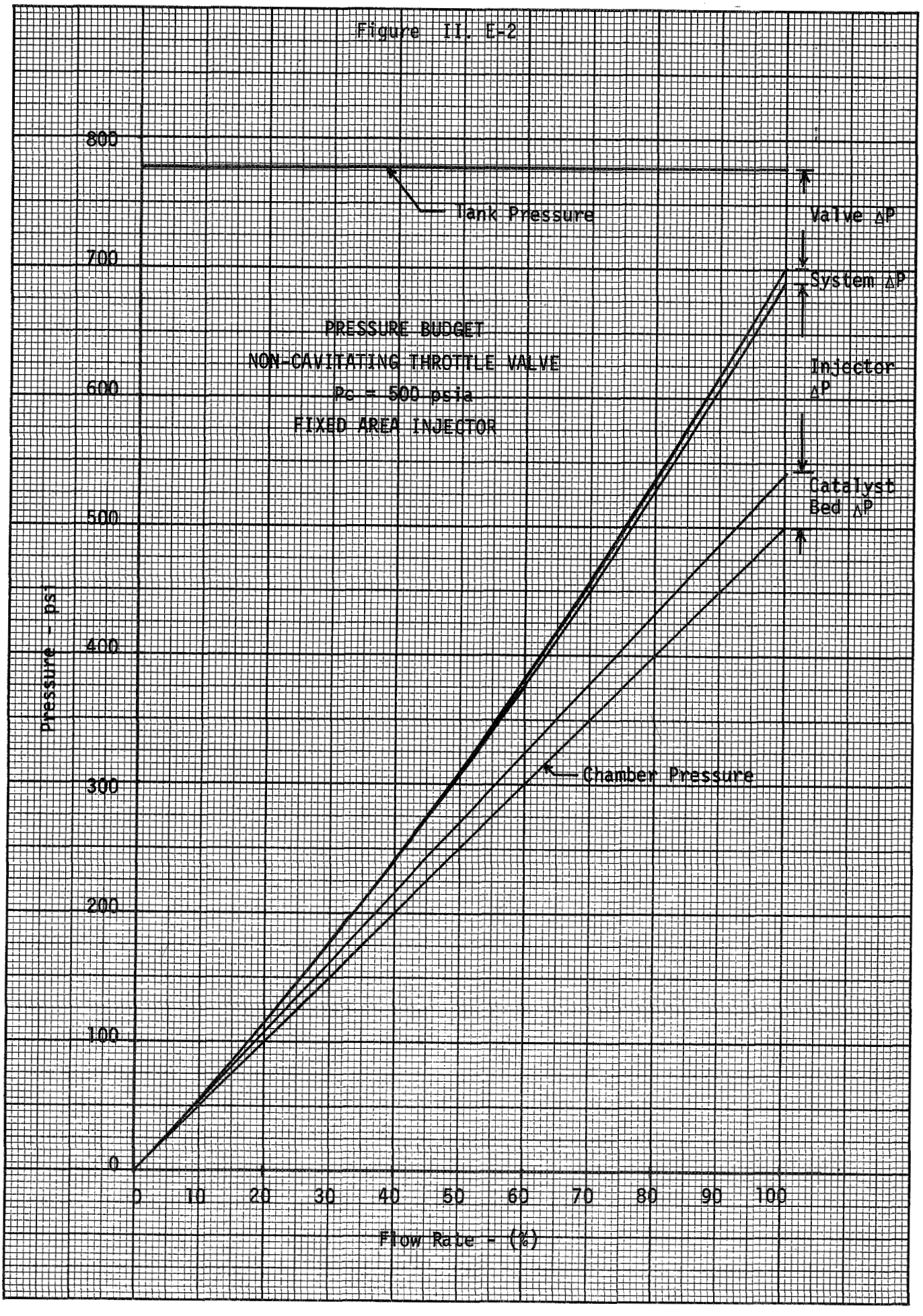
800
700
600
500
400
300
200
100
0
Pressure - psi
0
10
20
30
40
50
60
70
80
90
100
Flow Rate - (%)
PRESSURE BUDGET
NON-CAVITATING THROTTLE VALVE
Pc = 500 psia
FIXED AREA INJECTOR
Tank Pressure
Valve ΔP
System ΔP
Injector ΔP
Catalyst Bed ΔP
Chamber Pressure

Figure II. E-3

PRESSURE BUDGET

NON-CAVITATING THROTTLE VALVE

Pc = 900 psia

FIXED AREA INJECTOR

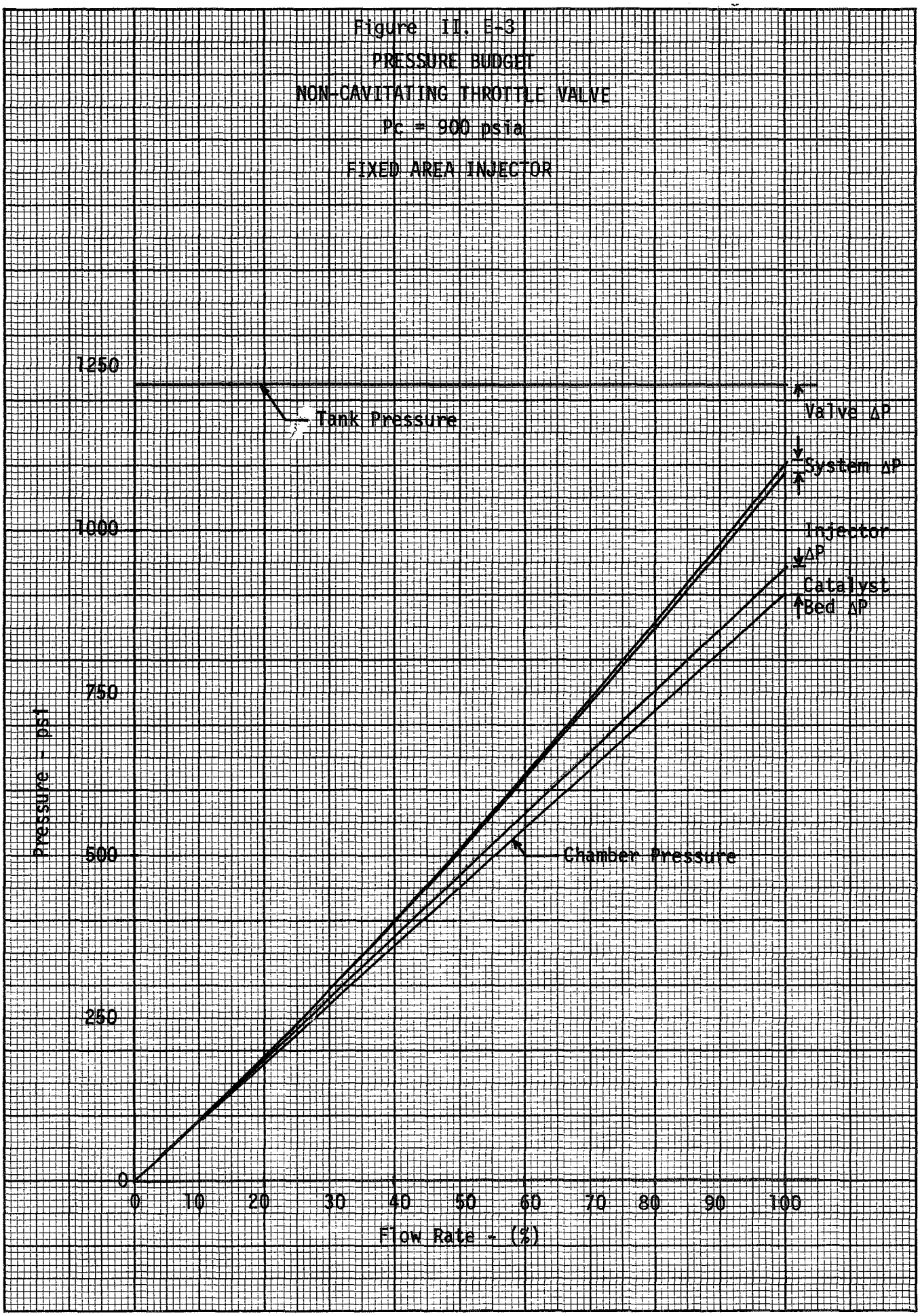

Figure II. E-4

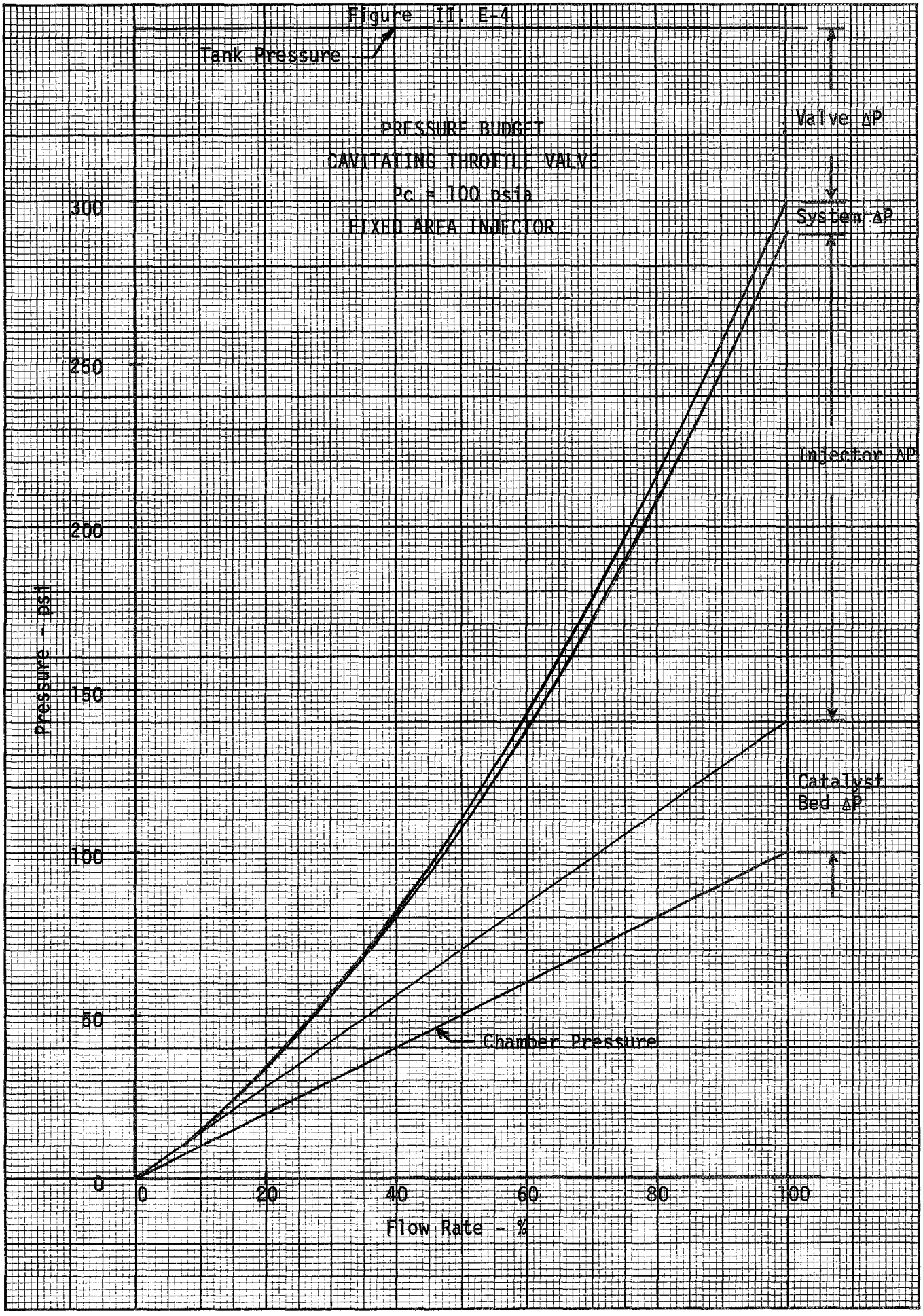
PRESSURE BUDGET
CAVITATING THROTTLE VALVE
Pc = 100 psia
FIXED AREA INJECTOR
Tank Pressure
Valve ΔP
System ΔP
Injector ΔP
Catalyst Bed ΔP
Chamber Pressure
Pressure - psi
Flow Rate - %
300
250
200
150
100
50
0
0
20
40
60
80
100

Figure II. E-5

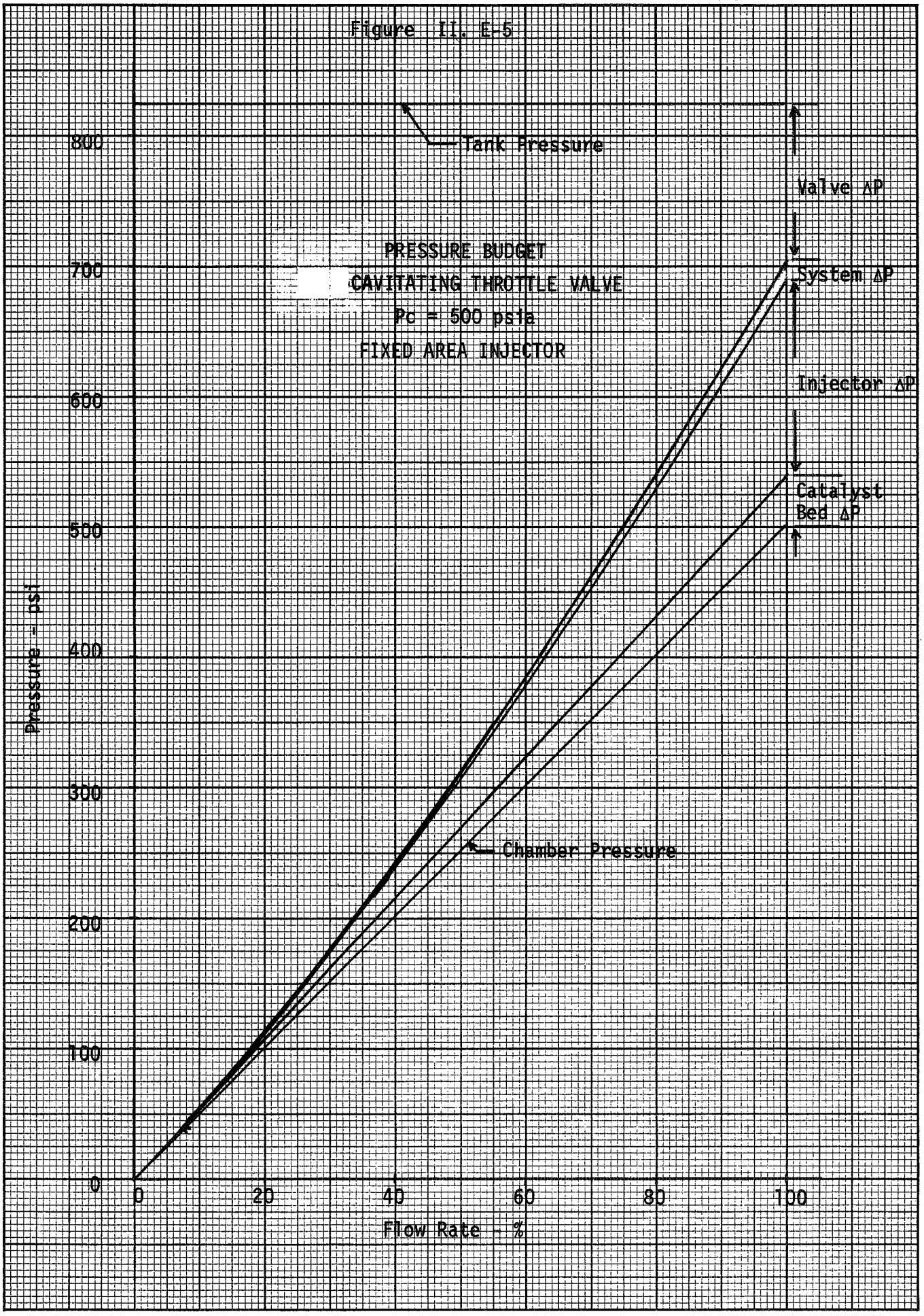
PRESSURE BUDGET
CAVITATING THROTTLE VALVE
Pc = 500 psia
FIXED AREA INJECTOR
Tank Pressure
Valve ΔP
System ΔP
Injector ΔP
Catalyst Bed ΔP
Chamber Pressure
Pressure - psi
Flow Rate - %
0
100
200
300
400
500
600
700
800
0
20
40
60
80
100

Figure II. E-6

PRESSURE BUDGET
CAVITATING THROTTLE VALVE
Pc = 900 psia
FIXED AREA INJECTOR

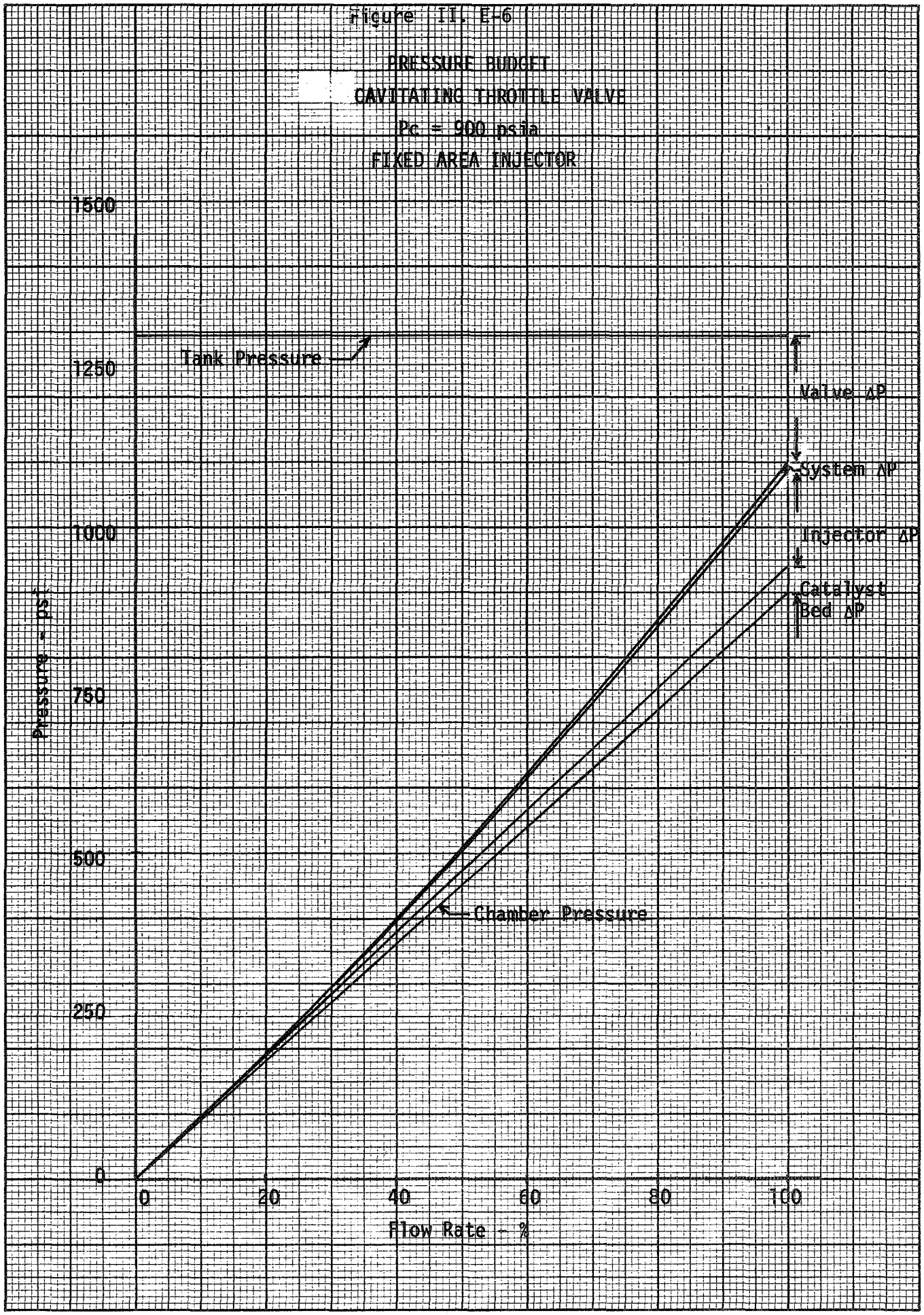

Figure II. E-7

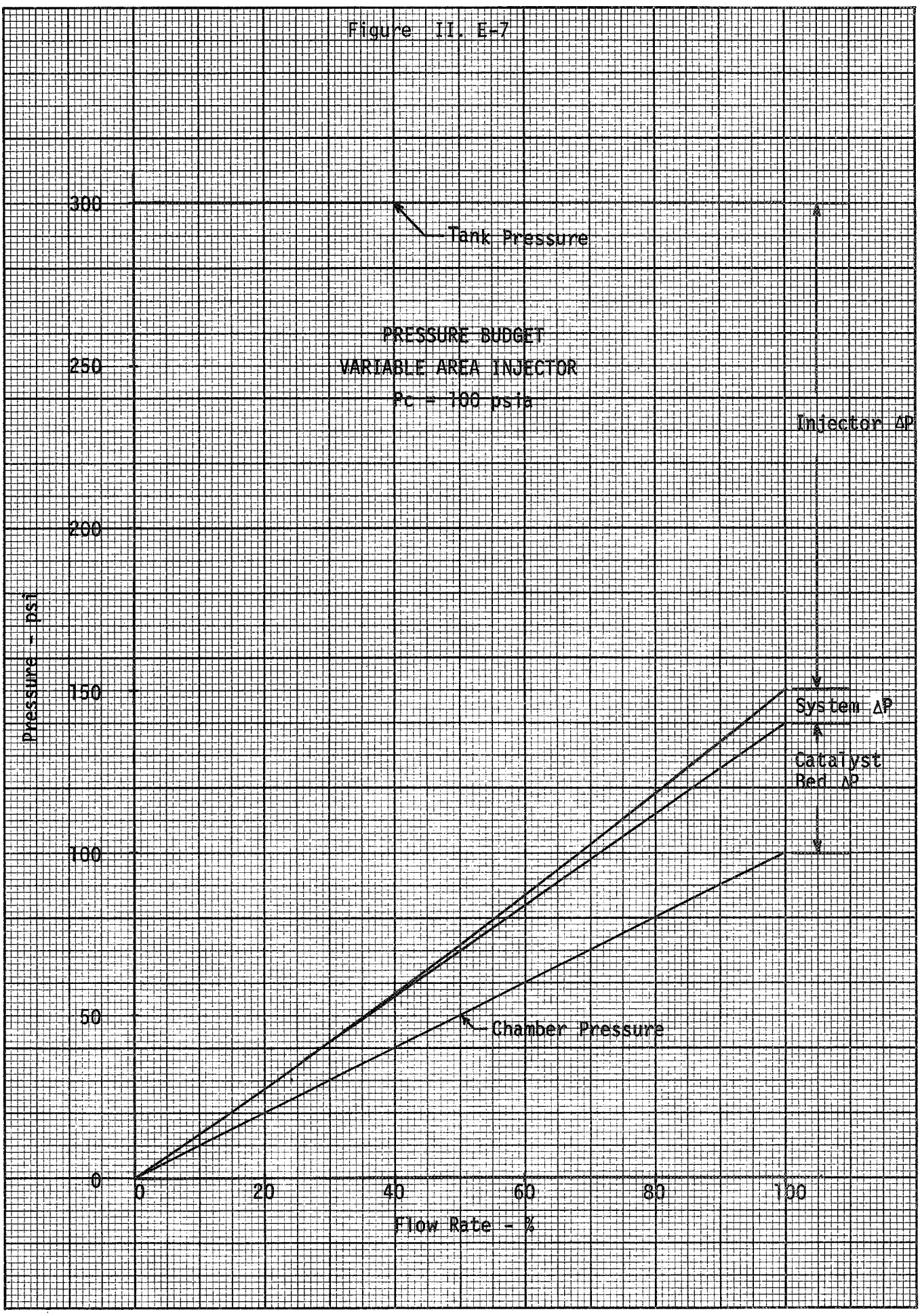
PRESSURE BUDGET
VARIABLE AREA INJECTOR
Pc = 100 psia
Tank Pressure
Injector ΔP
System ΔP
Catalyst Bed ΔP
Chamber Pressure
Pressure - psi
300
250
200
150
100
50
0
0
20
40
60
80
100
Flow Rate - %

Figure II. E-8

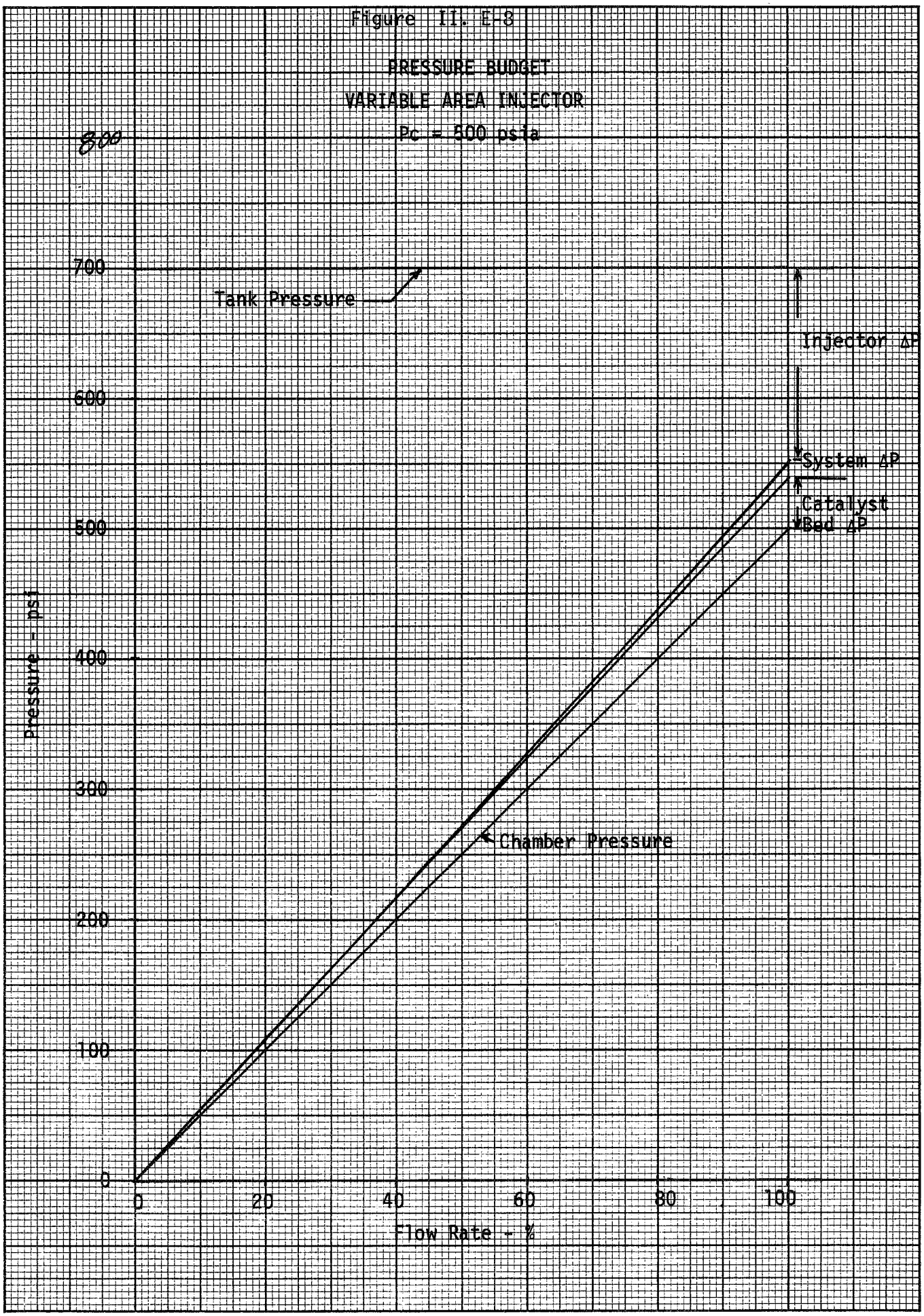
PRESSURE BUDGET
VARIABLE AREA INJECTOR
Pc = 500 psia
800
700
600
500
400
300
200
100
0
Pressure - psi
Tank Pressure
Injector ΔP
System ΔP
Catalyst Bed ΔP
Chamber Pressure
0
20
40
60
80
100
Flow Rate - %

Figure II. E-9

PRESSURE BUDGET
VARIABLE AREA INJECTOR
Pc = 900 psia

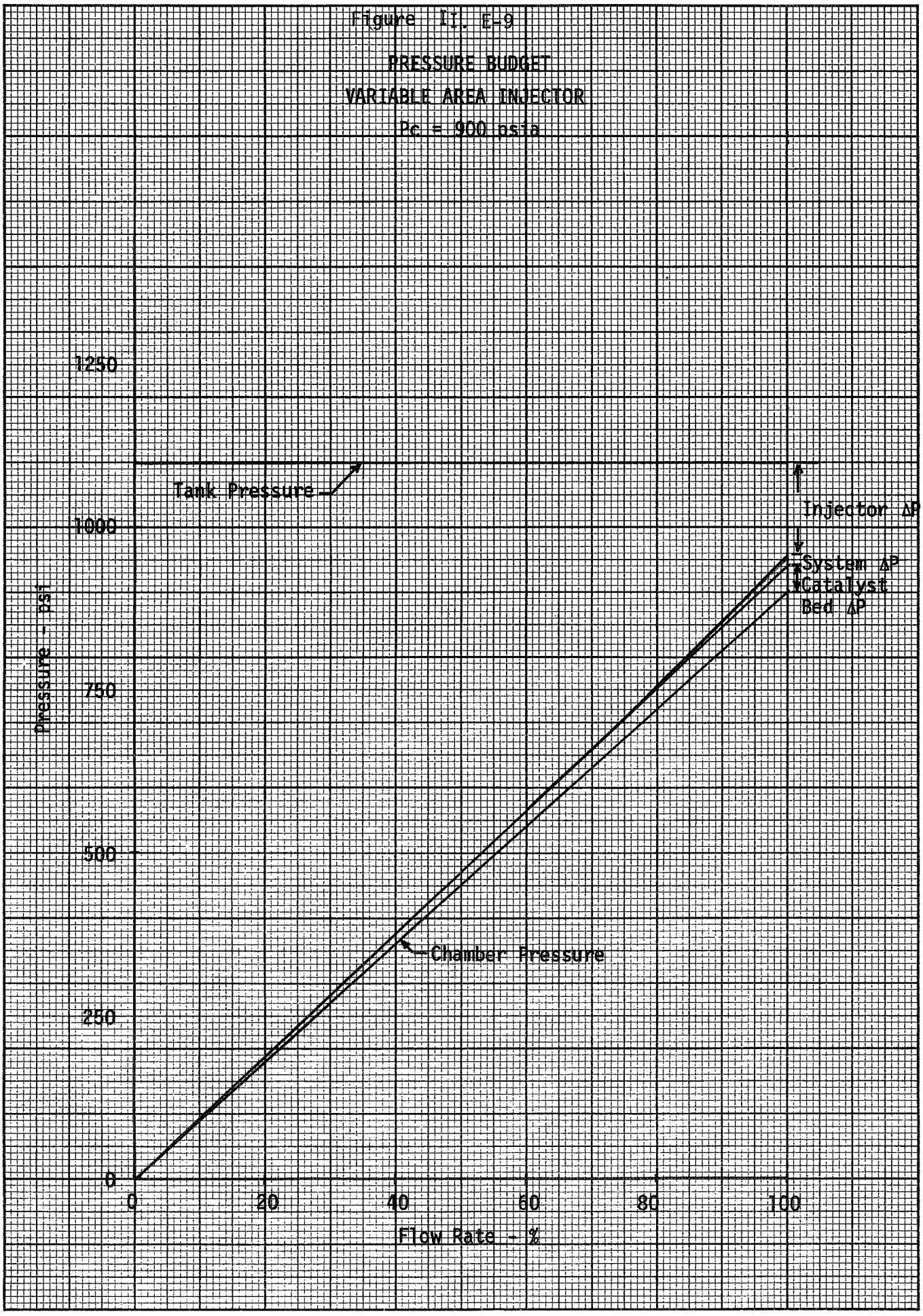

Figure II. E-10

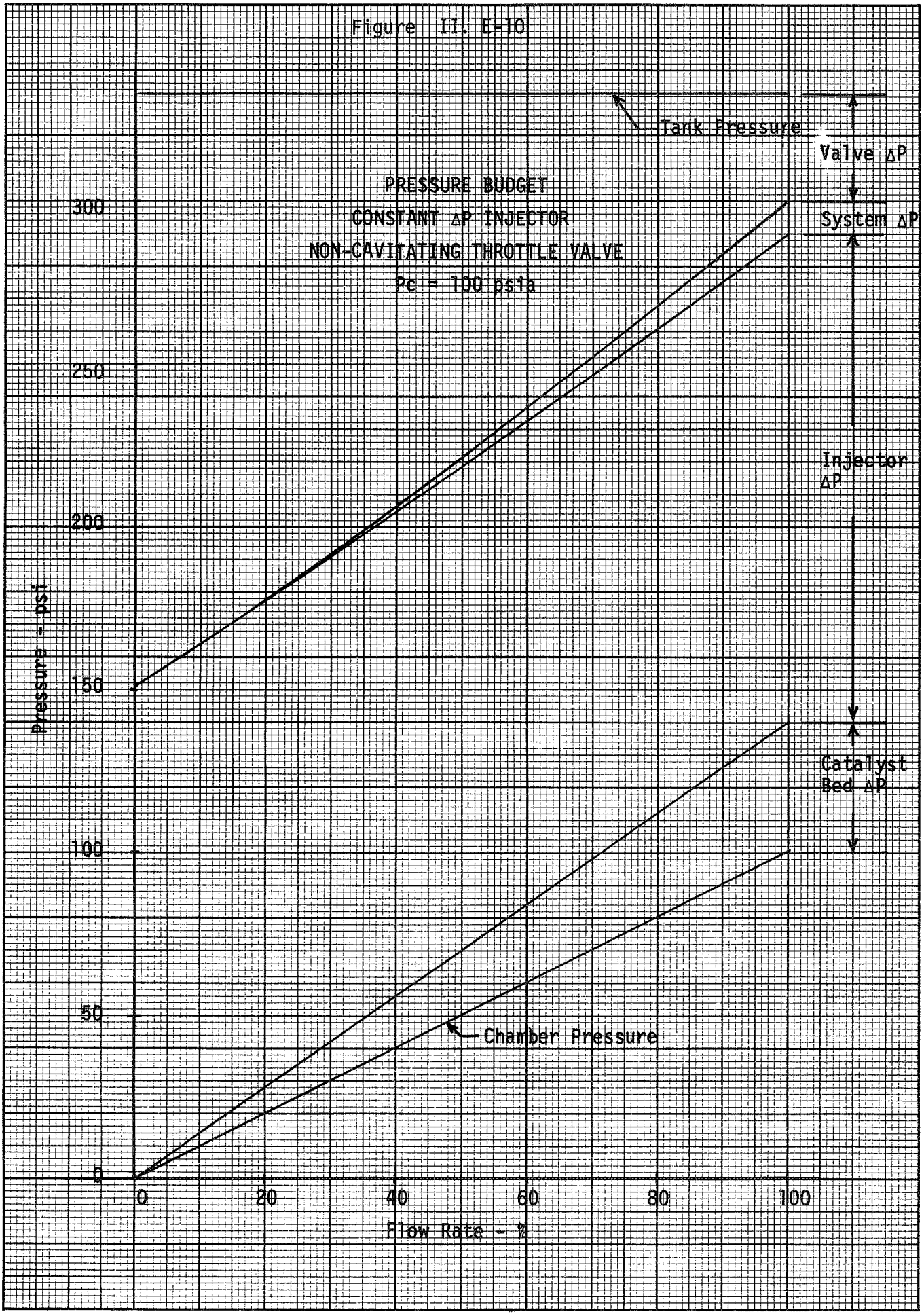

Figure II. E-11

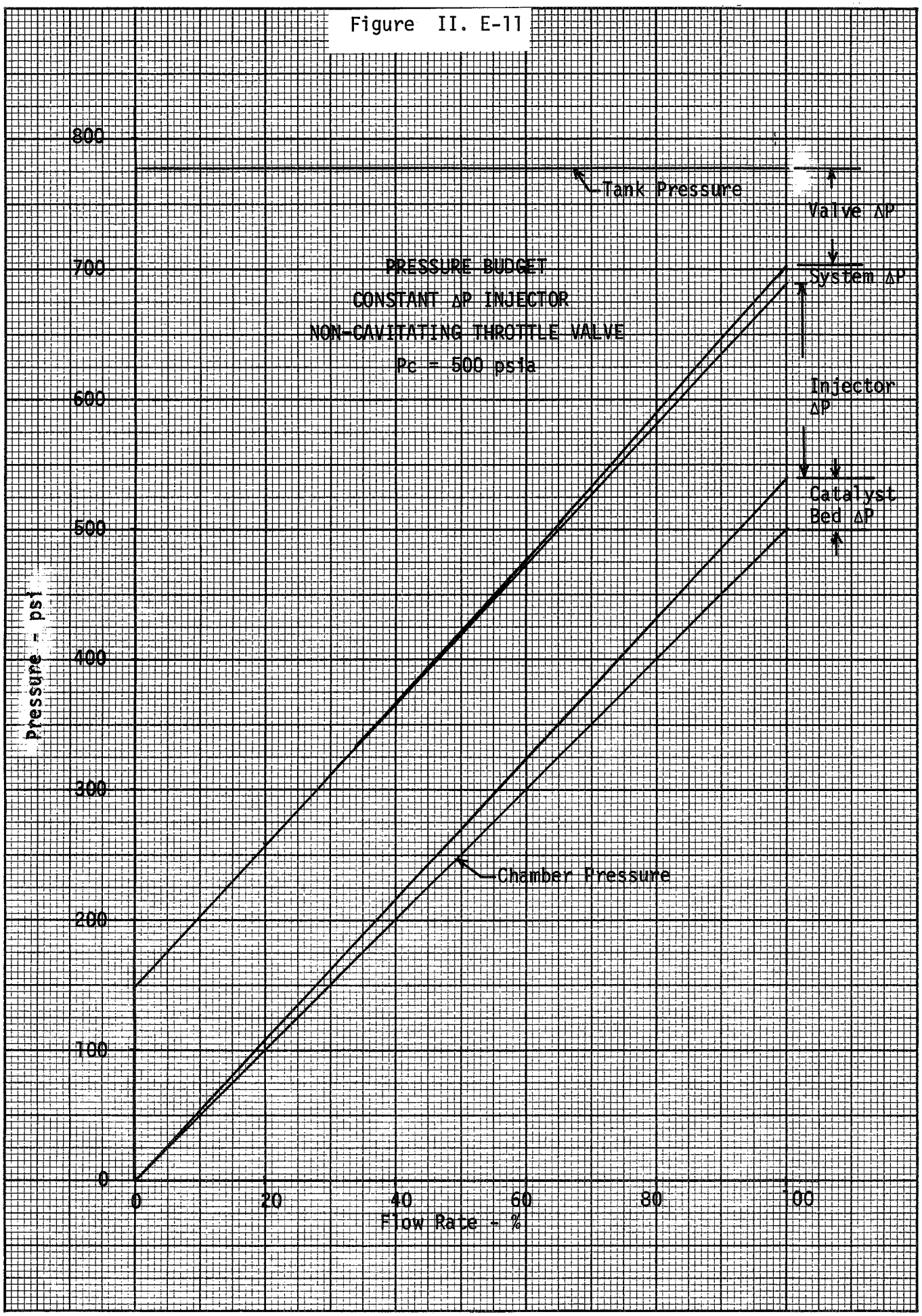

Figure II. E-12
PRESSURE BUDGET
CONSTANT ΔP INJECTOR
NON-CAVITATING THROTTLE VALVE
Pc = 900 psia

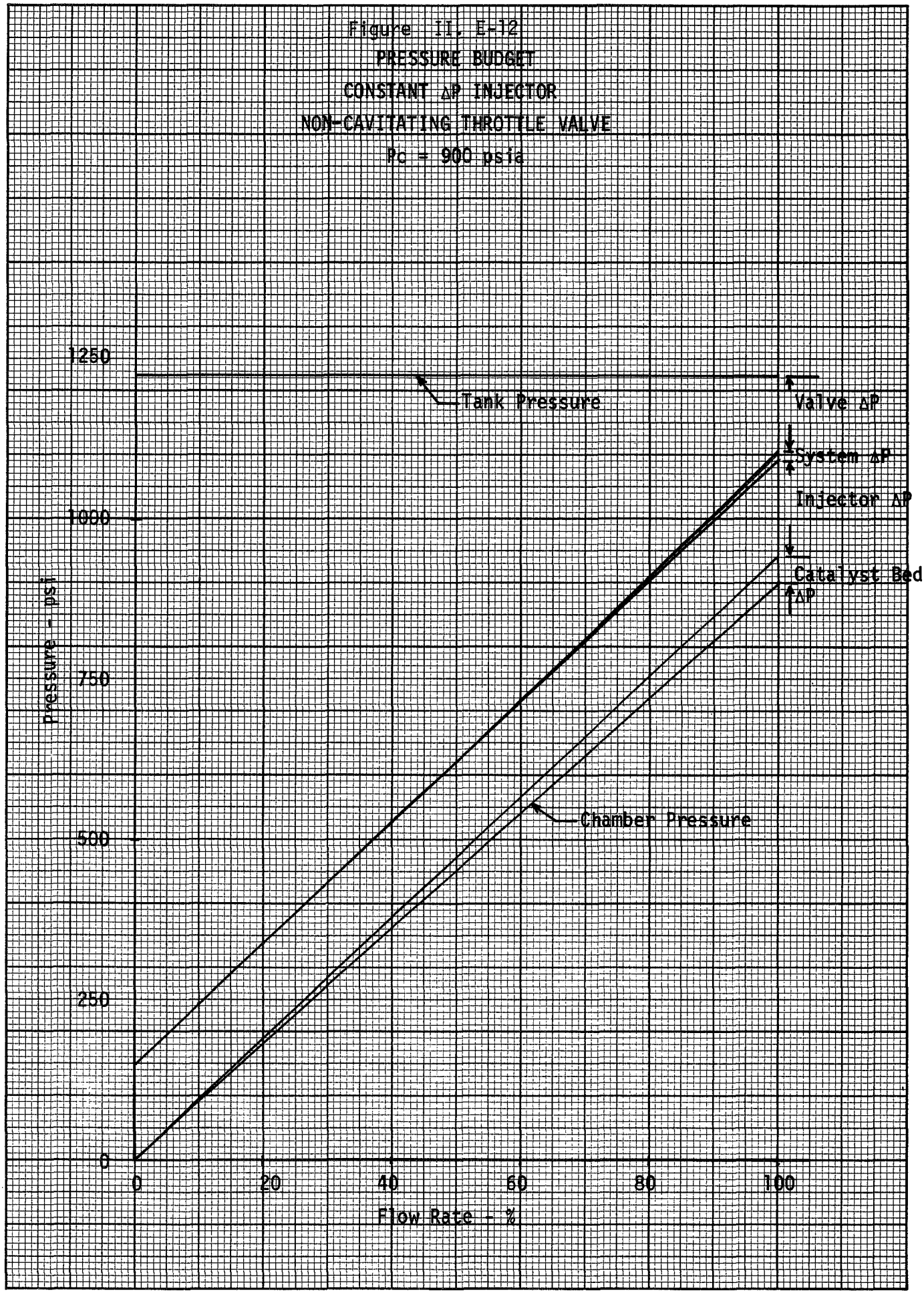

Figure II. E-13

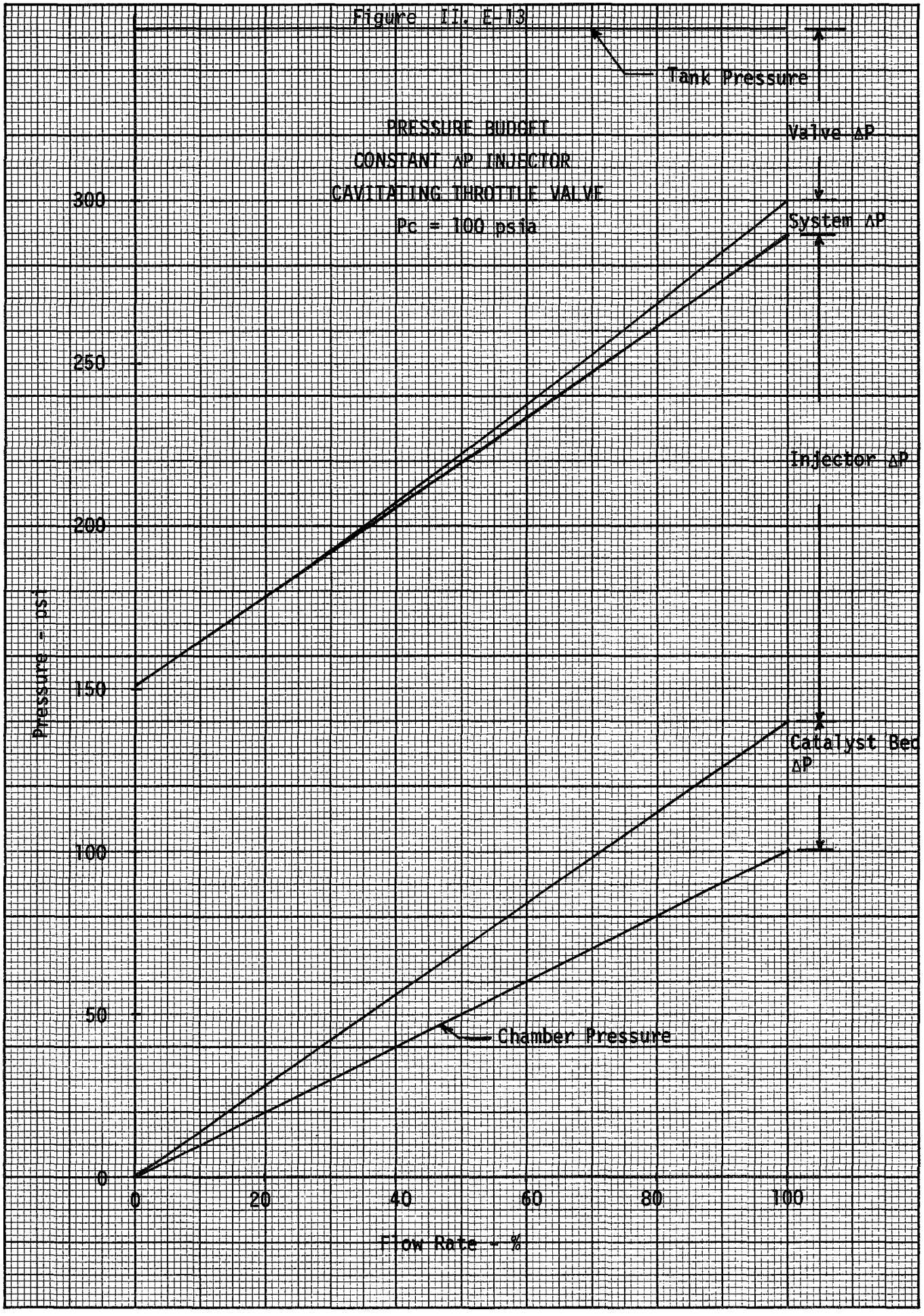

Figure II. E-14

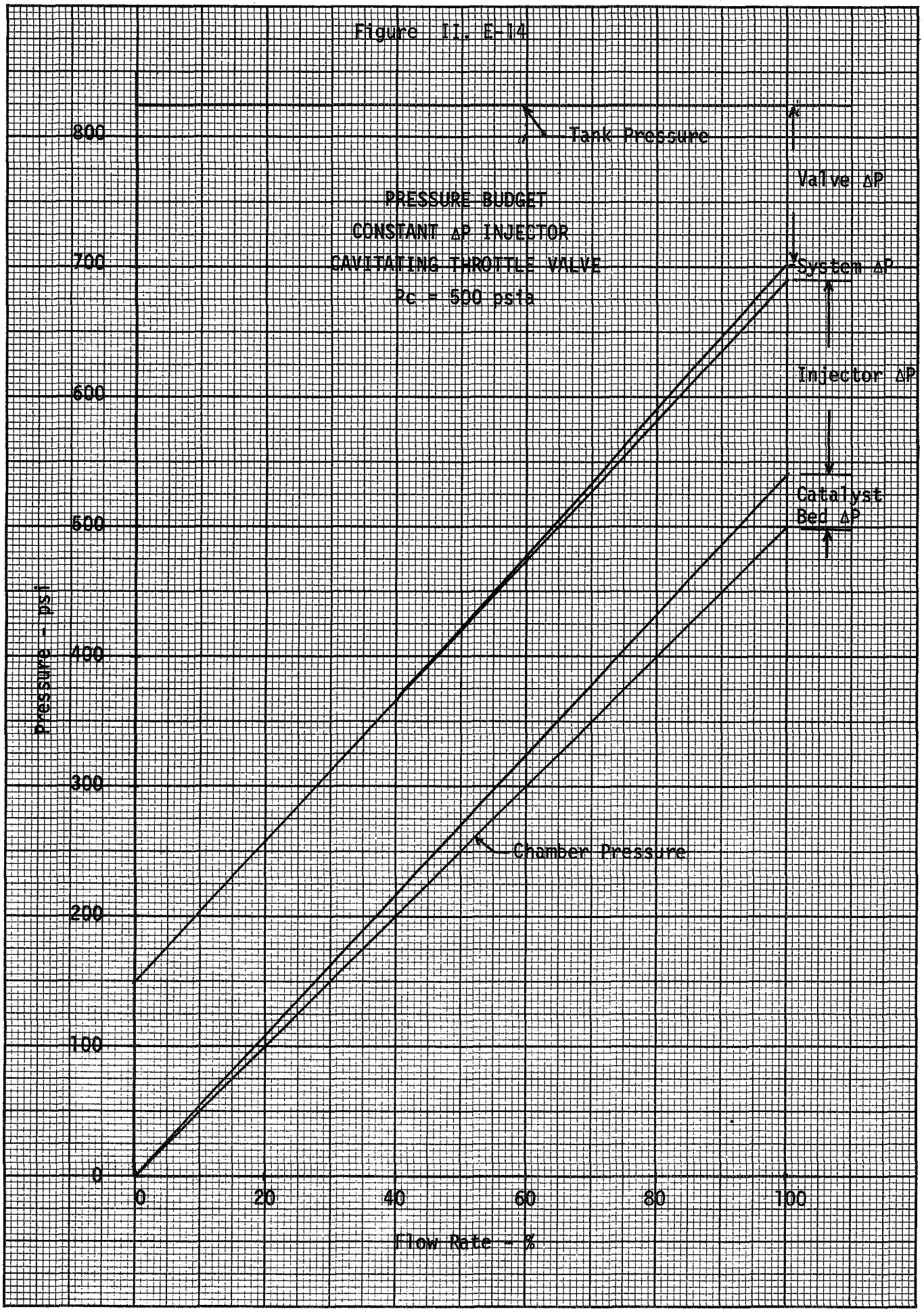

Figure II. E-15

PRESSURE BUDGET

CONSTANT ΔP INJECTOR

CAVITATING THROTTLE VALVE

Pc = 900 psia

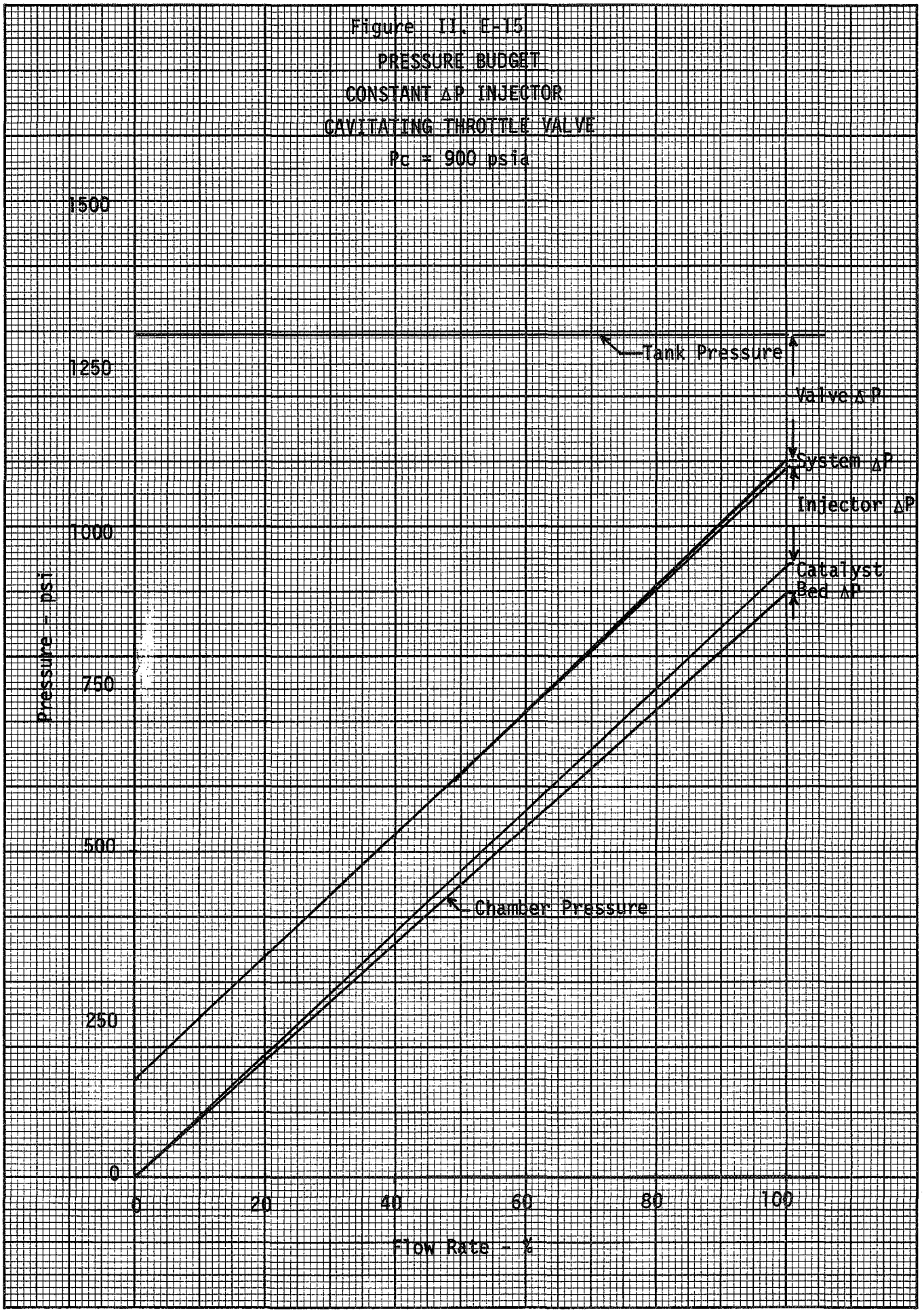

Figure II. E-16

PRESSURE BUDGET
VARIABLE AREA NOZZLE
100 PSIA CHAMBER PRESSURE
300 PSIA TANK PRESSURE

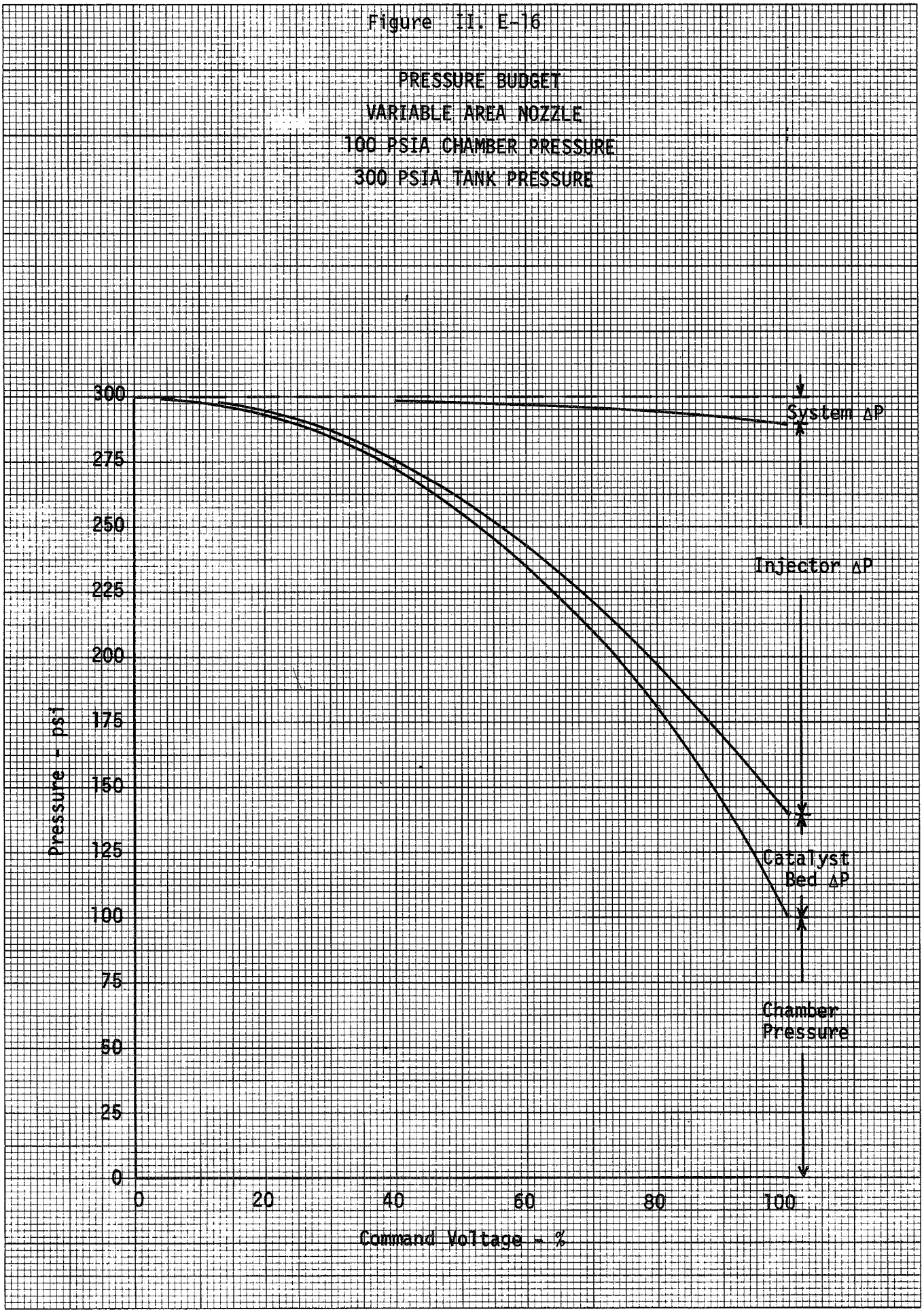

Figure II. E-17

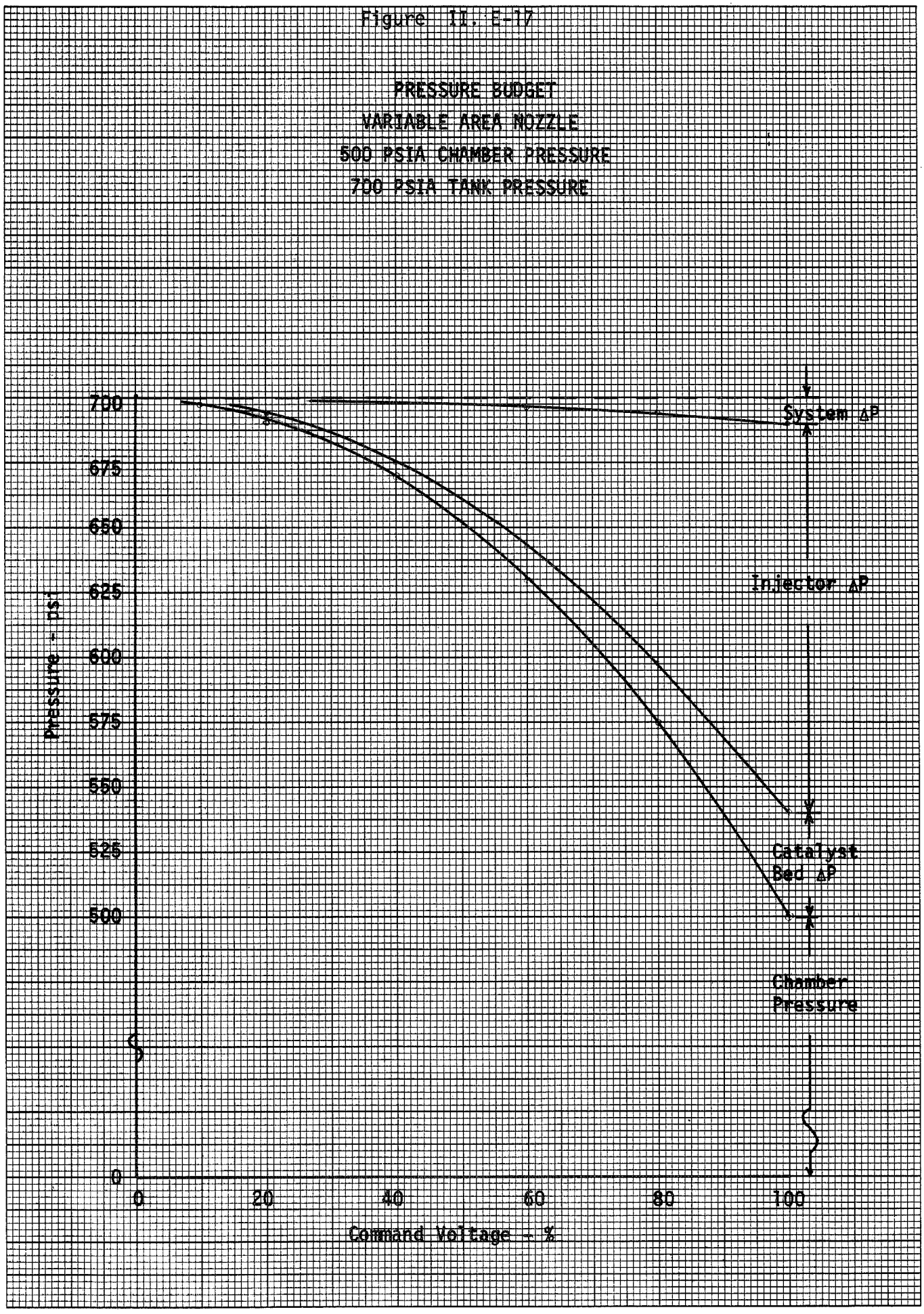

Figure II. E-18

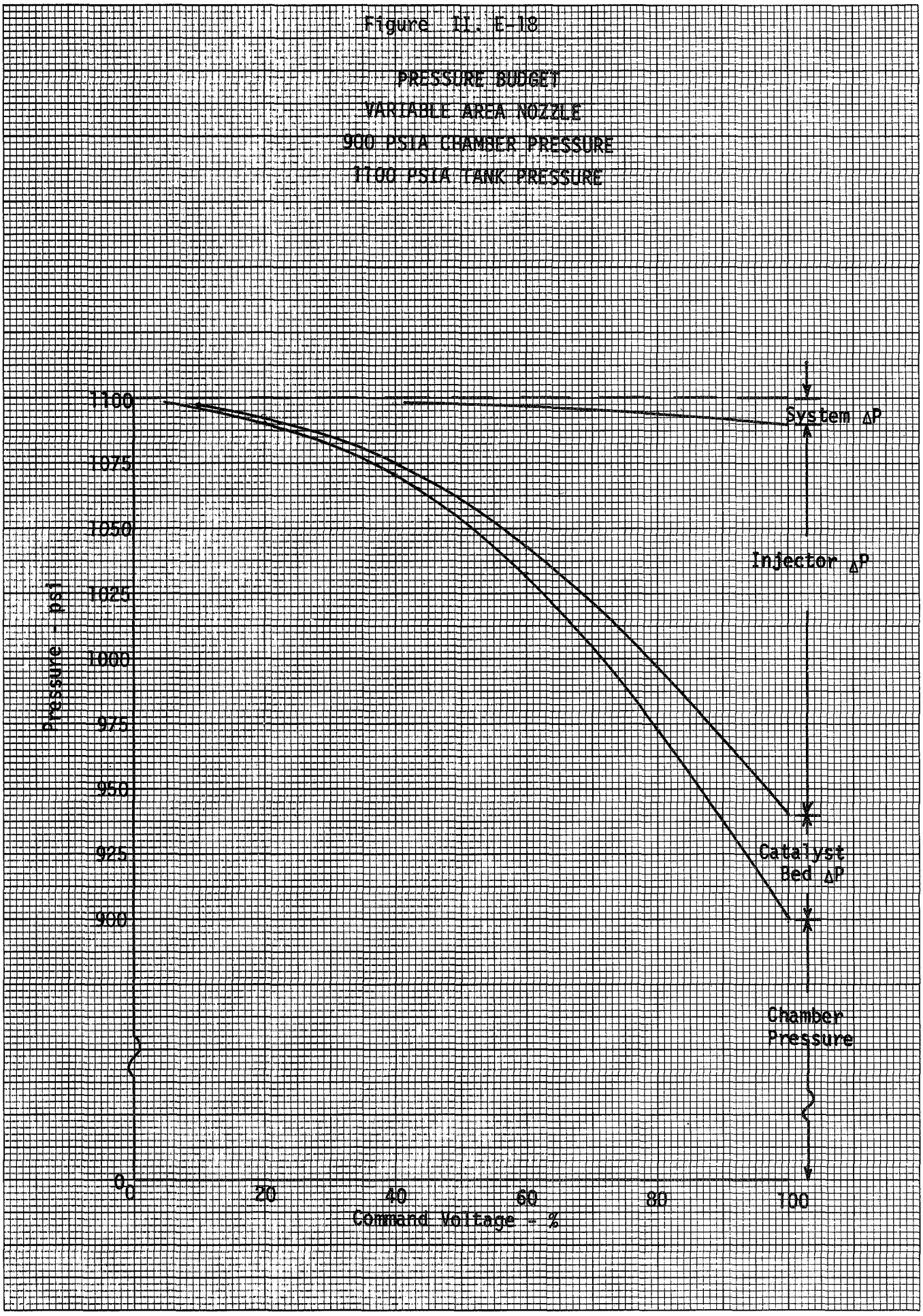

Figure II. E-19

TANK PRESSURE REQUIRED FOR
CATALYTIC DECOMPOSITION ENGINE

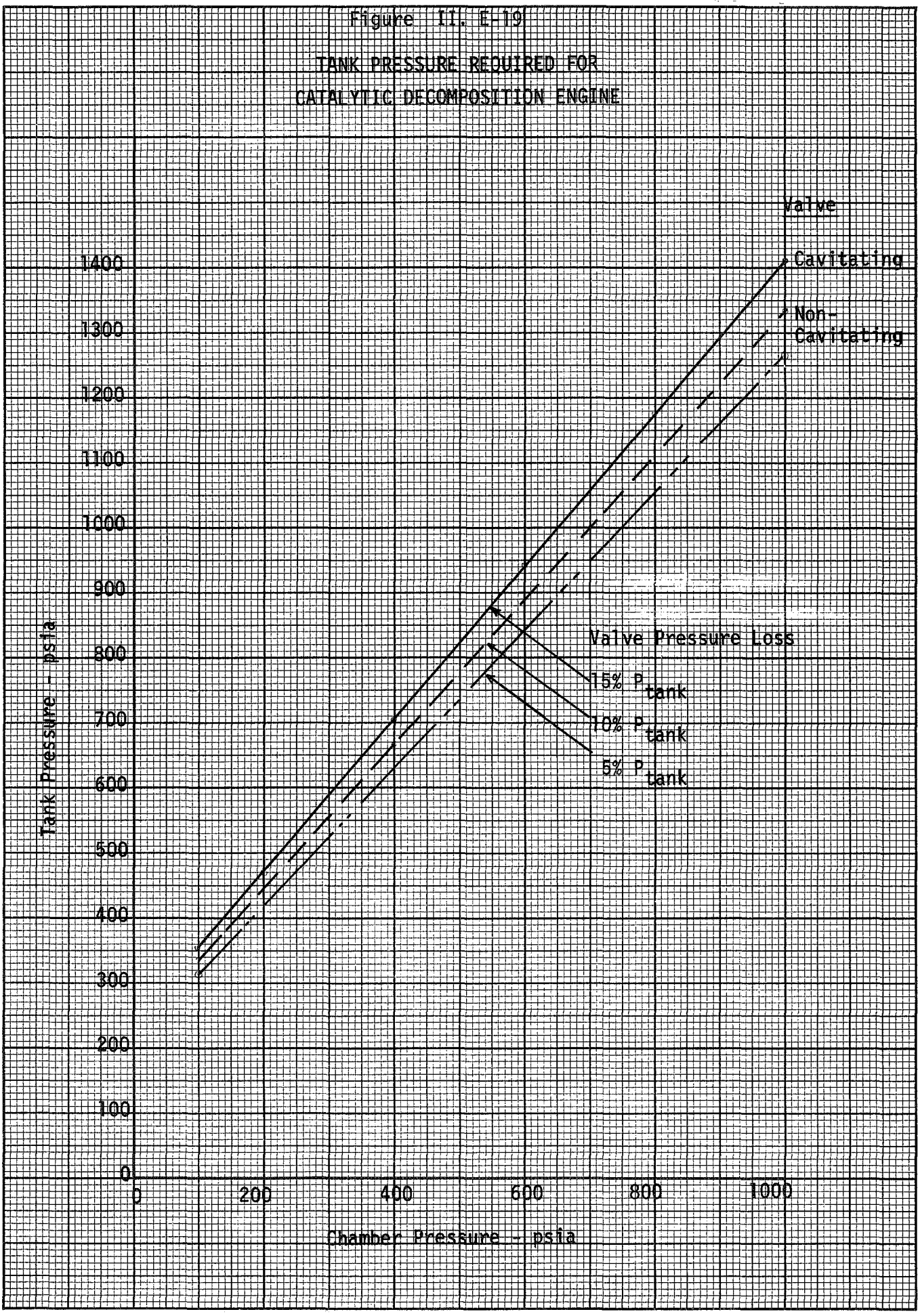

Figure II. E-20

TANK PRESSURE REQUIRED FOR
THERMAL DECOMPOSITION ENGINE

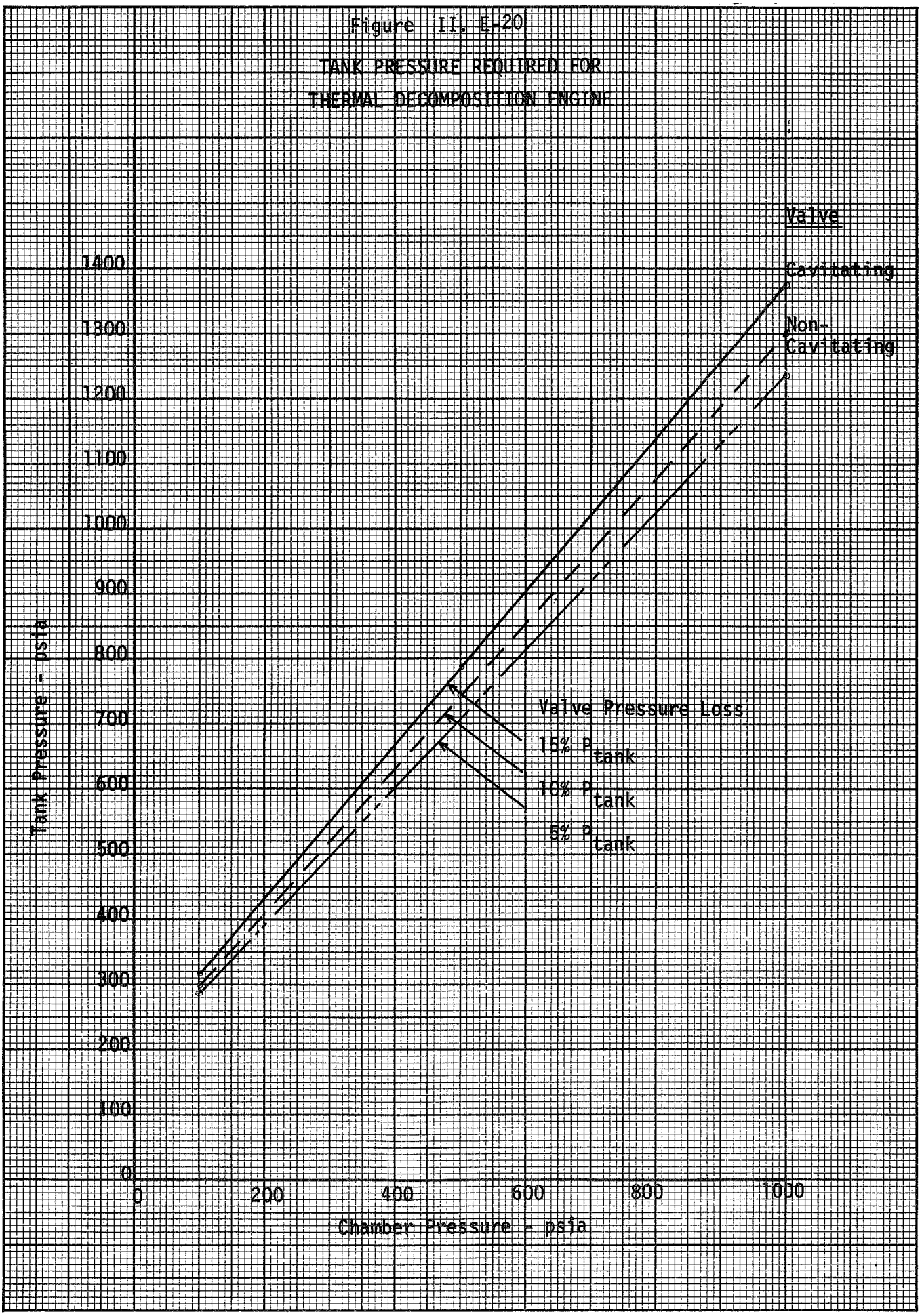

CATALYST DECOMPOSITION ENGINE

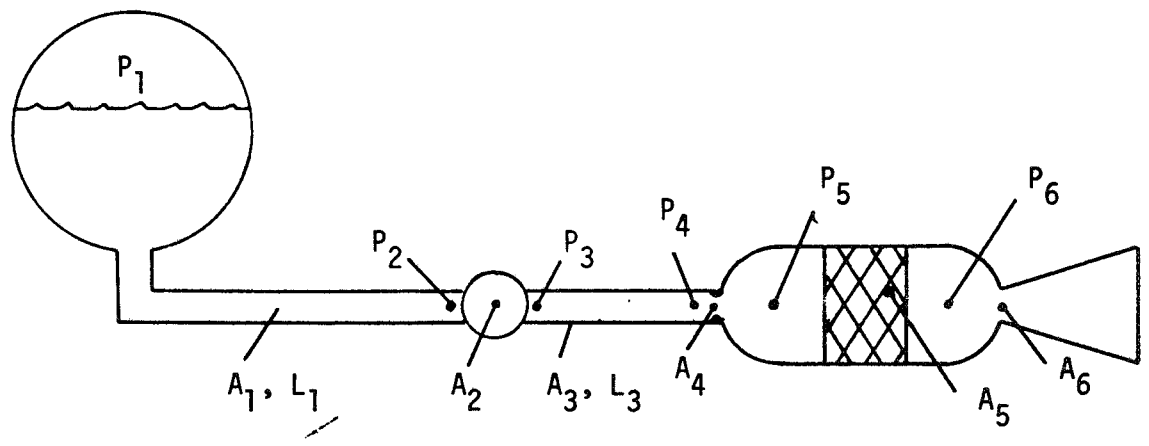

Chamber Pressure	$P_6 = \frac{\dot{w}}{C_1}$	$C_1 = A_6 \left[\frac{kg}{RT_6}\left(\frac{2}{k+1}\right)^{\frac{k+1}{k-1}}\right]^{1/2}$
Catalyst Bed ΔP	$P_5^2 - P_6^2 = C_2 \dot{w}^2$	$C_2 = 2K\left[\left(\frac{A_v}{F_v^{1.7}}\right)\left(\frac{L_c}{A_5^2}\right)\right]$
Injector Orifice ΔP	$P_4 - P_5 = \frac{\dot{w}^2}{C_3}$	$C_3 = C_{D4}^2 A_4^2 2g \gamma_L$
Injector Tube ΔP	$P_3 - P_4 = C_4 \dot{w}^2$	$C_4 = \left[\frac{4fL_2}{d_2} + \Sigma K_2\right] \frac{1}{2g \gamma_L A_3^2}$
Non-Cavitating Valve ΔP	$P_2 - P_3 = \frac{\dot{w}^2}{C_5}$	$C_5 = C_{D2}^2 A_2^2 2g \gamma_L$
Variable Area Injector Valve ΔP	$P_2 - P_5 = \frac{\dot{w}^2}{C_6}$	$C_6 = C_{D4}^2 A_4^2 2g \gamma_L$
Cavitating Valve ΔP	$P_2 - P_v = \frac{\dot{w}^2}{C_7}$	$C_7 = C_{D2}^2 A_2^2 2g \gamma_L$
Propellant Feed Line ΔP	$P_1 - P_2 = C_8 \dot{w}^2$	$C_8 = \left[\frac{4fL_1}{d_1} + \Sigma K_1\right] \frac{1}{2g \gamma_L A_1^2}$
Non-Cavitating Valve		(a) $P_1 = \left(C_8 + \frac{1}{C_5} + C_4 + \frac{1}{C_3}\right) \dot{w}^2 + \left(C_2 + \frac{1}{C_1^2}\right)^{1/2} \dot{w}$ (b) $P_1 = \left(C_8 + \frac{1}{C_5} + C_4 + \frac{1}{C_3}\right) \left(\frac{g}{C^*} P_6 A_6\right)^2 + \left(C_2 + \frac{1}{C_1^2}\right)^{1/2} \left(\frac{g P_6 A_6}{C^*}\right)$
Variable Area Injector Valve		(c) $P_1 = \left(C_8 + \frac{1}{C_6}\right) \dot{w}^2 + \left(C_2 + \frac{1}{C_1^2}\right)^{1/2} \dot{w}$ (d) $P_1 = \left(C_8 + \frac{1}{C_6}\right) \left(\frac{g}{C^*} P_6 A_6\right)^2 + \left(C_2 + \frac{1}{C_1^2}\right)^{1/2} \left(\frac{g P_6 A_6}{C^*}\right)$
Cavitating Valve		(e) $P_1 = P_v + \left(C_8 + \frac{1}{C_7}\right) \dot{w}^2$ (f) $P_1 = P_v + \left(C_8 + C_7\right) \left(\frac{g}{C^*} P_6 A_6\right)^2$

Figure II. E-21

THERMAL DECOMPOSITION ENGINE

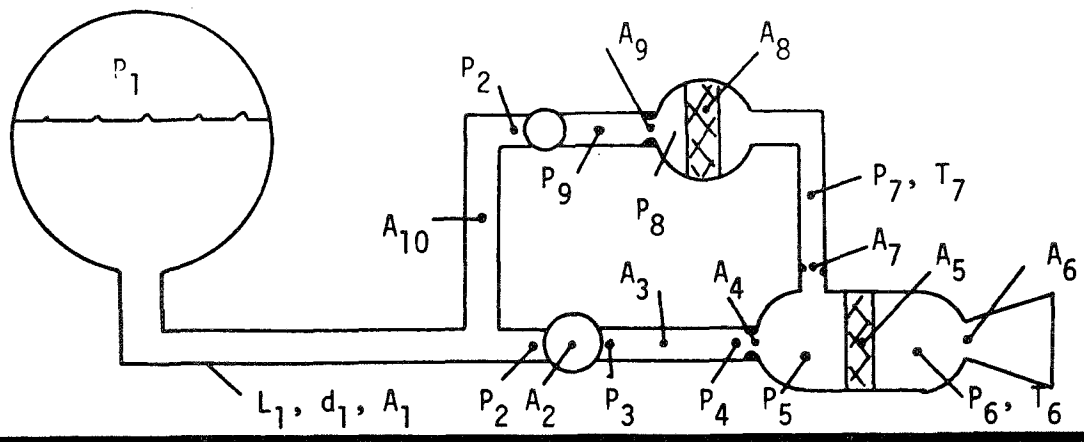

Chamber Pressure	$P_6 = \frac{\dot{w}}{C_1}$	$C_1 = [\frac{kg}{RT} (\frac{2}{k+1})^{\frac{k+1}{k-1}}]^{1/2} A_6$
Screen ΔP	$P_5^2 - P_6^2 = \frac{\dot{w}^2}{C_2}$	$C_2 = (K A_5)^2 \frac{a}{R_6 T_6}$
Injector ΔP	$P_4 - P_5 = \frac{\dot{w}_1^2}{C_3}$	$C_3 = C_{D4}^2 A_4^2 2g \gamma_L$
Injector Tube ΔP	$P_3 - P_4 = C_4 \dot{w}_1^2$	$C_4 = [\frac{4fL_2}{d_2} + \Sigma K_2] \frac{1}{2g \gamma_L A_3^2}$
Non-Cavitating Valve ΔP	$P_2 - P_3 = \frac{\dot{w}_1^2}{C_5}$	$C_5 = C_{D2}^2 A_2^2 2g \gamma_L$
Variable Injector Area Valve ΔP	$P_4 - P_5 = \frac{\dot{w}_1^2}{C_6}$	$C_6 = C_{D4}^2 A_4^2 2g \gamma_L$
Cavitating Valve ΔP	$P_2 - P_v = \frac{\dot{w}_1^2}{C_7}$	$C_7 = C_{D2}^2 A_2^2 2g \gamma_L$
Propellant Feed Line ΔP	$P_1 - P_2 = C_8 \dot{w}^2$	$C_8 = [\frac{4fL_1}{d_1} + \Sigma K_1] [\frac{1}{2g \gamma_L A_1^2}]$
Hot Gas Orifice ΔP	$P_7^2 - P_5^2 = \frac{\dot{w}_2^2}{C_9}$	$C_9 = C_{D7}^2 A_7^2 \frac{g}{R_7 T_7}$
Pre-Heater Catalyst Bed ΔP	$P_8^2 - P_7^2 = C_{10} \dot{w}_2^2$	$C_{10} = 2K [(\frac{A_v}{F_v 1.7}) (\frac{L_c}{A_8^2})]$
Pre-Heater Injector ΔP	$P_9 - P_8 = \frac{\dot{w}_2^2}{C_{11}}$	$C_{11} = C_{D9}^2 A_9^2 2g \gamma_L$
Pre-Heater Propellant Line ΔP	$P_2 - P_9 = C_{12} \dot{w}_2^2$	$C_{12} = (\frac{4fL}{d} + \Sigma K) \frac{1}{2g \gamma_L A_{10}^2}$
Pre-Heater Cavitating Valve Flow	$(P_2 - P_v) = \frac{\dot{w}_2^2}{C_{13}}$	$C_{13} = C_D^2 A_{10}^2 2g \gamma$
Non-Cavitating Valve	(a) $P_1 = (\frac{1}{C_1^2} + \frac{1}{C_2})^{1/2} \dot{w} + \{C_8 + \frac{1}{[\frac{1}{(\frac{1}{C_5} + C_4 + \frac{1}{C_3})^{1/2}} + \frac{1}{(C_{12} + \frac{1}{C_{11}} + \frac{C_{10} + 1/C_9}{P_5 + P_8})^{1/2}}]^2} \} \dot{w}^2$	
Cavitating Valve	(b) $\frac{[P_1 - C_8 w^2 - (\frac{1}{C_2} + \frac{1}{C_1^2})^{1/2} \dot{w}^2]^{1/2}}{[C_{12} + \frac{1}{C_{11}} + \frac{C_{10} + 1/C_9}{P_5 + P_8}]^{1/2}} + C_7^{1/2} [P_1 - P_v - C_8 w^2]^{1/2} = w$	
Variable Area Injector	(c) $P_1 = (\frac{1}{C_1^2} + \frac{1}{C_2})^{1/2} \dot{w} + \{C_8 + \frac{1}{[C_6^{1/2} + \frac{1}{(C_{12} + \frac{1}{C_{11}} + \frac{C_{10} + 1/C_9}{P_5 + P_8})^{1/2}}]^2} \} \dot{w}^2$	

Figure II. E-22

Figure II E-23
PROPELLANT FLOWRATE
NON-CAVITATING THROTTLE VALVE
2:1 TANK BLOWDOWN RANGE
400 LB_F THRUST ENGINE

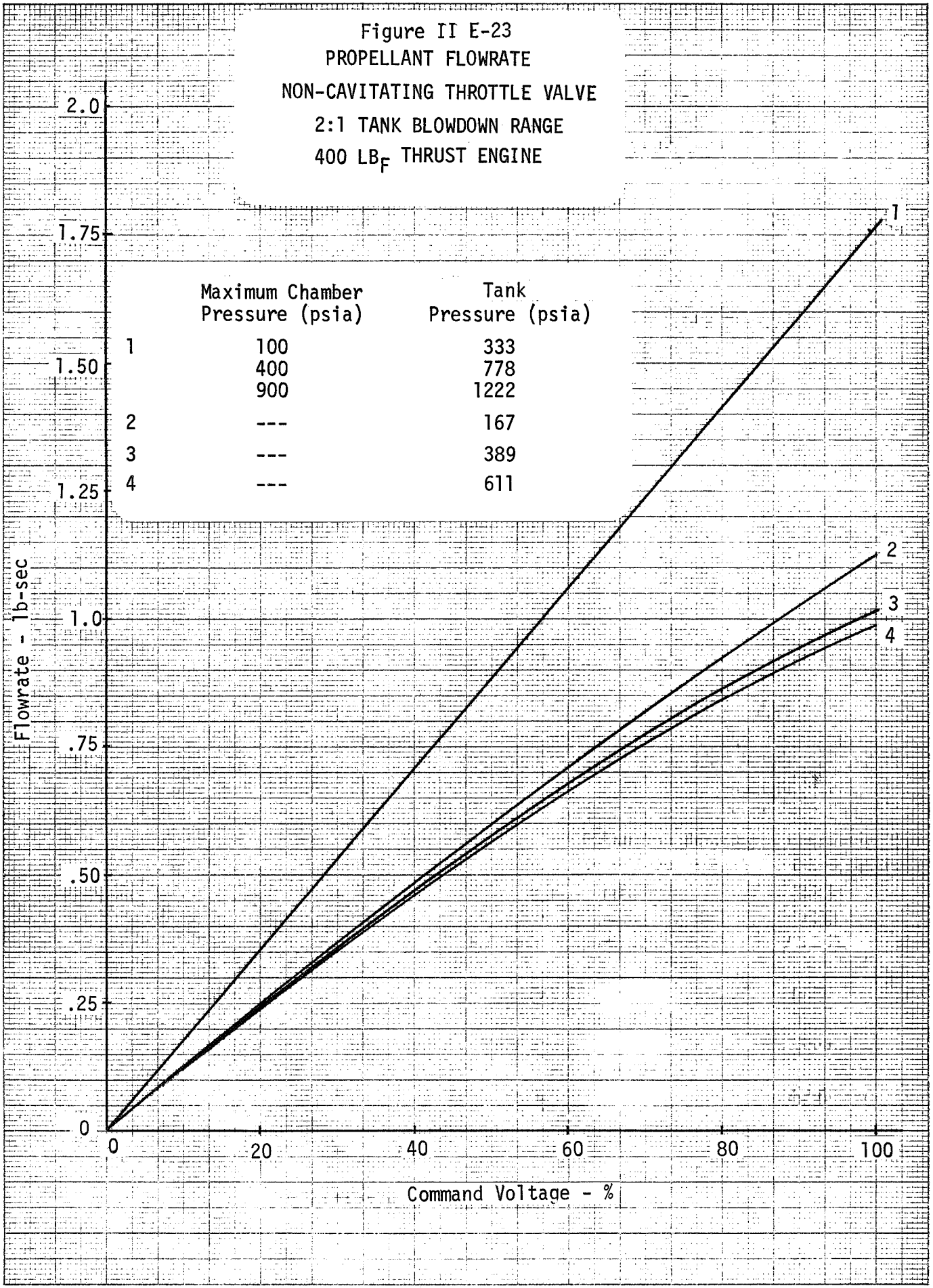

	Maximum Chamber Pressure (psia)	Tank Pressure (psia)
1	100	333
	400	778
	900	1222
2	---	167
3	---	389
4	---	611

Figure II. E-24
PROPELLANT FLOWRATE
NON-CAVITATING THROTTLE VALVE
2:1 TANK BLOWDOWN RANGE
800 LB_F THRUST ENGINE

	Maximum Chamber Pressure (psia)	Tank Pressure (psia)
1	100	333
	500	778
	900	1222
2	---	167
3	---	389
4	---	611

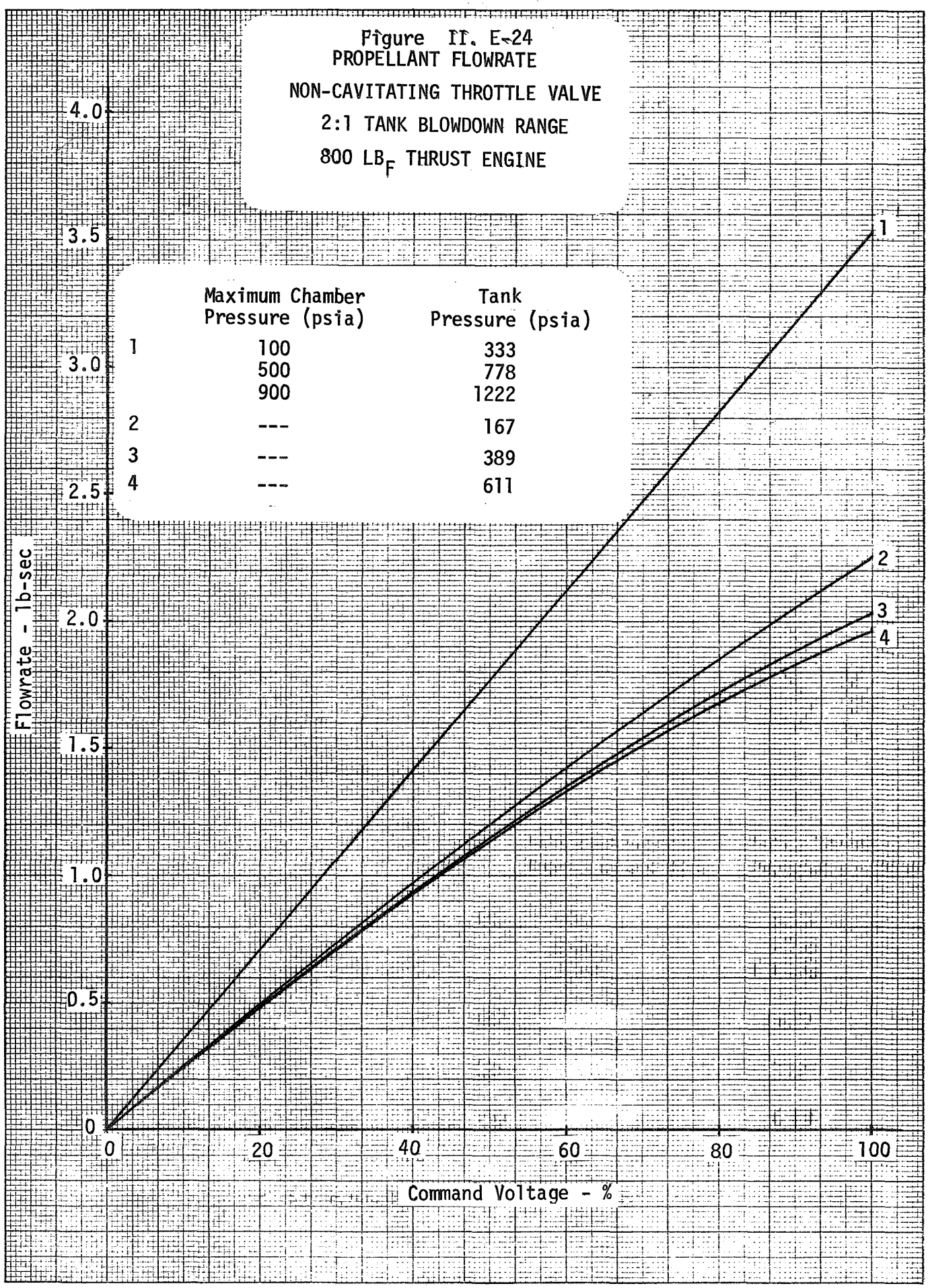

Figure II. E-25
PROPELLANT FLOWRATE
NON-CAVITATING THROTTLE VALVE
2:1 BLOWDOWN RANGE
1200 LB_F THRUST ENGINE

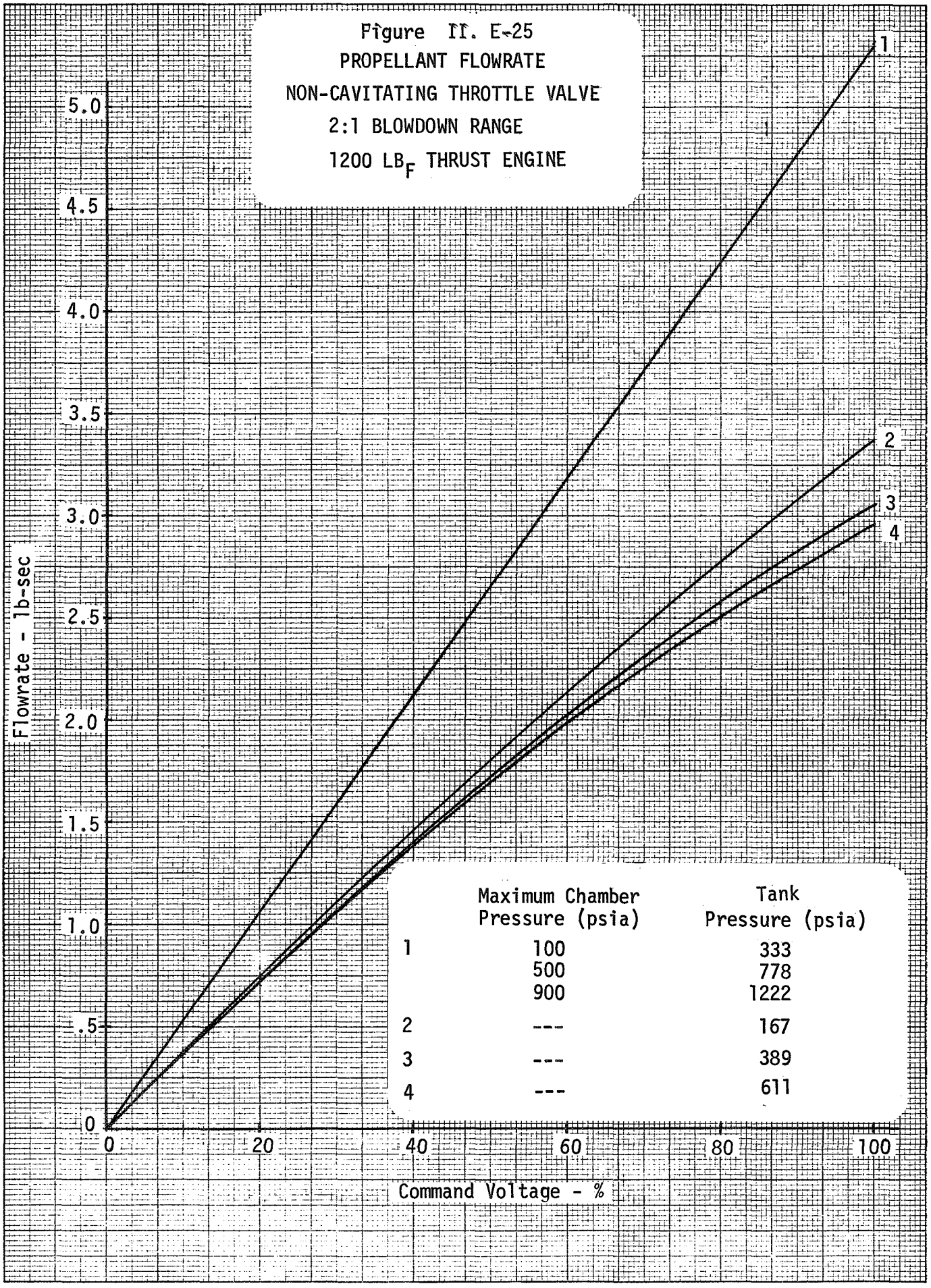

	Maximum Chamber Pressure (psia)	Tank Pressure (psia)
1	100	333
	500	778
	900	1222
2	---	167
3	---	389
4	---	611

Figure II. E-26

PROPELLANT FLOW RATE
CAVITATING THROTTLE VALVE
2:1 TANK BLOWDOWN RANGE
400, 800 AND 1200 LB_F THRUST ENGINE

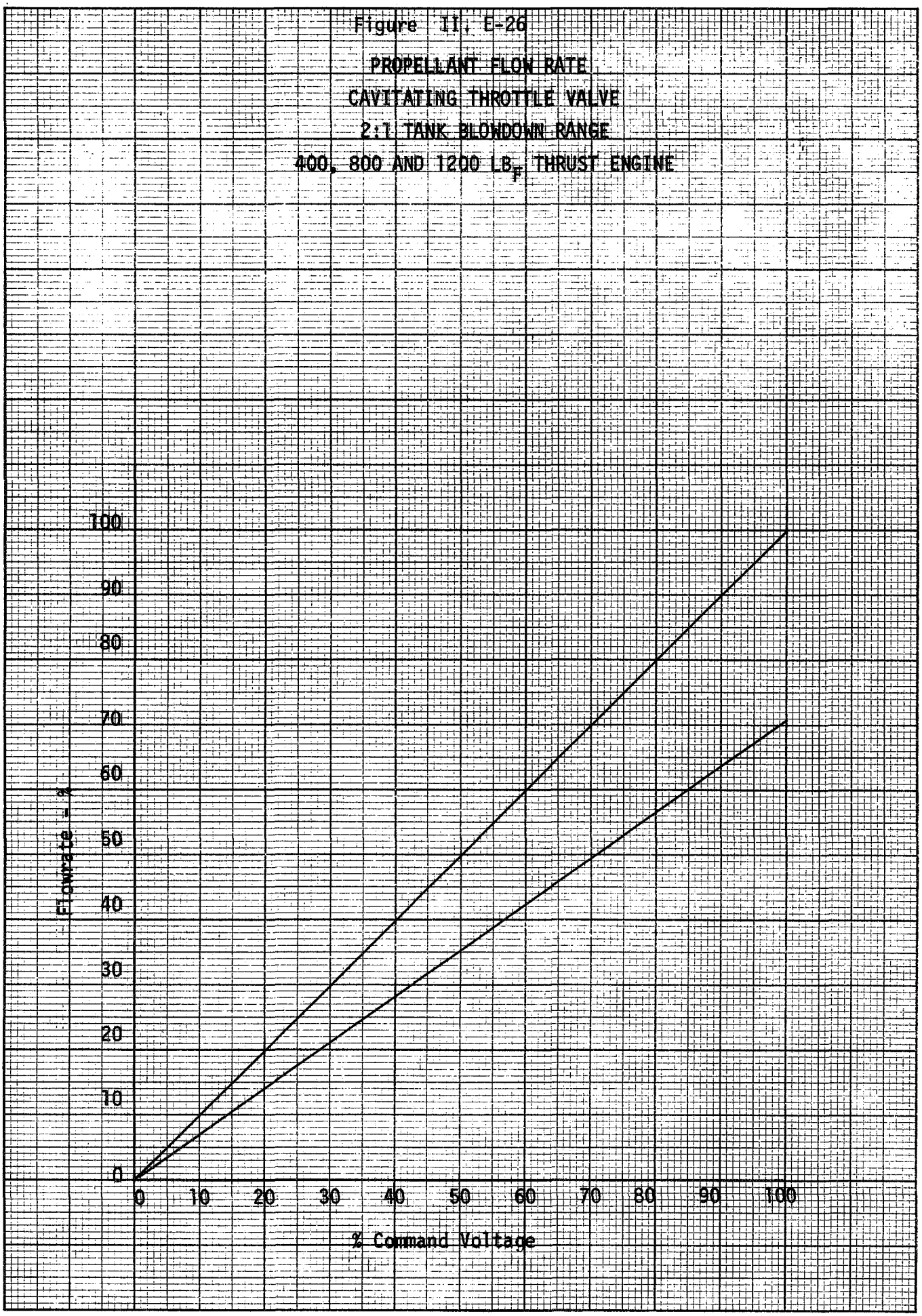

Figure II. E-27
PROPELLANT FLOWRATE
VARIABLE AREA INJECTOR
2:1 TANK BLOWDOWN RANGE
400 LB_F THRUST ENGINE

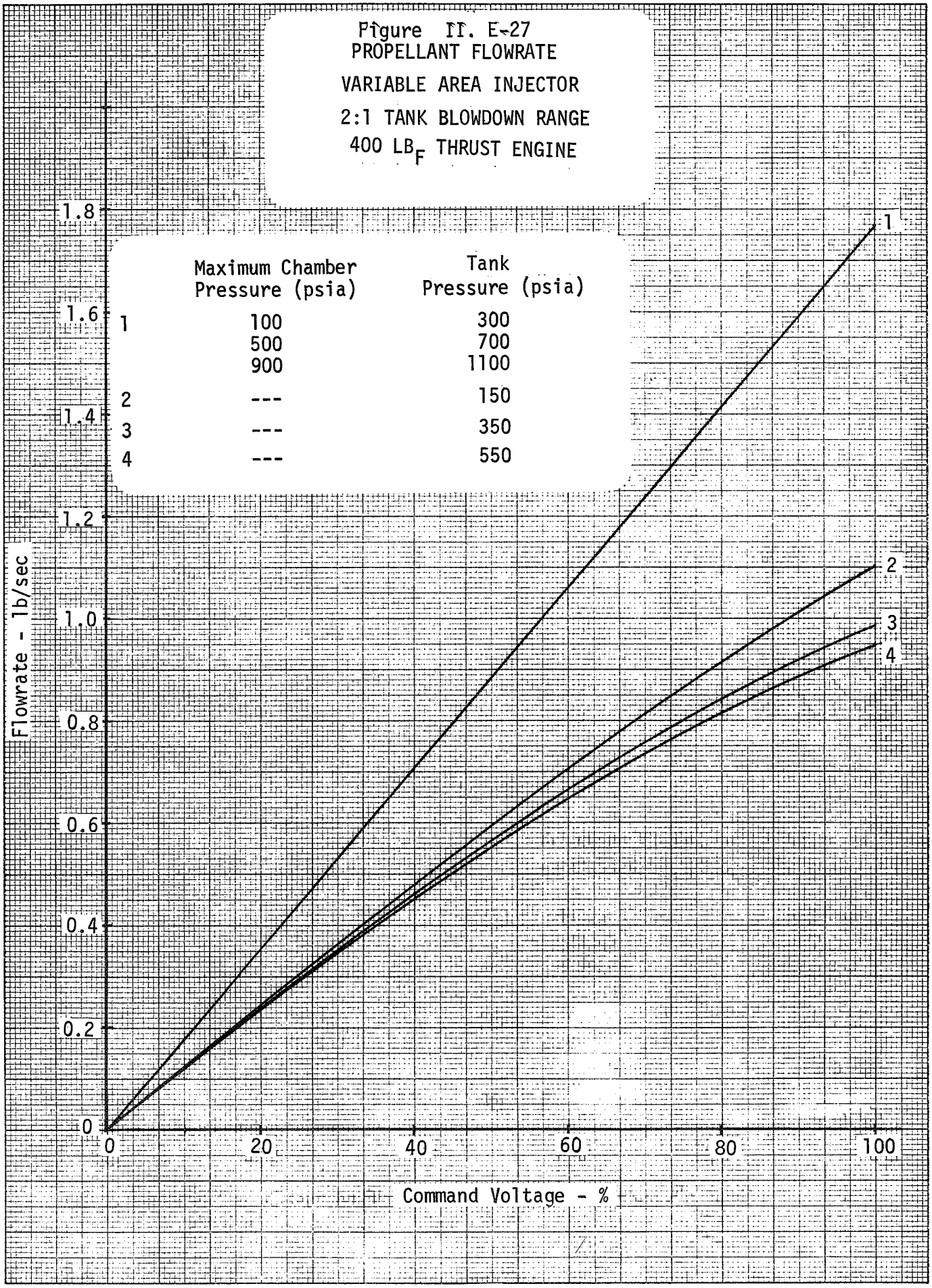

	Maximum Chamber Pressure (psia)	Tank Pressure (psia)
1	100	300
	500	700
	900	1100
2	---	150
3	---	350
4	---	550

Figure II. E-28

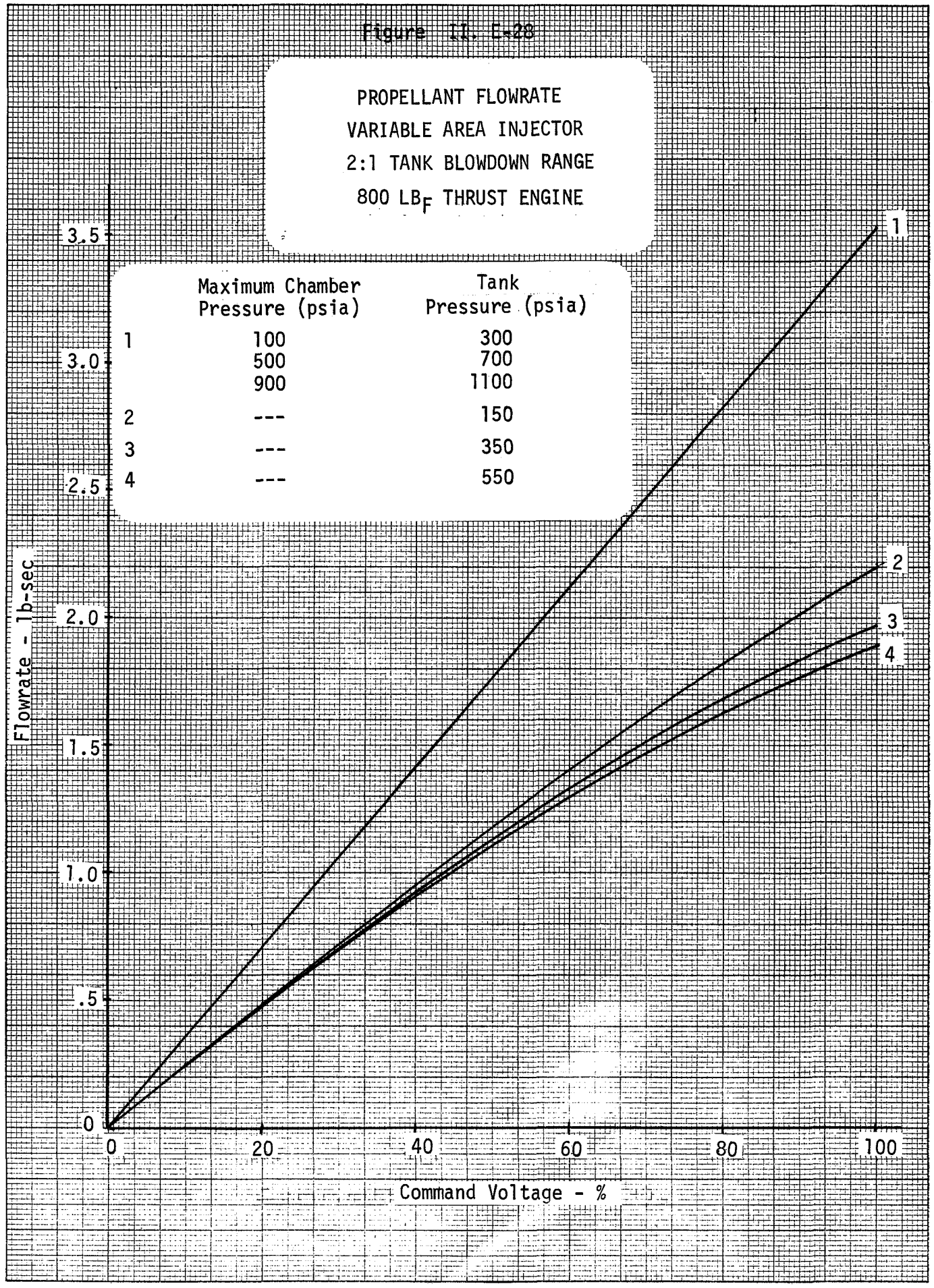

Figure II. E-29

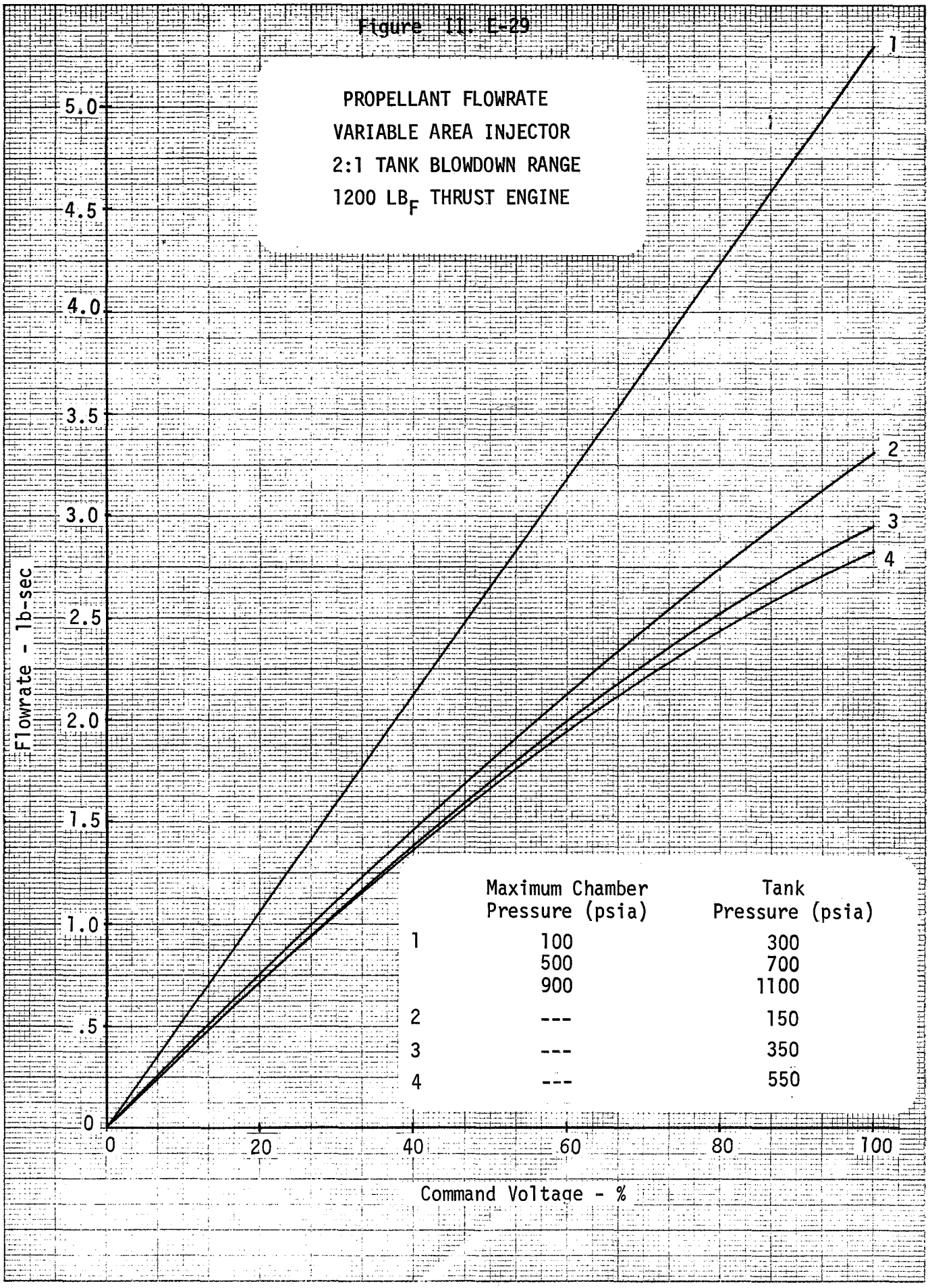

Figure II. E-30

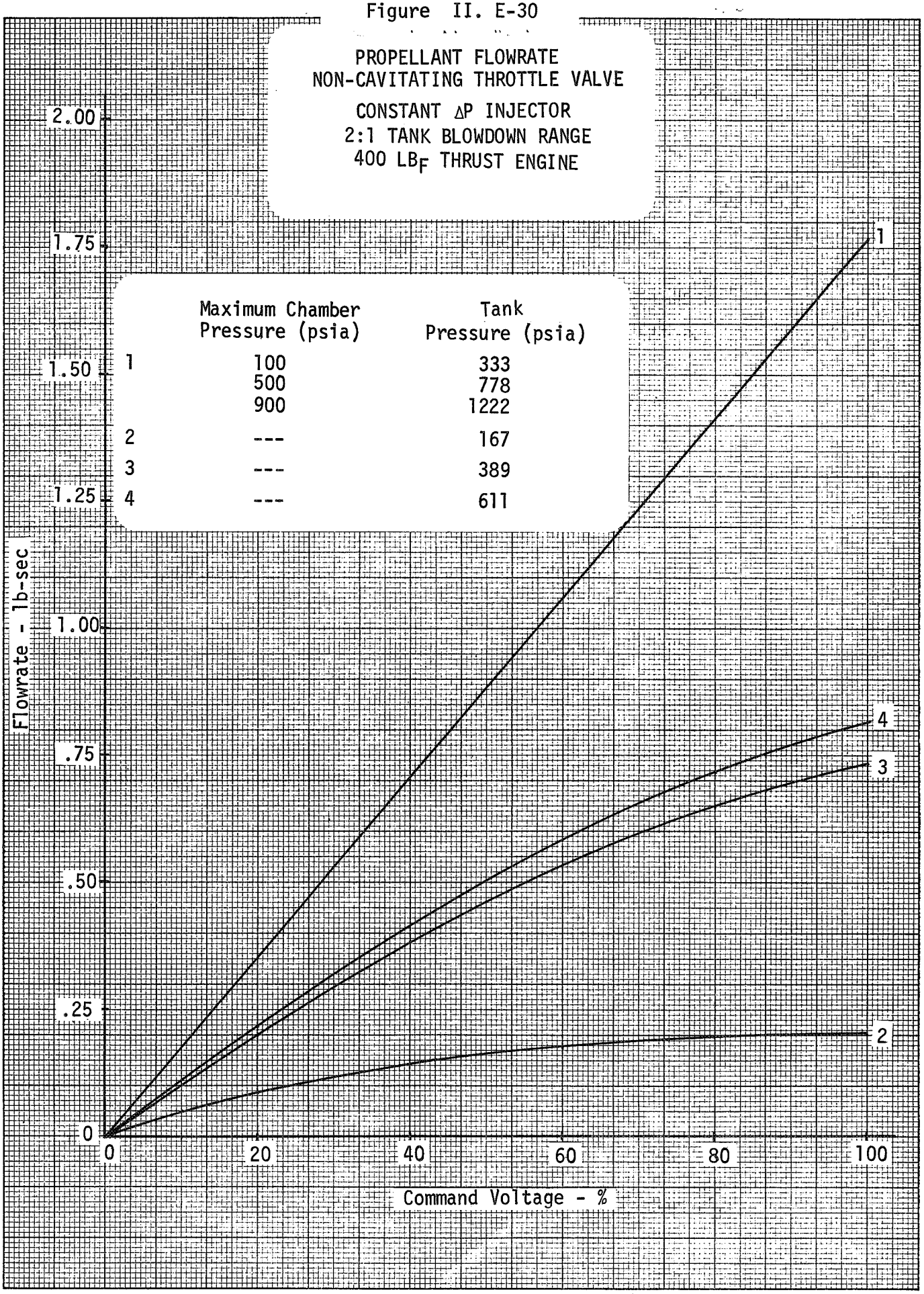

Figure II. E-31

PROPELLANT FLOWRATE
NON-CAVITATING THROTTLE VALVE

CONSTANT ΔP INJECTOR
2:1 TANK BLOWDOWN RANGE
800 LB_F THRUST ENGINE

	Maximum Chamber Pressure (psia)	Tank Pressure (psia)
1	100	333
	500	778
	900	1222
2	---	167
3	---	389
4	---	611

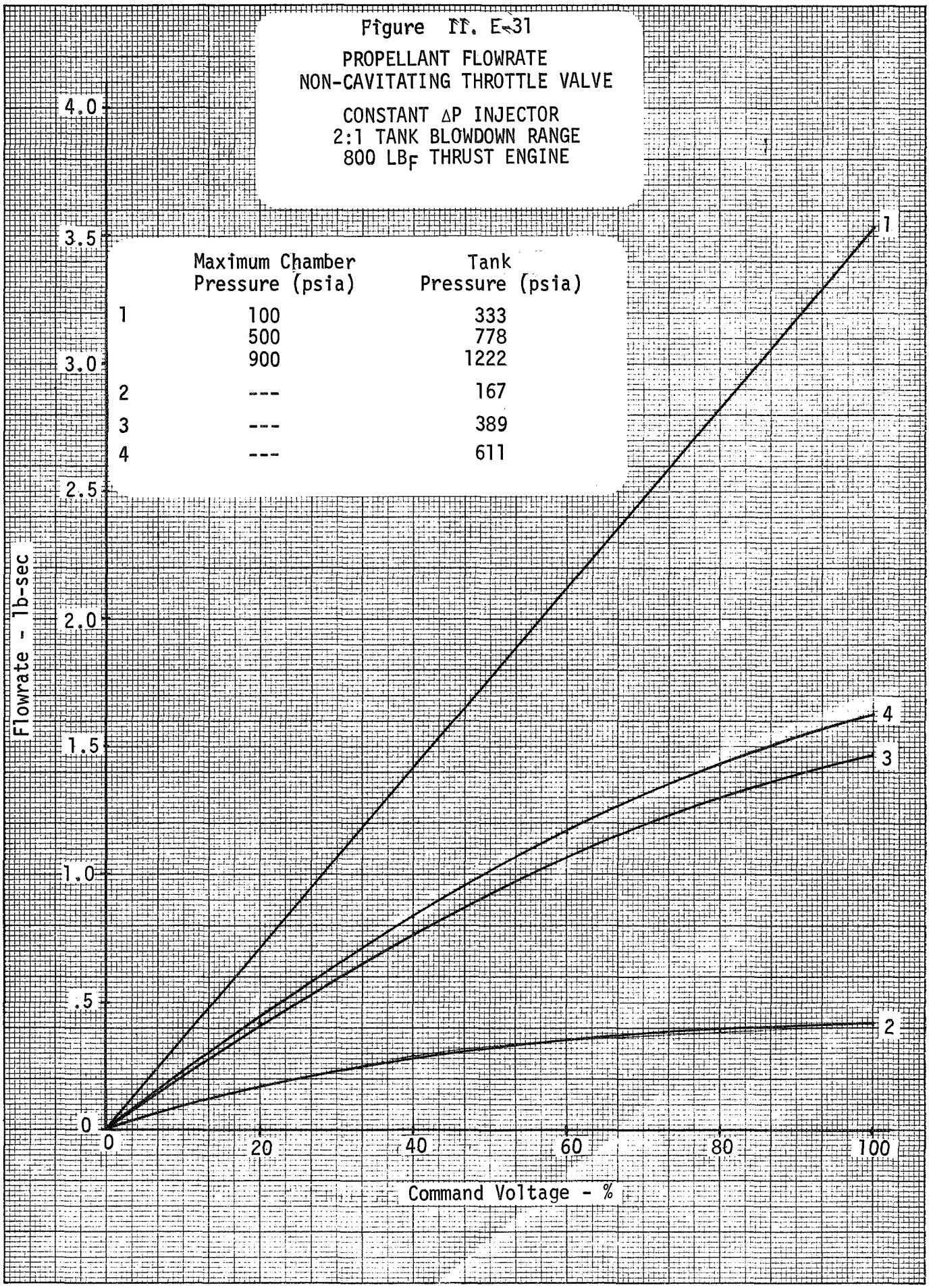

Figure II. E-32
PROPELLANT FLOWRATE
NON-CAVITATING THROTTLE VALVE

CONSTANT ΔP INJECTOR
2:1 TANK BLOWDOWN RANGE
1200 LB_F THRUST ENGINE

	Maximum Chamber Pressure (psia)	Tank Pressure (psia)
1	100	333
	500	778
	900	1222
2	---	167
3	---	389
4	---	611

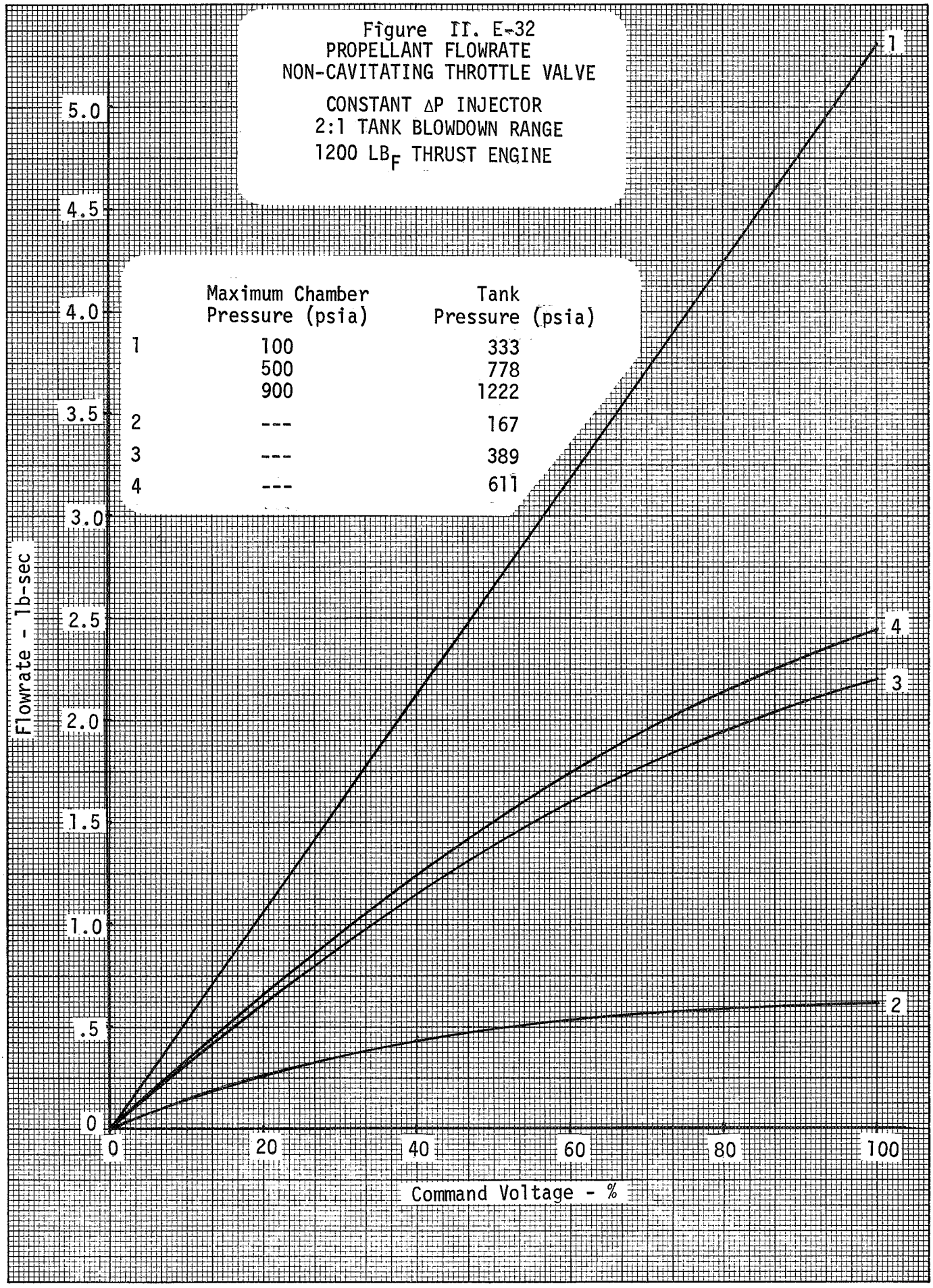

Figure II. E-33

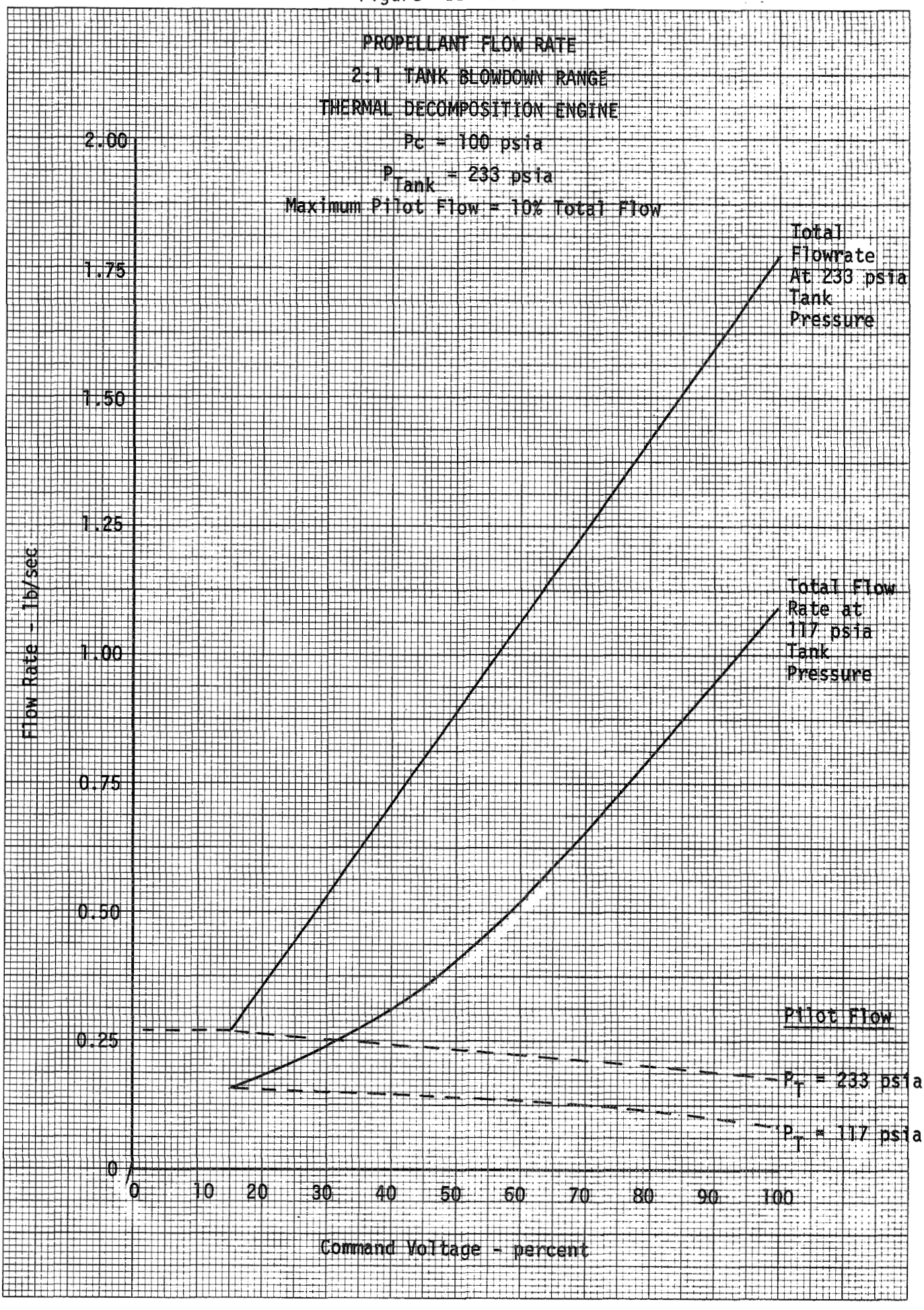

Figure II. E-34

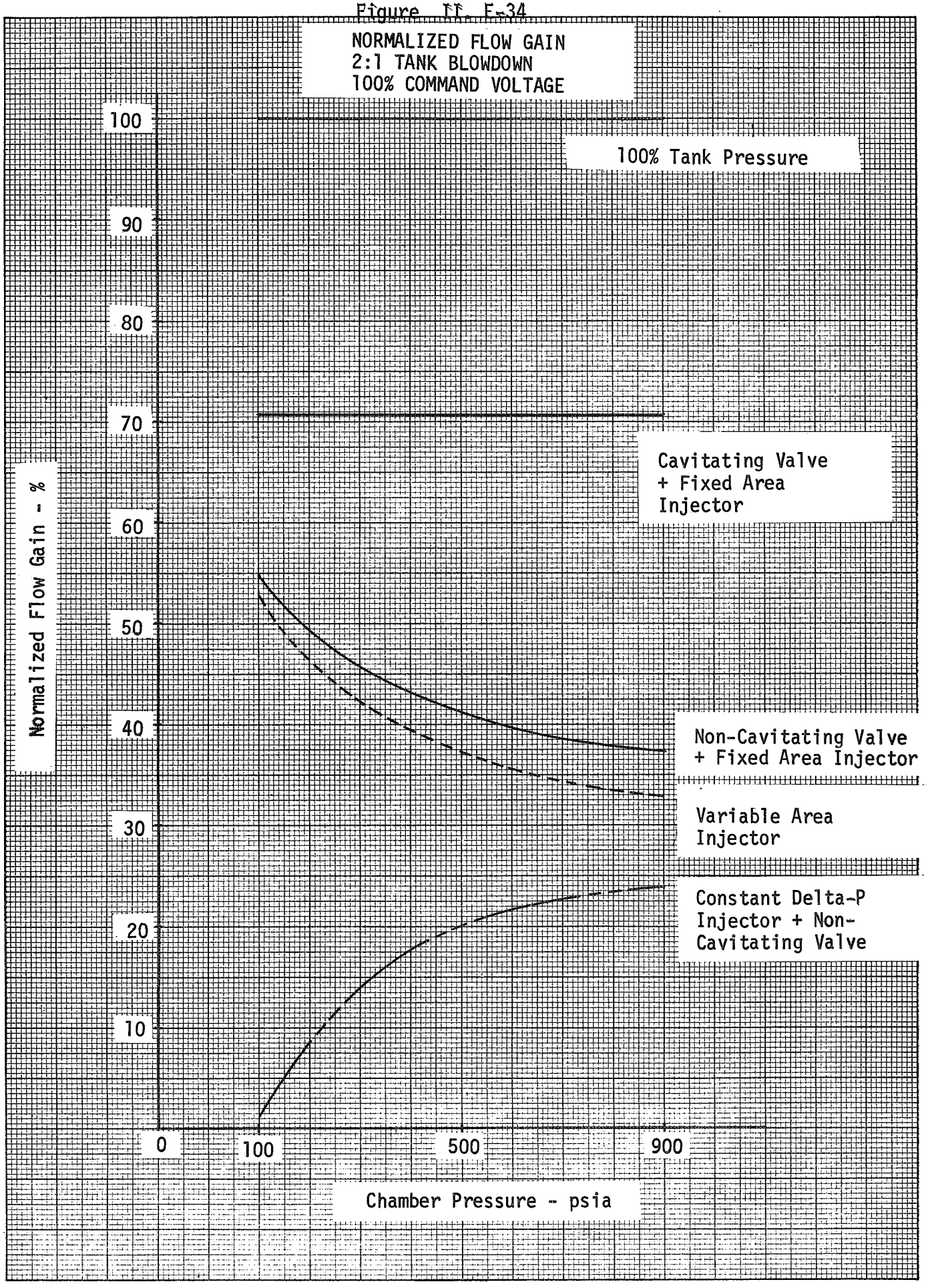

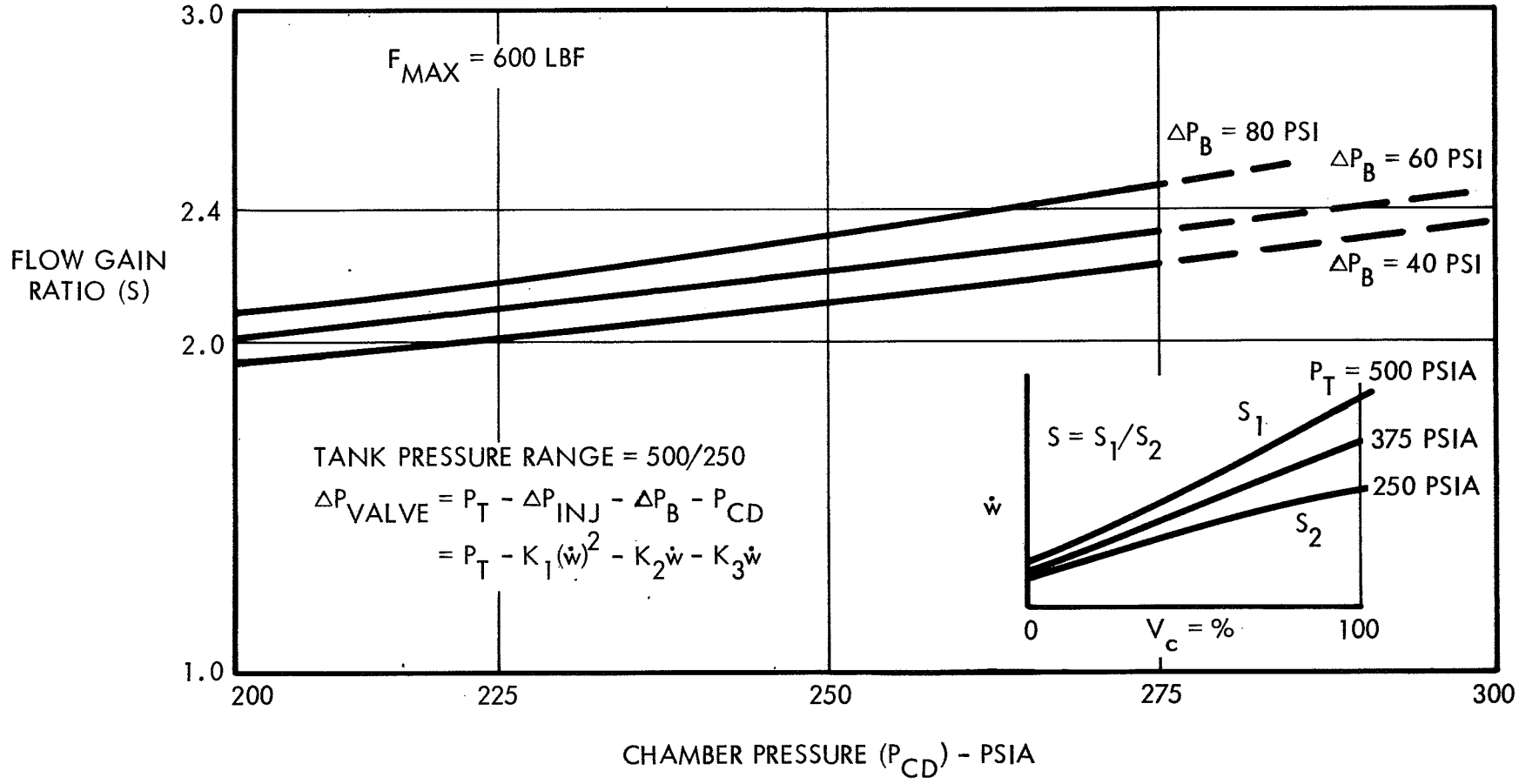

Figure II.E-35. Flow Gain Ratio vs Chamber Pressure

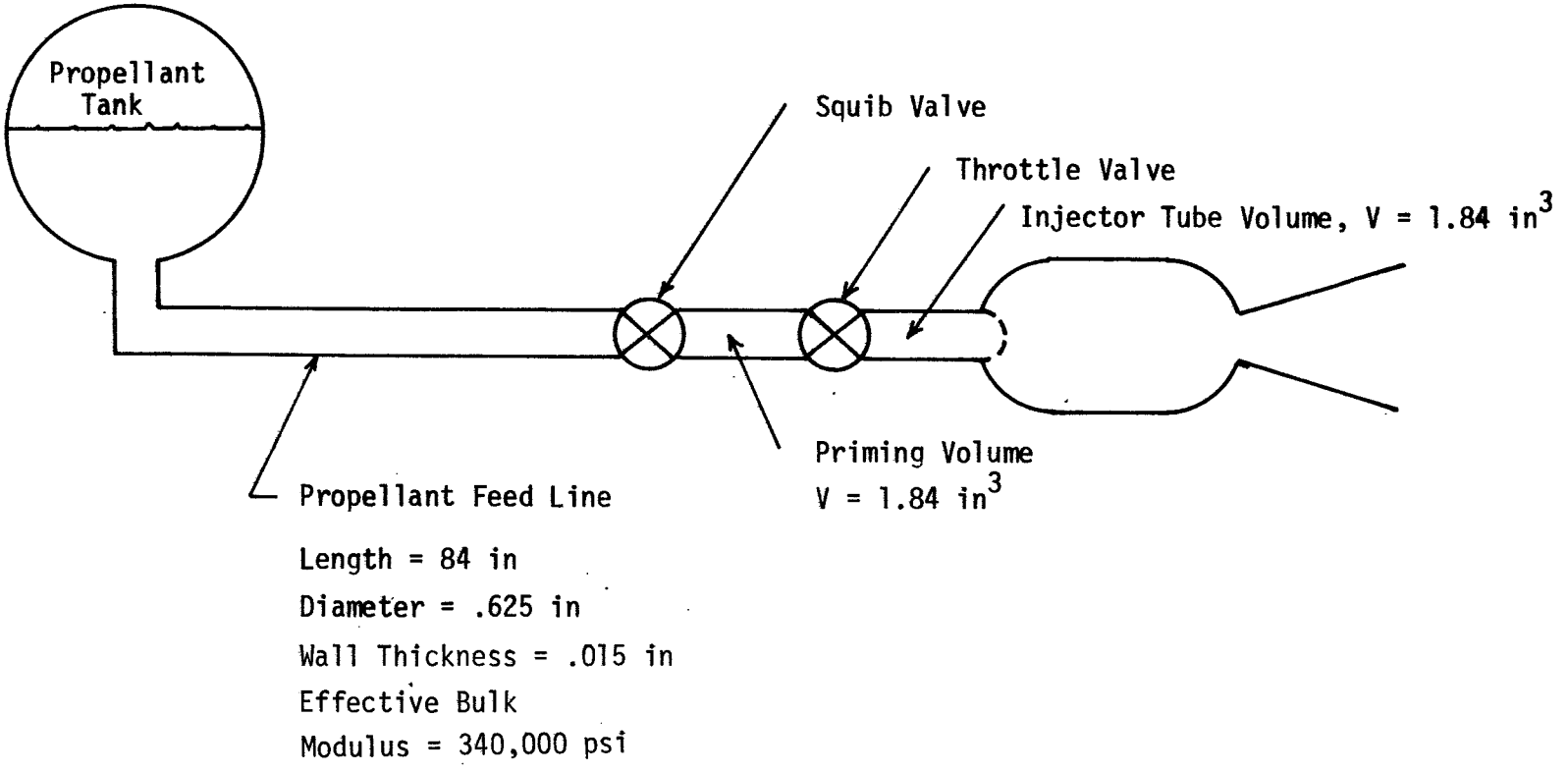

Figure II.E-36. Propellant Feed System Schematic
Hydraulic Surge Pressure Analysis

Figure II. E-37

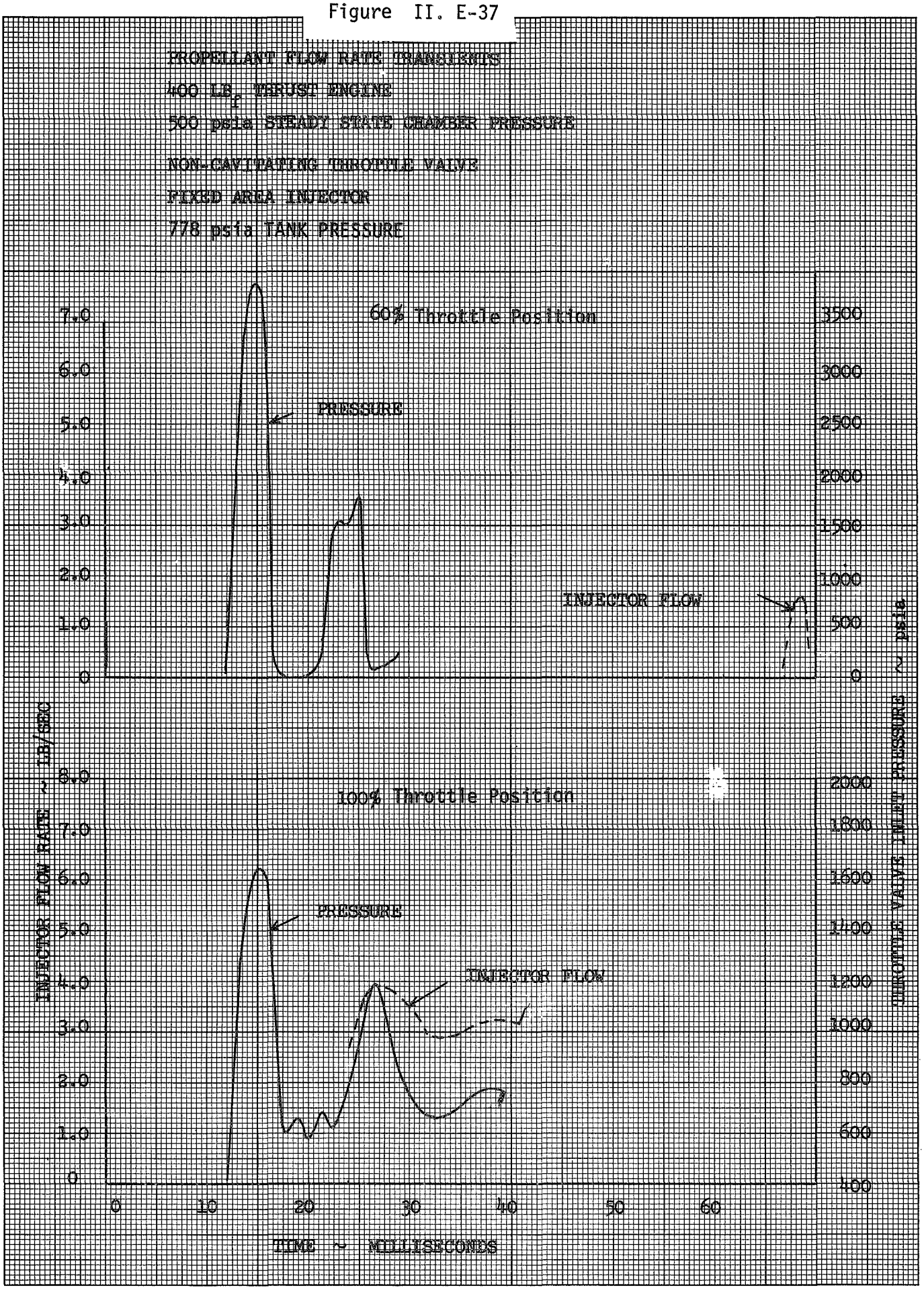

Figure II. E-33

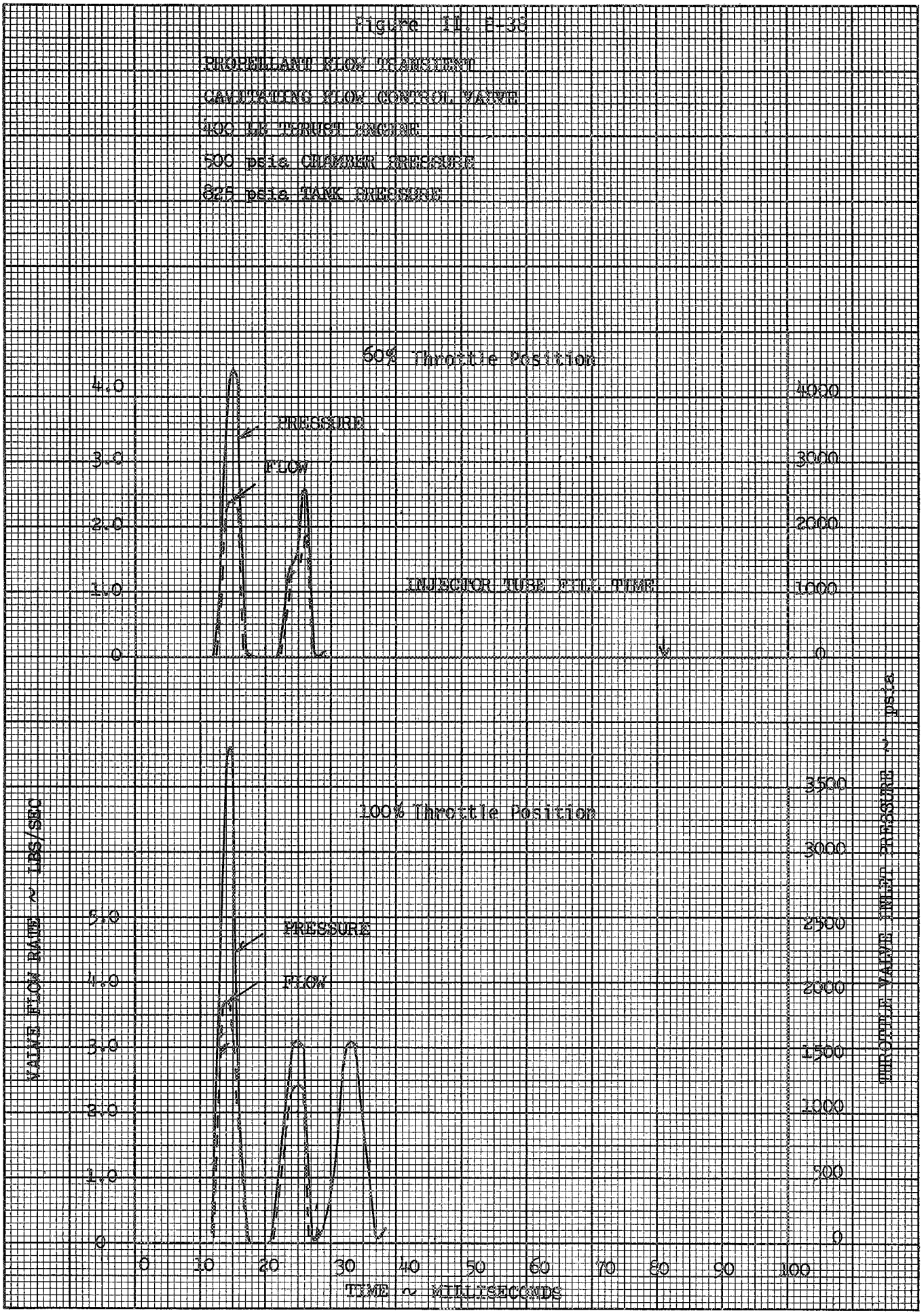

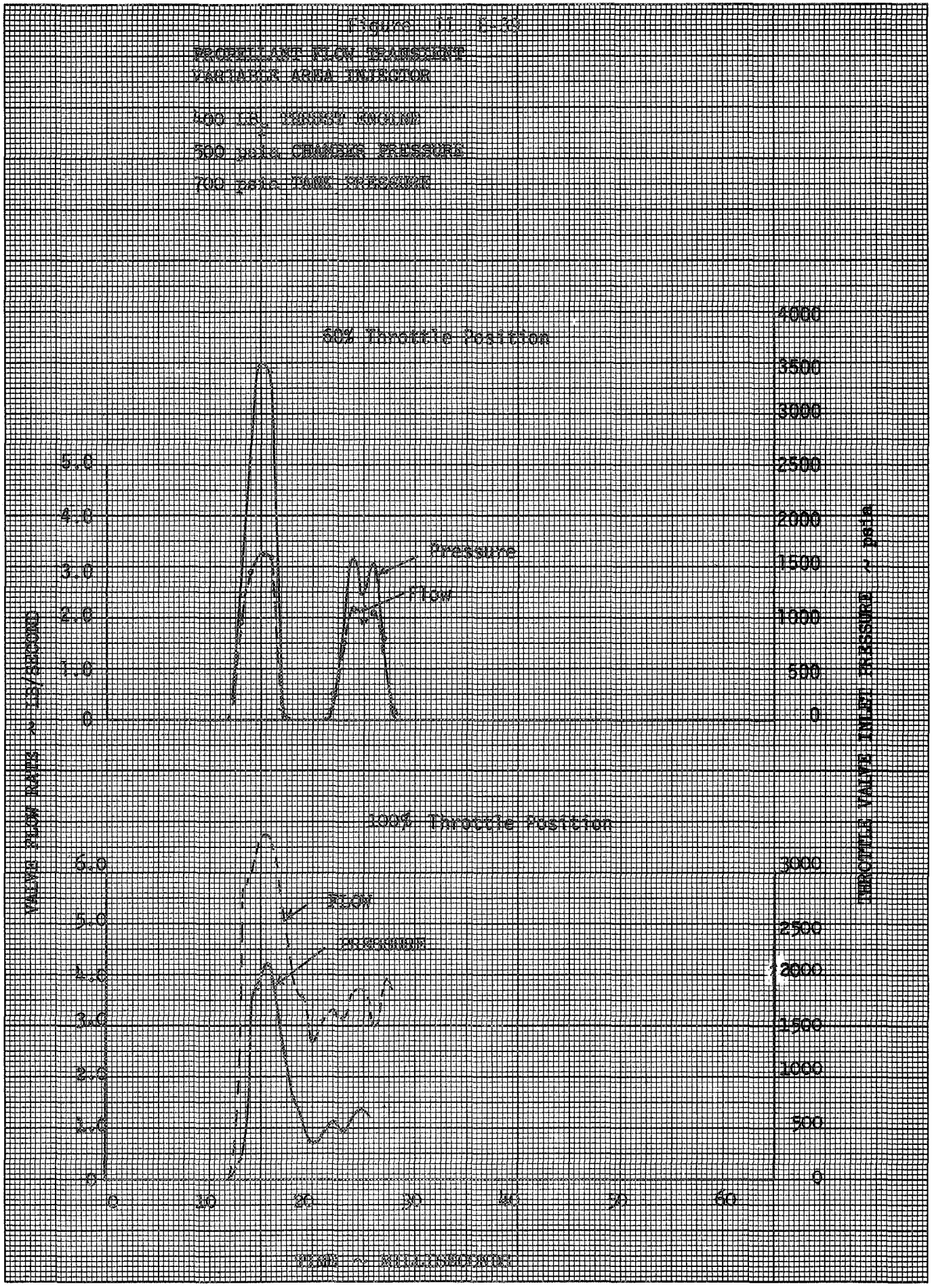
Figure II E-38
Propellant Flow Transient
Variable Area Injector
400 lb$_f$ Thrust Engine
500 psia Chamber Pressure
700 psia Tank Pressure
60% Throttle Position
Pressure
Flow
100% Throttle Position
Flow
Pressure
Flow Rate, lbm/sec
Throttle Valve Inlet Pressure, psia
Time, milliseconds

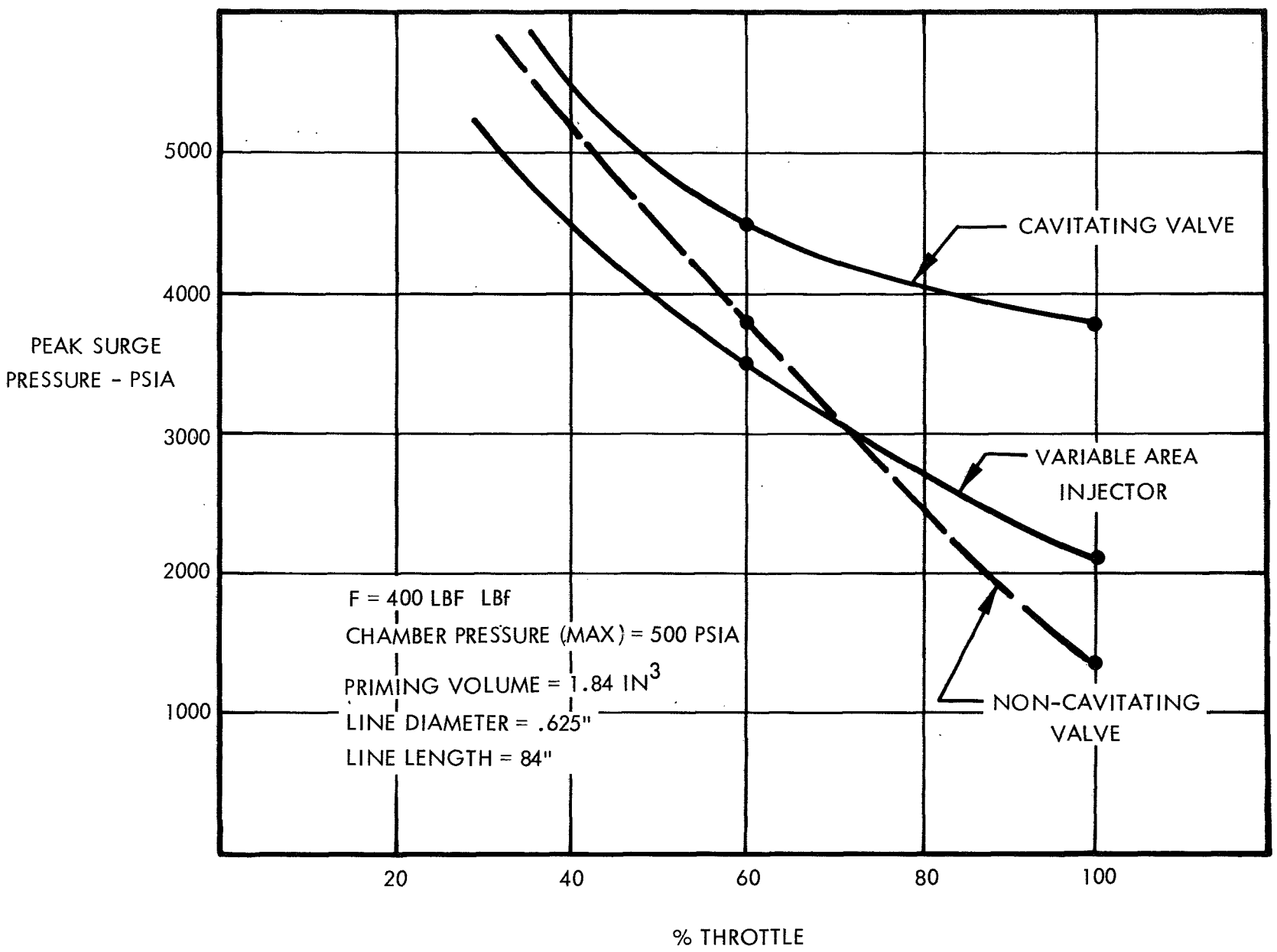

Figure II.E-40. Surge Pressure Characteristics

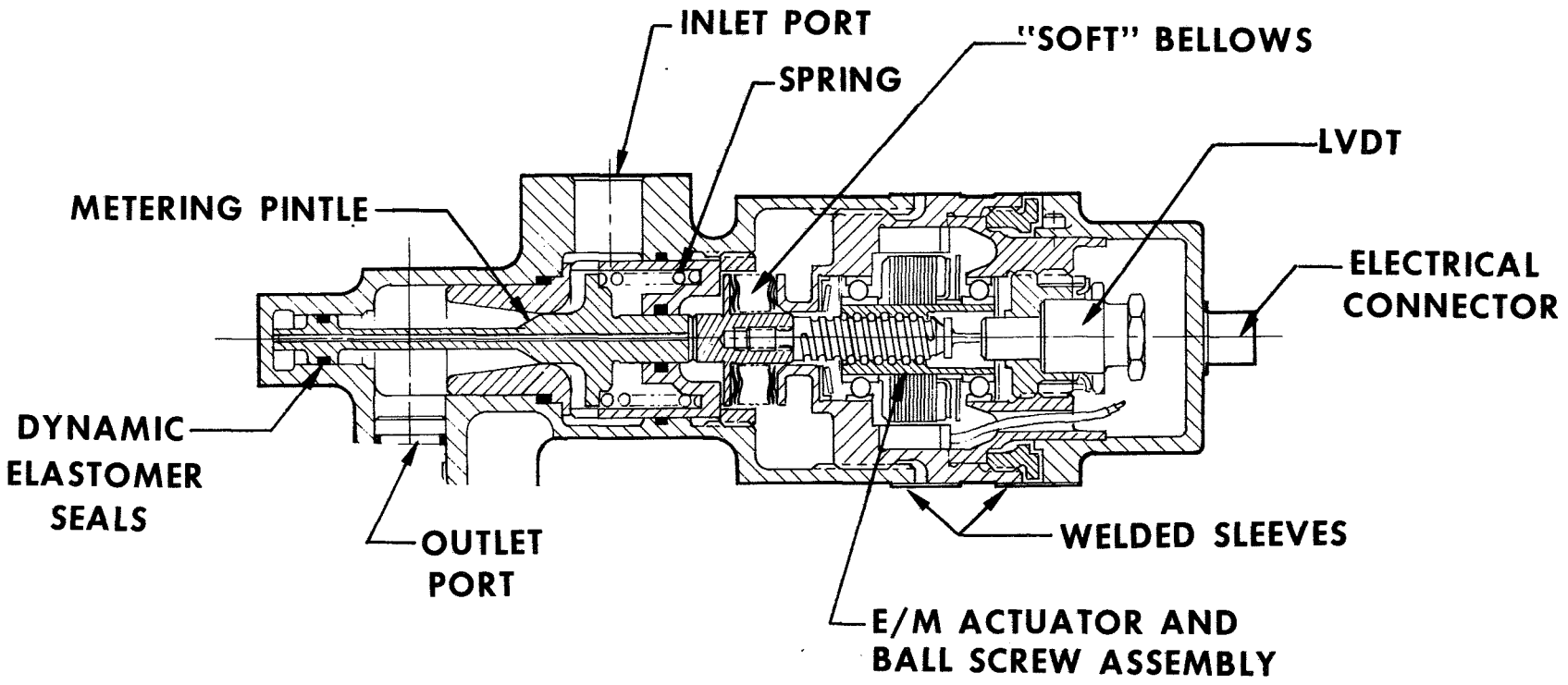

Figure II.E-41. Advanced E/M Actuator Non-Cavitating Throttle Valve Design

Figure II. E-42

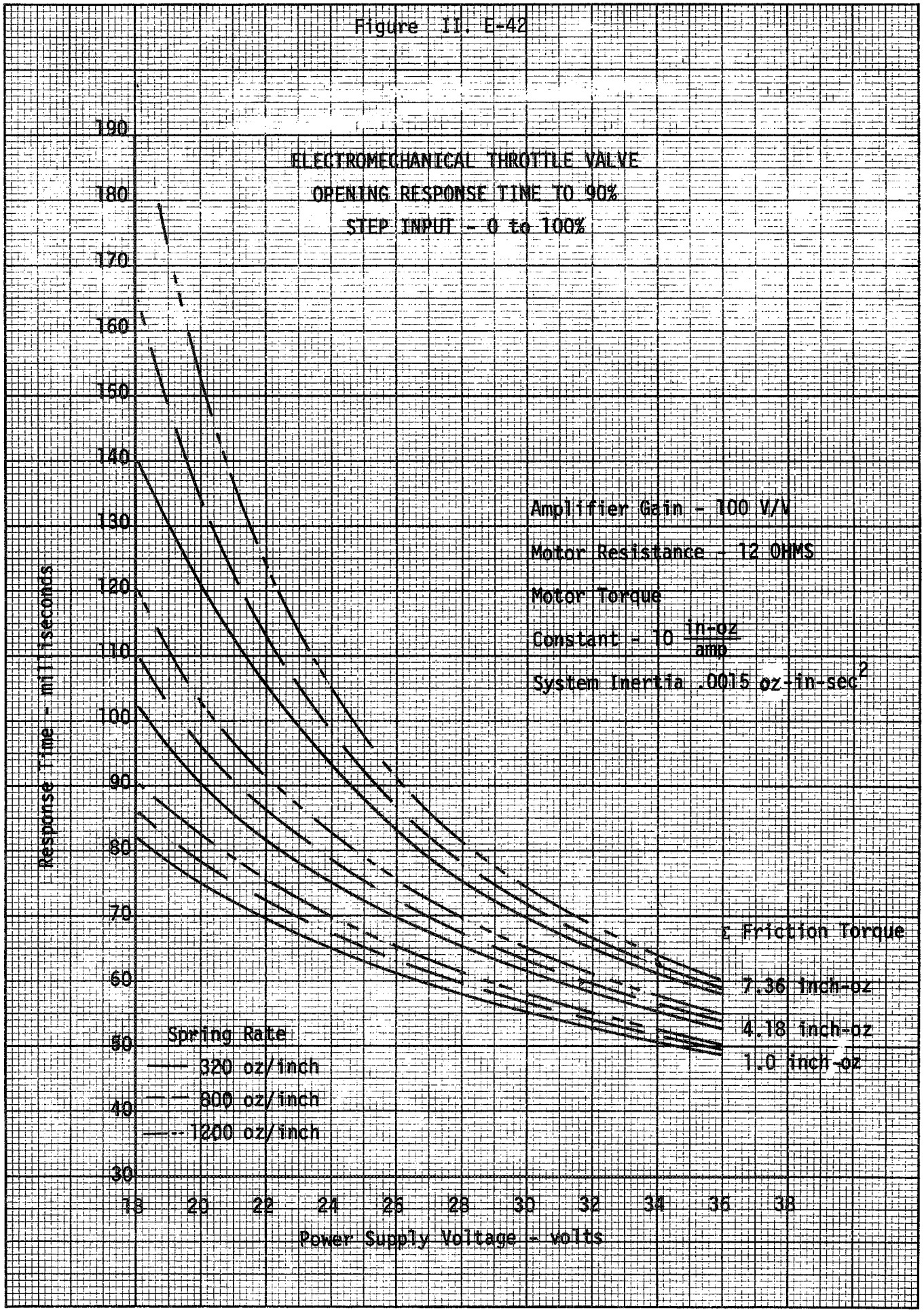

POSITION FEEDBACK

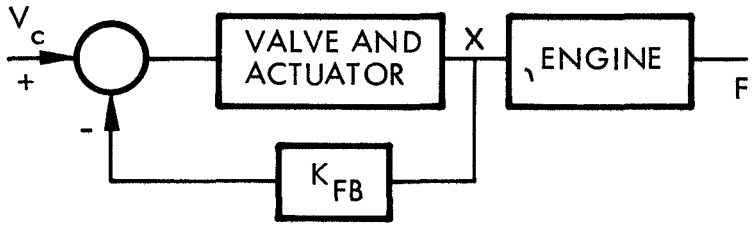

CHAMBER PRESSURE FEEDBACK

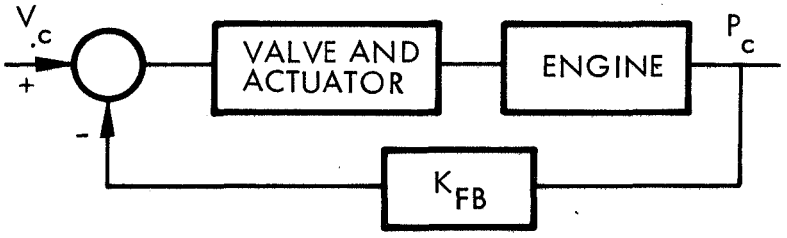

VEHICLE GUIDANCE FEEDBACK

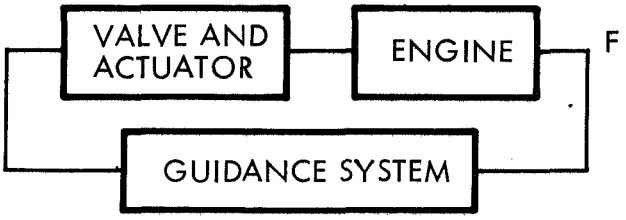

Figure II.E-43. Control Systems

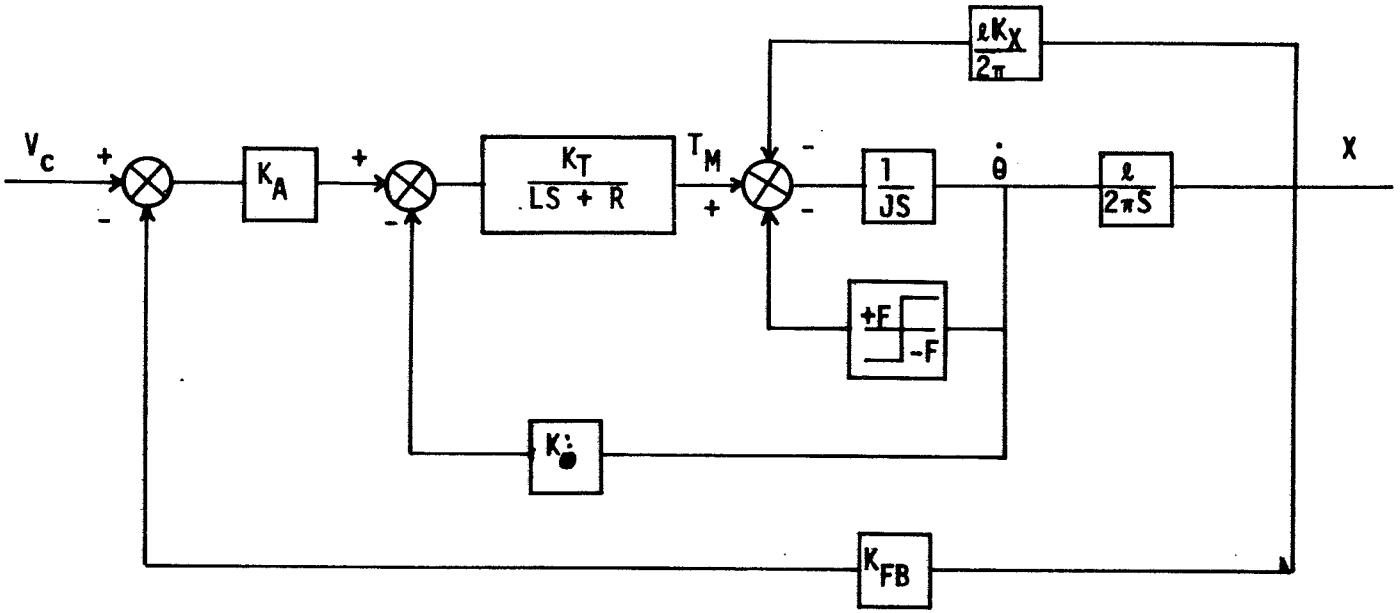

LINEARIZED TRANSFER FUNCTION

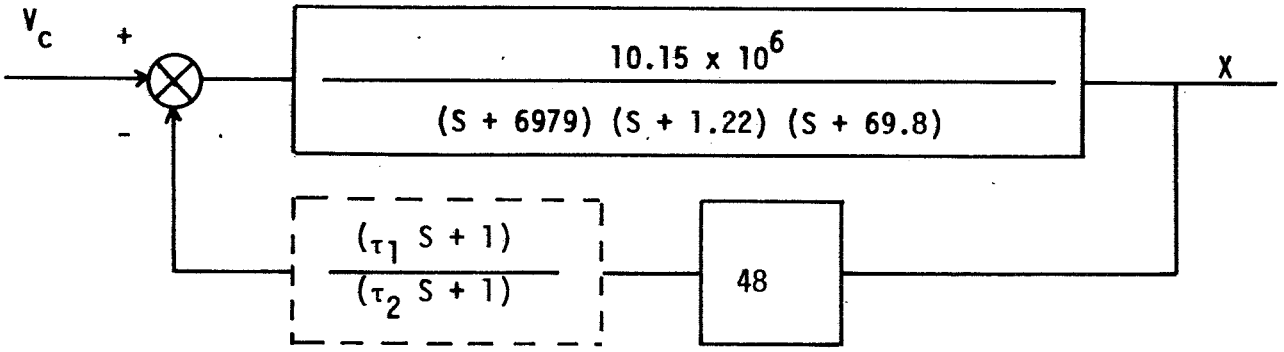

Figure II.E-44. Position Feedback Control Electromechanical Actuator

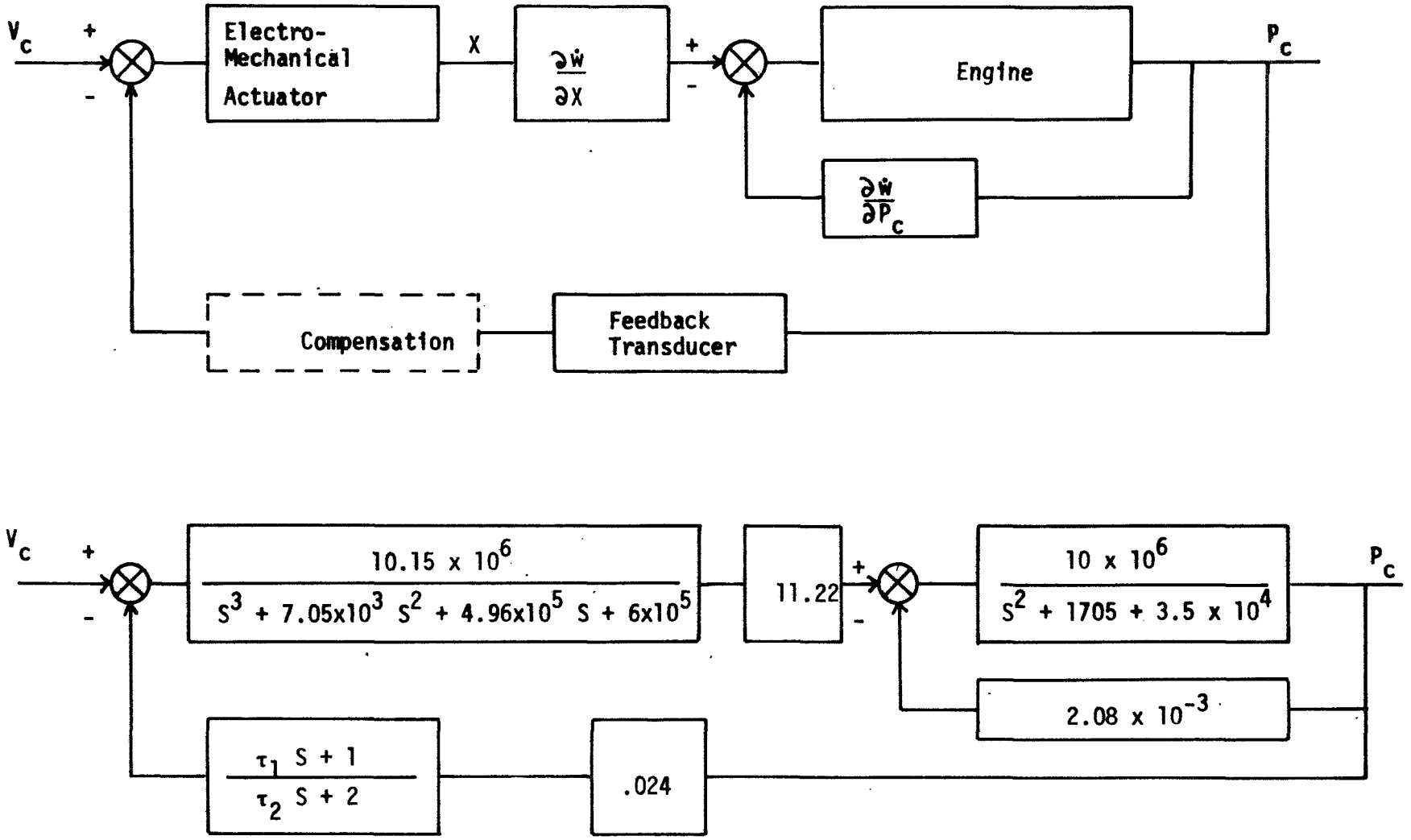

Figure II.E-45. Chamber Pressure Feedback Control Electromechanical Actuator

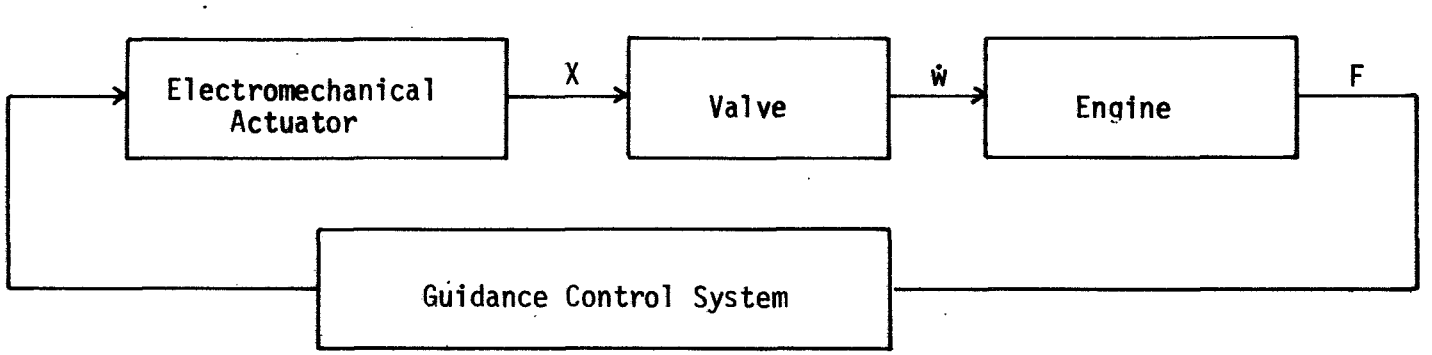

Figure II.E-46. Vehicle Guidance System Feedback Control Electromechanical Actuator

ELECTROMECHANICAL ACTUATOR

	POSITION FEEDBACK CONTROL	CHAMBER PRESSURE FEEDBACK CONTROL	VEHICLE GUIDANCE SYSTEM FEEDBACK CONTROL
	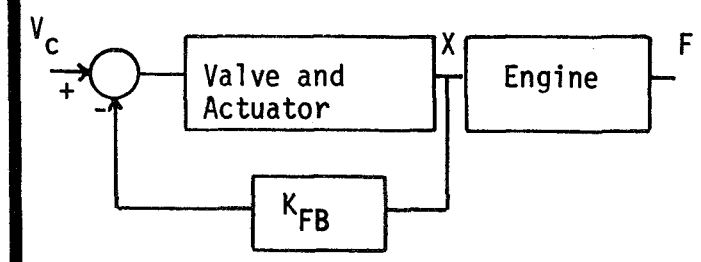	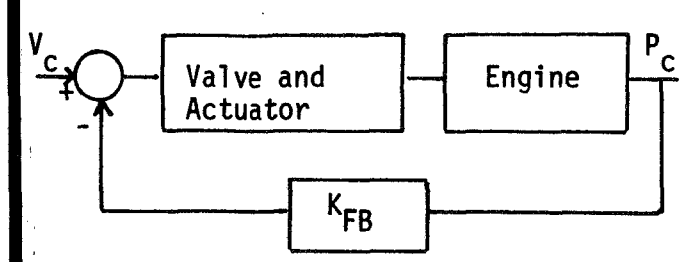	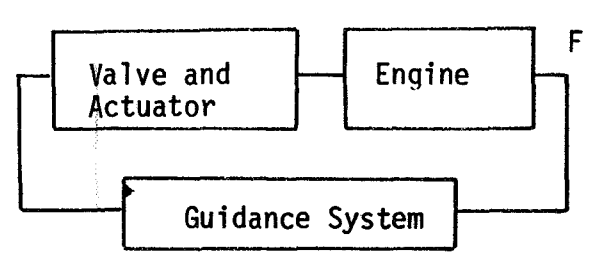
Resolution	$\Delta V_c = \frac{R}{K_A K_T} [(\frac{\ell}{2\pi})(F_{\text{seal friction}}) + T_{\text{motor friction torque}}]$ + Valve Control Electronic Resolution	$\Delta V_c = \frac{R}{K_A K_T} [(\frac{\ell}{2\pi})(F_{\text{seal friction}}) + T_{\text{motor friction torque}}]$ + Valve Control Electronic Resolution	$\Delta V_c = \frac{R}{K_A K_T} [(\frac{\ell}{2\pi})(F_{\text{seal friction}}) + T_{\text{motor friction torque}}]$ + Valve Control Electronic Resolution
Hysteresis	$\Delta V_c = (\frac{R}{K_A K_T}) [(\frac{\ell}{2\pi})(F_{\text{seal friction}}) + T_{\text{motor friction torque}}]$ + (position transducer hysteresis) + (valve control electronics hysteresis)	$\Delta V_c = (\frac{R}{K_A K_T}) [(\frac{\ell}{2\pi})(F_{\text{seal friction}}) + T_{\text{motor friction torque}}]$ + (chamber pressure feedback transducer hysteresis) + (valve control electronics hysteresis)	$\Delta V_c = (\frac{R}{K_A K_T})[(\frac{\ell}{2\pi})(F_{\text{seal friction}}) + T_{\text{motor friction torque}}]$ + (guidance system electronics hysteresis) + (valve control electronic hysteresis)
Static Error	$\Delta F = (\frac{\partial \dot{w}}{\partial X})(\frac{\partial F}{\partial \dot{w}})\frac{1}{K_{FB}}\{[\frac{R}{K_A K_T}][\frac{\ell}{2\pi}(K_s X + F_{\text{pintle preload}} + F_{\text{seal friction}} + \frac{F}{X} dx_{(\text{valve load})})] + T_{\text{motor friction torque}}]$ + position feedback transducer static error + valve control electronic static error}	$\Delta F = (\frac{\partial F}{\partial X})(\frac{1}{K_{FB}})\{(\frac{R}{K_A K_T})[(\frac{\ell}{2\pi})(K_s X + F_{\text{pintle preload}} + F_{\text{seal friction}} + \frac{\partial F}{\partial X} dx_{(\text{valve})})] + T_{\text{motor friction torque}}]$ + pressure feedback transducer static error + valve control electronic static error}	$\Delta F = \frac{1}{K_{FB}}\{\frac{\partial F}{\partial X}[(\frac{R}{K_A K_T})[(\frac{\ell}{2\pi})(K_S X + F_{\text{pintle preload}} + F_{\text{seal friction}} + \frac{F}{X} dx_{(\text{Valve})})] + T_{\text{motor friction torque}}]$ + Valve Control Electronic Static Error] + guidance system error}
Linearity	$\frac{\Delta F}{\Delta V_c} = (\frac{2P_T \dot{w}_o^2 X - 2R \dot{w}_o^2 \dot{W} X + R \dot{w}_o \dot{w}^2}{[P_{To} - R\dot{w}_o X] 2\dot{w} + R\dot{w}_o^2 X^2})(\frac{\partial X}{\partial V_c})(\frac{\partial F}{\partial \dot{w}})$	$(\frac{\Delta F_c}{\Delta V_c})$ = (chamber pressure transducer linearity)	$(\frac{\Delta F}{\Delta V_c})$ = (guidance system electronics linearity)

Figure II.E-47

Figure II. E-48

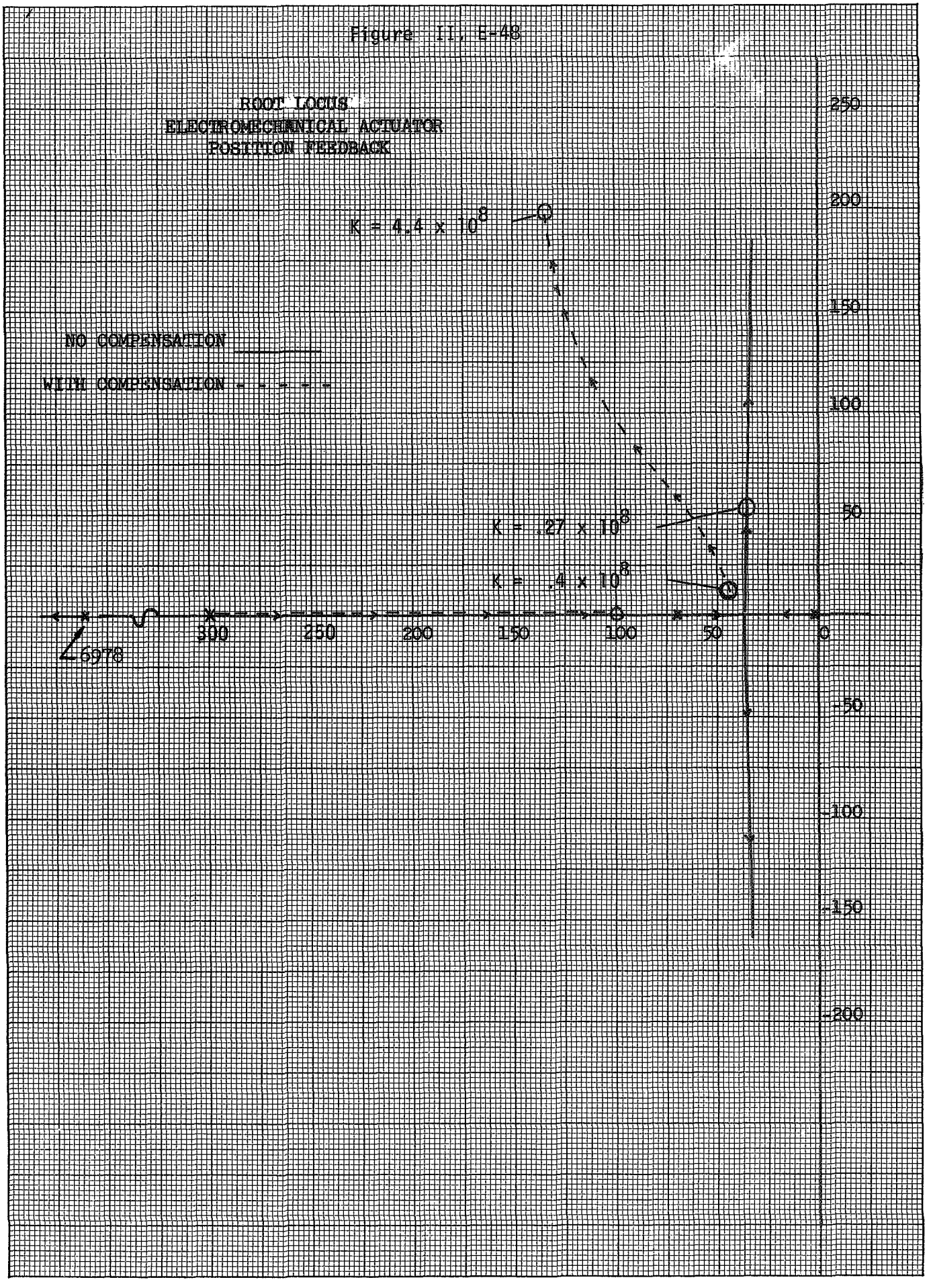

Figure II. E-49

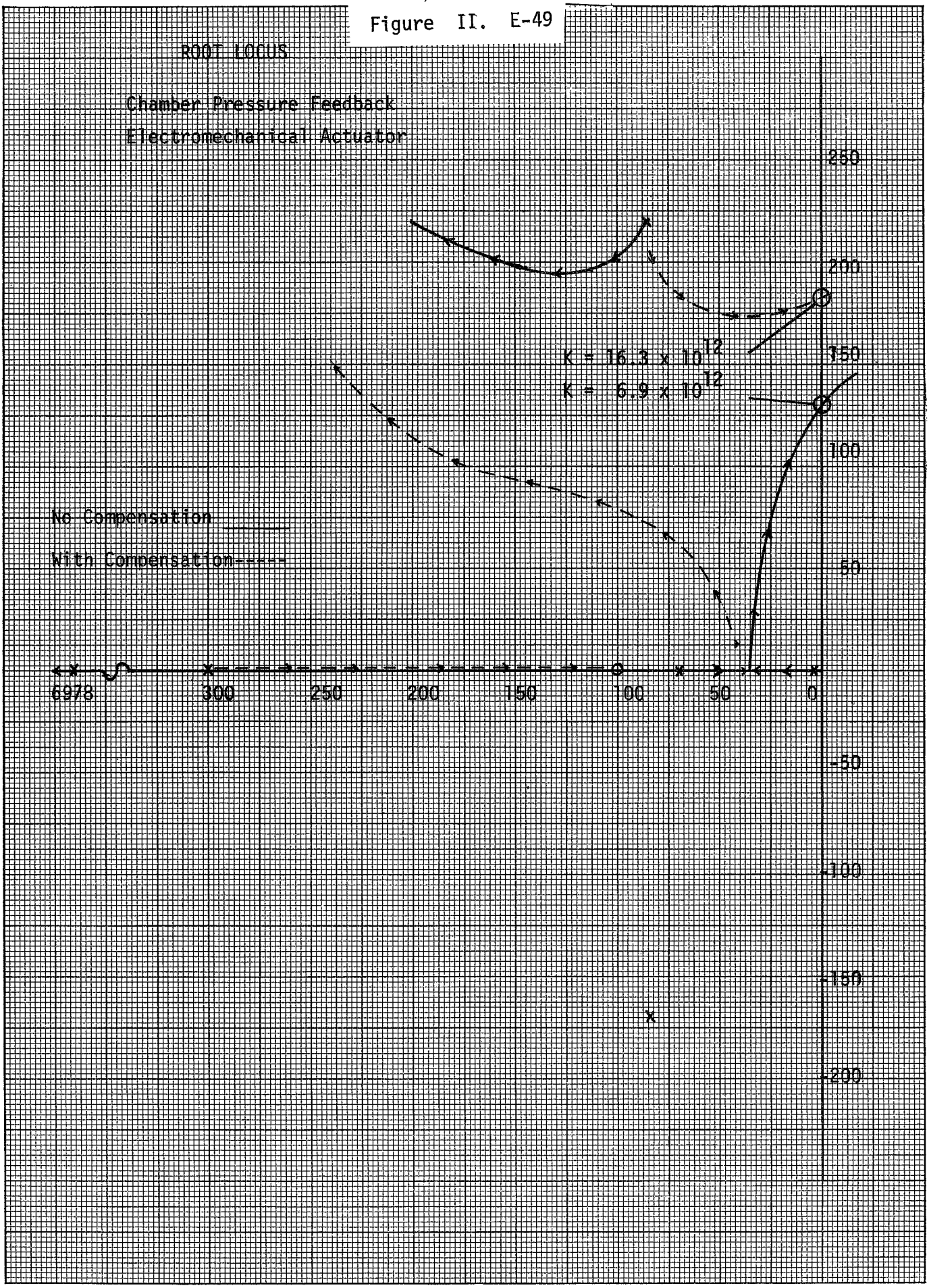

III. PHASE II RECOMMENDATION

Based on the data presented in Section II, the engine configuration recommended for Phase II was system number eight. This system employs a catalytic chamber and conventional nozzle with an electro-mechanically actuated, non-cavitating throttle valve. A nominal chamber pressure of 200 psia and an expansion ratio of 20:1 were also tentatively recommended pending the results of more detailed study in Phase II. Due to the simplified analytical approach used in the overall system weight and performance evaluations, a more detailed examination of optimum operating conditions will be performed. Areas of investigation will include an appraisal of the effects of variation in mass velocity (G) and catalyst bed pressure drop on the overall system weight and a more detailed examination of chamber and nozzle weight as a function of chamber pressure and expansion ratio.

The Phase II effort will also include practical considerations such as fabrication cost, time and material limitations in the design of the reactor shape and catalyst bed support. Since the performance is adversely affected under throttling conditions, possible methods to decrease the ammonia dissociation at low thrust levels will be considered. A determination of the thermal balance in the engine will provide insight into possible design modifications.

Detailed design and procurement of the flow control valve will be initiated during Phase II in order to meet the program schedule. At the present time, it appears that significant improvements in the performance characteristics of existing actuators can be made. In addition, suggestions regarding the development of an alternative advanced design concept have been received. A preliminary recommendation of the design approach has been submitted based on a modification to currently available designs and further tradeoffs among the alternates are being studied.

In keeping with the general philosophy of developing an advanced technology flight type engine design with a minimum of development risk, some margin will be provided in the basic engine configuration which would allow performance improvement or weight reduction in production versions.

Emphasis will be placed on the use of designs which have demonstrated feasibility in order to reduce the development risk. Primary objectives of the Phase II design effort will be to conceive a lightweight engine system with improved performance which will be suitable to demonstrate manufacturing, checkout and control capabilities.

At the present time, concurrence has been received from JPL in the Phase II recommendation and the detailed design studies are underway. Procurement action on the flow control valves will be initiated upon finalization and approval of the specific approach to be used.

IV. NEW TECHNOLOGY REPORTS

The conceptual design study described in Section II.B revealed several areas of improvment over current design practices. On the basis of a thorough evaluation of the possible combination of the various component parts of known designs, four New Technology Reports have been initiated as a result of the Phase I Program. These advanced designs are described in detail in the following paragraphs.

IV.1 Thermal Decomposition Engine

Hydrazine is presently one of the most useful monopropellants because of its relatively high performance and physical properties which are similar to water. Until "spontaneous" catalysts became available, initiating the decomposition process in a repeatible and reliable manner was a cumbersome procedure requiring external energy sources. The spontaneous catalysts will decompose liquid hydrazine upon contact so the starting procedure for engines and gas generators running on hydrazine is much simpler than before. These catalysts must be present in large quantities, however, if the entire decomposition process is to be completed within the catalyst pack. Such large quantities are very expensive, are heavy, and are subject to deterioration as operating time increases. Fortunately, hydrazine can also be decomposed in a purely thermal process provided a suitable mechanism is available where heat can be transferred from the hot products to the liquid drops so they will vaporize and decompose. Although this process is self-sustaining, it must be initiated by the introduction of a considerable amount of thermal energy.

This innovation combines the spontaneous initiation capability of catalyst beds with the light weight, economy, and durability of a thermal reactor. In essence it is a small catalytic reactor which decomposes a pilot flow of hydrazine during the starting period and sprays the resulting hot gases into a thermal reactor to provide the energy necessary to start decomposing the main flow of liquid fuel injected directly into the thermal reactor. Since the small catalytic reactor starts quickly and spontaneously and it delivers such a large and diffuse source of energy, the main reactor can be started merely by sequencing the opening of its valves with relation

to the opening of the valves on the small reactor. Once the main reactor is functioning, the small reactor is shut down to minimize its total operating time and thereby to maximize the useful life of the catalyst.

As can be seen in the Figure IV-1, the small starter reactor is much smaller than ordinary full-size catalytic reactors. This means that less catalyst is needed so the cost and weight of catalyst are far less than for ordinary catalytic reactors.

The novelty of this invention is the combination of a spontaneously-startable catalytic reactor and a large thermal reactor so as to achieve the advantages of spontaneous starting for the thermal reactor without the penalties of expense, weight and deterioration which are characteristic of large catalytic reactors.

IV.2 Radial Flow Reactor

Within the reactor sections of hydrazine monopropellant rocket engines, the liquid fuel must be vaporized and decomposed to ammonia, nitrogen, and hydrogen gases. This process releases chemical energy in the form of heat which is then available to be converted into directed kinetic energy by the nozzle producing thrust by expelling the gases. The processes of vaporization and decomposition should be accomplished in a compact volume if the size of the engine is to be minimized. This invention arranges the elements of such an engine so as to provide an efficient reactor configuration within a shorter overall length than has been conventional to date.

Hydrazine vaporization and decomposition require heating the liquid fuel but external sources of heat cannot be provided efficiently so this heat must be obtained from the hydrazine itself. A common means of doing this is to use a catalytic substance which upon contact causes the hydrazine to spontaneously increase in temperature until it vaporizes and decomposes. Because the catalytic reaction is a surface phenomenon, achieving a high rate of reaction requires that the catalyst surface to volume ratio be maximized. Catalysts are currently available which will initiate this reaction when the propellant and catalyst are at ambient temperatures; however, such catalysts are very expensive. A much cheaper type of catalyst is available which will initiate the reaction with ambient

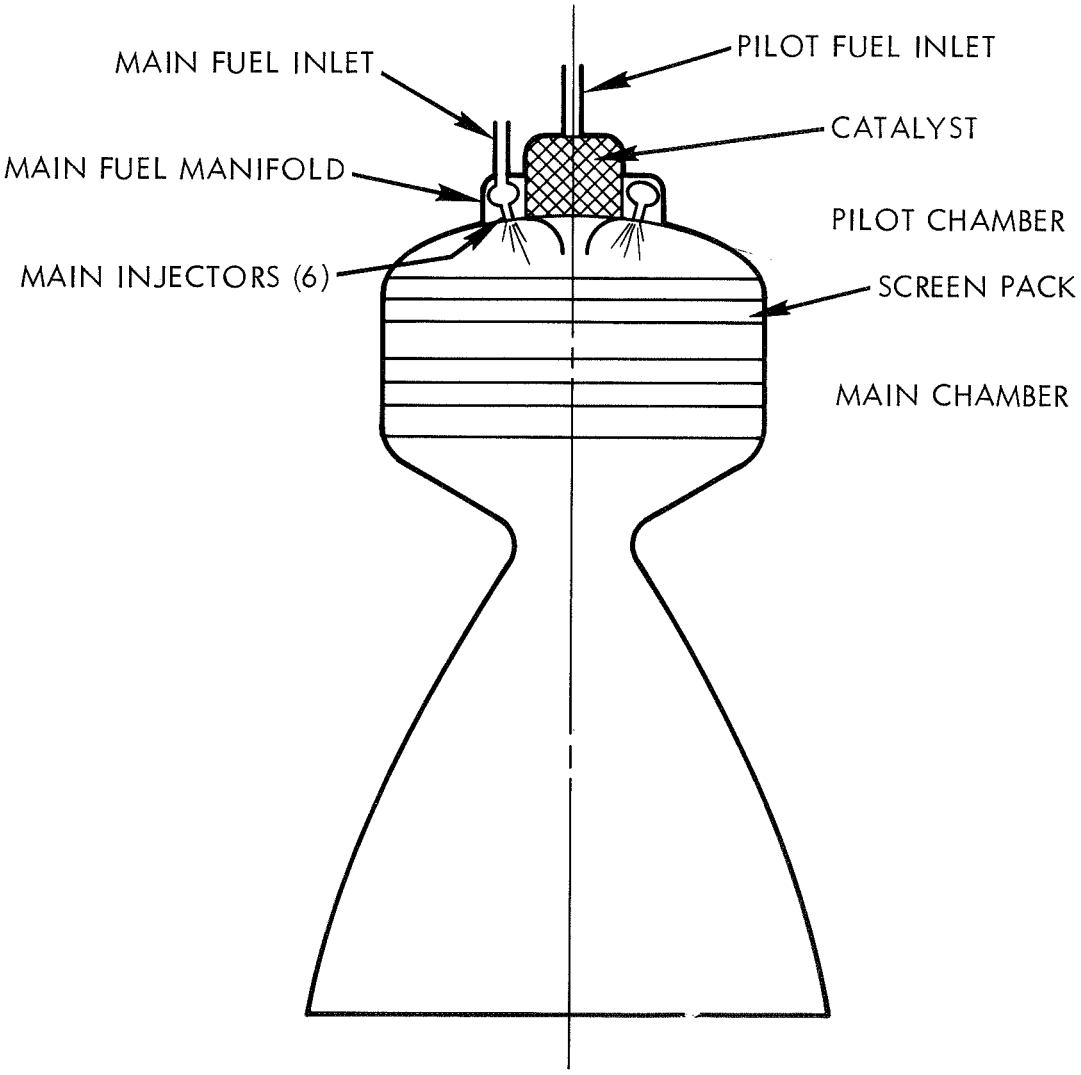

Figure IV-1. Thermal Decomposition Engine

propellant if the catalyst can be initially raised to 400 to 500°F. Both types of catalyst are in the form of a coating on refractory pellets.

The cost of catalyst may thus be minimized by using a minimum of the spontaneous catalyst to initiate the reaction and then directing the partially decomposed stream into a volume of the cheaper pellets to complete the process. Once this process has progressed to the state where a considerable fraction of the flow has been converted to hot gases, it can be completed without further contact with catalyst if the heat in the gases is effectively transferred to the remaining fraction which is still liquid so as to vaporize and decompose it. Completing the process without catalyst is desirable to minimize the catalyst weight and expense and maximize performance by reducing the ammonia dissociation. One means of hastening the vaporization process in a space void of catalyst is to place a multitude of narrow obstructions in the flow path so that many small turbulent eddies are produced. If the ratio of the width of the obstructions to the distance between them is correct for the existing flow velocity, essentially all of the hot gases and droplets will be caught up in the eddies downstream of the obstructions. This turbulence will tend to shatter the drops of liquid so the surface to volume ratio increases, and to mix the resulting droplets with the hot gases in a most intimate manner so the heating and vaporization rate increases.

The present invention combines these most efficient and economic elements in a compact configuration which is nearly disc-shaped or an oblate spheroid (see Figure IV-2). Several equally-spaced injector elements, located near the outer periphery, spray liquid fuel into adjacent conical volumes filled with fine mesh spontaneous catalyst contained in individual screen assemblies, one per injector element. The partially-decomposed fuel emerges from these into an annulus filled with non-spontaneous coarse mesh catalyst pellets where the process of decomposition continues as the fuel flows radially inward. Near the center is an open space kept free of catalyst by a screen; within this space the flow direction is reversed so the fuel leaves by flowing radially outward. The decomposition process is completed in a space filled with a highly porous refractory material (layers of metal screens, concentric metal plates with

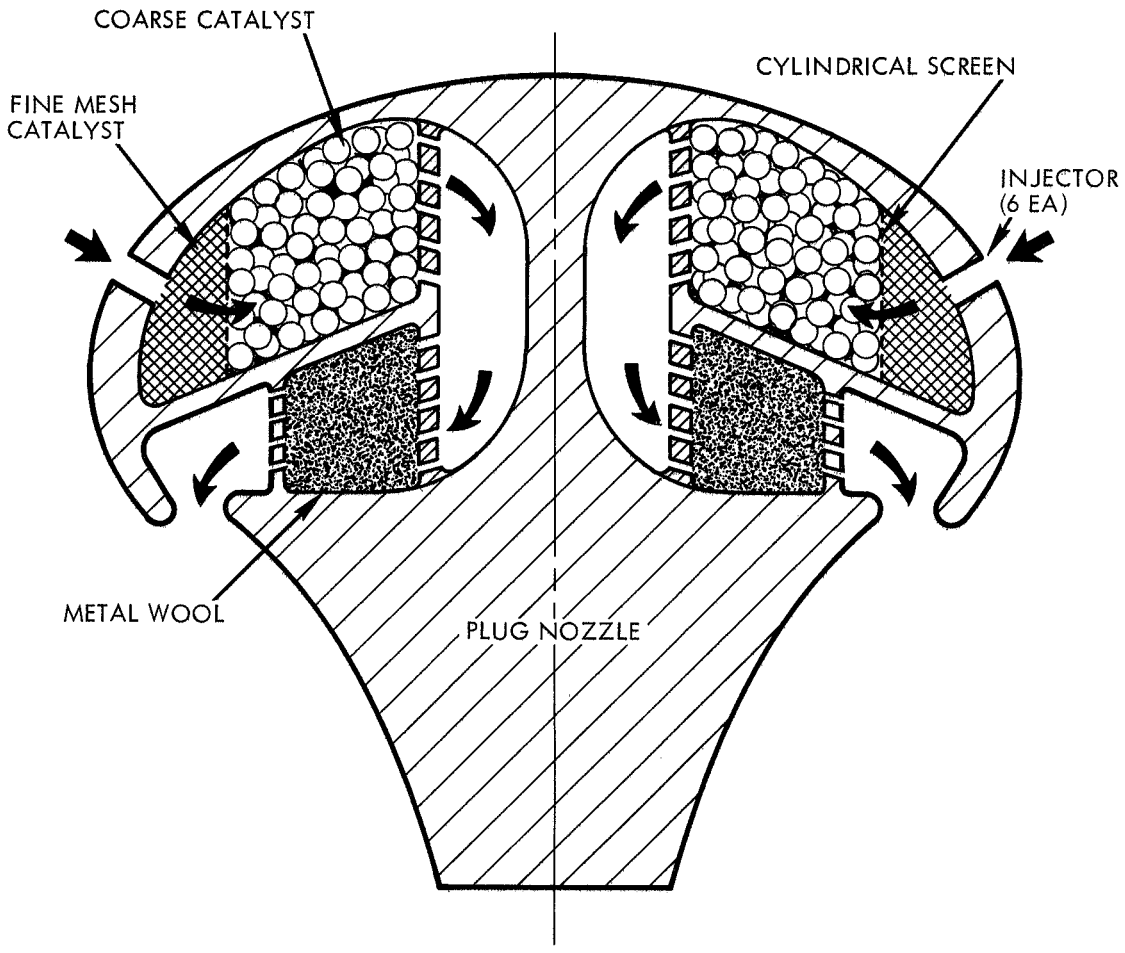

Figure IV-2. Radial Flow Reactor

many holes, metal wool, or other suitable materials). The nozzle throat is an annulus near the exit of the reactor. (A truncated plug nozzle is shown in Figure IV-2 to illustrate the shortest configuration.)

The advantage of this configuration compared to conventional cylindrical reactors is that the overall length is much shorter for a given flow path length. This configuration is novel in that a folded radial flow path is used to obtain a maximum path length in the shortest axial length. Within the path, a combination of the most efficient and economic reactor design elements have been combined in a manner which is most likely to achieve high performance along a given length path.

IV.3 High Efficiency Monopropellant Reactor

When monopropellant such as hydrazine are decomposed in catalyst beds, the rate of decomposition is controlled by the rate of liquid temperature increase. Heat is available from two sources internal to the reactor; the catalytic reaction of the fuel on the surface of the catalyst and the hot gaseous products of the fuel which has been fully decomposed exothermically. The purpose of this innovation is to make more efficient use of these two sources of heat than is done in the convetional monopropellant catalyst bed so that the reactor bed can be smaller, lighter in weight, and have better response.

To appreciate the significance of the innovation, it is necessary to understand that the catalyst beds currently in use consist of spaces (cylindrical in most cases) filled with catalyst-coated pellets. These pellets are used in several sizes, the smaller (fine mesh) pellets being more reactive. Usual practice is to use a thin layer of small pellets where the liquid fuel is sprayed onto the bed, and a thicker layer of the larger pellets which constitutes the remainder of the bed. Fuel sprayed onto the small pellets begins to heat up rapidly. A pressure differential across the bed causes the fuel to flow into the layer of large pellets where the decomposition process is completed by both catalytic reaction and heat transfer from the hot gases is restricted by the resistance to recirculation flow of the densely packed pellets (i.e., the interstitial spaces constitute the flow path for both the liquid fuel and the gaseous products).

It has been established that increasing the degree of hot gas recirculation upstream to the colder zone will increase the rate of reaction due to both direct convective heating of the liquid flow and heating of the catalyst pellets. Furthermore, lateral maldistributions of fuel flow across the bed lead to flooded zones where reaction rates are considerably slower than the average. The purpose of this invention is to provide suitable flow paths and a positive driving mechanism to insure an increased amount of hot gas recirculation. Further, the occurence of local flooding is reduced by controlling the lateral distribution of the fuel and by providing a lateral mixing zone within the bed where inequalities can be reduced by cross-flow.

Figure IV-3 shows the configuration of this invention. Fuel from a high pressure source is sprayed by suitable injector mechanisms into mixing cans which are comprised of converging-diverging nozzles attached to right cylinders. By centrally locating an injector at the entrance to each nozzle, the high velocity jet of fuel issuing from the injector will entrain a quantity of ambient gas from the space above the nozzles and carry it into the mixing can; this action is commonly referred to as "jet pumping". The resulting mixture of gas and liquid impinges on and passes through the space of highly reactive, fine-mesh catalyst pellets in the cylinder. Here the decomposition process begins. Uniformity of flow across the reactor is assured by the arrangement of one injector per mixing can. The mixed phase flow issuing from these cans exhausts into a plenum which allows cross-wise equalization if any of the injectors fails to flow at the average rate.

Since the cylinders are round in cross-section, a considerable space exists between them which presents a series of flow passages for some of the gas to flow from the plenum back to upper space where it provides the ambient gas to be entrained by the jet pumping action. Due to the catalytic action, these gases will be hot. When mixed with the injected liquid and being pumped through the bed, these gases regeneratively heat the liquid and the pellets.

The larger fraction of the flow, which is a mixture of gases and undecomposed liquid, will not recirculate but instead will flow into the

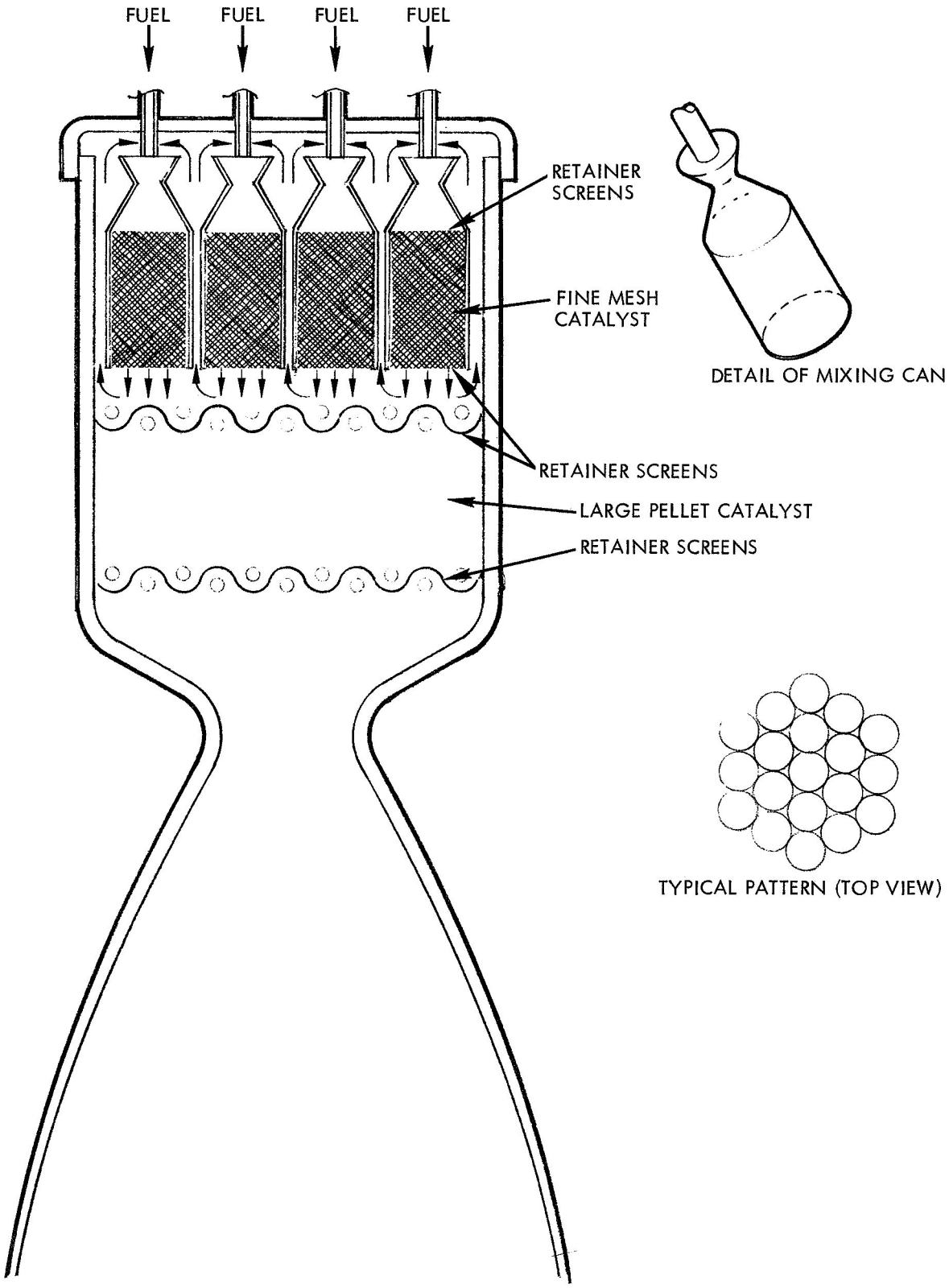

Figure IV-3. High Efficiency Monopropellant Reactor

main portion of the bed which is a thick layer of large size catalyst pellets. Here the remaining liquid is decomposed to hot gases. The efflux from the bed passes out through the bottom retainer screen to the downstream plenum.

The novelty of this invention is in the use of nozzles, in proximity to the jets of fuel, which act as jet pumps; the containment of the fine mesh catalyst in an array of cylindrical containers to control lateral spreading of the flow and to create an array of parallel flow channels connecting the center plenum with the space above the jet pumps; and the containment of the larger catalyst pellets in a separate discrete layer below the center plenum so the entire cross-section of the bed has an equal potential for receiving flow via the plenum.

IV.4 Throttleable Monopropellant Rocket Engine

A fixed configuration of rocket engine theoretically will operate at maximum efficiency at only one set of operating conditions: the pressures and flow rates for which the different parts were designed. This means that throttleable rockets must be operated at off-optimum conditions or the configuration must be variable. This innovation consists of a configuration of a monopropellant liquid rocket engine (typically fueled with hydrazine) combining those features which allow most of the pertinent variables to be controlled so as to achieve nearly uniform efficiency as the thrust level is modulated. These features will be described according to the location in the engine (see Figure IV-4), starting with the expansion nozzle.

Inequality between the lowest pressure to which the gases are expanded in the nozzle (exit pressure) and the local ambient pressure results in pressure forces which decrease thrust below the maximum obtainable at the same conditions with equality of these pressures. Therefore, a nozzle in which the flow will naturally expand to, but not lower than, the ambient will experience no loss in performance due to exit pressure mismatch. Two kinds of nozzles which achieve this are the "plug" nozzle and the "expansion-deflection" nozzle. Either may be used in this engine.

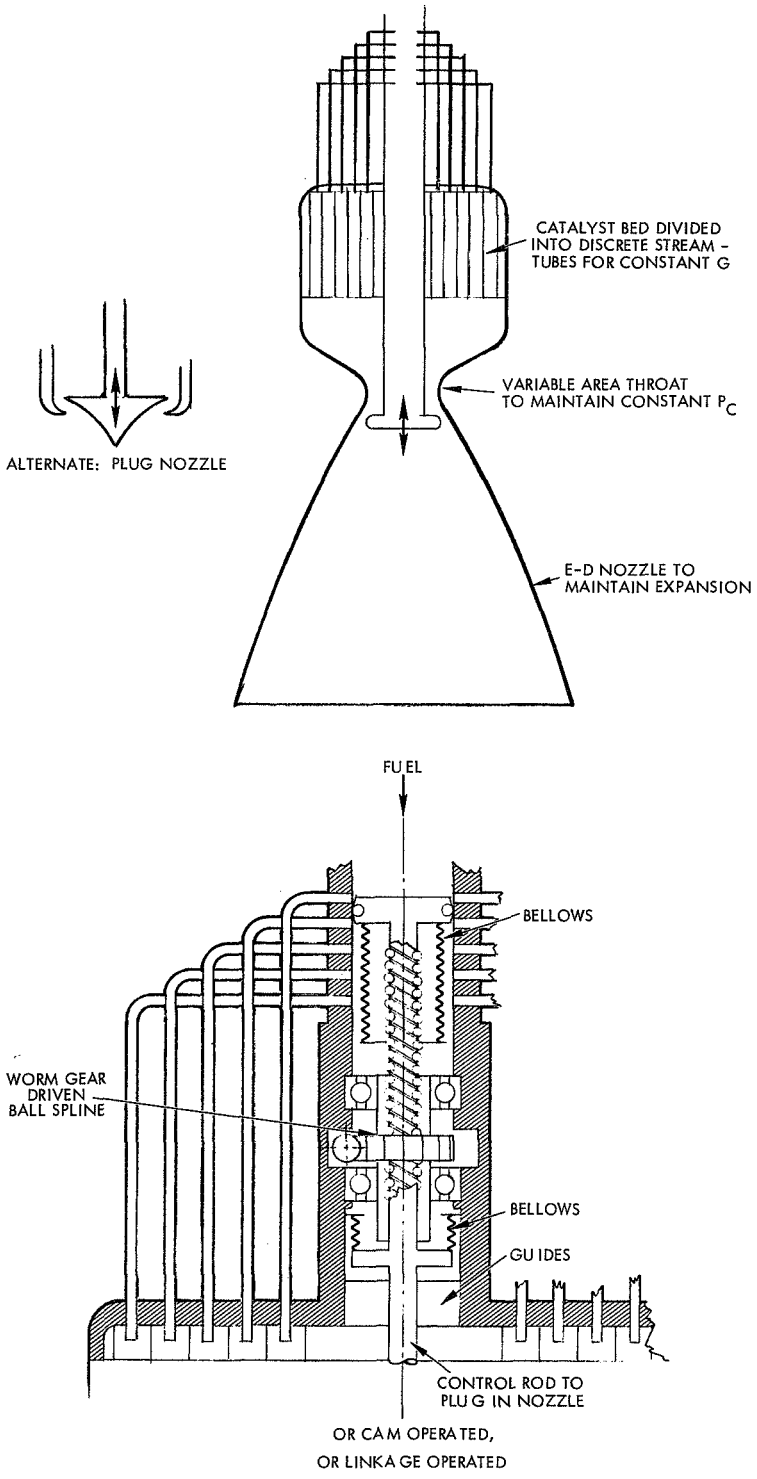

NOTE: TRAVEL OF PLUG IS LESS THAN VALVE BY A FACTOR OF 4 TO 10.

Figure IV-4. Throttleable Monopropellant Rocket Engine

If chamber pressure decreases as thrust decreases, the thermodynamic performance of the nozzle will decrease (all other factors being constant) because the pressure ratio decreases. Therefore, a variable area nozzle throat which is changed in concert with the propellant flow rate so as to maintain a constant chamber pressure, will eliminate this cause of performance degradation. For plug and expansion-deflection nozzles this can be accomplished by moving the plug or deflector so as to change the annular throat area. A suitable seal is required on the actuation rod; in this case, a metal bellows is shown.

Monopropellant engines in which the decomposition process is controlled by a catalyst pack or bed are likewise designed for optimum operation at only one set of conditions; in this case, for a given mass flow rate per unit cross-sectional area. Off-optimum operation yields lower performance. Higher than optimum flow rates cause the fuel concentration in the catalyst bed to increase so that some fuel may leave the bed before being decomposed. Lower than optimum flow rates allow the decomposition to be completed too far upstream of the exit from the bed so that dissociation of the products occurs before the gases exit, and since dissociation endothermically cools the products, the performance is lowered. One solution to this problem is to divide the bed into many separate but parallel paths, each of which carries only its optimum flow rate for best performance. Throttling is accomplished by varying the number of paths being used (i.e., each is fed by its own separate injector element and the valving, discussed below, turns these on and off to throttle the engine).

The process of injecting propellant usually affects performance as the stream velocity and stream size varies. Most throttling injectors operate over a range of velocities and/or stream sizes and, therefore, operate for part of the duty cycle at less than maximum performance. The present configuration operates at constant velocity and stream size by virtue of the constant pressure differential across the orifices (both feed pressure and chamber pressure are constant) and the fixed geometry of each injector orifice. In other words, the injector operation is incremental with the individual elements (orifices) being turned either

full on or full off by appropriate valving. Thus, the orifices geometry may be selected for best performance with assurance that they will be operated at the design point.

Several means can be used to valve the orifice entries so as to start and stop the fuel flow by progressively opening or closing an array of orifices. A piston in the manifold which uncovers the orifice entries is shown in the sketch. A mechanical actuation device is used to operate the valve and the nozzle plug in unison.

The novelty of this invention is the unique combination of features which results in the most uniform performance as the thrust level is varied.

APPENDIX A. SYSTEM PERFORMANCE PROGRAM

This section describes the basic digital computer programs used in the system and engine weight analysis and ideal velocity increment determination. The program for system 6 was identical to that for 1, 2 and 8 except for updating of the format and the necessary changes in the input data. A listing is presented for systems 1, 2 and 8. Systems 3, 4, 5 and 7 were computed in an identical manner to systems 1, 2 and 8 except for the altitude compensation feature which adjusts the area ratio depending on the exit pressure to avoid separation. System 3 employs a variable area nozzle which requires an iteration loop to adjust the throat area for maintaining a constant chamber pressure and establishing the corresponding thrust coefficient.

The programs required an initial input of engine weight as a function of thrust, chamber pressure and expansion ratio. The output is presented for engine performance, system ideal velocity increment and system weight (3 engines + hardware + propellant) with a breakdown of propellant, engine (1 each) and hardware weight. Program options include varying the type of throttle valve, blowdown pressure ratio, injector ΔP, reactor ΔP and ambient pressure.

```
C: PROGRAM FOR AL HARPER  7-15-69
   WRITE (1,5)
 5 FORMAT(//,$WOULD YOU LIKE THE OPTION OF PRINTING$/$MOST OF
    THE VARIABLES?$//3X$TYPE  0 FOR NO$/9X$1 FOR YES$)
   ACCEPT IPRINT
   DIMENSION E(6,7),PC(6),F(3),DTBP(16),WFBP(16),CFVBP(3,12),
   CFEBP(12),CFCBP(3),CSTBP(12),CSTCBP(12),PRCTF(7),WEPCBP(8)
   ,WEEBP(6),WEBP4(6,8),WEBP5(6,8),WEBP6(6,8),WC(3),ZIS(6),CS
   TAR(6),CFVAC(6),CF(6)
   DATA KEND,((E(I,J),J=1,7),I=1,6)/6,5.,10.,15.,20.,30.,40.,
   0.,5.,10.,15.,20.,30.,40.,0.,5.,10.,15.,20.,30.,40.,0.,5.,
   10.,20.,30.,40.,60.,0.,5.,10.,20.,30.,40.,60.,80.,5.,10.,2
   0.,30.,40.,60.,80./
   DATA JPCEND,(PC(I),I=1,6)/6,50.,75.,100.,200.,300.,500./
   DATA IFEND,(F(I),I=1,3)/3,300.,600.,1200./
   DATA (WC(I),I=1,3)/4.,5.,6./
   DATA T,R,G,RHOT,RHOP,SIGMA/530.,643.,32.174,.16,.0361,6810
   0./
   DATA DELPS,PI/10.,3.14159265/
   DATA (DTBP(I),I=1,16)/1.,2.,3.,4.,5.,6.,7.,8.,9.,10.,12.5,
   15.,20.,25.,35.,43./
   DATA (WFBP(I),I=1,16)/1.63,1.515,1.442,1.4,1.361,1.33,1.30
   5,1.285,1.265,1.247,1.21,1.18,1.133,1.095,1.038,1.005/
   DATA (CFVBP(1,I),I=1,12)/1.6,1.624,1.66,1.687,1.706,1.72,1
   .73,1.737,1.743,1.753,1.761,1.7715/
   DATA (CFVBP(2,I),I=1,12)/1.61,1.635,1.672,1.7,1.717,1.732,
   1.743,1.7515,1.758,1.769,1.778,1.7885/
   DATA (CFVBP(3,I),I=1,12)/1.62,1.644,1.685,1.7135,1.733,1.7
   48,1.759,1.767,1.774,1.786,1.7955,1.8085/
   DATA (CFEBP(I),I=1,12)/7.5,10.,15.,20.,25.,30.,35.,40.,45.
   ,55.,65.,80./
   DATA (CFCBP(I),I=1,3)/20.,60.,100./
   DATA (CSTBP(I),I=1,12)/4150.,4193.,4233.,4272.,4287.,4302.
   ,4315.,4325.,4334.,4345.,4352.,4358./
   DATA (CSTCBP(I),I=1,12)/10.,20.,30.,40.,45.,50.,55.,60.,65
   .,75.,85.,100./
   DATA (PRCTF(I),I=1,7)/20.,30.,40.,60.,80.,100./
   DATA (WEPCBP(I),I=1,5)/50.,100.,200.,300.,500./
   DATA (WEEBP(I),I=1,6)/5.,10.,20.,40.,60.,80./
   DATA (WEBP4(1,I),I=1,5)/5.39,5.25,5.29,5.5,5.99/
   DATA (WEBP4(2,I),I=1,5)/5.82,5.55,5.5,5.68,6.12/
   DATA (WEBP4(3,I),I=1,5)/6.6,6.1,5.89,5.99,6.37/
   DATA (WEBP4(4,I),I=1,5)/8.09,7.01,6.53,6.52,6.77/
   DATA (WEBP4(5,I),I=1,5)/10.5,7.8,7.09,6.97,7.12/
   DATA (WEBP4(6,I),I=1,5)/13.15,9.27,7.51,7.32,7.39/
   DATA (WEBP5(1,I),I=1,5)/8.83,8.72,9.23,9.94,11.56/
   DATA (WEBP5(2,I),I=1,5)/10.15,9.66,9.89,10.48,11.98/
```

```
      DATA (WEBP5(3,I),I=1,5)/12.26,11.15,10.94,11.34,12.65/
      DATA (WEBP5(4,I),I=1,5)/15.7,13.57,12.66,12.74,13.74/
      DATA (WEBP5(5,I),I=1,5)/18.34,15.44,13.98,13.82,14.57/
      DATA (WEBP5(6,I),I=1,5)/20.3,16.97,15.06,14.7,15.25/
      DATA (WEBP6(1,I),I=1,5)/12.74,11.61,11.75,12.35,13.9/
      DATA (WEBP6(2,I),I=1,5)/16.,13.92,13.38,13.69,14.93/
      DATA (WEBP6(3,I),I=1,5)/22.19,18.3,16.48,16.21,16.88/
      DATA (WEBP6(4,I),I=1,5)/32.59,25.64,21.68,20.45,20.16/
      DATA (WEBP6(5,I),I=1,5)/41.59,32.07,26.19,24.14,23.01/ .
      DATA (WEBP6(6,I),I=1,5)/48.39,36.82,29.56,26.89,25.15/
      KSYST=8
      PAMB=.3
   99 WRITE (1,10)
   10 FORMAT(/,$INJECTOR PRESSURE DROP(DELPI) = $,Z)
      ACCEPT DELPI
      WRITE (1,20)
   20 FORMAT(/,$REACTOR PRESSURE DROP(DELPB) = $,Z)
      ACCEPT DELPB
      WRITE (1,30)
   30 FORMAT(/,$V = $,Z)
      ACCEPT V
      WRITE (1,40)
   40 FORMAT(/,$Z = $,Z)
      ACCEPT Z
      WRITE(1,41) KSYST
   41 FORMAT(8(/)15X$SYSTEM$I3///)
      IF(IPRINT) 70,70,75
   70 WRITE (1,76)
   76 FORMAT(//2X,$THRUST$,5X,$PC$,8X,$E$,7X,$WS$,10X,$PT$,7X,$W
      E$,10X$WP$/)
   75 CONTINUE
      DO 1 I=1,IFEND
      DO 2 J=1,JPCEND
      KEND=6
      IF(J.GT.4) KEND=7
      DO 3 K=1,KEND
      DO 4 L=1,6
      CFVAC(L)= FUN2[PRCTF(L),CFCBP,E(J,K),CFEBP,CFVBP,3,12]
      CF(L)=.99*CFVAC(L)-PAMB*E(J,K)/PRCTF(L)/PC(J)/.010
      CALL INTRPOL[PRCTF(L),C1234,CSTCBP,CSTBP,DELY,12]
      CSTAR(L)=C1234
      ZIS(L)=CSTAR(L)*CF(L)/G
    4 CONTINUE
      WP=3.*F(I)*(1./ZIS(1)+1./ZIS(6)+4.8/ZIS(5)+3.6/ZIS(4)+2.4/
      ZIS(3)+.6/ZIS(2))
      DT=(6.*Z*WP/RHOP/PI)**(1./3.)
      CALL INTRPOL[DT,WF,DTBP,WFBP,DELY,16]
      PT=(PC(J)+DELPB+DELPI+DELPS)/(1.-V)
```

```
      WT=3.*Z*WP*PT*RHOT*WF/2./RHOP/SIGMA
      WN=(Z-1.)*PT*WP/RHOP/R/T
      IF(I-2) 100,150,200
  100 WE=FUN2[E(J,K),WEEBP,PC(J),WEPCBP,WEBP4,6,5]
      GO TO 300
  150 WE=FUN2[E(J,K),WEEBP,PC(J),WEPCBP,WEBP5,6,5]
      GO TO 300
  200 WE=FUN2[E(J,K),WEEBP,PC(J),WEPCBP,WEBP6,6,5]
  300 WS=WP+WT+WN+WC(I)+3.*WE
      IF(IPRINT) 50,50,60
   50 WRITE (1,52) F(I),PC(J),E(J,K),WS,PT,WE,WP
   52 FORMAT(2X,F5.0,4X,F5.0,4X,F5.0,3X,F8.2,3X,F7.1,3X,F7.2,3X,
      F8.2)
      GO TO 3
   60 WRITE (1,65) F(I),PC(J),E(J,K),DT,WN,WP,WT,WE,WS,PT,WF
      WRITE (1,66) (PRCTF(L),CSTAR(L),CFVAC(L),CF(L),ZIS(L),L=1,
      6)
   66 FORMAT(6(F5.0,2X,E14.8,2X,E14.8,2X,E14.8,2X,E14.8/)///)
   65 FORMAT(///$THRUST = $E14.8/$PC = $E14.8/$E = $E14.8/$DT =
      $E14.8/$WN = $E14.8/$WP = $E14.8/$WT = $E14.8/$WE = $E14.8
      /$WS = $E14.8/$PT = $E14.8/$WF = $E14.8//2X,$%F$,7X,$CSTAR
      $,12X,$CFVAC$,10X,$CF$16X$IS$/)
    3 CONTINUE
      DISPLAY " "
    2 CONTINUE
      DISPLAY " "
    1 CONTINUE
      STOP
      END



      SUBROUTINE INTRPOL[XPT,YPT,X,Y,DELY,N]
      DIMENSION X(100),Y(100)
      IF(XPT-X(1)) 8,9,2
    2 IF(XPT-X(N)) 3,10,11
    3 DO 1 I=1,N
      IF(XPT-X(I)) 4,5,1
    4 Z=(XPT-X(I-1))/(X(I)-X(I-1))
      YPT=Z*(Y(I)-Y(I-1))+Y(I-1)
      DELY=(Y(I)-Y(I-1))/(X(I)-X(I-1))
      RETURN
    5 YPT=Y(I)
      DELY=(Y(I+1)-Y(I))/(X(I+1)-X(I))
      RETURN
    1 CONTINUE
    8 WRITE (1,101)
    9 YPT=Y(1)
```

```
      DELY=0.0
      RETURN
   11 WRITE (1,101)
   10 YPT=Y(N)
      DELY=0.0
  101 FORMAT($INPUT FOR X IS OUTSIDE OF RANGE INPUT FOR INTERPOL
      ATION$/)
      RETURN
      END



      FUNCTION FUN2(ARG1,ARG1BP,ARG2,ARG2BP,FUN2BP,I1,I2)
      DIMENSION ARG1BP(10),ARG2BP(10),FUN2BP(10,10)
      DO 200 J1=2,I1
      IF(ARG1-ARG1BP(J1)) 21,21,200
  200 CONTINUE
   21 DO 301 J2=2,I2
      IF(ARG2-ARG2BP(J2)) 13,13,301
  301 CONTINUE
   13 ARG=ARG1BP(J1-1)
      FUN=FUN2BP(J1-1,J2-1)
      DX=(ARG1-ARG)/(ARG1BP(J1)-ARG)
      DY=(ARG2-ARG2BP(J2-1))/(ARG2BP(J2)-ARG2BP(J2-1))
      FUNX=FUN+DX*(FUN2BP(J1,J2-1)-FUN)
      FUNY=FUN2BP(J1-1,J2)+DX*(FUN2BP(J1,J2)-FUN2BP(J1-1,J2))
      FUN2=FUNX+DY*(FUNY-FUNX)
      RETURN
      END
```

APPENDIX B. THRUST LEVEL SELECTION

1. Mars Lander Requirements

Selection of an "optimum" hydrazine monopropellant rocket engine design and associated flow control components is dependent upon many factors including proposed mission, operational and non-operational environmental requirements, and development schedule limitations. Independent design parameters include thrust level, chamber pressure, total impulse and engine duty cycle or throttle range. In order to select an engine design at least two of these parameters should be constrained as to avoid an unwieldly parametric study. This program, has, therefore, been based on the selection of hydrazine rocket engine designs for Mars landing vehicles such as Mars '73 and subsequent applications where a vehicle growth potential is anticipated. This section presents the results of a brief study which was conducted to determine the effect of engine thrust level on lander payload.

Since it was not possible to conduct a complete flight control study which would by necessity include attitude control and guidance component considerations, only the requirements for achieving near zero horizontal and vertical velocity components at lander touchdown were considered. It was also assumed that parachutes, aeroshells or other decelerating devices would provide the following initial conditions at engine ignition:

- Total lander mass
- Vertical velocity
- Horizontal velocity
- Altitude above the planet surface.

By fixing the initial conditions, the effect of engine thrust level on relative landed payload could be examined. The study was also based on a Surveyor type vehicle configuration where three engines are used to provide pitch and yaw stabilization as well as velocity vector control. The following paragraphs present the basic assumptions and equations for the study and the resulting conclusions.

2. Payload Optimization

As previously outlined, this study was aimed at determining the effect of thrust level on lander payload capability without considering explicitly the requirements resulting from attitude stabilization or the guidance and control loops. This approach is justified in that proposed engine differential throttling provides stability control and, therefore, (1) requires only that some delta thrust be added to the nominal thrust level, and (2) does not appreciably change the total impulse requirement. In addition, a fixed tank pressure was assumed; the use of a blowdown system would, therefore, imply setting the maximum thrust level at a higher value.

a. Basic Assumptions and Equations

In order to achieve the desired results of this study, the following assumptions were made:

- Flat planet
- Constant gravitational acceleration
- Constant thrust landing
- Zero aerodynamic forces

While variations in each of these parameters would be of interest to the guidance engineer, they do not measurably affect the results of this study. It was also assumed that the vehicle could be aligned with the net lander velocity vector such that both the vertical and horizontal velocity components would simultaneously be cancelled. The conventional equations describing the vertical profile as a function of thrust level, specific impulse, vehicle mass and landing or engine burn time are (B-1), (B-2) and (B-3).

$$\frac{d\,(dh/dt)}{dt} = g_m + \frac{\dot{m}\, g_e\, I_{sp}}{m} \qquad \text{(B-1)}$$

$$\dot{h}_o = g_e\, I_{wp}\, \ln\left[\frac{m_i}{m_i + \dot{m}t}\right] - g_m t \qquad \text{(B-2)}$$

$$\dot{h}_o = 1/2\ g_m t^2 + \dot{h}_o t + \frac{g_e I_{sp} m_i}{\dot{m}} \left[\frac{m_i + \dot{m}t}{m_i} \left(\ln \frac{m_i + \dot{m}t}{m_i} - 1 \right) + 1 \right] \quad \text{(B-3)}$$

Calculation of the rate of vehicle mass change is determined from equation (B-4) assuming that propellant expenditure is the only source of that change

$$\dot{m} = \frac{-3\ F_v}{I_{sp}\ g_e} \quad \text{(B-4)}$$

Using these basic equations and assumptions, the effect of thrust level on landed payload can be determined.

b. Relative Payload Determination

Figure B-1 shows the effect of thrust level on landing time and total impulse as a function of ignition altitude for a Viking class lander. The mass of the lander after parachute and aeroshell separation is on the order of 1200 lbm. As can be seen, for a fixed total impulse there is a maximum ignition attitude which occurs at an engine thrust level[1] of just under 300 lbf. As thrust level increases, the burn time and ignition altitude converge to zero. Similarly, as thrust level is reduced to the point where the total thrust to Mars weight ratio approaches one, the ignition altitude as well as the initial vertical velocity must gain approach zero. This is best shown in Figure B-2 and B-3. The former is a cross plot of Figure B-1 where landing time is replaced by initial vertical velocity and the latter is the same plot for an initial lander weight of 2400 lbm. As the initial lander weight is doubled, the thrust level at maximum ignition altitude is also doubled. Typical free fall lines have also been added to these curves. Free fall line (2) in Figure B-2 is representative of a Viking class vehicle where the following initial conditions exist.

[1] Unless otherwise noted, specified thrust levels refer to a single engine where total thrust is three times that value.

- Ignition altitude = 4000 feet
- Vertical velocity = 280 ft/sec.
- Horizontal velocity = 250 ft/sec.

It can be seen from these figures that as the lander free-falls from the initial altitude and vertical velocity, (1) the thrust level required to land increases and (2) the total impulse decreases rapidly at first but then much more slowly as the free fall line begins to almost parallel the total impulse lines. This characterization is best shown in Figure B-4 and B-5. The former shows the variation in gross landed mass fraction as a function of ignition altitude and thrust level and implies the existence of some peak value. The latter shows the same mass fraction plotted against thrust level for the two different sized vehicles and the two different free fall lines. It can be concluded that the characteristic curve merely moves (1) vertically as a function of initial velocity and altitude (or free fall line) and (2) horizontally as a function of initial lander mass. This can also be shown by reducing equations (B-2) and (B-3) to final mass fractions for fixed landing times.

In order to determine the existence of a relative maximum payload mass fraction, the increase in propulsion system weight with thrust level and total impulse must be considered. Based on parametric engine and tank weight data, equation (B-5) was used to adjust the results of Figure B-5.

$$\frac{\Delta m}{m_i} = -3 \cdot \frac{(\partial Meng/\partial F)\ \Delta F + (\partial m_t/\partial m_p)\ \Delta m_p}{m_i} \qquad \text{(B-5)}$$

By making this adjustment, the results of Figure B-6 were derived which show that for a Viking class vehicle an optimum engine thrust level of approximately 450 lbf exists based on vertical velocity control only. This gives a total thrust to initial vehicle Mars weight ratio of 3.0:1. As the initial vehicle weight is doubled (2400 lbm), the optimum thrust also appears to double (900 lbf)

but the peak becomes less pronounced due to the fact that the sensitivity of total engine mass to thrust level does not change. If initial vehicle mass were halved, the peak would be more obvious and would be more desirable to pinpoint. It should be noted that the mass fractions presented in Figure B-6 are relative values; fixed weight for the propulsion system using 200 lbf engines must be injected to determine absolute values. Up to this point, the horizontal velocity component has not been considered. Solving equation (B-6) for the appropriate conditions gives a horizontal impulse requirement of approximately 10,000 lbf-sec while the vertical impulse required is on the order of 20,000 lbf-sec. This results in an actual total impulse requirement of about 23,000 lbf-sec.

$$\dot{y}_o = g_e \, I_{sp} \, \ln\left(\frac{m_i}{m_f}\right) \tag{B-6}$$

Since a single set of fixed thrust vector engines is to be used, the relationship of total thrust to vertical thrust can be determined from equation (B-7).

$$\begin{aligned} \frac{F}{F_v} &= \frac{\left[\left(F_v t\right)^2 + \left(F_h t\right)^2\right]^{1/2}}{F_v t} \\ &= \frac{\left[\left(I_{t_v}\right)^2 + \left(I_{t_h}\right)^2\right]^{1/2}}{I_{t_v}} \end{aligned} \tag{B-7}$$

Solving this equation gives a ratio of about 1.1 which implies that the actual engine thrust level should be about 500 lbf (thrust to weight ratio of 3.3:1) excluding stability considerations. More detailed studies would be required to determine how much higher the thrust level should be raised to provide adequate stability margins as well as to account for a decaying thrust capability if a blowdown pressurization system is used. A 2:1 blowdown ratio (i.e., 600 psia/300 psia) for example would require an increase in maximum thrust level to approximately 625 lbf to maintain an average thrust level of 500 lbf.

3. Conclusions

Based on the results of this study, the following conclusions were reached:

- A maximum thrust level of about 500 lbf (thrust-to-weight ratio of 3.3:1) is desirable for a Viking class vehicle based on payload optimization only.
- The "optimum" thrust to weight ratio remains constant with increasing vehicle initial weight although the peak in the payload mass fraction versus thrust level becomes less pronounced as vehicle weight increases.
- A more detailed evaluation is required to establish the effects of aerodynamic forces and required landing maneuvers on absolute thrust level selection. Pitch up and hovering requirements as well as guidance logic and sensor requirements, for example, will dictate a throttle range as well as altering to some degree the results of a fixed thrust landing profile analysis.

For the purpose of this program which is to select an engine design, it can be concluded that a fixed thrust to weight ratio of approximately 3.3:1 should be used and that a fixed engine duty cycle is valid for determining system requirements for increasing thrust levels. The duty cycle shown in Figure II.A-1 is representative of such a duty cycle and was used for subsequent analyses.

Figure B-1

IGNITION ALTITUDE

vs.

BURN TIME

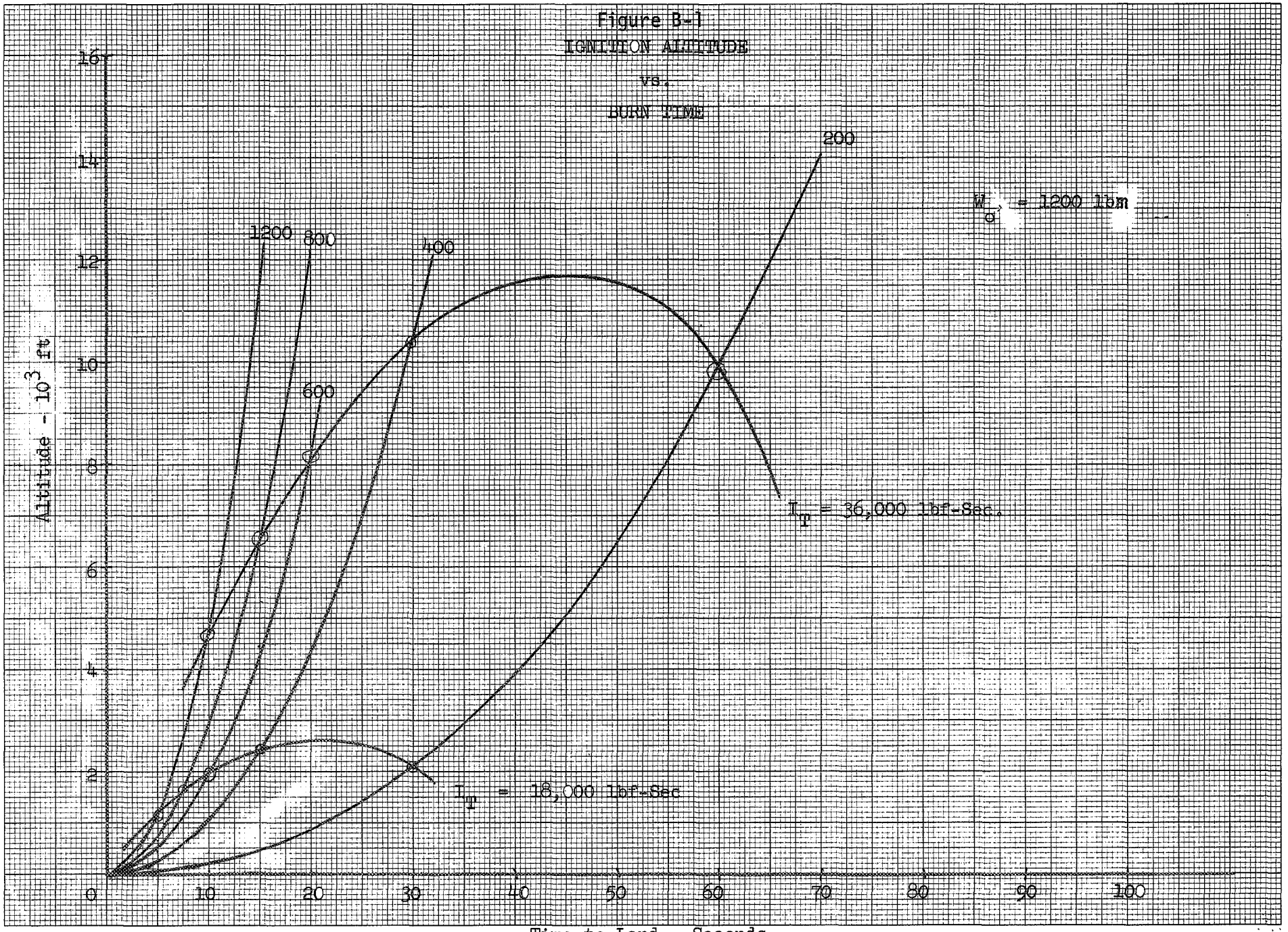

Figure 8-2

LANDER VERTICAL VELOCITY

VS.

IGNITION ALTITUDE

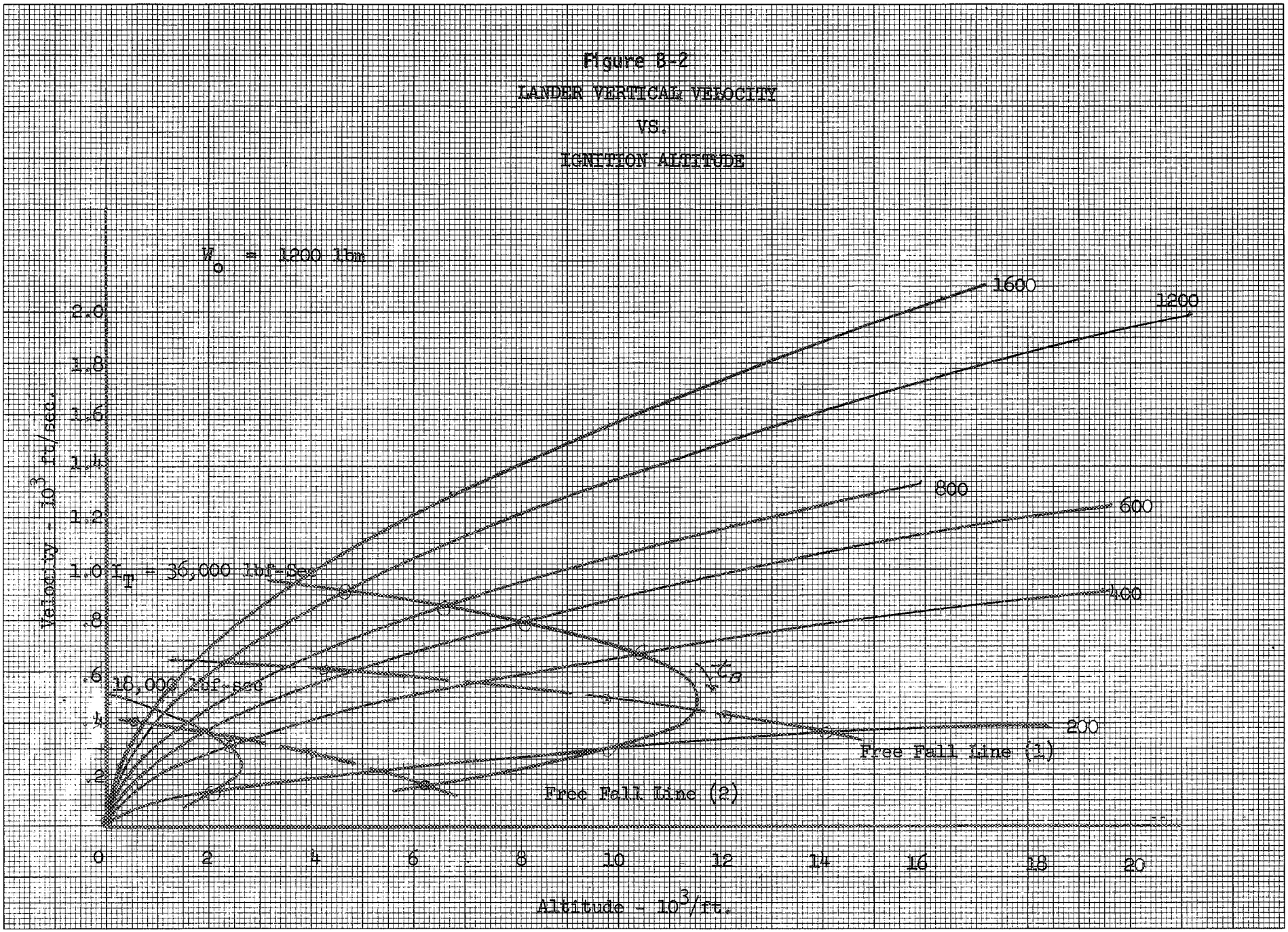

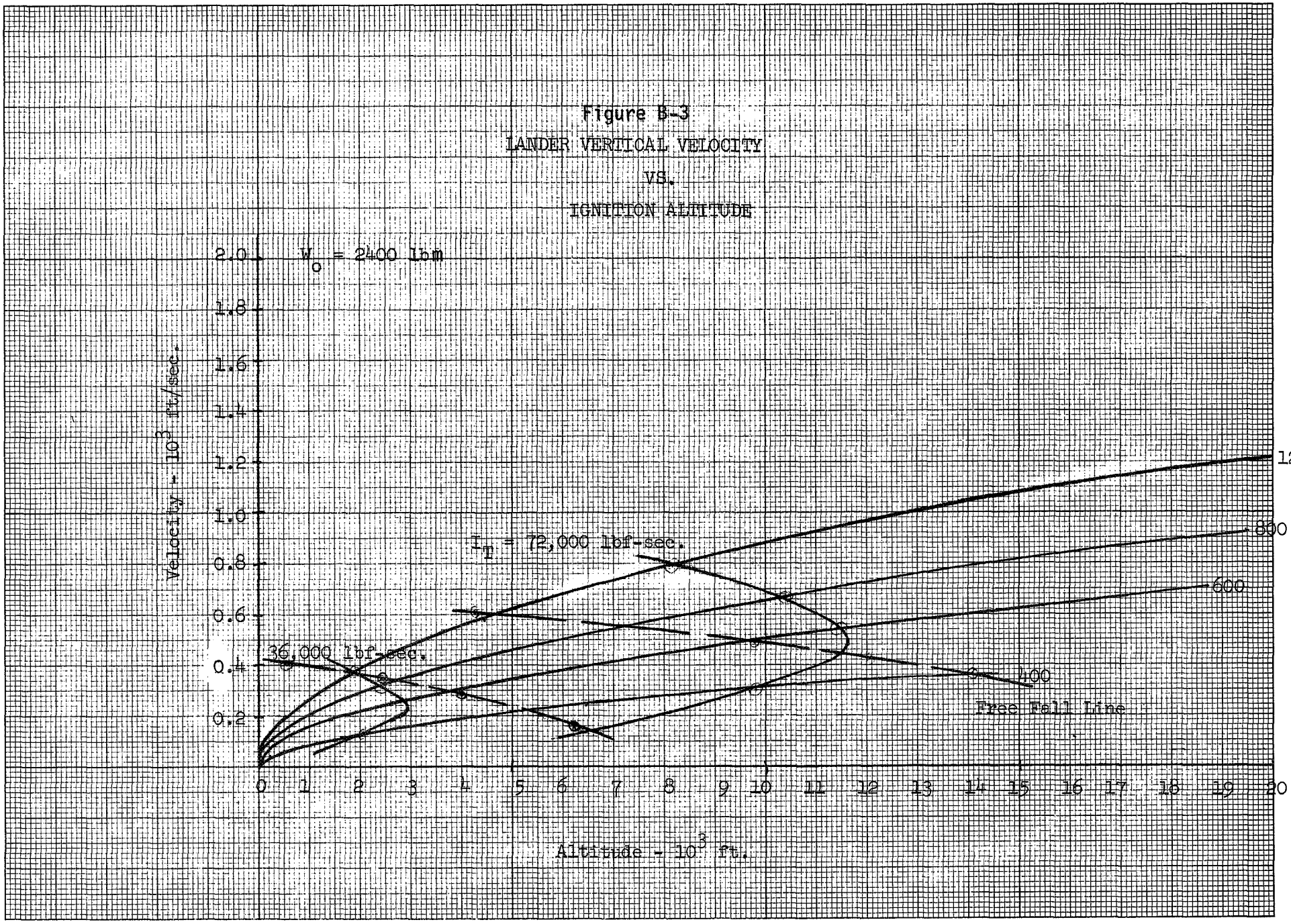
Figure B-3
LANDER VERTICAL VELOCITY
VS.
IGNITION ALTITUDE
W_o = 2400 lbm
I_T = 72,000 lbf-sec.
36,000 lbf-sec.
1200
800
600
400
Free Fall Line
Velocity - 10^3 ft/sec.
Altitude - 10^3 ft.
2.0
1.8
1.6
1.4
1.2
1.0
0.8
0.6
0.4
0.2
0
1
2
3
4
5
6
7
8
9
10
11
12
13
14
15
16
17
18
19
20

Figure B-4

MASS FRACTION

vs.

IGNITION ALTITUDE

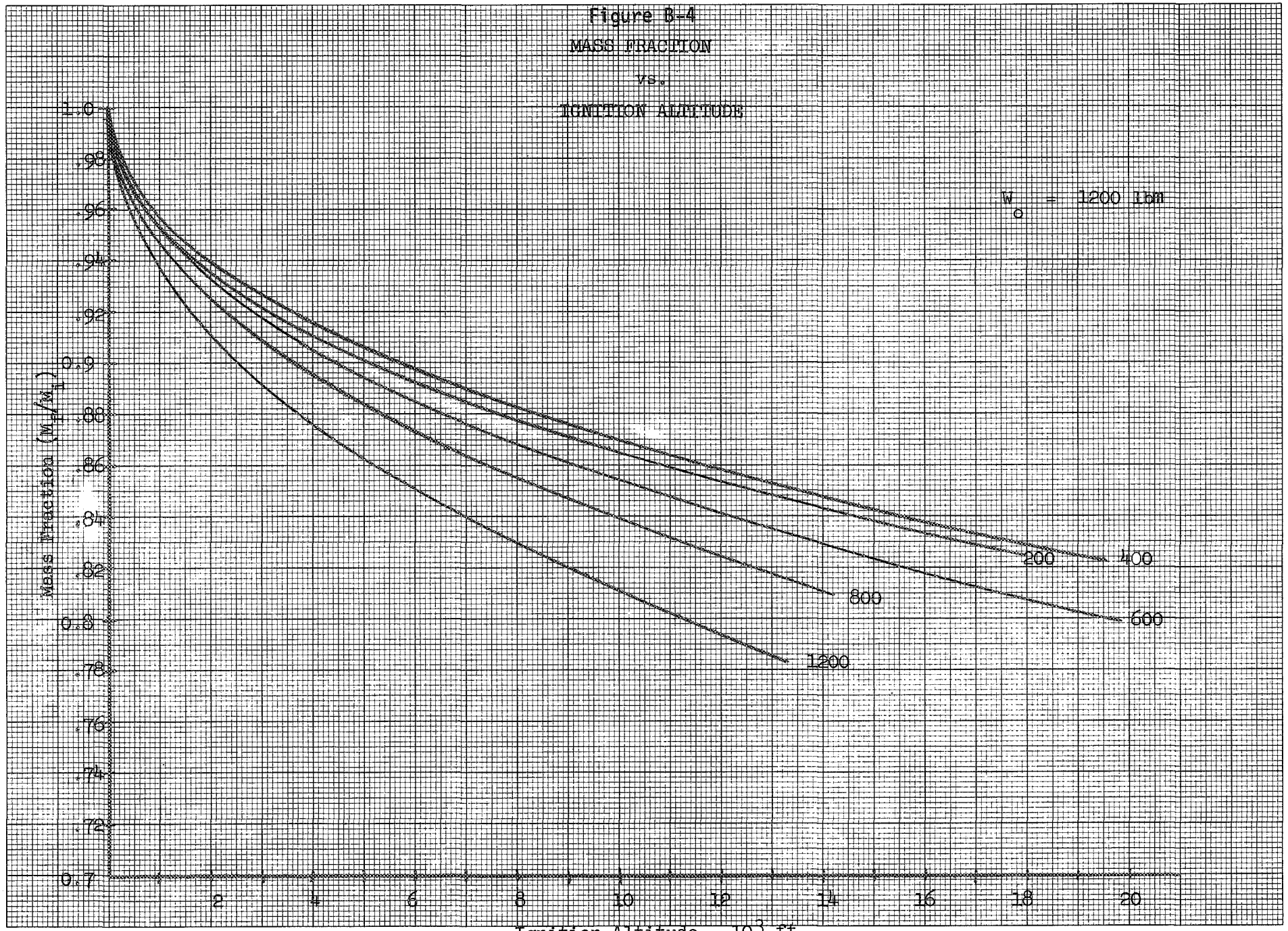

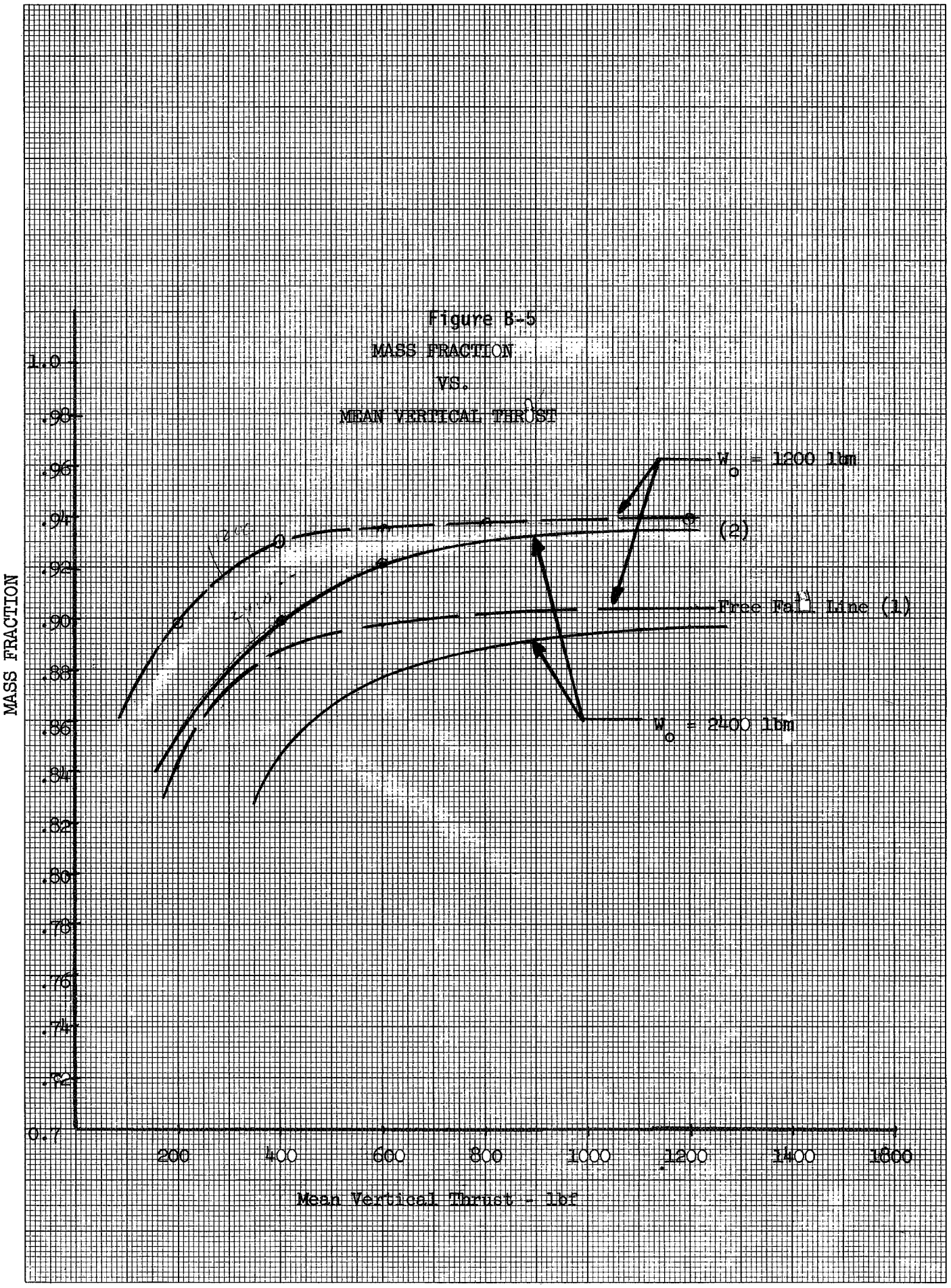
Figure B-5
MASS FRACTION
VS.
MEAN VERTICAL THRUST
MASS FRACTION
1.0
.98
.96
.94
.92
.90
.88
.86
.84
.82
.80
.78
.76
.74
.72
0.7
W_o = 1200 lbm
(2)
Free Fall Line (1)
W_o = 2400 lbm
200
400
600
800
1000
1200
1400
1600
Mean Vertical Thrust - lbf

Figure B-6

PAYLOAD MASS FRACTION

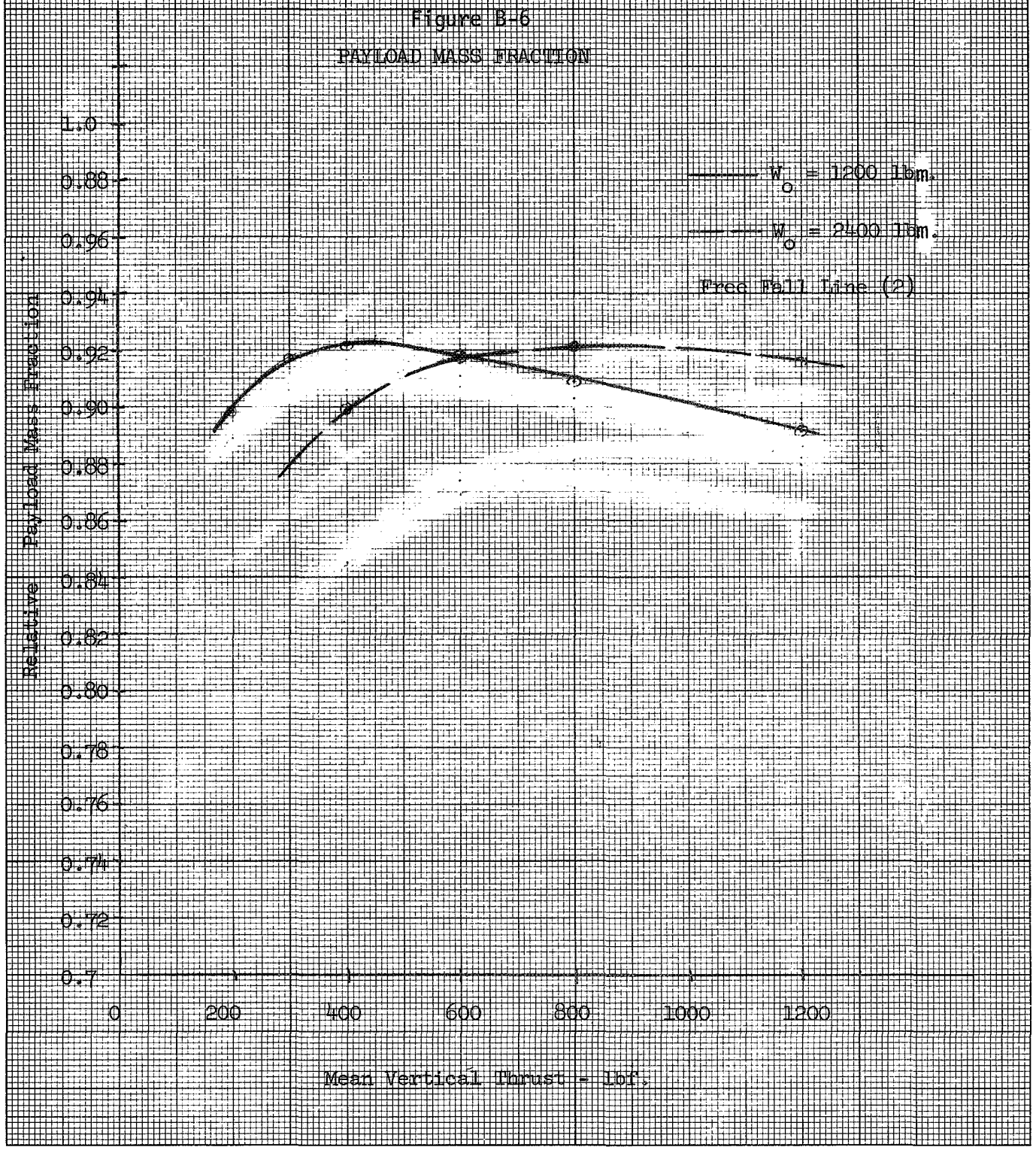

APPENDIX C. THRUST LINEARITY EVALUATION

The thrust linearity requirements for Viking type lander vehicles include the requirement that at any given valve position the flowgain ratio or ratio of slopes ($\partial F/\partial V_c$) over an inlet pressure range of 2:1 shall be less than some value. In order to minimize this ratio the thrust versus command voltage map should be linear at the mid-inlet pressure. In order to establish an optimum chamber pressure, pressure schedule and valve metering plug contour, a parametric evaluation of the effects of chamber pressure, catalyst bed pressure drop and valve pressure drop at maximum thrust must be conducted. The following paragraphs present the results of a typical study for a maximum thrust level of 600 lbf and a tank pressure range from 500 to 250 psia.

1. Basic Equations

The pressure balance equations are as follows:

$$P_T - \Delta P_\ell - \Delta P_v - \Delta P_{inj} - \Delta P_B - P_c = 0 \qquad \text{(C-1)}$$

$$\Delta P_\ell = R_\ell (\dot{w})^2 \qquad \text{(C-2)}$$

$$\Delta P_v = R_v (\dot{w})^2 \qquad \text{(C-3)}$$

$$\Delta P_{inj} = R_{inj} (\dot{w})^2 \qquad \text{(C-4)}$$

$$\Delta P_B = R_B \dot{w} \qquad \text{(C-5)}$$

$$P_c = R_n \dot{w} \qquad \text{(C-6}$$

The relationship between flow rate and command voltage at mid-tank pressure (P_1 = 375 psia) is as follows where I_{sp} is assumed fixed and valve position is proportional to command voltage (V_c).

$$\dot{w} = K_1 + K_2 V_c \qquad \text{(C-7)}$$

The required valve resistance as a function of command voltage can, therefore, be expressed as follows:

$$R_v = \frac{P_1}{(K_1 + K_2 V_c)^2} - (R_{inj} + R_1) - \frac{(R_B + R_N)}{(K_1 + K_2 V_c)} \qquad (C\text{-}8)$$

Equation (C-7) can also be used to solve system flow rate for any tank pressure and valve setting per equation (C-9).

$$\dot{w} = - \frac{(R_B + R_N)}{2(R_v+R_1+R_{inj})} + \frac{\left[\left(\frac{R_B + R_N}{R_v+R_1+R_{inj}}\right)^2 + \frac{4 P_T}{R_v+R_1+R_{inj}}\right]^{1/2}}{2} \qquad (C\text{-}9)$$

The slope at any given point can now be determined.

$$\frac{\partial \dot{w}}{\partial V_c} = \left(\frac{\partial \dot{w}}{\partial R_v}\right) \left(\frac{\partial R_v}{\partial V_c}\right) \qquad (C\text{-}10)$$

$$\frac{\partial \dot{w}}{\partial R_v} = \frac{(R_B + R_N)}{2(R_v+R_1+R_{inj})^2} - \frac{\left[\frac{2(R_B+R_N)^2}{(R_v+R_1+R_{inj})^3} + \frac{4 P_T}{(R_1+R_v+R_{inj})^2}\right]}{\left[4\left(\frac{R_B + R_N}{R_v+R_1+R_{inj}}\right)^2 + \frac{4 P_T}{(R_v+R_1+R_{inj})}\right]^{1/2}} \qquad (C\text{-}11)$$

$$\frac{\partial R_v}{\partial V_c} = \frac{-2P_1K_2}{(K_1+K_2V_c)^3} + \frac{(R_B + R_N)K_2}{(K_1 + K_2 V_c)^2} \qquad (C\text{-}12)$$

2. Results

The ratio of slopes at the maximum throttle setting as a function of chamber pressure and bed pressure drop has been presented in Figures II.E-35. For a nominal bed drop of 40 psi, the chamber pressure could be increased to almost 300 psia before a typical ratio requirement of 2.4:1 is exceeded. Once bed drop and chamber pressure are set, the distribution of remaining pressure between propellant lines, injector and valve does not affect this ratio. This can be seen by examination of equation (C-11) which shows that these resistances (R_v, R_1 and R_{inj}) are additive in each term.